July 2016

Inhibition of DNA Methylation in Acquired Tamoxifen-Resistant Breast Cancer: Cell Line Model and Clinical Implications

Stephanie Zimmers
University of Massachusetts Amherst

INHIBITION OF DNA METHYLATION IN ACQUIRED TAMOXIFEN-RESISTANT BREAST CANCER: CELL LINE MODEL AND CLINICAL IMPLICATIONS

A Dissertation Presented

by

STEPHANIE MARIE ZIMMERS

Submitted to the Graduate School of the
University of Massachusetts Amherst in partial fulfillment
of the requirements for the degree of

DOCTOR OF PHILOSOPHY

May 2016

Molecular and Cellular Biology Graduate Program

INHIBITION OF DNA METHYLATION IN ACQUIRED TAMOXIFEN-RESISTANT BREAST CANCER: CELL LINE MODEL AND CLINICAL IMPLICATIONS

A Dissertation Presented

by

STEPHANIE MARIE ZIMMERS

Approved as to style and content by:

_____
Kathleen F. Arcaro, Chair

_____
Lisa M. Minter, Member

_____
Sallie Smith Schneider, Member

_____
Patricia Wadsworth, Member

_____
Dominique Alfandari, Director
Molecular and Cellular Biology Program

DEDICATION

To my grandparents, Virginia and Joseph Andrejcik and Galia and Charles Zimmers, whom I miss dearly and I know would be very proud of all of my accomplishments.

ACKNOWLEDGMENTS

I would like to extend my sincere thanks to my advisor, Dr. Kathleen Arcaro. My first project in the Arcaro lab was developing an analytical extraction method to measure bisphenol-A (BPA) in breast milk. This was a challenging project that gave me the opportunity to develop skills I otherwise never would have. Kathleen has been both supportive and understanding and I am honored to have such a great scientist as my mentor.

Working on the BPA project, I was introduced to a number of people who were always willing to offer advice and help with equipment and lab issues. I never would have completed the project had it not been for the help from Dr. David Reckhow, Dr. Patrick O'Keefe, Larry Kramer, Sherrie Webb-Yagodzinski and Karen Mason. Dr. Reckhow was kind enough to let us use his HPLC and mass spectrometer. I would also like to thank Eva Browne and Ashley Silvia for their help with method development and sample processing.

I would also like to thank the members of my committee: Dr. Sallie Schneider, Dr. Lisa Minter and Dr. Patricia Wadsworth. I am honored to have them on my committee. They were instrumental in providing advice on experiments and at other key points throughout my graduate career. I was also fortunate to have the opportunity to be a TA in classes taught by Dr. Minter and Dr. Wadsworth. I enjoyed working with them and am grateful for this opportunity.

I am also extremely grateful to have such wonderful lab mates throughout my graduate career. Thank you Dr. Katerina Fagan-Solis, Eva Browne, Elizabeth

Punska, Kristin Williams, Kasie Auger and Ana Caballero for providing help and support both inside and out of the lab.

After our lab moved from Morrill into the Life Sciences Laboratories, we shared a research cluster with other labs both inside and outside of the Veterinary and Animal Sciences (VASCI) Department. I am so glad I had the opportunity to get to know these professors and their lab members better. Specifically, I would like to thank the following professors for generously sharing some of their equipment and reagents: Dr. John Clark, Dr. Joseph Jerry, Dr. Jungwoo Lee, Dr. Michele Klingbeil, Dr. Sarah Perry, Dr. Sandra Peterson, Dr. Shelly Peyton, Dr. Yasu Morita, Dr. Sallie Schneider, Dr. Elizabeth Stuart and Dr. Wilmore Webley. I would also like to thank Stephen Ball who has been helpful with all sorts of equipment and building issues over the past few years.

I was very fortunate to utilize an ongoing collaboration with the Pathology Department at Baystate Medical Center. The work presented here could not have been completed without the help of Dr. Christopher Otis, Dr. Rahul Jawale, Brooke Bentley and Lynn Eaton. It was an honor to work with them and I am thankful to have such a great learning experience.

I thank the Molecular and Cellular Biology (MCB) Program and the Institute for Cellular Engineering, specifically Sarah Czerwonka and Shana Passonno, for their help with keeping track of administrative matters. I am grateful for the opportunity to participate in these graduate programs. Through these programs I met amazing scientists and made some great friends. Thank you also to Dr. Daniel Hebert, with whom I did my second rotation in the MCB Program. I would also like to thank the

members of the VASCI Department, specifically Jimmy Wright and Laura Looman, for helping me to keep things in order. I also thank members of the Biology Department for their support and help through the semesters when I taught undergraduate lab courses specifically, Robbie Cairl and Dr. Caleb Rounds.

I have made some amazing friends throughout my time at UMass. They have been incredibly supportive and I am so grateful for their friendship. In particular, I would like to thank Elsina Hagan, Eva Browne, Kasie Auger, Santiago Vidales, Kristin Williams, Weam Zaky and Dr. Katerina Fagan-Solis for letting me stay in their extra rooms numerous times so I could work longer in lab and not have to drive an hour back to my house late at night or when the weather was bad. Thank you also Dr. Tina Kuksin for your friendship and the numerous times we carpooled together. I would also like to thank my friends from The Ohio State University, to whom I am forever grateful for their support and friendship even though we live so far away.

Last but certainly not least, I thank my family for their continuous love and support. My mother, Laurie Zimmers, is and always has been there for me sending care packages and calling on the phone to send her support. I would not be the person I am today without such a great role model to look up to. Thank you to my husband, Kevin Handy, to whom I am forever grateful for his support. He has always stood by my side to encourage me through each year. I would also like to thank my father, Vaughn Zimmers, grandparents, aunts, uncles, in-laws, cousins, nieces and nephews as well as close family friends. This journey would have been impossible without the love and support from my family.

ABSTRACT

INHIBITION OF DNA METHYLATION IN ACQUIRED TAMOXIFEN-RESISTANT BREAST CANCER: CELL LINE MODEL AND CLINICAL IMPLICATIONS

MAY 2016

STEPHANIE MARIE ZIMMERS, B.S., THE OHIO STATE UNIVERSITY

Ph.D., UNIVERSITY OF MASSACHUSETTS AMHERST

Directed by: Professor Kathleen F. Arcaro

One out of every eight American women will develop invasive breast cancer throughout their lifetime. Approximately 70% of breast cancers are estrogen receptor alpha (ER)-positive and can therefore be treated with an anti-estrogen such as tamoxifen. Although tamoxifen treatment has been successful at reducing breast cancer death rates, nearly one-third of women treated with tamoxifen for 5 years will have disease recurrence. Therefore, it is imperative that researchers investigate the mechanisms involved in developing acquired tamoxifen resistance and identify biomarkers that are predictive of acquired resistance.

DNA methylation is known to play a role in the development of breast cancer and is thought to be involved in drug resistance as well. Although genome-wide hypomethylation occurs frequently in breast cancer, gene-specific hypermethylation and a corresponding decrease in expression are known to occur in breast cancer. The primary objective of this study is to evaluate how changes in DNA methylation in response to the DNMT1 inhibitor, 5-Aza-2'-deoxycytidine, affect gene expression and cell behavior in the ER-negative cell line model of tamoxifen-resistance.

In the present study, I utilize a cell line model of acquired tamoxifen resistance, TMX2-28. This cell line, along with two other tamoxifen-resistant lines, were generated by culturing MCF-7 cells in the presence of Tamoxifen (10^{-6} M) for 6 months. Cloning by limiting dilution lead to the discovery of three tamoxifen-resistant cell lines. Two of which retained expression of ER, TMX2-4 and TMX2-11, and one that no longer expressed ER, TMX2-28. Initial studies of genome-wide methylation with the Illumina Human Methylation 450 BeadChip found TMX2-28 is hypermethylated compared to the parental cell line, MCF-7. Specifically, promoter methylation is involved in regulating the expression of at least two genes in TMX2-28. Promoter methylation of these genes decreased in response to treatment with the DNMT-inhibitor, 5-Aza-2'-deoxycytidine, and a corresponding increase in mRNA expression was observed. Unpublished data from our lab indicate that 5-Aza-2'-deoxycytidine also decreases TMX2-28 cell proliferation. However, it is unclear how changes in methylation and gene expression induced by 5-Aza-2'-deoxycytidine affect the behavior of TMX2-28 cells.

I tested the hypothesis that changes in cell behavior in response to 5-Aza-2'-deoxycytidine are caused by changes in gene expression induced by decreased promoter methylation. First I utilized the Illumina Human Methylation 450 BeadChip to study changes in DNA methylation in the parental cell line, MCF-7, as well as the three tamoxifen-resistant cell lines. I confirmed results from previous studies indicating that TMX2-28 is hypermethylated compared to the parental cell line, MCF-7. I also discovered that treatment with 5-Aza-2'-deoxycytidine results in cell line-specific changes in DNA methylation. The ER-negative, tamoxifen-resistant

cell line, TMX2-28, is most sensitive to treatment with the DNMT-inhibitor. To determine the genes most likely to have altered expression after 5-Aza-2'-deoxycytidine treatment, I first identified CpG sites that are hypermethylated in TMX2-28 compared to MCF-7. Of these 37,501 CpGs, there are 707 CpGs with decreased methylation after treatment with 5-Aza-2'-deoxycytidine. This corresponds to 27 genes with changes in at least 2 CpGs located in the promoter.

To determine other cell behaviors that may be affected by inhibition of methylation in TMX2-28, I conducted a 2-dimensional scratch/wound assay. I found that treatment of TMX2-28 with 5-Aza-2'-deoxycytidine inhibits 2-dimensional migration and induces detachment of cells from the monolayer. Treatment with 5-Aza-2'-deoxycytidine also decreased cell viability. One of the 27 genes I identified as differentially methylated and altered by 5-Aza-2'-deoxycytidine, *TACSTD2*, seemed likely to play a role in regulating these behaviors in TMX2-28. Expression of the protein encoded by this gene, tumor-associated calcium signal transducer 2, TROP2, is regulated by promoter methylation in lung cancer and TROP2 is involved in development, intracellular signaling and epithelial cancers. Expression of TROP2 in lung cancer cell lines inhibits proliferation, colony formation and blocks phosphorylation of important intracellular signaling molecules involved in growth signaling and transcription. Promoter methylation of *TACSTD2* is low in MCF-7 and TROP2 expression is high while promoter methylation is high in TMX2-28 and TROP2 expression is low. This is consistent with the idea that promoter methylation is regulating expression. Therefore, I tested the hypothesis that the

behavior of TMX2-28 in response to 5-Aza-2'-deoxycytidine was due to increased expression of TROP2.

To test this hypothesis, I first confirmed that treatment of TMX2-28 with 5-Aza-2'-deoxycytidine decreases *TACSTD2* promoter methylation and increases TROP2 expression. Next, I generated stable cell lines with increased TROP2 expression (TMX2-28-Trop2) and knocked down TROP2 expression in MCF-7 (MCF-7-Trop2-Kd). I quantified proliferation, adhesion to fibronectin and migration of these cell lines. Contrary to my predictions, expression of TROP2 in TMX2-28 did not affect proliferation and increased both adhesion to fibronectin and migration. Interestingly, knockdown of TROP2 expression in MCF-7 increased proliferation but did not alter adhesion or migration.

To further evaluate the role of TROP2 in breast cancer, *TACSTD2* methylation and TROP2 expression were analyzed in a total of 70 primary and recurrent clinical breast cancer samples. *TACSTD2* promoter methylation was lower in the clinical samples than the cell lines. In agreement with the cell line data, methylation of the three *TACSTD2* CpG sites was higher in ER-negative recurrent tumors that were initially ER-positive primary tumors. However, there was no correlation between promoter methylation and TROP2 expression in the clinical samples. In contrast to previous reports, I found no association between TROP2 expression and tumor grade or Ki67 status. Despite the small size, the clinical sample data indicate that our cell line model may be relevant for studying ER-negative, tamoxifen resistant breast cancer.

Additionally, I characterized DNA methylation and protein expression patterns of several luminal and basal cytokeratins. According to the methylation status determined by the 450 BeadChip and protein expression determined by IHC for the parental cell line and the three tamoxifen-resistant cell lines, promoter methylation seems to play a role in regulating expression of p40, the basal cytokeratins CK5 and CK14, and the luminal cytokeratins CK8, CK17, CK18 and CK20. I found that MCF-7, TMX2-4 and TMX2-11 express luminal (low molecular weight) cytokeratins while TMX2-28 express a combination of luminal and basal cytokeratins. These new IHC data are consistent with previously published work from our lab and demonstrate that TMX2-28 have a mixed basal-luminal phenotype. DNA methylation of cytokeratin genes may be useful as an alternative indicator of tumor subtype and provide insight into mechanisms controlling expression of these important prognostic markers.

The results presented in the present study demonstrate that DNA methylation may play an important role in ER-negative, tamoxifen resistant breast cancer. TMX2-28 cells rely on a TROP2-independent mechanism to sustain proliferative signals. TROP2 acts to promote adhesion and migration in TMX2-28. Further studies are necessary to determine the mechanism by which TROP2 increases adhesion and migration as well as the role of TROP2 in drug resistant breast cancer. Due to the high percentage of clinical samples positive for TROP2 expression, TROP2 may serve as a method for targeted drug delivery for recurrent breast cancer.

TABLE OF CONTENTS

Page

ACKNOWLEDGMENTS v

ABSTRACT viii

LIST OF TABLES xvi

LIST OF FIGURES xviii

CHAPTER

1. INTRODUCTION 1

Breast Cancer and Biology of the Breast 1
Etiology of Breast Cancer 2
The Hallmarks of Cancer 3
Epigenetics and DNA Methylation 4
Tamoxifen Resistance and DNA Methylation 5
Tamoxifen-Resistant Cell Line Model 8
Cell Proliferation, Adhesion and Migration 9
Tumor-Associated Calcium Signal Transducer 2 (TROP2) 12

2. DNA METHYLATION ANLYSIS 26

Introduction 26
Materials and Methods 31
Results 34
5-Aza-2'-deoxycytidine Alters Global DNA Methylation 34
Top 5 Genes With Decreased Methylation in TMX2-28 After 5-Aza-2'-deoxycytidine Treatment 36
Top 7 Genes With More Than One CpG Site in the Promoter Region With Decreased Methylation in TMX2-28 After 5-Aza-2'-deoxycytidine Treatment 37
Genes Likely Re-expressed in TMX2-28 by 5-Aza-2'-deoxycytidine Treatment 37
Genes With Differential Methylation in the Promoter Region and Demethylated by 5-Aza-2'-deoxycytidine 39
Distribution of CpG Sites that are Hypermethylated in TMX2-28 and Have Decreased Methylation After 5-Aza-2'-deoxycytidine Treatment 40
Methylation Pattern of *TACSTD2* in Control- and 5-Aza-2'-deoxycytidine-Treated Cell Lines 40

Further Characterization of Target Genes Identified by Changes in Promoter Methylation 41
Discussion 43

3. 5-AZA-2'-DEOXYCYTIDINE INHIBITS PROLIFERATION, MIGRATION AND ADHESION IN TMX2-28 72

Introduction 72
Materials and Methods 78
Results 81
5-Aza-2'-deoxycytidine Inhibits Proliferation in TMX2-28 81
5-Aza-2'-deoxycytidine Inhibits Cell Migration (Scratch/Wound) in TMX2-28 82
Optimization of Seeding Densities for Quantitative Adhesion Assay 83
Variability With Initial Experiments and Switch to Pre-coated Fibronectin Plates 84
5-Aza-2'-deoxycytidine Inhibits Adhesion in TMX2-28 85
Validation of Changes in Methylation Identified on 450 BeadChip 87
Discussion 87

4. THE ROLE OF TROP2 IN REGULATION OF ADHESION, MIGRATION AND PROLIFERATION IN TMX2-28 102

Introduction 102
Materials and Methods 107
Results 114
Overexpression of TROP2 Alters Adhesion and Migration in TMX2-28, Not Proliferation 114
Knockdown of TROP2 in MCF-7 Alters Proliferation Only 116
Analysis of *TACSTD2* Methylation and TROP2 Expression in Clinical Samples 117
Discussion 125

5. FURTHER CHARACTERIZATION OF TAMOXIFEN-RESISTANT BREAST CANCER CELL LINES BY KERATIN EXPRESSION 161

Introduction 161
Materials and Methods 165
Results 167
TMX2-28 Cells Have a Mixed Cytokeratin Expression Profile 167

Expression of Several Cytokeratins and p40 May Be Regulated by Promoter Methylation 168
Expression of Luminal Cytokeratins, CK8, CK17, CK18 and CK20, May Be Regulated by Promoter Methylation 170
Expression of the Basal Cytokeratins, CK1, CK6 and CK10, the Luminal Cytokeratin, CK17, and p63 Does Not Appear to Be Regulated by Promoter Methylation 173
Discussion 175

6. DISCUSSION AND FUTURE DIRECTIONS 208

Introduction 208
DNA Methylation Patterns Differ Between the Parental and Tamoxifen-resistant Cell Lines 209
5-Aza-2'-deoxycytidine Alters DNA Methylation, Proliferation, Migration and Adhesion in TMX2-28 211
Role of TROP2 in Regulation of Proliferation, Migration and Adhesion in Cell Line Model 213
TACSTD2 Methylation and TROP2 Expression in Clinical Samples 217

APPENDICES

A. COMPARISON OF CELL LINE REPLICATES ON 450 BEADCHIP 221
B. OPTIMIZATION OF SEEDING DENSITIES FOR ADHESION ASSAY 226
C. INNITIAL ADHESION ASSAY EXPERIMENTS 230
D. ADHESION OF ADHERENT AND FLOATING CELL POPULATIONS TREATED WITH 5-AZA-2'-DEOXYCYTIDINE 233

BIBLIOGRAPHY 237

LIST OF TABLES

Table Page

2.1 Primers Used to Detect Relative mRNA Expression of Genes 48

2.2 Changes in Global Methylation Between Tamoxifen-Resistant Cell Lines and MCF-7 49

2.3 Changes in Global Methylation Between TMX2-28-5-Aza-2'-deoxycytidine-Treated and TMX2-28-Control 50

2.4 Top 5 Genes in TMX2-28 Containing CpG Sites With the Largest Decrease in Methylation After 5-Aza-2'-deoxycytidine Treatment 51

2.5 Top 7 Genes in TMX2-28 Containing CpG Sites With the Largest Decrease in Methylation in the Promoter After 5-Aza-2'-deoxycytidine Treatment 52

2.6 Differences in mRNA Expression Between TMX2-28 and MCF-7 53

2.7 Hypermethylated CpG Sites in TMX2-28 CpG That Have Decreased Methylation After 5-Aza-2'-deoxycytidine Treatment 54

2.8 Genes With More Than One CpG Site in the Promoter Differentially Methylated in TMX2-28 and Decreased by 5-Aza-2'-deoxycytidine 55

2.9 Average Promoter Methylation (Beta value) from Illumina Human Methylation 450 BeadChip and mRNA Expression (Cycle Number) for MCF-7 and TMX2-28 Cells from the 72-hr. Aza Exposure Experiment 56

2.10 Average Cycle Thresholds for Control and 5-Aza-2'-deoxycytidine for Previously Validated Genes 58

4.1 Summary of Previous Results and Predictions 133

4.2 Predictions for Tumor Samples Based on Cell Line Data 134

4.3 Predictions for Tumor Samples Based on Literature 135

4.4 Patient and Tumor Characteristics 136

4.5 TROP2 Staining in Breast Tumors 138

4.6 Descriptive Statistics for Average Beta Values by ER Status.....139

4.7 Descriptive Statistics for Membrane TROP2 Scores 140

4.8 Descriptive Statistics for Cytoplasmic TROP2 Scores 141

5.1 Cytokeratin, p40 and p63 Expression Determined by IHC for Cell Lines ...181

LIST OF FIGURES

Figure Page

1.1: Normal Breast Anatomy....16

1.2: Two General Types of Breast Cancer....17

1.3: Basal Verses Luminal Breast Cancers....18

1.4: The Hallmarks of Cancer....20

1.5: Chromatin Structure and Epigenetics in Normal Cells....21

1.6: DNA Methyltransferase (DNMT) Converts Cytosine to 5-Methylcytosine....22

1.7: Treatment of Recurrent Breast Cancer....23

1.8: Development of Tamoxifen-Resistant Cell Lines....24

1.9: Summary of Metastatic Cascade in Breast Cancer....25

2.1: Structure and Intracellular Metabolism of 5-Aza-2'-deoxycytidine....59

2.2: Distribution of Sites on the HM450 BeadChip....60

2.3 Global Methylation Patterns Differ Among Tamoxifen-Resistant Cell Lines....61

2.4: 5-Aza-2'-deoxycytidne Treatment Causes Cell Line-Specific Changes in Global Methylation....63

2.5: TMX2-28 Differs from MCF-7 in Global mRNA Expression....65

2.6: Summary of Selection Process for Target Genes....66

2.7: Functional Genomic Location and Neighborhood Distribution of Differentially Methylated CpG Sites in TMX2-28 with Decreased Methylation After 5-Aza-2'-deoxycytidine Treatment....67

2.8: Methylation Patterns for *TACSTD2* in DMSO-Control and 5-Aza-2'-deoxycytidine-Treated Cell Lines....68

2.9: Relative mRNA Expression of Target Genes in DMSO-Control and 5-Aza-2'-deoxycytidine-Treated Cells....70

3.1: Treatment With 5-Aza-2'-deoxycytidine for 96 Hours Decreases Proliferation in TMX2-28....93

3.2: 5-Aza-2'-deoxycytidine Treatment Decreases Proliferation in TMX2-28....94

3.3: 5-Aza-2'-deoxycytidine Treatment Inhibits Migration in Scratch/Wound Assay in TMX2-28....95

3.4: 5-Aza-2'-deoxycytidine Treatment Results in Detachment of Cells Independent of Scratch....96

3.5: 5-Aza-2'-deoxycytidine Treatment Decreases Viability in TMX2-28....97

3.6: Schematic of Experimental Design for 5-Aza-2'-deoxycytidine Treatment and Adhesion Assay....98

3.7: 5-Aza-2'-deoxycytidine Treatment Decreases Adhesion in TMX2-28....99

3.8: 5-Aza-2'-deoxycytidine Treatment Decreases Adhesion in TMX2-28 (n = 16)....100

3.9: 5-Aza-2'-deoxycytidine Treatment Decreases Promoter Methylation of *TACSTD2*....101

4.1: TROP2 Expression in the Cloned Cell Lines....142

4.2: TROP2 Overexpression Does Not Affect Proliferation in TMX2-28....144

4.3: TROP2 Increases Adhesion to Fibronectin in TMX2-28....145

4.4: TROP2 Promotes Migration of TMX2-28....146

4.5: Knockdown of TROP2 in MCF-7 Increases Proliferation....147

4.6: TROP2 Knockdown Has Variable Results on MCF-7 Adhesion to Fibronectin....148

4.7: Average Methylation for *TACSTD2* in Tumor Samples by ER status....150

4.8: Average Methylation for *TACSTD2* in Primary and Recurrent Tumor Samples....151

4.9: *TACSTD2* Methylation in Tumor Samples....152

4.10: TROP2 IHC Scoring in Tumor Samples....155

4.11: Summary of Membrane and Cytoplasmic TROP2 IHC Scoring in Tumor Samples....156

4.12: Expression of Membrane TROP2 in ER-Positive Primary Tumors that Recur as ER-Negative....157

4.13: Expression of TROP2 in Tumor Samples by ER/HER2 Status....158

4.14: Expression of TROP2 in Non-Recurrent Samples and Primary Samples that Recur....159

4.15: Tumor Grade and Ki67 Score by Expression Level of Membrane TROP2....160

5.1: Components of the Cytoskeleton....182

5.2: p40 is Highly Methylated in All Cell Lines....183

5.3: CK5 Expression May Be Regulated by Promoter Methylation in TMX2-28....185

5.4: CK14 Expression May Be Regulated by Promoter Methylation....187

5.5: CK8 Expression May Be Regulated by Promoter Methylation....189

5.6: CK17 Expression May Be Regulated by Promoter Methylation....191

5.7: CK18 Expression May Be Regulated by Promoter Methylation....194

5.8: CK20 Expression May Be Repressed by Promoter Methylation....196

5.9: Expression of CK1 Does Not Appear to be Regulated by Promoter Methylation....197

5.10: CK6 Expression Does Not Appear to be Regulated by Promoter Methylation....199

5.11: Expression of CK10 Does Not Appear to be Regulated by Promoter Methylation....203

5.12: IHC Staining with Pan Cytokeratin Antibodies and Individual CK Antibodies 205

5.13: Expression of p63 is Not Regulated by Promoter Methylation 206

A.1: Scatter Plots Comparing DNA Methylation in Cell Line Replicates 222

A.2: Scatter Plots Comparing DNA Methylation in Cell Line Replicates from the 5-Aza-2'-deoxycytidine Experiment 224

B.1: Serial Dilution to Determine Seeding Density for Adhesion Assay 228

B.2: Adhesion Assay Standard Curve with MCF-7 229

C.1: Variability in Initial Adhesion Assay Experiments 231

D.1: Adhesion of Adherent Cell Populations and Combined Cell Populations 235

CHAPTER 1

INTRODUCTION

Breast Cancer and Biology of the Breast

The breast is composed of glands or lobules, which are capable of producing milk, ducts that connect the milk-producing glands to the nipple, connective stromal and fat tissue. Breast cancer results from the uncontrolled growth of cells in the breast. Most breast cancers arise from cells in the lobules or ducts (Figure 1.1). Breast cancer has two general categories, *in situ (non-invasive)* and invasive. *In situ* cancers remain in the ducts or lobules while invasive cancers begin in a duct or lobule but spread into the surrounding normal tissue (Figure 1.2). Breast cancers can be further categorized by stage to indicate whether the cancer is located in one area of the breast or has spread to healthy tissue within the breast or other areas of the body.[1] Expression of hormone receptors is also used for classification and evaluation of therapeutic options.

According to the American Cancer Society, breast cancer is the most common type of cancer among women in the United States, excluding skin cancer.[2] Approximately one out of every eight American women will develop invasive breast cancer throughout their lifetime. Breast cancer is the second leading cause of cancer-related deaths among women. Roughly 290,000 women were estimated to be diagnosed with breast cancer in 2015. It was estimated that about 40,000 women would die of breast cancer in 2015.[2] The majority of breast cancer-related deaths occur due to metastasis to other sites within the body.[3] Only 5-10% of breast

cancers result from inherited genetic mutations in genes such as BRCA1 and BRCA2. Nearly 85% of breast cancers occur in women with no family history of the disease. These cancers occur as a result of accumulated genetic and/or epigenetic mutations acquired over the course of one's lifetime.[1]

Etiology of Breast Cancer

Breast cancer is a heterogeneous disease in which decisions about therapeutic options are often based on gene expression and histological profiles. Breast cancers can be classified into 4 subtypes, as reviewed by Eroles and colleagues.[4] The most common breast cancer subtype is Luminal A (73% of breast cancers).[5] These cancer cells have a gene expression signature similar to normal luminal epithelial cells that line mammary ducts (Figure 1.3).[4,6] They express estrogen receptor alpha (ER), progesterone receptor (PR), B-cell lymphoma 2 (Bcl-2) and cytokeratins CK8/18 and are epidermal growth factor receptor 2 (HER2) negative. Patients with Luminal A breast cancers have a better overall prognosis than those with other breast cancer subtypes.[4,5] Luminal B breast cancers which represent about 10% of breast cancers are more aggressive than luminal A and have a higher histological grade and proliferative index.[4,5] These breast cancers express ER and HER2 and have increased expression of proliferative genes. HER2 positive tumors have high or overexpression of HER2 and other genes in the HER2 pathway, along with overexpression of genes involved in proliferation.[4] Approximately 5% of breast cancers are HER2 positive.[5] Basal-like cancers have a gene expression signature similar to basal/myoepithelial cells, which line the mammary ducts.

These cancers express high molecular weight cytokeratins CK5 and CK17, P-cadherin, caveolin 1 and 2, nestin, CD44 and epidermal growth factor receptor (EGFR) and are usually ER- and PR-negative. Triple negative breast cancers lack expression of ER, PR and HER2 and some are also considered basal-like. Basal-like cancers have a worse prognosis than luminal cancers and make up roughly 12% of all breast cancers.[4,5]

The Hallmarks of Cancer

Hanahan and Weinberg first described six hallmarks of cancer cells in 2000.[7] The hallmarks are characteristics of cancer cells that allow for escape of normal cell function and malignant growth. They defined the six hallmarks as sustained proliferative signaling, escape of growth suppression, activation of invasion and metastasis, induction of angiogenesis, resistance of cell death and replicative immortality (Figure 1.4).[7] Cancer cells can employ a variety of different mechanisms in order to achieve these hallmarks, including dysregulation of normal cell signaling pathways and altered protein function. Researchers in the cancer field have therefore focused on understanding how cancer cells attain these hallmarks and developing novel therapeutic strategies to inhibit them. Hanahan and Weinberg have since modified their initial list of the hallmarks of cancer. In 2011, they added two emerging hallmarks; altered cell metabolism and evading immune surveillance. They also identified two enabling characteristics that facilitate and promote tumor growth: genomic instability/mutations and inflammation (Figure 1.4).[8] The research presented in this dissertation focuses on epigenetic alterations, which are

related to genomic instability, one of the enabling characteristics of cancer cells, and aspects related to two of the six hallmarks of cancer: sustaining growth and promoting invasion/metastasis. Specifically, the goal of this project is to investigate the role of epigenetic alterations in drug resistant breast cancer and determine the effects of inhibition of DNA methylation on proliferation, adhesion and migration in a drug resistant breast cancer cell line.

Epigenetics and DNA Methylation

Epigenetics is the study of heritable changes in gene expression that are not a result of changes in the underlying DNA sequence. [9-11] Epigenetic control of gene expression is important for regulating many different cellular processes including development, tissue-specific differentiation and X-chromosome inactivation. When epigenetic regulation is altered, it can lead to diseases including cancer.

Epigenetic mechanisms include DNA methylation and histone modifications, which alter chromatin structure and accessibility of DNA to regulate gene expression. [9,11] Chromosomes are made of condensed DNA called chromatin. Chromatin is composed of nucleosomes, which contain DNA wrapped around an octamer of four core histone proteins (H3, H4, H2A and H2B). [12] In normal cells, condensed chromatin is not transcriptionally active and has dense nucleosomes, DNA methylation and deacetylated histones, while transcribed regions of the genome have open nucleosome positioning, unmethylated DNA and acetylated histones (Figure 1.5). [13] As reviewed by Baylin and Jones, gene expression is regulated by a combination of DNA methylation, nucleosome positioning and

histone modifications which are controlled by the Polycomb group (PcG) complex.[14] DNA methylation occurs in DNA where a cytosine is followed by a guanine residue (CpG dinucleotides). Methyl groups from S-adenosylmethionine (SAM) are added to position 5 of cytosine by DNA methyltransferases (DNMTs) (Figure 1.6).[15-18]

Epigenetic alterations such as global hypomethylation, regional hypermethylation and chromatin remodeling are known to occur during carcinogenesis.[13] Specifically, aberrant DNA methylation is known to occur early in tumorigenesis[13,16] and is often seen in breast cancer.[16] Hypermethylation of CpG-rich regions of the genome approximately 1 kb in length (CpG islands)[19] clustered in the promoter region of genes can lead to suppression of gene expression and often silencing of tumor suppressors and transcription factors.[11,20,21] Because these epigenetic changes associated with breast cancer are thought to occur early during disease progression, they could potentially be used as biomarkers. Targeting DNA methylation could be an effective therapy for breast cancer because DNA methylation may be reversed by epigenetic therapies or dietary changes.[11,22]

Tamoxifen Resistance and DNA Methylation

Estrogen (17-Beta-estradiol or E2) signaling regulates cell proliferation and survival and is critical for many aspects of normal female physiology such as reproduction and behavior. E2 binds to ER and regulates ligand-activated genomic as well as non-genomic signaling pathways in normal and cancerous breast tissue. Approximately 70% of breast cancers are ER-positive and can therefore be treated with an anti-estrogen such as tamoxifen.[23] Tamoxifen is one of the drugs used as

endocrine therapy and it acts as a selective estrogen receptor modulator (SERM).[24] It works by competing with estrogen for binding to the ligand-binding domain of the ER. Binding of tamoxifen to ER induces a conformational change, which inactivates the AF-2 domain of ER resulting in receptor stabilization.[25] Although tamoxifen treatment has been successful at reducing breast cancer death rates, approximately one-third of women treated with tamoxifen for 5 years will have disease recurrence.[26] This initial response to therapy followed by disease progression is known as acquired resistance.[23] Therefore, it is imperative that researchers identify biomarkers that are predictive of acquired resistance. These biomarkers may also be utilized as novel therapeutic targets for tamoxifen-resistant breast cancers.

There are several mechanisms that lead to acquired resistance to endocrine therapies and disease recurrence. Acquired resistance can result from loss of ER expression, epigenetic modifications, expression of altered forms of ER, post-translational modifications of ER, increased activity of transcription factors along with deregulation of ER co-activators, increased signals from receptor tyrosine kinase signaling pathways, improper regulation of the cell cycle and apoptosis, mutations in the gene encoding ER, ESR1, altered drug metabolism and selection of pre-existing cancer initiating cells or cancer stem cells.[23,27,28] Cancer cells utilize these alterations to give themselves a survival advantage and continue to grow despite suppression of estrogen signaling.[29] Interestingly, DNA methylation is known to play a role in breast cancer[16] and has been shown to be involved in tamoxifen resistance as well.

Genome-wide hypomethylation occurs frequently in breast cancer. However, as reviewed by *Connolly and Stearns*,[30] certain breast cancer-related genes are known to be hypermethylated in tumor samples. Our lab as well as others have demonstrated that changes in DNA methylation across the genome occur in ER-positive, tamoxifen-resistant breast cancer cell lines.[25,27,31] However, the role of promoter methylation and regulation of gene expression is poorly understood in ER-negative, tamoxifen-resistant disease. The majority of cell-line models of tamoxifen resistance are ER-positive. This is indicative of recurrence patterns in patients, as the majority of recurrences from ER-positive tumors retain ER expression.[32,33] However, approximately 10-12% of local or metastatic recurrences from primary tumors lose expression of ER (Figure 1.7).[32,33] Patients with these ER-negative, recurrent tumors have limited treatment options. Tamoxifen is the main drug used to treat premenopausal women with ER-positive disease after surgery and radiation/chemotherapy.[34] ER-positive patients with disease progression are then treated with another ER antagonist, such as fulvestrant, or aromatase inhibitors.[34] However, these drugs will not benefit patients with ER-negative recurrent disease. If the recurrent disease is HER2-positive, anti-HER2 therapy may be utilized. The other options for patients with ER-negative recurrent disease are targeted therapies such as mTOR or PI3K inhibitors or other experimental treatments.[34] Hyperactivation of the PI3K/AKT/mTOR pathway has been shown to contribute to disease progression of ER-positive breast cancer and resistance to endocrine therapy.[35] Although there is a lack of biomarkers that predict benefit from treatment of advanced breast cancer with mTOR inhibitors, there is evidence

that PI3K/AKT/mTOR inhibition can improve the benefit of endocrine therapy in ER-positive breast cancer. However, due to the ability of cancer cells to compensate for alterations in signaling pathways, it is likely that tumors resistant to mTOR targeting will emerge.[36] Further studies are needed to determine whether PI3K/AKT/mTOR inhibitors should be used with existing endocrine therapy or inhibitors of upstream or downstream effectors and whether isoform-specific or pan-PI3K inhibition is better. There is also a need to develop new methods for identifying patients who are likely to respond to PI3K/AKT/mTOR inhibition by either molecular signatures of biomarkers or large-scale genomic screening. Therefore, additional targets are needed for treatment of advanced, endocrine resistant breast cancer. The goal of this project is to evaluate the role of DNA methylation in ER-negative, tamoxifen-resistant disease and the use of the DNMT1-inhibitor, 5-Aza-2'-deoxycytidine, as a potential epigenetic therapy for ER-negative recurrent disease.

Tamoxifen-Resistant Cell Line Model

This study focuses primarily on an ER-negative, tamoxifen-resistant cell line, TMX2-28. This cell line, and two other tamoxifen-resistant lines, were generated by culturing MCF-7 cells in the presence of Tamoxifen (10^{-6} M) for 6 months.[37] Cloning by limiting dilution lead to the discovery of three tamoxifen-resistant cell lines. Two of which retained expression of ERα, TMX2-4 and TMX2-11, and one that no longer expressed ERα, TMX2-28 (Figure 1.8). All three tamoxifen-resistant cell lines retain an epithelial-like phenotype, similar to the parental line, MCF-7. Previous work in

our lab demonstrated that TMX2-28 cells have a Ras Homolog Gene Family Member, A (RhoA)-dependent invasion mechanism and express S-phase kinase-associated protein 2 (SKP2), which targets the cyclin-dependent kinase (CDK) inhibitor p27 for degradation and facilitates cell cycle progression and increased proliferation.[38,39] Initial studies of genome-wide methylation with the HM450K BeadChip found over 33,000 hypermethylated CpG sites in TMX2-28 compared to the parental cell line, MCF-7. Specifically, promoter methylation is involved in regulating the expression of at least two genes in TMX2-28, zinc finger 350 (ZNF350) and melanoma antigen family D1 (MAGED1).[31] Promoter methylation of ZNF350 and MAGED1 decreased in response to treatment with the DNMT-inhibitor, 5-Aza-2'-deoxycytidine, and a corresponding increase in mRNA expression was observed for both genes. Unpublished data from our lab indicate that 5-Aza-2'-deoxycytidine decreases TMX2-28 cell proliferation. However, it is unclear how changes in methylation and gene expression induced by 5-Aza-2'-deoxycytidine affect the behavior of TMX2-28 cells.

Cell Proliferation, Adhesion and Migration

Sustaining proliferation, altering adhesion and promoting migration are some of the key characteristics of all cancer cells.[7,8] The majority of breast cancer deaths are caused by metastases.[3] Therefore, understanding what promotes the growth and migration of breast cancer cells is indispensable for developing new therapeutics. In tamoxifen-resistant disease, breast cancer cells have circumvented

estrogen signaling and rely on alterative signaling pathways to sustain malignant progression.

Growth signaling pathways such as the phosphatidylinositol 3-kinase (PI3K)/AKT and insulin-like growth factor 1 receptor (IGF1-R) are activated in anti-estrogen-resistant cell lines.[28,40] AKT phosphorylates effector proteins that are involved in cell survival, proliferation and metabolic signaling.[41] IGF signaling is known to regulate angiogenesis, proliferation, metastasis and apoptosis resistance. The two main pathways involved in IGF signaling are the mitogen-activated protein kinase (MAPK) and PI3K/AKT pathways.[42] Overexpression of IGF1-R has been implicated in cell culture models of antiestrogen resistance.[28] IGF1 promotes terminal end bud growth and extension of the ductal network in the normal breast and is important for mammary gland development. Anti-apoptotic signals are generated through IGF1-R signaling via the PI3K/AKT and RAS/MAPK pathways. IGF1R signaling also works to control cell cycle progression through the MAPK/ extracellular signal-related kinase (ERK) pathway. Although some tamoxifen- and aromatase-resistant cell culture and mouse tumor models express low levels of IGF1-R, protein phosphorylation remains high resulting in constitutive activation of signaling pathways.[43] Understanding how these signaling pathways work both on their own and collectively to facilitate disease progression will help identify new targets for the personalized treatment of breast cancer.

Another important aspect of disease progression is metastasis, or the spread of cancer to secondary sites throughout the body. Metastasis begins when tumor cells invade the local surrounding tissue. The cancer cells must then invade blood or

lymphatic vessels though a process known as intravasation. The blood stream or lymphatic vessels then transport the cancer cells to other areas of the body. If they succeed in exiting the vessel (extravasation) and establishing a new tumor at this secondary location, then the metastatic cascade is complete (Figure 1.9).[3,44]

Metastasis begins with growth of the primary tumor and invasion of the surrounding local tissue. This is accomplished by altering cell-cell adhesion and cell adhesion to the extracellular matrix (ECM). Cadherins are known to regulate cell-cell adhesion and are important for breast cancer metastasis.[3] Cell adhesion to the ECM is facilitated by integrins and is important for both invasion and extravasation.[3,44] Additionally, cancer cells can degrade the ECM with metalloproteinases (MMPs) and the urokinase plasminogen activator (uPA) system.[3] Various adhesion and signaling molecules are involved in facilitating extravasation. Ras-related C3 botulinum toxin substrate 1 (rho family, small GTP binding protein) (Rac1) and Rho associated coiled-coil containing protein kinase 1 (ROCK1) are involved in regulating the formation of stress fibers and regulating intracellular tension. ERK, SRC proto-oncogene, non-receptor tyrosine kinase (SRC) and PI3K signaling aids in loosening endothelial cell junctions. Then β1 integrin and focal adhesion kinase (FAK) signaling are important for establishing protrusions which help cancer cells invade the basement membrane surrounding the vasculature and ultimately establish a new tumor at the secondary site.[44] In addition to these mechanisms, cancer cells recruit and interact with host cells to facilitate metastasis. The release of cytokines and proteases from stromal cells can stimulate proliferation of cancer cells and metastasis. Mesenchymal stem cells

(MSCs) can be recruited to the tumor where they differentiate into fibroblasts. Host-derived, tumor-associated macrophages are important for migration and invasion as well as suppression of the immune system.[45] Therefore, it is also important to consider these aspects of the tumor microenvironment when developing therapies for preventing metastasis or targeting secondary tumors.

Tumor-Associated Calcium Signal Transducer 2 (TROP2)

TROP2 (trophoblast antigen protein 2 or tumor-associated calcium signal transducer 2) is a 35.7 kDa transmembrane protein encoded by the intronless gene *TACSTD2*.[46,47] TROP2 was first identified as a marker of trophoblast cells which are cells that invade the uterine wall during placental implantation.[48] TROP2 is closely related to Trop1 or epithelial cell adhesion molecule (Epcam). The two proteins have 49% sequence identity and 67% similarity, the greatest homology occurs in the transmembrane region and the thyroglobulin repeat domain.[49] TROP2 has a short cytoplasmic tail that is involved in intracellular signaling. The cytoplasmic tail of TROP2 can be phosphorylated by protein kinase c (PKC)[50] and also contains a phosphatidylinositol 4,5 bisphosphate (PIP_2) binding site.[51] The cytoplasmic tail is similar to a HIKE domain[52] and may be involved in binding pleckstrin homology domains such as those found in G-proteins, kinases, ankyrin and kinesin.[53] The HIKE domain similarity also indicates the potential role for TROP2 in calcium signaling as the calcium signaling molecule, Calmodulin, can bind HIKE domains in G-proteins.[53,54] Mutations in *TACSTD2* are known to cause the autosomal recessive disorder Gelatinous drop-like corneal dystrophy (GDLD) in humans, a disease causing corneal amyloidosis and ultimately blindness.[55]

As reviewed by McDougall [54] and others, TROP2 is known to regulate various aspects of lung and kidney development, and is also involved in intracellular signaling and expressed in many epithelial cancers. By binding to neuregulin 1 (NRG1), TROP2 can sequester NRG in the cytoplasm, therefore blocking release of NRG1 ectodomain and preventing ErbB3 signaling. [56] TROP2 can regulate focal adhesion dynamics by recruiting RACK1 to the membrane and binding β1 integrin, which increases FAK phosphorylation leading to increased cell motility and decreased adhesion. [57] When cleaved by regulated intramembrane proteolysis, the resulting intracellular TROP2 fragment can interact with β-catenin to promote transcription of Cyclin D1 and c-myc. [58] TROP2 has been shown to affect MAPK signaling by regulating ERK phosphorylation. [59-62] Activation of TROP2 can increase intracellular calcium concentrations. [63] This presumably occurs via the predicted PIP_2 binding site in the cytoplasmic tail of TROP2. Hydrolysis of PIP_2 yields diacylglycerol (DAG) and inositol 1,4,5-triphosphate (IP3). DAG can then activate the PKC and MAPK pathways, while IP3 binds to its receptor on the endoplasmic reticulum, which causes calcium to be released from intracellular stores. [54] TROP2 may be involved in promoting tumor growth and metastasis, [54] however TROP2 seems to have the opposite effect in lung cancer as expression of TROP2 inhibits tumor growth.[61]

Interestingly, *Lin and colleagues* [61] found that *TACSTD2* expression is regulated by promoter methylation in lung cancer cell lines and lung adenocarcinoma tissues. Low TROP2 mRNA expression was observed along with hypermethylation of the *TACSTD2* promoter. Normal tissues had high TROP2

expression, while tumor tissues had promoter methylation and low TROP2 expression. Furthermore, treatment of CL1-0 and A549 cell lines with the DNMT inhibitor, 5-aza-2'-deoxycytidine, decreased methylation and restored TROP2 mRNA and protein expression. Forced *TACSTD2* expression in lung cancer cell lines inhibits proliferation and colony formation and blocks phosphorylation of AKT and ERK. Knockdown of *TACSTD2* increases proliferation, colony formation and phosphorylation of AKT and ERK. Additionally, *TACSTD2* knockdown increases tumor volume in a mouse xenograft model. The authors also found that TROP2 interacts directly with IGF-1. The region between the EGF-like and thyroglobulin type-1 domain of TROP2 mediated this interaction. Overexpression of Trop2 inhibits IGF-1R signaling by blocking phosphorylation of AKT and decreasing β-catenin expression. They conclude that silencing of *TACSTD2* expression in lung cancer results in increased IGF-1R signaling, activation of AKT and ERK and increased expression of β-catenin and Slug, which contribute to tumor invasion, metastasis and angiogenesis.[61]

Although TROP2 seems to suppress tumor growth in lung cancer, it has been found to promote the growth of other types of cancer. TROP2 mRNA has been found in normal tissues including breast, cervix, endometrium, oesophagus, fallopian tubes, kidney, pancreas, placenta, prostate, respiratory tract, salivary glands, seminal vesicles, stomach, tonsils, thymus and vagina.[64] Increased TROP2 expression in tumor tissue compared to normal tissue has been found in lung, breast, stomach, pancreas, liver, kidney, colorectal and ovarian cancers.[64] In breast cancer, membrane localization of TROP2 is correlated with a poor prognosis while

intracellular TROP2 is associated with increased survival.[65] However, it is not known whether TROP2 expression is regulated by promoter methylation in breast cancer and the role of TROP2 in tamoxifen resistance is not clear. Therefore, another objective of this project is to evaluate the role of TROP2 in tamoxifen resistance.

(A) **(B)** **(C)**

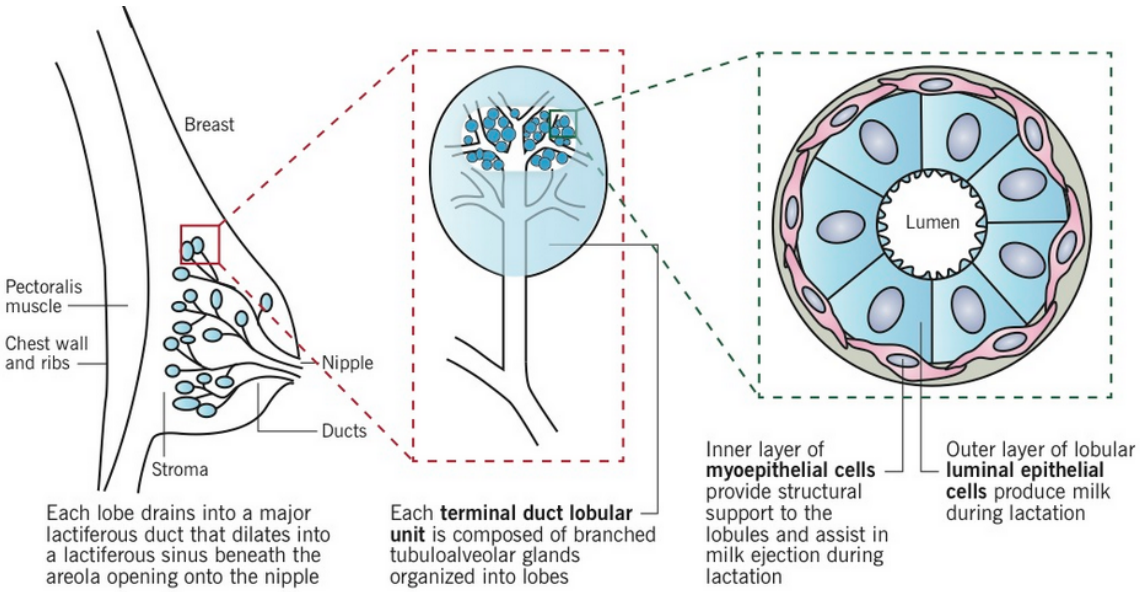

Figure 1.1: Normal Breast Anatomy. Profile of normal breast (A). Structure of terminal duct lobular unit where milk is produced (B). Cross section of breast duct showing myoepithelia/basal cells and luminal epithelial cells (C). Image from http://www.pathophys.org/breast-cancer/.[6]

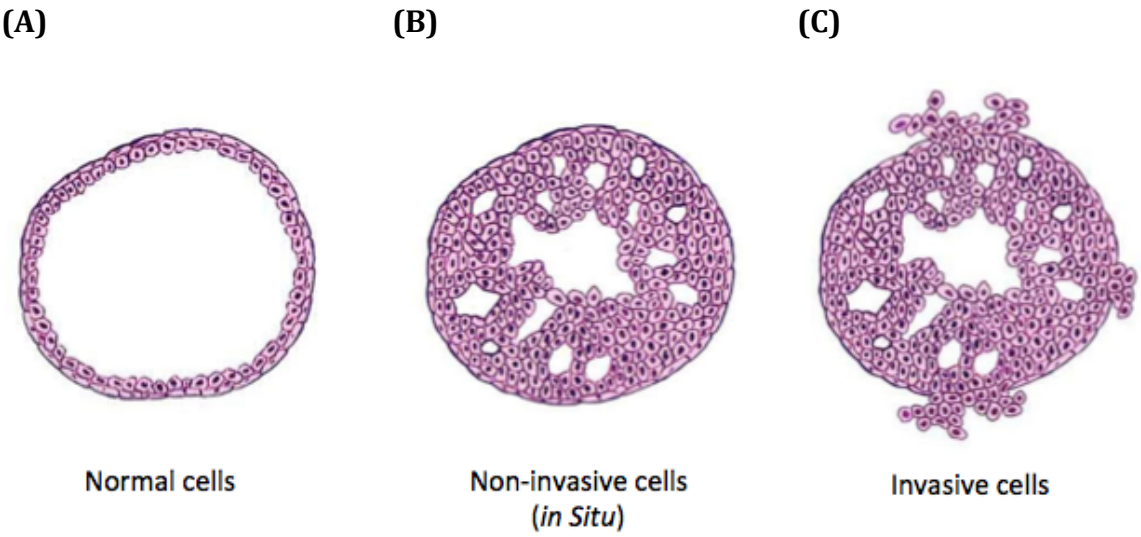

Figure 1.2: Two General Types of Breast Cancer. Cross section of duct with normal cells (A), non-invasive cancer cells (B) contained within the duct and invasive cancer cells (C) that have spread into the surrounding normal tissue. Images from http://www.breastcancer.org/symptoms/diagnosis/invasive.[1]

(A)

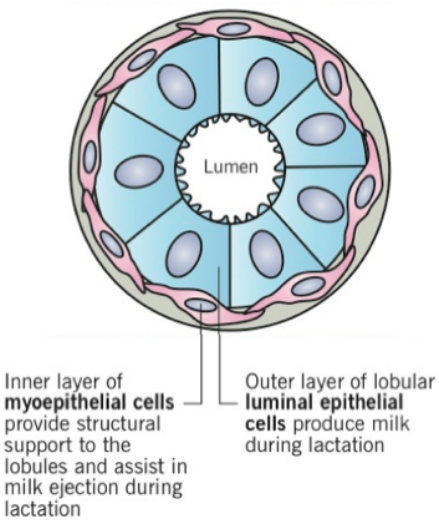

(B)

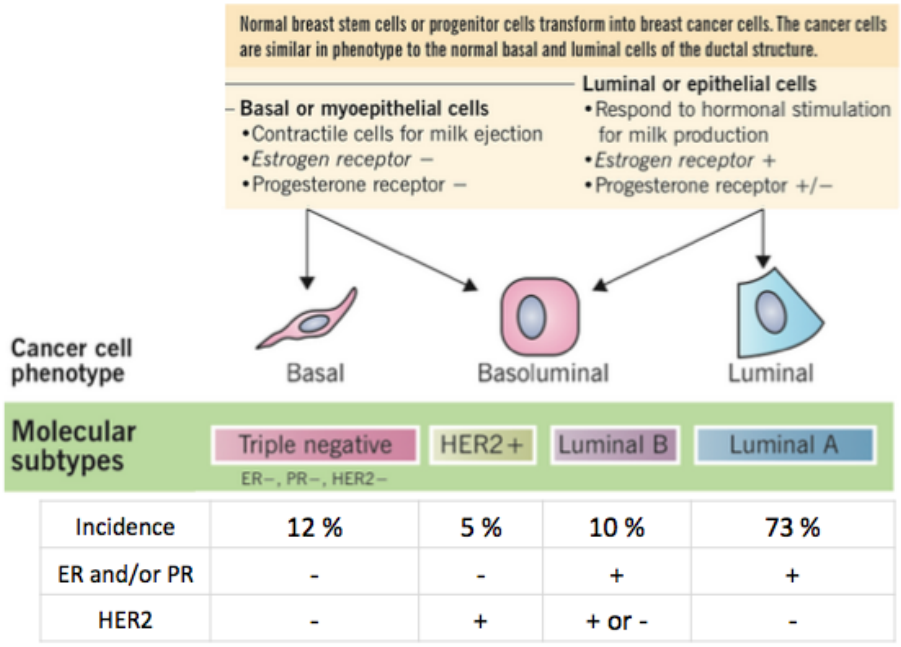

Incidence	12 %	5 %	10 %	73 %
ER and/or PR	-	-	+	+
HER2	-	+	+ or -	-

(Figure 1.3)

Figure1.3: Basal Verses Luminal Breast Cancers. Cross sectional view of mammary duct showing location of luminal epithelial and myoepithelial cells (A). Summary of molecular subtypes of breast cancer and the cells from which they originate. Incidences of molecular subtypes, hormone receptor expression (estrogen receptor (ER) and progesterone receptor (PR) and human epidermal growth factor receptor (HER2) status based on general U.S. populations in 2010 from the NCI SEER Database and adapted from[5] (B). Modified from http://www.pathophys.org/breast-cancer/.[6]

(A)

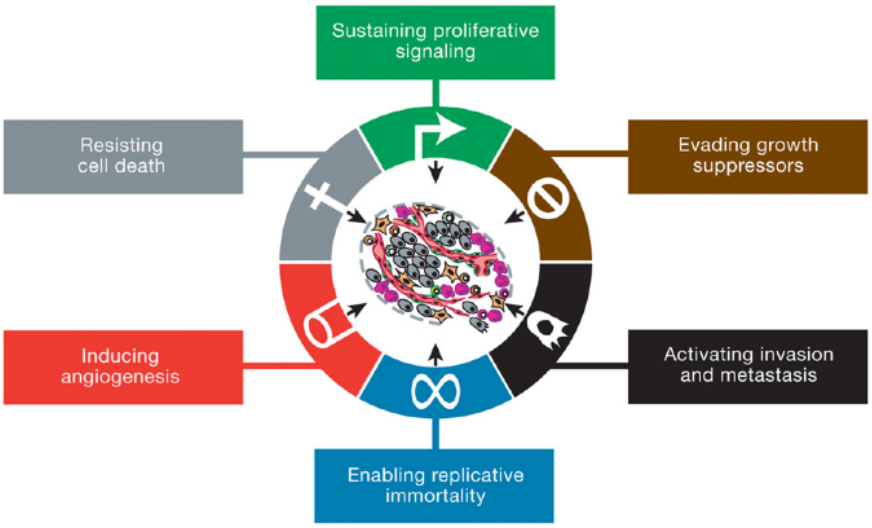

(B)

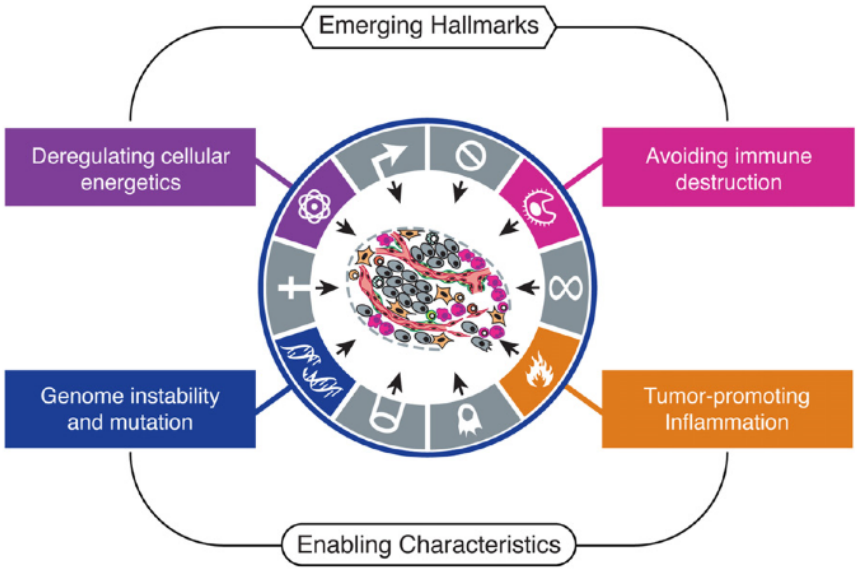

Figure 1.4: The Hallmarks of Cancer. The six original Hallmarks of Cancer as defined by Hanahan Weinberg in 2000 (A). Two additional hallmarks and two enabling characteristics of cancer cells as defined by Hanahan and Weinberg in 2011 (B). Images from *Hanahan and Weinberg. Cell. 2011.*[8]

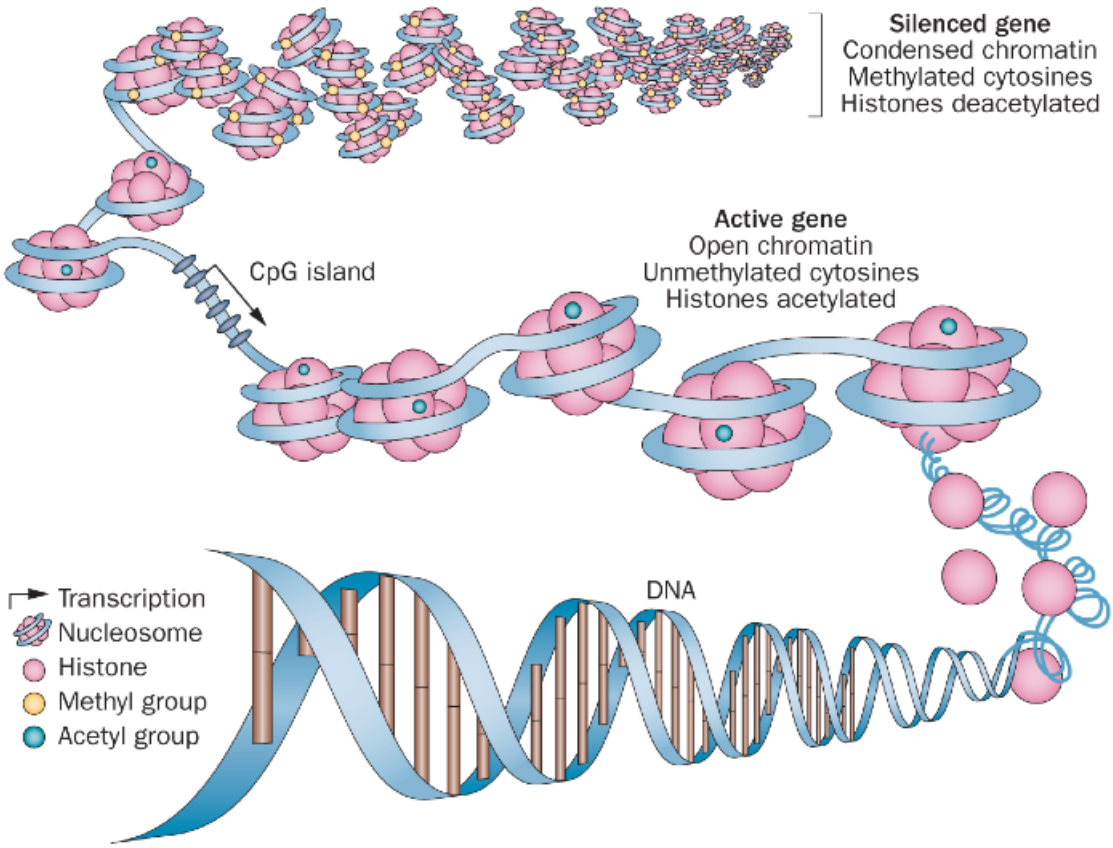

Figure 1.5: Chromatin Structure and Epigenetics in Normal Cells. In normal cells, untranscribed regions of the genome have condensed chromatin (heterochromatin) with tightly packed nucleosomes, methylated CpG sites and deacetylated histones. Transcribed regions of the genome (euchromatin) are characterized by open nucleosome positioning with unmethylated CpG sites and acetylated histones. Image from *Azad et al. 2013*.[13]

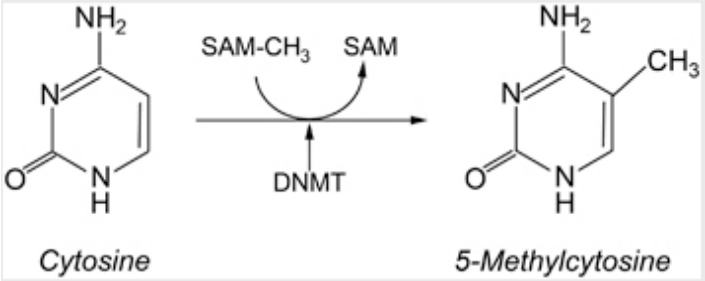

Figure 1.6: DNA Methyltransferase (DNMT) Converts Cytosine to 5-Methylcytosine. DNMT catalyzes the conversion of cytosine to 5-methylcytosine by transferring a methyl group (CH_3) from S-adenosylmethionine (SAM) to the 5-carbon position of cytosine. Figure from of *Gibney and Nolan 2010*.[18]

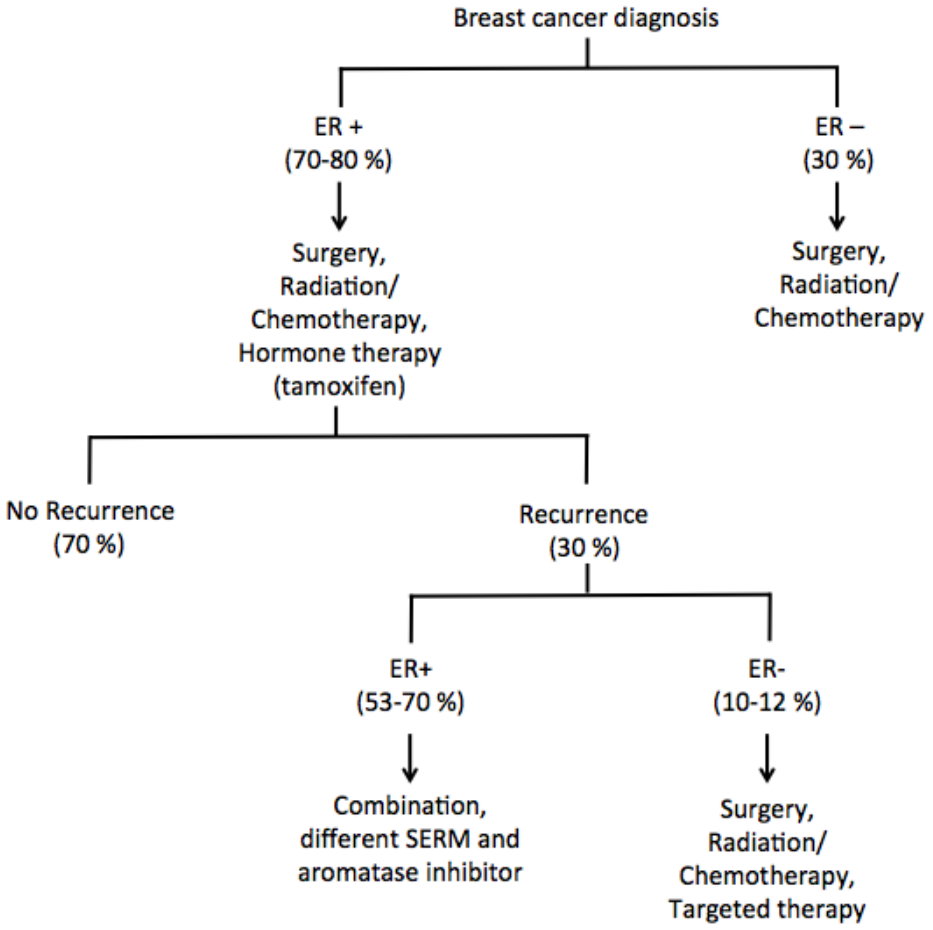

Figure 1.7: Treatment of Recurrent Breast Cancer. Flow chart depicting treatment of recurrent breast cancer with approximate percentages of cases indicated in parentheses. (ER+: ER-positive, ER-: ER-negative, SERM: selective estrogen receptor modulator). Information summarized from [24,28,29,32,33].

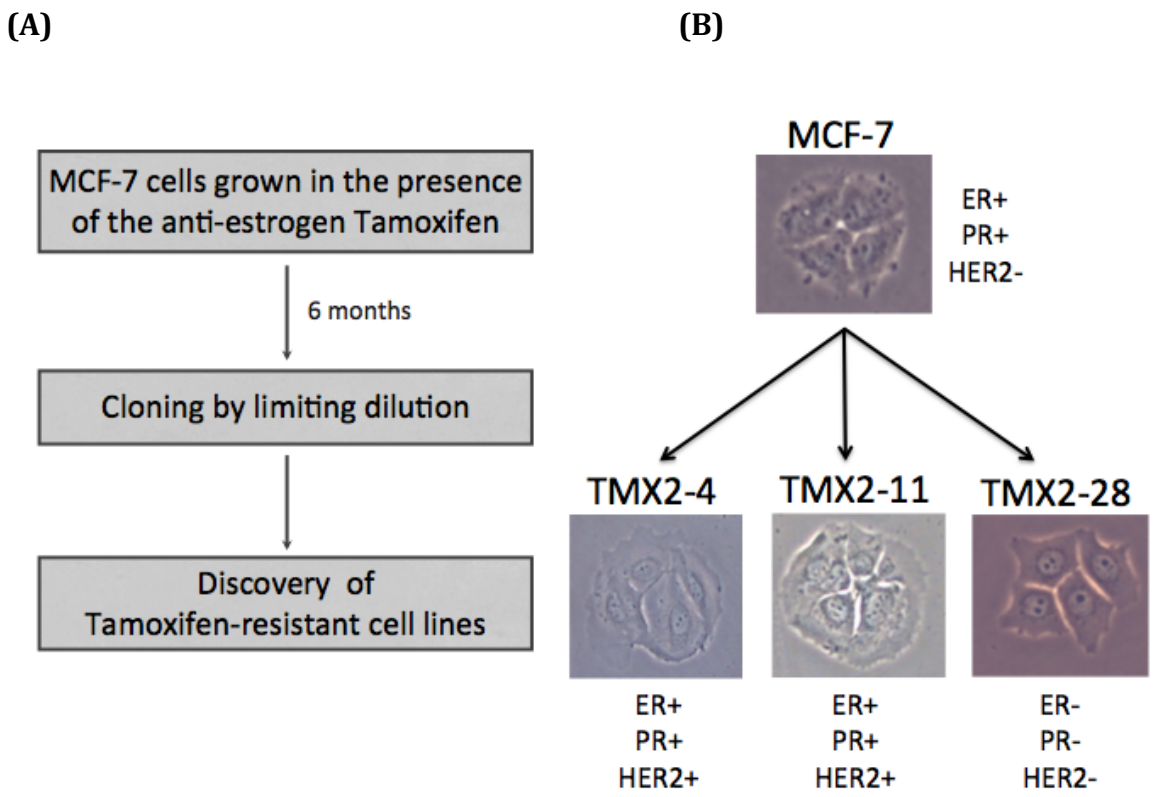

Figure 1.8: Development of Tamoxifen-Resistant Cell Lines. Schematic of Tamoxifen selection (A) (adapted from[37]). Estrogen receptor (ER), progesterone receptor (PR) and human epidermal growth factor receptor-2 (HER-2) status for the parental line, MCF-7, and the three tamoxifen-resistant lines, TMX2-4, TMX2-11 and TMX2-28 (B) (positive: +, negative: -).

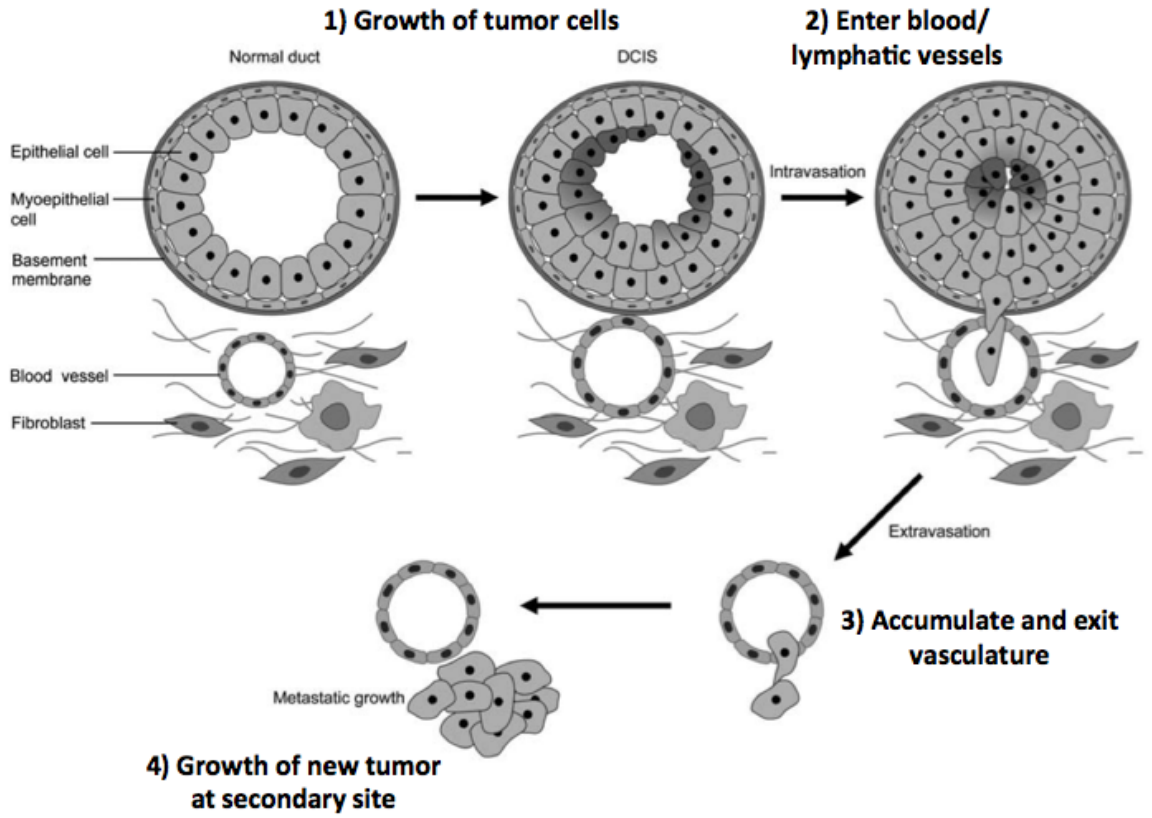

Figure 1.9: Summary of Metastatic Cascade in Breast Cancer. Summary of the major steps involved in the metastatic cascade of breast cancer. First, cancer cells proliferate and invade local surrounding tissue and eventually enter the blood of lymphatic system (intravasation). If the tumor cells survive in the vasculature and accumulate, they may eventually exit the vasculature (extravasation) and establish a new tumor at secondary site. Figure modified from *Scully et al. 2012*.[3]

CHAPTER 2

DNA METHYLATION ANLYSIS

Introduction

Aberrant DNA methylation is known to occur early during tumorigenesis and is often seen in breast cancer. Methyl groups are added to the cytosines of CpG dinucleotides by DNA methyltransferases (DNMTs).[16] CpG-rich regions of the genome that are approximately 1kb in length are known as CpG islands.[19] Although global hypomethylation is characteristic of cancer cells and genomic instability, methylation of CpG islands is frequently observed in cancer. Hypermethylation of CpG islands clustered in the promoter region of genes leads to suppression of gene expression and often silencing of tumor suppressors and transcription factors.[21] Because these epigenetic changes associated with breast cancer are thought to occur early during disease progression, they could potentially be used as biomarkers. Targeting DNA methylation could be an effective therapy for breast cancer because DNA methylation may be reversed by epigenetic therapies or dietary changes. However, it will be necessary to identify the patients who are likely to benefit from epigenetic therapy in order to minimize off-target effects.

Treatment with the DNMT1 inhibitor, 5-Aza-2'-deoxycytidine, decreases methylation and is known to restore expression of genes that are hypermethylated in cancer.[66-69] Upon incorporation into DNA, 5-Aza-2'-deoxycytidine binds covalently with DNMT1 (forming an irreversible intermediate), which leads to enzyme degradation, loss of methylation with subsequent cell divisions and re-

expression of genes silenced by promoter methylation (Figure 2.1).[70,71] Treatment with 5-aza-2'-deoxycytidine is an effective epigenetic therapy for myelodysplastic syndrome (MDS).[72] Currently, it is being evaluated as a possible treatment for solid tumors. However, it is not known whether 5-aza-2'-deoxycytidine treatment would be an effective therapy for ER-negative, recurrent breast cancer. Therefore, I will examine the effect of 5-Aza-2'-deoxycytidine on methylation in the ER-negative, tamoxifen-resistant cell line, TMX2-28, and determine the role of promoter methylation in regulation of gene expression and cell behavior.

Endocrine resistance causes changes in gene expression in various signaling pathways including estrogen receptor (ER), growth factor, cytoplasmic, cell cycle, apoptosis and cell survival signaling.[23] Aberrant DNA methylation is known to be an early event during tumorigenesis and occurs frequently in breast cancer.[13,16] Several studies involving endocrine resistance and DNA methylation use ER-positive, tamoxifen-resistant cell line models. Changes in DNA methylation across the genome have been observed in ER-positive, tamoxifen-resistant breast cancer cell lines.[25,27,31] Gene-specific differences in DNA methylation have been shown to correlate with changes in mRNA expression in other ER-positive, tamoxifen-resistant lines.[73] However, there is little information on the role of methylation in the development of ER-negative, acquired tamoxifen resistance. These patients have limited treatment options available upon disease recurrence and could possibly benefit from epigenetic therapy.

According to *Lin et al. 2013*, there are three methods for the development of tamoxifen resistance. The first is that ER-positive cells acquire epigenetic

alterations, which result in changes in mRNA expression of genes important for estrogen-dependent growth. Second, tamoxifen treatment results in the selection of pre-existing cancer initiating cells/cancer stem cells. The third mechanism is a combination of the two mechanisms. Modified DNA methylation-specific digital karyotyping (MMSDK) and digital gene expression (DGE) combined with next-generation parallel sequencing was used to compare DNA methylation and gene expression profiles of parental and MCF-7-derived, ER-positive tamoxifen-resistant cell lines. Two different resistant cell models were used. Both were treated with 4-hydroxy tamoxifen but in different methods. The TAM^R cell lines were grown in the presence of 1μM tamoxifen and the LCC1/LCC2 cells were cultured in media with increasing doses of tamoxifen. Differences in global methylation (all CpG sites interrogated) and global gene expression were observed between the parental cell line and the TAM^R cell lines. Overall, the TAM^R cell lines had higher methylation than MCF-7. In general, the authors conclude that DNA methylation in the promoter region is associated with decreased gene expression. Some of the genes identified in their analyses with high expression in the TAM^R cell lines were associated with pluripotency and differentiation, such as SOX2. Therefore, the authors conclude that stem cell-like cells and cancer-initiating cells may play a role in ER-positive, acquired tamoxifen resistance.[27]

In an earlier study, Fan and colleagues examined DNA methylation and gene expression in tamoxifen- and fulvestrant-resistant clones of MCF-7 cells. Tamoxifen- and fulvestrant-resistant cell lines were derived from a clone of MCF-7 cells, stably transfected with an ERα-responsive luciferase reporter and exposed to

4-hydroxytamoxifen or Fulvestrant for 12 months. MCF-7-T (tamoxifen-resistant) cells expressed ERα protein at a higher level than MCF-7 cells. MCF-7-F (fulvestrant-resistant) cells had a 90% decrease in ERα protein compared to MCF-7 cells. The authors examined gene expression using the Affymetrix Human Genome U133 Plus 2.0 Array and DNA methylation using a custom 60-mer oligonucleotide microarray covering approximately 44,000 CpG-rich fragments and 12,000 promoters. They found that activation of genes that promote cell growth was correlated with promoter hypomethylation in the antiestrogen-resistant line more frequently than inactivation of genes due to hypermethylation. Gene expression in the tamoxifen-resistant line and the parental cell line was more similar than gene expression in the fulvestrant-resistant and parental cell line. Genes in the EGFR/ErbB2 pathway were involved in regulating cell growth in both the MCF-7-T and MCF-7-F cell lines. Altered signaling pathways in MCF-7-T included PKA, caveolins, annexins, S100 calcium binding proteins, MAPK phosphatases and inhibitors of differentiation. Activation of β-catenin was important in the fulvestrant-resistant cell line. In contrast to results from our lab and results from other labs, activation of genes due to promoter hypomethylation was more common in these antiestrogen-resistant cell lines than inactivation due to promoter hypermethylation.[25]

Interestingly, *Stone et al. 2012* found that tamoxifen treatment caused promoter methylation and silencing of estrogen-responsive genes in another ER-positive cell line models of tamoxifen resistance. MCF-7 cells were treated with 4-hydroxytamoxifen (1×10^{-7} M) for 10 months and then withdrawn from tamoxifen

(grown in tamoxifen-free media for up to 6 months). The TAM-R cells still expressed ER protein, but had reduced protein expression levels. Withdraw from tamoxifen restored expression of ER, but the cells were still resistant to tamoxifen. Increased promoter methylation was observed for pS2 and PR in the resistant and withdrawn cells. Combined treatment of 5-Azacytidine with 17-Beta-estradiol (E2) decreases methylation and restores gene expression of pS2 and PR. The authors found that combined 5-Azacytidine (analog that is incorporated into DNA and RNA) treatment with E2 inhibits proliferation in the withdrawn cells. The authors conclude that tamoxifen exposure causes silencing of estrogen-responsive genes via increased promoter methylation. These genes normally function to inhibit proliferation and reactivation of these genes with 5-Azacytidine could be a potential therapeutic for tamoxifen-resistant breast cancer.[73]

Prior studies in our lab have shown that ER-negative, TMX2-28 cells have increased DNA methylation compared to the parental line, MCF-7. The Illumina Human Methylation 450 BeadChip was used to examine differences in DNA methylation between two tamoxifen-resistant cell lines, TMX2-11 (ER-positive) and TMX2-28 (ER-negative), and the parental cell line, MCF-7. The ER-negative, TMX2-28 cell line had more hypermethylated CpG sites compared to the parental cell line than TMX2-11. Treatment with 5-Aza-2'-deoxycytidine decreased promoter methylation of two genes, MAGED1 and ZNF350, which were hypermethylated in both TMX2-11 and TMX2-28. Promoter methylation seems to regulate expression of MAGED1 and ZNF350 in TMX2-28, as 5-Aza-2'-deoxycytidine treatment increased mRNA expression in this cell line.[31] However, little is known about the relationship

between DNA methylation, regulation of gene expression and disease progression in this model of acquired Tamoxifen-resistance. Therefore, I will examine the effect of 5-Aza-2'-deoxycytidine on methylation in the ER-negative, tamoxifen-resistant cell line, TMX2-28, using the Human Methylation 450 BeadChip. I will also investigate the role of promoter methylation in regulation of gene expression and cell behavior by determining the effect of treating cells with the methylation inhibitor, 5-Aza-2'-deoxycytidine, on cell proliferation, adhesion and migration.

Materials and Methods

Cell culture: MCF-7 cells were purchased from the American Type Culture Collection (ATCC). TMX2-4, TMX2-11 and TMX2-28 cells were provided by John Gierthy (Wadsworth Center Albany, NY). Cells were grown in Dulbecco's modified eagle medium (without phenol red). Medium was supplemented with 5% cosmic calf serum (Hyclone Cat. No. SH30087.03), 2.0 mM of L-glutamine, 0.1 mM of nonessential amino acids and 250 ng/mL of insulin. Cells were maintained at 37°C, 5% CO_2 in a humidified incubator and passaged at subconfluence or media exchanged every 2 days.

5-Aza-2'-deoxycytidine Treatment: Cells were seeded into 6-well plates and allowed to adhere overnight at 37°C, 5% CO_2. Cells were treated with either 0.1% DMSO (vehicle control) or 2.5 μM 5-Aza-2'-deoxycytidine (Aza or 5-Aza-CdR) (Sigma-Aldrich Cat. No. A3656) in 0.1% DMSO for 96 hours, with media exchanged every other day.

DNA and RNA Isolation: DNA was isolated with the QIAamp DNA Mini Kit (Qiagen Cat. No. 51304) as per manufacturer instructions and protocols described previously.[74,75] RNA was isolated using TriReagent (Molecular Research Center, Inc. Cat. No. TR118). Purified DNA and RNA were quantified using a NanoDrop 8000 (Thermo Scientific).

Illumina Human Methylation 450 BeadChip: DNA samples from control and Aza-treated MCF-7, TMX2-4, TMX2-11 and TMX2-28 cells were sent to the University of Southern California for HM450 BeadChip (Illumina Cat. No. WG-314-1003) analysis. Briefly, DNA was quantified using an Alu PCR reaction and bisulfite-treated. Bisulfite-treated DNA was then quantified by additional PCR reactions prior to running on the array. Then the DNA was enzymatically fragmented at 37 °C for 1 hour and precipitated in 100% 2-propanol at 4 °C for 30 min. followed by centrifugation at 3000 × g at 4 °C for 20 min. After resuspension in hybridization buffer of dried pellets, samples were incubated at 48 °C for 1 hour followed by 95 °C for 20 min. after which the samples were loaded onto the HM450 BeadChip and incubated at 48 °C for 16-24 hours. After hybridization of DNA to the primers on the BeadChip, wash buffers were used to remove non-specific and unhybridized DNA. A single-base extension of the hybridized primers was then conducted using labeled nucleotides and the BeadChip was stained with Cy-3 and Cy-5 fluorescent dyes. The BeadChip was then read using the Illumina iScan Reader. Illumina GenomeStudio was then used to analyze the image data to determine the efficiency of the reaction. The ratio of the fluorescent signals of methylated to unmethylated sites (beta values) was used to calculate the methylation of interrogated CpG loci.

The HM450 BeadChip includes 485,764 cytosine sites across the human genome and is enriched for gene promoters (482,421 of the sites are CpG sites and 3,343 are CNG sites).[76] The functional distribution, as defined by Illumina, of the sites is as follows: 200,339 sites are located in the promoter (within 200-1500 bp upstream of the transcription start site, 5'-UTR or exon 1), 15,383 are in the 3'-UTR, 150,212 are in the gene body and 119,830 sites are intergenic. When considering the CpG content or neighborhood distribution of sites, 150,254 are located in a CpG island, 112,072 and 47,161 are located in CpG shores and shelves, respectively and the remaining 176,277 are isolated CpG's in the "open sea." The majority of sites on the HM450 BeadChip, 361,766, are located in genes that encode RNA transcripts. While 4,168 sites are non-coding and 119,830 are intergenic (Figure 2.2).

mRNA Expression Array: RNA was isolated from two biological replicates of MCF-7 and TMX2-28 cells (cultured under normal conditions without Aza) as described above. The total quantity of RNA sent to the Troester Lab at the University of North Carolina Chapel Hill ranged from 3.7 – 6.8 μg. Samples were run on the Agilent 4x44k V2 Microarray with 2-color, low input quick amp labeling kit (Agilent). Collaborators at the University of North Carolina Chapel Hill conducted preliminary data analysis.

Data Analysis: The methylation data obtained from the HM450 BeadChip was analyzed using Genome Studio Methylation Module (v.1.9.0). Detection p-values of < 0.01 were used to select statistically significant CpG site data. Figures were made in either Microsoft Excel or PowerPoint for Mac 2011. Statistical

analysis was conducted using the SatPlus application (v. 5.8.2.0). RT-PCR data was analyzed using an un-paired Student t test (StatPlus for Mac v. 5.8.2.0).

Two-Step Reverse Transcriptase PCR (RT-PCR): Changes in gene expression after treatment with 5-Aza-2'-deoxycytidine were confirmed by two-step RT-PCR. RNA was reverse transcribed using the High-Capacity cDNA Reverse Transcription Kit (Applied Biosytems) supplemented with the RNase Inhibitor, RNasin (Promega). cDNA was then quantified using a NanoDrop 8000 (Thermo Scientific) and diluted to 50 ng/μL. Primers for RT-PCR were designed to span an exon-exon junction using Primer-BLAST (NIH) (Table 2.1). RT-PCR was conducted using the FastStart Universal SYBR Green Master (with Rox Reference Dye) (Roche) on the Stratagene MxPro (Mx3005P, Agilent). Relative mRNA expression will be quantified using the Standard Curve Method normalized to beta-actin or by comparison of cycle thresholds.

Results

5-Aza-2'-deoxycytidine Alters Global DNA Methylation

Previous studies in cell line models have indicated that DNA methylation may be involved in tamoxifen resistance.[25,27,73] However, the majority of these studies involve ER-positive, tamoxifen-resistant cell lines and little is known about the role of DNA methylation in ER-negative, acquired tamoxifen resistance. Using the HM450 BeadChip, our lab found global differences (among the CpG sites included on the HM450 BeadChip) in DNA methylation between tamoxifen-resistant cell lines compared to the parental cell line, MCF-7.[31] DNA methylation in the ER-negative,

tamoxifen-resistant cell line, TMX2-28, differed the most from the parental cell line, MCF-7. Overall, TMX2-28 is hypermethylated compared to the parental cell line. However, it is not known how the DNMT1 inhibitor, 5-Aza-2' -deoxycytidine, affects global methylation in MCF-7 or the tamoxifen-resistant cell lines.

To examine the effect of 5-Aza-2'-deoxycytine treatment on DNA methylation in the parental cell line, MCF-7, and the three tamoxifen-resistant cell lines were treated with 2.5 μM 5-Aza-2'-deoxycytidine or vehicle control for 96 hours. DNA was isolated and sent to the University of Southern California for HM450 analysis. The data were analyzed using Illumina Genome Studio software. First, global DNA methylation (among the CpG sites included on the HM450 BeadChip) in each tamoxifen-resistant cell line (vehicle control-treated sample) was compared to the parental cell line, MCF-7 vehicle control. In agreement with previously published data, [31] the ER-negative cell line, TMX2-28, displayed the greatest difference in DNA methylation from MCF-7 and had a large number of hypomethylated CpG sites (Figure 2.3). This confirmed previous findings from a single experiment in our lab. Comparing TMX2-28-Control to MCF-7-Control and filtering beta values to include those greater than or equal to 0.1 and a fold-change greater than or equal to 1.8, there are 37,501 (8%) CpG sites hypermethylated in TMX2-28, 14,956 (3%) CpG sites are hypomethylated and 432,294 (89%) are the same between the two cell lines (Table 2.2).

To determine the changes in methylation induced by 5-Aza-2'-deoxycytine treatment for each cell line, beta values for 96-hour 5-Aza-2'-deoxycytine treated cells were compared to those for vehicle control treated samples for each cell line.

Treatment with 5-Aza-2'-deoxycytidine affects global methylation in all four cell lines (Figure 2.4). The ER-negative cell line, TMX2-28, has the greatest change in DNA methylation in response to the DNMT1 inhibitor. A large number of CpG sites are hypomethylated in TMX2-28 while there is little change in methylation in MCF-7 treated with Aza. Using the same criteria described above to compare TMX2-28-Aza to TMX2-28-Control, 59 (0.01%) CpG sites are hypermethylated, 6,637 (1%) CpG sites are hypomethylated and 478,145 (99%) are unchanged (Table 2.3).

Top 5 Genes With Decreased Methylation in TMX2-28 After 5-Aza-2'-deoxycytidine Treatment

To determine the top CpG sites in TMX2-28 that were demethylated upon 5-Aza-2'-deoxycytidine treatment, beta values in TMX2-28-Control and TMX2-28-Aza ≥ 0.1 with detection p-value ≤ 0.01 were filtered by negative fold change ≥ 1.8 (average beta value of TMX2-28-Control over average beta value of TMX2-28-Aza). There are 6,637 CpG sites with decreased methylation in TMX2-28 after 5-Aza-2'-deoxycytidine treatment (Table 2.3). The genes containing CpG sites with the greatest fold change are NADH dehydrogenase (ubiquinone) iron-sulfur protein 6, mitochondrial (NDUFS6), chromosome 21 open reading frame 91 (C21orf91), mitogen-activated protein kinase 8 interacting protein 3 (MAPK8IP3), chromosome 1 open reading frame 115 (C1orf115) and chromosome 1 open reading frame 31 (C1orf31) (Table 2.4). However, most of these single CpG sites were either located in the gene body where the relationship between methylation and gene expression is less direct or in open reading frames not a gene coding region. Therefore, further

analysis was necessary to determine genes with more than one CpG site in the promoter region, which were demethylated upon 5-Aza-2'-deoxycytidine treatment in TMX2-28. Demethylation of CpG sites in the promoter region is likely to have an effect on gene translation.

Top 7 Genes With More Than One CpG Site in the Promoter Region With Decreased Methylation in TMX2-28 After 5-Aza-2'-deoxycytidine Treatment

To better identify decreases in methylation induced by 5-Aza-2'-deoxycytidine that are likely to affect gene expression, the same filtering criteria described in the previous section but only genes with more than one differentially methylated CpG site in the promoter region were included. The top seven genes that contain more than one CpG with decreased methylation after 5-Aza-2'-deoxycytidine treatment are chromosome 1 open reading frame 31 (C1orf31), mitogen-activated protein kinase 15 (MAPK15), HtrA serine peptidase 1 (HTRA1), zinc finger protein (ZNF677), NK6 homeobox 2(NKX6-2), delta-like 1 homolog (DLK1) and trophoblast antigen protein 2 or tumor-associated calcium signal transducer 2 (*TACSTD2*) (Table 2.5). To identify a set of genes with decreased promoter methylation and changes in gene expression, this list was compared with data from the mRNA expression array comparing MCF-7 to TMX2-28.

Genes Likely Re-expressed in TMX2-28 by 5-Aza-2'-deoxycytidine Treatment

Because I want to identify genes that are regulated by promoter methylation that are likely re-expressed by 5-Aza-2'-deoxycytidine, data from the mRNA

expression array comparing MCF-7 to TMX2-28 was also examined. If promoter methylation is regulating expression of a gene in TMX2-28, I predict that gene expression would be decreased in TMX2-28 compared to the parental cell line, MCF-7, because global methylation is higher in TMX2-28 (Figure 2.3 and Table 2.2). According to the analysis of the mRNA expression array, there are 2,414 genes with decreased mRNA expression in TMX2-28 compared to MCF-7 (Table 2.6). Using the criteria above for CpG sites with decreased methylation after 5-Aza-2'-deoxycytidine treatment in TMX2-28, I identified genes that have lower expression in TMX2-28 compared to MCF-7 and that have decreased methylation in TMX2-28 after 5-Aza-2'-deoxycytidine treatment. There are 6,637 CpG sites that are hypomethylated in TMX2-28 after treatment with 5-Aza-2'-deoxycytidine. However, some of these decreases in methylation occur in areas outside the promoter region. The genes with decreased expression in TMX2-28 compared to MCF-7 and decreased methylation in TMX2-28 after 5-Aza-2'-deoxycytidine treatment are listed in Table 2.8. Because this analysis identified genes with demethylation in areas other than the promoter, I decided to revise our analysis to better identify genes whose expression could be regulated by methylation in the promoter region and are affected by treatment with 5-Aza-2'-deoxycytidine. I predict genes which have low expression in TMX2-28 compared to MCF-7 and have CpG sites in the promoter region that are demethylated by 5-Aza-2'-deoxycytidine may be more likely to be re-expressed in TMX2-28 after 5-Aza-2'-deoxycytidine treatment.

Genes With Differential Methylation in the Promoter Region and Demethylated by 5-Aza-2'-deoxycytidine

To better identify genes possibly regulated by promoter methylation, I examined CpG sites that were differentially methylated in the promoter region in TMX2-28 compared to MCF-7 and demethylated by 5-Aza-2'-deoxycytidine. I filtered the HM450 data, using the same criteria described above, to include CpG sites with an average β-value greater than or equal to 0.1, a fold-change greater than or equal to 1.8 and a detection p-value less than 0.01 (Table 2.2). Using these criteria to compare TMX2-28-Control to the parental cell line, MCF-7-Control, 37,501 (8%) CpG sites are hypermethylated, 14,956 (3%) CpG sites are hypomethylated and 432,294 (89%) are unchanged. Using the same criteria to compare TMX2-28-Aza to TMX2-28-Control, 59 (0.01%) CpG sites are hypermethylated, 6,637 (1%) CpG sites are hypomethylated and 478,145 (99%) are unchanged (Table 2.3). Of the 37,501 CpG sites with increased methylation in TMX2-28 compared to MCF-7, there are 707 CpG sites which are hypermethylated in TMX2-28 compared to the parental line, MCF-7, and also have decreased methylation in TMX2-28 after treatment with 5-Aza-2'-deoxycytidine (Table 2.7). I predict that these differentially methylated CpG sites, which have decreased methylation after 5-Aza-2'-deoxycytidine treatment, are likely to regulate expression of genes that may be re-expressed by 5-Aza-2'-deoxycytidine.

Distribution of CpG Sites that are Hypermethylated in TMX2-28 and Have Decreased Methylation After 5-Aza-2'-deoxycytidine Treatment

To identify genes for which expression was likely regulated by promoter methylation, I examined the distribution of the 707 CpG sites identified as hypermethylated in TMX2-28 with decreased methylation by 5-Aza-2'-deoxycytidine. (A summary of the selection process and HM450K filtering is presented in Figure 2.6). Of these CpG sites, 251 (35%) are located in the promoter (TSS200 or TSS1500 region), 129 (18%) are in the 5'UTR/1st Exon, 223 (32%) are in the body, 13 (2%) are in the 3'UTR and 91 (13%) are intergenic (Figure 2.7 (A)). The neighborhood distribution for these CpG sites is as follows: 268 (38%) are located within a CpG island, 230 (32%) are in north or south shores, 27 (4%) are in north or south shelves and 182 (26%) are found in the open sea (Figure 2.7 (B)). Out of the 251 GpG sites in the promoter region that are hypermethylated in TMX2-28 and have decreased methylation after 5-Aza-2'-deoxycytidine treatment, there are 27 genes for which there are 2 or more CpG sites with significant changes in methylation (Table 2.8). I predict that these target genes are likely re-expressed after 5-Aza-2'-deoxycytidine treatment.

Methylation Pattern of *TACSTD2* in Control- and 5-Aza-2'-deoxycytidine-Treated Cell Lines

TACSTD2 is one of the genes identified as being differentially methylated in TMX2-28 compared to MCF-7 and has decreased methylation after 5-Aza-2'-deoxycytidine treatment. *TACSTD2* encodes the protein tumor-associated calcium

signal transducer 2 (TROP2).[46,47] TROP2 plays an important role in development, intracellular signaling and epithelial cancers.[54] Expression of TROP2 is regulated by promoter methylation in lung cancer. Forced expression of TROP2 in lung cancer cell lines inhibits proliferation and colony formation and blocks phosphorylation of AKT and ERK.[61] Three CpG cites in the promoter of *TACSTD2* were identified as hypermethylated in TMX2-28 with decreased methylation after treatment with 5-Aza-2'-deoxycytidine (Table 2.8). The mean average beta values for these 3 CpGs (MAPINFO numbers: 59043370, 59043280 and 59043255) in MCF-7-Control, TMX2-28-Control and TMX2-28-5-Aza-2'-deoxycytidine-treated cell lines are 0.04, 0.71 and 0.32, respectively (Figure 2.8, A). Mean methylation of these 3 CpGs in TMX2-28 decreased by approximately 0.40 after treatment with 5-Aza-2'-deoxycytidine. Interestingly, methylation of *TACSTD2* in TMX2-28 was most sensitive to treatment with the DNMT-1 inhibitor (Figure 2.8, B). Therefore, it would be interesting to investigate the role of TROP2 in our cell line model of ER-negative, tamoxifen-resistant breast cancer.

Further Characterization of Target Genes Identified by Changes in Promoter Methylation

I then consulted the mRNA expression array to determine if any of the 27 target genes were differentially expressed between TMX2-28 and MCF-7. If translation is regulated by promoter methylation, I predict that these genes would have decreased expression in TMX2-28 compared to MCF-7. Eight of the genes were identified on the array; 5 have decreased expression in TMX2-28 as I predicted

(CGNL1, CKB, NFIA, SPRED2 and *TACSTD2*) however, 3 have increased expression in TMX2-28 (SERPINB5, SGCE and ZNF331) (Table 2.8). This is not unusual as promoter methylation is not the only regulatory factor that determines mRNA expression. Translation also depends on chromatin structure and position of nucleosomes as well as the availability of transcription factors, coactivators and corepressors.

Based on our predictions for genes regulated by promoter methylation, I predict that the targets I identified will have lower methylation and higher mRNA expression in MCF-7 than TMX2-28 and that treatment with 5-Aza-2'-deoxycytidine will increase mRNA expression in TMX2-28 due to decreased methylation. I therefore wanted to evaluate the expression level of these genes in MCF-7. I consulted the Human Protein Atlas, Cell Line Atlas online database to determine approximate mRNA expression levels in MCF-7. I then narrowed our list of target genes to those with predicted moderate or high expression levels in MCF-7. Additionally, I also consulted published literature regarding protein function and possible role in cancer or breast cancer. Gene-specific RT-PCR primers were designed to span an exon-exon junction using Primer-BLAST (NIH) for 10 genes that had predicted moderate expression in MCF-7, interesting predicted function in breast cancer or unknown role in breast cancer. Eight of the 10 primers amplified a single product as determined by melting curve analysis and the MCF-7 and TMX2-28 5-Aza-2'-deoxycytidine-treated and control samples were analyzed for mRNA expression based on cycle thresholds. Average cycle thresholds and beta-values are listed in Table 2.9. By comparison of cycle thresholds (non-normalized RT-PCR

data), two genes had increased expression in TMX2-28-5 Aza-2'-deoxycytidine-treated (PCR product amplified at an earlier cycle), *TACSTD2* and SERPINB5. Because so few of the mRNA expression patterns matched our predictions, I examined the expression of ERα and two previously examined genes, MAGED1 and ZNF350 and compared cycle thresholds with the 5-Aza-2'-deoxycytidine-treated samples (Table 2.10). Expression patterns for ERα agreed with previously published data for MCF-7 and TMX2-28.[38] Importantly, expression patterns for MAGED1 in 5-Aza-2'-deoxycytidine-treated MCF-7 and TMX2-28 cells were verified, as previously reported.[31]

mRNA expression of four target genes was examined by RT-PCR using the standard curve method and normalized to beta-actin (Figure 2.9). As predicted if regulated by promoter methylation, mRNA expression of two genes, *TACSTD2* and CGNL1, was increased in TMX2-28 by 5-Aza-2'-deoxycytidine whereas expression was unchanged in MCF-7. However, mRNA expression of ZNF331 increased in TMX2-28-5-Aza-2'-deoxycytidine-treated which does not agree with our prediction.

Discussion

In American women, breast cancer is the most common cancer diagnosis and it is the second-leading cause of cancer-related deaths.[2] About 70% of breast cancers are ER-positive.[26,77] These patients can be treated with hormonal therapy, such as Tamoxifen. However, about one-third of ER-positive patients treated with Tamoxifen for five years have recurrence.[26] This acquired resistance is a huge obstacle in the clinic because of limited treatment options. There are several

studies, including one from our lab, indicating that DNA methylation may be involved in the development of Tamoxifen resistance.[25,27,31,73] Therefore, epigenetic therapies that alter DNA methylation may prove to be promising therapy for tamoxifen-resistant disease. However, it is unclear how DNMT inhibitors such as 5-Aza-2'-deoxycytidine affect cell behavior, specifically in ER-negative, acquired Tamoxifen resistance.

The objective of the present study was to investigate how 5-Aza-2'-deoxycytidine affects global methylation in our cell line model of acquired Tamoxifen resistance and identify genes regulated by promoter methylation that are re-expressed by 5-Aza-2'-deoxycytidine treatment. To accomplish this, I first confirmed previous results from a single experiment,[31] examining global methylation differences between the tamoxifen-resistant cell lines and the parental cell line, MCF-7. In agreement with this initial study, TMX2-28 is hypermethylated compared to MCF-7. Also, the same trend of decreasing methylation was observed for CpG sites in the promoter regions of MAGED1 and ZNF350, two genes previously identified as being differentially methylated.[31] Expanding on these results, I also examined the effect of 5-Aza-2'-deoxycytidine treatment on global methylation in the parental cell line and the tamoxifen-resistant cell lines. I found that 5-Aza-2'-deoxycytidine treatment alters global methylation in a cell-line specific manner. The ER-negative, tamoxifen-resistant cell line, TMX2-28, is most sensitive to inhibition of methylation by 5-Aza-2'-deoxycytidine. I then sought to identify genes with changes in promoter methylation that might be re-expressed by 5-Aza-2'-deoxycytidine. I did this by identifying genes with CpG sites in the promoter that

are differentially methylated between TMX2-28 and MCF-7 and also have decreased methylation in TMX2-28 after 5-Aza-2'-deoxycytidine treatment.

I predicted that if gene expression is regulated by promoter methylation, genes with hypermethylated CpG sites in TMX2-28 compared to MCF-7 will have lower mRNA expression in TMX2-28 and that treatment with the DNMT1 inhibitor, 5-Aza-2'-deoxycytidine, will decrease methylation and result in increased mRNA expression in TMX2-28. Indeed, there were five genes in our target list of 27 genes (Table 2.8) for which mRNA expression determined by microarray is lower in TMX2-28 than MCF-7 (CGNL1, CKB, NFIA, SPRED2 and *TACSTD2*). I predict that 5-Aza-2'-deoxycytidine treatment will likely increase expression of these genes in TMX2-28. However, three of the 27 target genes have increased expression in TMX2-28 compared to MCF-7 (SERPINB5, SGCE and ZNF331). It is likely that other epigenetic modifications or availability of transcription factors and/or coactivators are acting to regulate expression of these genes. I then determined which genes are predicted to have moderate to high expression in MCF-7 using the Human Protein Atlas. Ultimately RT-PCR primers were designed for 10 of the target genes based on predicted expression in MCF-7 and information regarding protein function in the literature. Comparing average cycle thresholds for control and 5-Aza-2'-deoxycytidine-treated cells, mRNA expression of two genes (*TACSTD2* and SERPINB5) increased in TMX2-28 after 5-Aza-2'-deoxycytidine treatment. This increase in mRNA expression agrees with our prediction if gene expression is regulated by promoter methylation in TMX2-28. However, the mRNA expression array found that expression of SERPINB5 is higher in TMX2-28 than the parental cell

line, MCF-7, which does not agree with our prediction because I know that methylation is higher in TMX2-28. Therefore, expression of SERPINB5 does not seem to be regulated by promoter methylation. Because our predictions for differences in *TACSTD2* expression, which seems to be regulated by promoter methylation, agree with the mRNA expression array and RT-PCR data, I decided to explore the role of *TACSTD2* in our Tamoxifen resistance model.

The *TACSTD2* gene encodes the protein TROP2. [46,47] TROP2 is related to Trop1/ epithelial cell adhesion molecule (Epcam) [49] however, TROP2 has different roles in cell signaling. As reviewed by *McDougall et al. 2014*, [54] TROP2 is expressed in a variety of epithelial cancers and can affect many different aspects relating to cancer cell proliferation, migration and intracellular signaling. TROP2 is involved in regulating intracellular calcium levels, [63] which may contribute to increased proliferation due to activation of PKC signaling.[54]Another mechanism by which TROP2 can promote proliferation is through binding β-catenin and promoting transcription of Cyclin D1 and c-myc. [58] TROP2 is involved in regulating focal adhesion dynamics, a central aspect involved in cell migration. [57] TROP2 can also regulate activation of ERK signaling, an important pathway for sustaining cell proliferation. [59-62] Interestingly, *TACSTD2* expression is regulated by promoter methylation in lung adenocarcinoma. [61] Here the authors demonstrate the TROP2 interacts with IGF1 to inhibit IGF1-R signaling. This prevents activation of AKT and ERK and inhibits proliferation and colony formation. [61] Previously unpublished data from our lab indicates that 5-Aza-2'-deoxycytidine, which decreased promoter methylation of *TACSTD2* and increases mRNA expression of TROP2, inhibits

proliferation in TMX2-28 (*Kristin Williams, unpublished)*. Therefore, I want to test the hypothesis that increased expression of TROP2, resulting from decreased promoter methylation, inhibits proliferation in TMX2-28.

Additionally, TROP2 may have an important role in breast cancer as intracellular localization was found to be an important prognostic factor.[65] Ambrogi and colleagues found that TROP2 localized to the membrane was indicative of poor prognosis while intracellular TROP2 was associated with increased patient survival.[65] However, the role of TROP2 in tamoxifen resistance is unknown. Therefore, I will utilize our cell line model of tamoxifen resistance to investigate the role of TROP2 in drug resistant breast cancer as well as the potential role of methylation in regulation of *TACSTD2* expression.

Table 2.1 Primers Used to Detect Relative mRNA Expression of Genes			
Gene	**Accession Number**	**Forward Sequence (5'-3')**	**Reverse Sequence (5'– 3')**
Beta-actin	NM_001101.3	GGACTTCGAGCAAGAGATGG	AGCACTGGTTGGCGTACAG
CGNL1	NM_032866.4	GGCTGAGGAGGAAATCGACA	CTCGGCAGCTTCTTCAGTCTTA
ERα	NM_000125	ATGATCAACTGGGCGAAGAG	GATCTCCACCATGCCCTCTA
GFI1	NM_001127216.1	GACCGTTTGTCCCCCGAAT	CATTGACTTCTCCGAGGCTGG
MAGED1	NM_001005332	CCTTCTTCGTCAAGCCCCCAG	AGGCAGCATTTGGACCCTTT
MYEOV2	NM_138336.1	TCAGGACTGCCCAGGACAAG	CCCGTTCAGTTCACATCTCTCT
PDGFB	NM_033016.2	TTTATCATGGGCCTCGGGGA	CGGGTCATGTTCAGGTCCAA
PLOD2	NM_000935.2	GGGTCTCTGCGTTCTCGC	ATAATTTATCTGTGGGGATGCTCG
SERPINB5	NM_002639.4	CAGAGTCAACAAGACAGACACCA	TGGACTCATCCTCCACATCCT
SGCE	NM_001099400.1	TCAACGCTTCCTGTGTTCCA	CGAAAATCTCCTGTAGTCTGCTG
SND1	NM_014390.2	GCAGGGGAGAGTTCTGCATT	GGACCTCTCTGTTGCCGTAG
TACSTD2 (3'UTR)	NM_002353.2	AATGTATCCCCTTTCGGTCC	TCCCGGGTTGTCATACAGAT
TACSTD2 (orf)	NM_002353.2	GCCTTCAACCACTCAGACCT	GAGACTCGCCCTTGATGTCC
ZNF331	NM_018555.5	CACGAGATGGCAGTTTTGGA	CTGAAGGCCAGCTCTTTCTTCC
ZNF350	NM_021632	CCCAGTTGAATGCTGTCTTCC	CCACTCCTCCCAAGTGAAGTC

Table 2.2 Changes in Global Methylation Between Tamoxifen-Resistant Cell Lines and MCF-7			
	Change in Methylation	**Filter**	**No. of CpG Sites**
TMX2-28 v. MCF-7	Hypermethylated	Fold change ≥1.8 in TMX2-28-Control (TMX2-28-Control/MCF-7-Control), β-value ≥0.1 in TMX2-28-Control, Detection p-value ≤ 0.01 for TMX2-28-Control and MCF-7-Control	37,501 (8%)
	Hypomethylated	Fold change ≥1.8 in MCF-7-Control (MCF-7-Control/TMX2-28-Control), β-value ≥0.1 in MCF-7-Control, Detection p-value ≤ 0.01 for TMX2-28-Control and MCF-7-Control	14,956 (3%)
	No Change	Detection p-value ≤ 0.01 for TMX2-28-Control and MCF-7-Control (484,751) minus No. of hypermethylated and hypomethylated CpG sites	432,294 (89%)
TMX2-4 v. MCF-7	Hypermethylated		3,563 (0.7%)
	Hypomethylated		13,810 (3%)
	No Change		467,566 (96%)
TMX2-11 v. MCF-7	Hypermethylated		5,887 (1%)
	Hypomethylated		4,802 (0.99%)
	No Change		474,257 (98%)

Table 2.3 Changes in Global Methylation Between TMX2-28-5-Aza-2'-deoxycytidine-Treated and TMX2-28-Control		
Change in Methylation	**Filter**	**No. of CpG Sites**
Hypermethylated	Fold change ≥1.8 in TMX2-28-Aza (TMX2-28-Aza/TMX2-28-Control), β-value ≥0.1 in TMX2-28-Aza, Detection p-value ≤ 0.01 for TMX2-28-Aza and TMX2-28-Control	59 (0.01%)
Hypomethylated	Fold change ≥1.8 in TMX2-28-Control (TMX2-28-Control/TMX2-28-Aza), β-value ≥0.1 in TMX2-28-Control, Detection p-value ≤ 0.01 for TMX2-28-Aza and TMX2-28-Control	6,637 (1%)
No Change	Detection p-value ≤ 0.01 for TMX2-28-Control and MCF-7 control (484,841) minus No. of hypermethylated and hypomethylated CpG sites	478,145 (99%)

Table 2.4 Top 5 Genes in TMX2-28 Containing CpG Sites With the Largest Decrease in Methylation After 5-Aza-2'-deoxycytidine Treatment					
MAPINFO no.	**Refgene Name**	**Accession**	**Fold Change**	**Refgene Group**	**Relation to CpG Island**
1809712	NDUFS6	NM_004553	6.09	Body	n/a
19191892	C21orf91	NM_017447, NM_001100421, NM_001100420	5.68	TSS200	Island
1787806	MAPK8IP3	NM_001040439, NM_015133	5.44	Body, Body	N Shelf
220863263	C1orf115	NM_024709	5.00	TSS1500	N Shore
234509074	C1orf31	NM_001012985	4.87	TSS1500	Island

Table 2.5 Top 7 Genes in TMX2-28 Containing CpG Sites With the Largest Decrease in Methylation in the Promoter After 5-Aza-2'-deoxycytidine Treatment

MAPINFO no.	Refgene Name	Accession	Fold Change	Refgene Group	Relation to CpG Island
234509074	*C1orf31*	NM_001012985	4.87	TSS1500	Island
234509059	*C1orf31*	NM_001012985	51.8	TSS1500	Island
144798331	*MAPK15*	NM_139021	4.11	TSS200	N Shore
144798354	*MAPK15*	NM_139021	2.70	TSS200	N Shore
124220854	*HTRA1*	NM_002775	3.54	TSS200	Island
124220856	*HTRA1*	NM_002775	2.08	TSS200	Island
124220504	*HTRA1*	NM_002775	1.91	TSS1500	Island
53758233	*ZNF677*	NM_182609	3.00	TSS200	S Shore
53758521	*ZNF677*	NM_182609	1.82	TSS1500	S Shore
134600848	*NKX6-2*	NM_177400	2.90	TSS1500	Island
134599807	*NKX6-2*	NM_177400	2.29	TSS1500	Island
134599934	*NKX6-2*	NM_177400	2.21	TSS1500	Island
134600858	*NKX6-2*	NM_177400	1.94	TSS1500	Island
101192973	*DLK1*	NM_003836	2.89	TSS1500	Island
101193017	*DLK1*	NM_003836	2.06	TSS1500	Island
59043255	*TACSTD2*	NM_002353	2.69	TSS200	Island
59043280	*TACSTD2*	NM_002353	2.05	TSS200	Island
59043370	*TACSTD2*	NM_002353	1.92	TSS1500	S Shore

Table 2.6 Differences in mRNA Expression Between TMX2-28 and MCF-7*	
Change in mRNA Expression in TMX2-28	**No. of Genes**
Decreased	2,414 (72%)
Increased	958 (28%)

* Total no. of genes with significant changes in mRNA expression between TMX2-28 and MCF-7 is 3,372 (12% of total)

Table 2.7 Hypermethylated CpG Sites in TMX2-28 CpG That Have Decreased Methylation After 5-Aza-2'-deoxycytidine Treatment		
Change in Methylation	**Filter**	**No. of CpG Sites**
Hypermethylated	Fold change ≥1.8 in TMX2-28-Control (TMX2-28-Control/MCF-7-Control), β-value ≥0.1 in TMX2-28-Control, Detection p-value ≤ 0.01 for TMX2-28-Control and MCF-7-Control	37,501
Hypomethylated	Filter criteria from above and Fold change ≥1.8 in TMX2-28-Control (TMX2-28-Control/TMX2-28-Aza), β-value ≥0.1 in TMX2-28-Control, Detection p-value ≤ 0.01 for TMX2-28-Aza	707

Table 2.8 Genes With More Than One CpG Site in the Promoter Differentially Methylated in TMX2-28 and Decreased by 5-Aza-2'-deoxycytidine		
UCSC Refgene Name	**No. of CpG Sites**	**mRNA Expression in TMX2-28 v. MCF-7**
ASZ1	2	n/a
C17orf102; TMEM132E	2	n/a
CGNL1	2	Decreased
CKB	2	Decreased
CRMP1	2	n/a
ENTPD7	2	n/a
GFI1	3	n/a
HTRA1	2	n/a
IGF2BP1	2	n/a
KIAA1826	2	n/a
MAP9	2	n/a
MAPK15	2	n/a
MYEOV2	2	n/a
NFIA	2	Decreased
PDGFB	2	n/a
PIK3R1	2	n/a
PLOD2	2	n/a
PON2	2	n/a
RAET1L	3	n/a
SERPINB5	2	Increased
SGCE	2	Increased
SND1;LRRC4	3	n/a
SPRED2	2	Decreased
TACSTD2	3	Decreased
TMEM216	2	n/a
ZFR2	2	n/a
ZNF331	3	Increased

Table 2.9 Average Promoter Methylation (Beta value) from Illumina Human Methylation 450 BeadChip and mRNA Expression (Cycle Number) for MCF-7 and TMX2-28 Cells from the 72-hr. Aza Exposure Experiment.										
	TACSTD2		**SND1**		**PDGFB**		**ZNF331**		**CGNL1**	
	MCF-7	**TMX2-28**	**MCF-7**	**TMX2-28**	**MCF-7**	**TMX2-28**	**MCF-7**	**TMX2-28**	**MCF-7**	**TMX2-28**
Control Methylation Beta value	0.042	0.71	0.18	0.78	0.057	0.64	0.15	0.63	0.11	0.48
Aza Methylation Beta value	0.039	0.32	0.14	0.38	0.039	0.31	0.14	0.30	0.084	0.21
Control Expression Cycle No.	24.33	34.24	27.26	26.48	40.44	39.01	30.74	27.74	34.01	36.55
Aza Expression Cycle No.	24.35	28.99 ↑	28.29	29.09 ↓	41.68	41.31 ↓	31.37	30.99 ↓	33.50	36.75

Arrows represent the direction of the change in expression in TMX2-28-Aza compared to TMX2-28-Control

Table 2.9 con't										
	SGCE		**GFI1**		**SERPINB5**		**PLOD2**		**MYEOV2**	
	MCF-7	**TMX2-28**	**MCF-7**	**TMX2-28**	**MCF-7**	**TMX2-28**	**MCF-7**	**TMX2-28**	**MCF-7**	**TMX2-28**
Control Methylation Beta value	0.17	0.69	0.098	0.38	0.063	0.43	0.23	0.73	0.28	0.66
Aza Methylation Beta value	0.15	0.34	0.079	0.18	0.062	0.22	0.19	0.38	0.22	0.35
Control Expression Cycle No.	40.49	34.95	35.11	33.89	37.44	32.91	n/a	n/a	n/a	n/a
Aza Expression Cycle No.	41.38	39.90 ↓	34.62	35.92 ↓	37.09	31.69 ↑	n/a	n/a	n/a	n/a

Arrows represent the direction of the change in expression in TMX2-28-Aza compared to TMX2-28-Control

Table 2.10 Average Cycle Thresholds for Control and 5-Aza-2'-deoxycytidine for Previously Validated Genes			
Cell line – Treatment	**ERα**	**MAGED1**	**ZNF350**
MCF-7-Control	27.51	34.29	31.28
MCF-7-Aza	28.41	33.37	31.17
TMX2-28-Control	37.65	39.57	31.35
TMX2-28-Aza	38.11	33.85	31.35

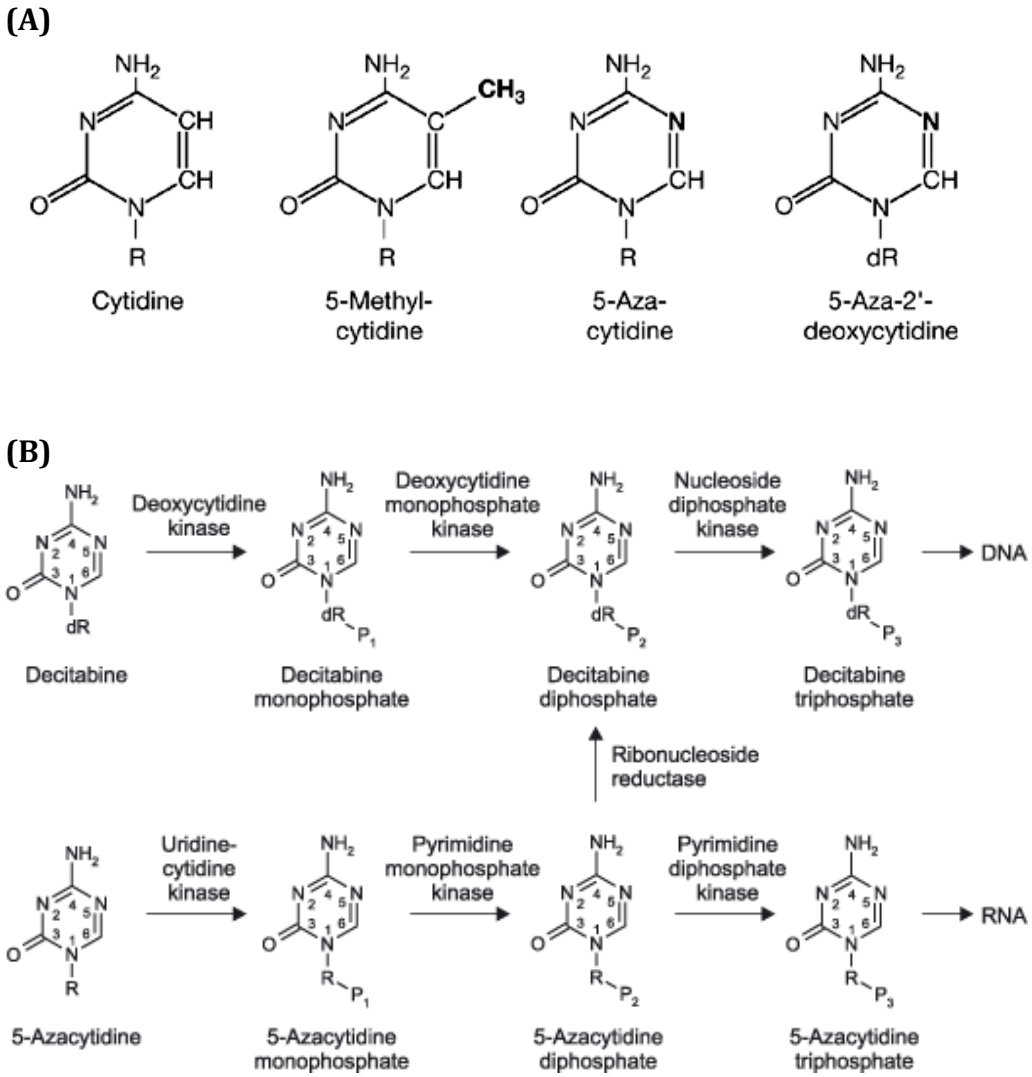

Figure 2.1: Structure and Intracellular Metabolism of 5-Aza-2'-deoxycytidine. (A) Structure of cytidine, 5-Methyl-cytidine, 5-Azacytidine and 5-Aza-2'-deoxycytidine. R = ribose. dR = deoxyribose. Image from *P. Fenaux 2005*.[78] (B) Intracellular metabolism of 5-Aza-2'-deoxycytidine or Decitabine (top) and 5-Azacytidine (bottom). R = ribose, dR = deoxyribose, P = phosphate. Image from *Ghoshal and Bai, 2007*.[70]

(A)

FGD	CpGs	Subgroup	CpGs
Promoter	200,339	TSS200	62,625
		TSS1500	77,379
		5'UTR	49,525
		1stExon	10,810
Body	150,212		
3'UTR	15,383		
Intergenic	119,830		

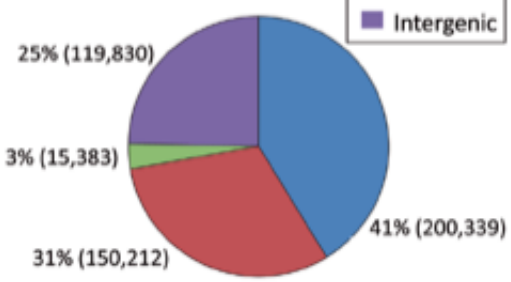

(B)

CpG content	CpGs
Island	150,254
Shore	112,072
Shelf	47,161
Others	176,277

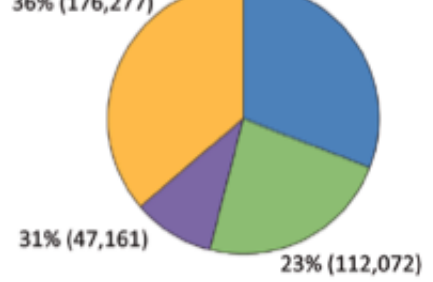

(C)

Associated RNA Transcripts	CpGs
Coding	361,766
Non-Coding	4,168
Intergenic	119,830

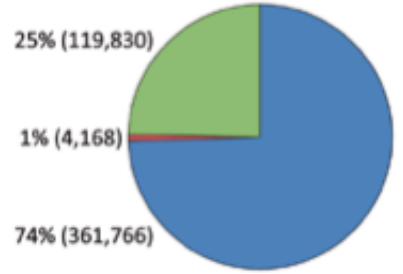

Figure 2.2: Distribution of Sites on the HM450 BeadChip. Summary of the functional genomic distribution (FGD) listed as promoter (within 200-1500 bp upstream of the transcription start site, 5'-UTR, or exon 1), 3'-UTR, gene body or intergenic (A). Distribution of sites in terms of CpG content and neighborhood, as defined by Illumina (B). Distribution of sites with respect to RNA transcripts (C). Images from *Sandoval et al. 2011.*[76]

(A)

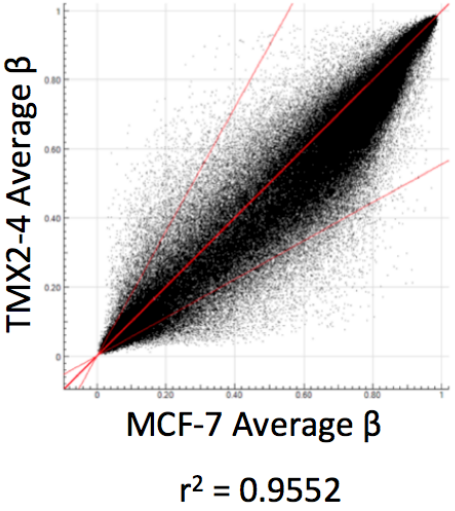

(B)

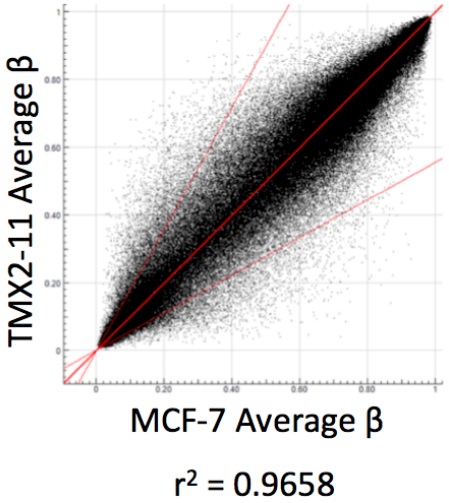

(C)

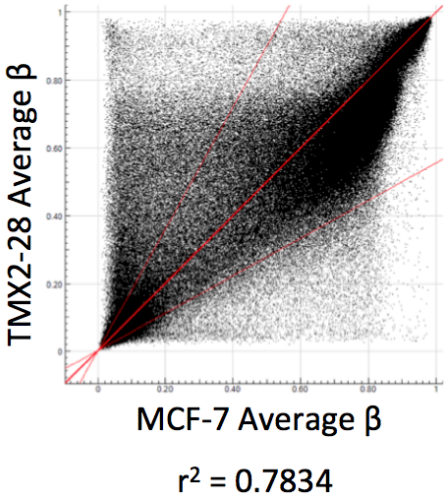

(Figure 2.3)

Figure 2.3: Global Methylation Patterns Differ Among Tamoxifen-Resistant Cell Lines. Scatter plots indicating genome-wide methylation differences between tamoxifen-resistant cell lines, (A) TMX2-4, (B) TMX2-11 and (C) TMX2-28 compared with the parental line, MCF-7. Each black dot on the plot represents a CpG site analyzed on the Human Methylation 450 BeadChip. Center red line represents equal average beta values in the two samples and outer red lines indicate a 1.8-fold change in average beta values. Value of r^2 from Genome Studio represents goodness-of-fit of linear regression.

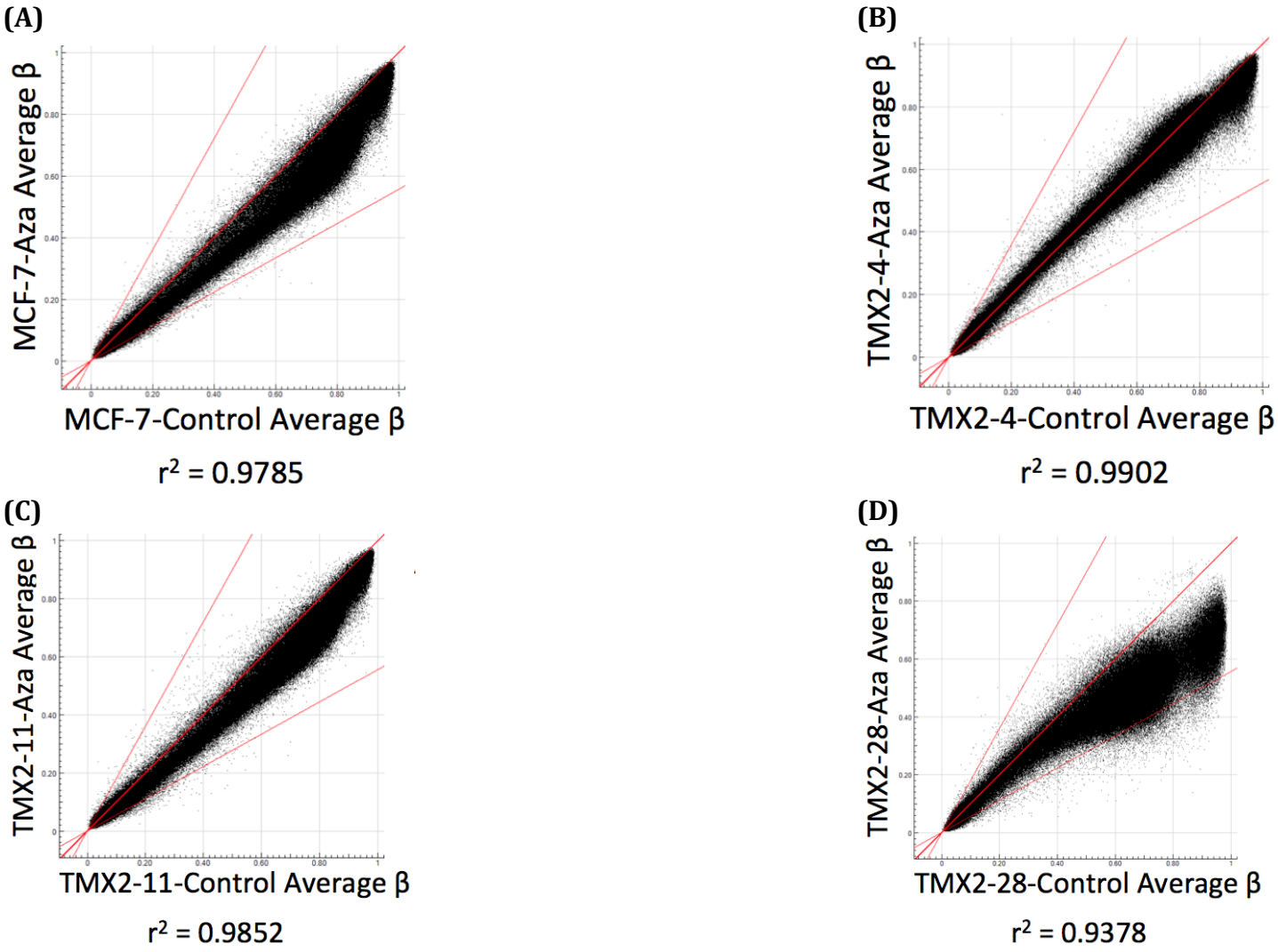
(A)
MCF-7-Aza Average β
MCF-7-Control Average β
r² = 0.9785
(B)
TMX2-4-Aza Average β
TMX2-4-Control Average β
r² = 0.9902
(C)
TMX2-11-Aza Average β
TMX2-11-Control Average β
r² = 0.9852
(D)
TMX2-28-Aza Average β
TMX2-28-Control Average β
r² = 0.9378

(Figure 2.4)

Figure 2.4: 5-Aza-2'-deoxycytidine Treatment Causes Cell Line-Specific Changes in Global Methylation.
Scatter plots indicating genome-wide differences in methylation for 72-hour 5-Aza-2'-deoxycytidine-treated (A) MCF-7, (B) TMX2-4, (C) TMX2-11 and (D) TMX2-28 compared to control for each cell line. Each black dot on the plot represents a CpG site analyzed on the Human Methylation 450 BeadChip. Center red line represents equal average beta values in the two samples and outer red lines indicate a 1.8-fold change in average beta values. Value of r^2 from Genome Studio represents goodness-of-fit of linear regression.

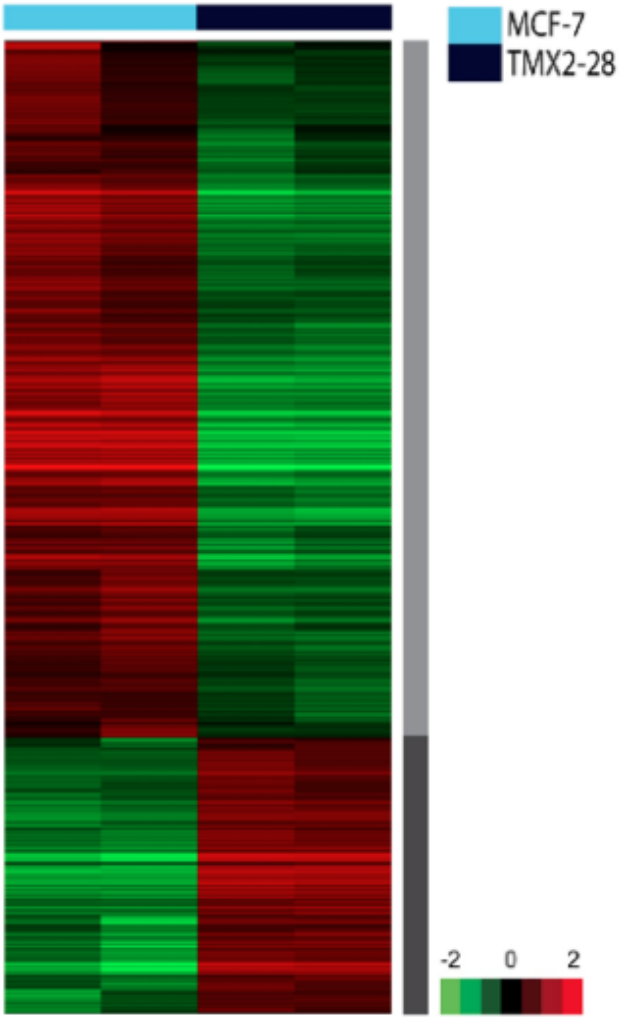

Figure 2.5: TMX2-28 Differs from MCF-7 in Global mRNA Expression.
Heatmap showing results from gene expression array analysis (Agilent 4x44k V2 Microarray) for MCF-7 and TMX2-28. Red: upregulated. Green: down-regulated.

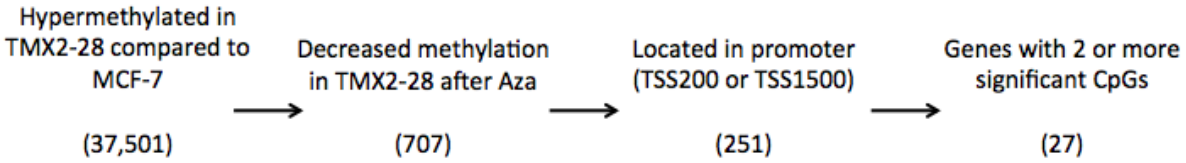

Figure 2.6: Summary of Selection Process for Target Genes. Flow chart describing the selection process and filtering utilized to identify genes with CpG sites located in the promoter that were hypermethylated in TMX2-28 compared to MCF-7 and had decreased methylation when TMX2-28 cells were treated with 5-Aza-2'-deoxycytidine. Number of CpG sites indicated in parentheses. (See also Table 2.7)

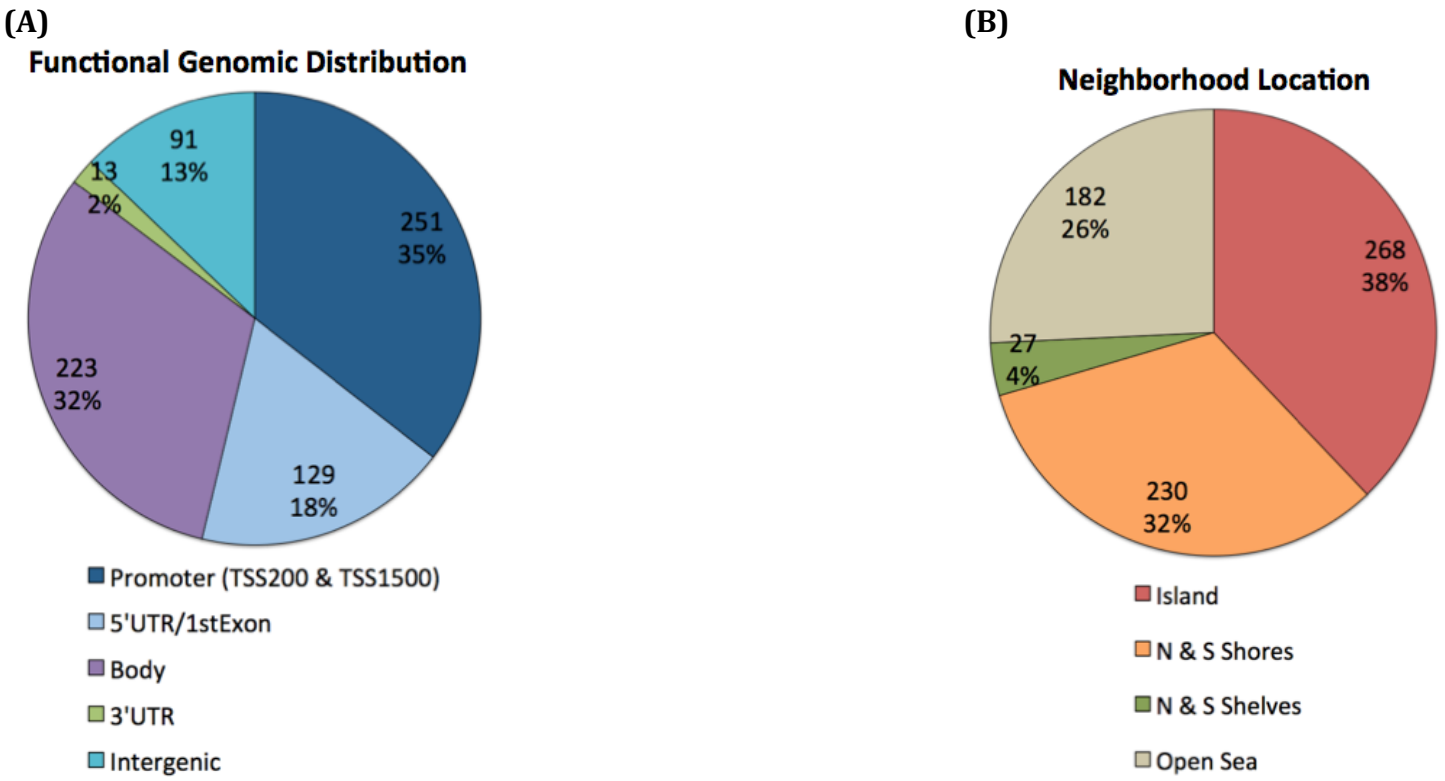

Figure 2.7: Functional Genomic Location and Neighborhood Distribution of Differentially Methylated CpG Sites in TMX2-28 with Decreased Methylation After 5-Aza-2'-deoxycytidine Treatment. Pie charts indicated the (A) functional genomic distribution and (B) neighborhood locations for the 707 CpG sites identified as having increased methylation in TMX2-28 compared to MCF-7 and also decreased methylation in TMX2-28 after 5-Aza-2'-deoxycytidine treatment.

(A)

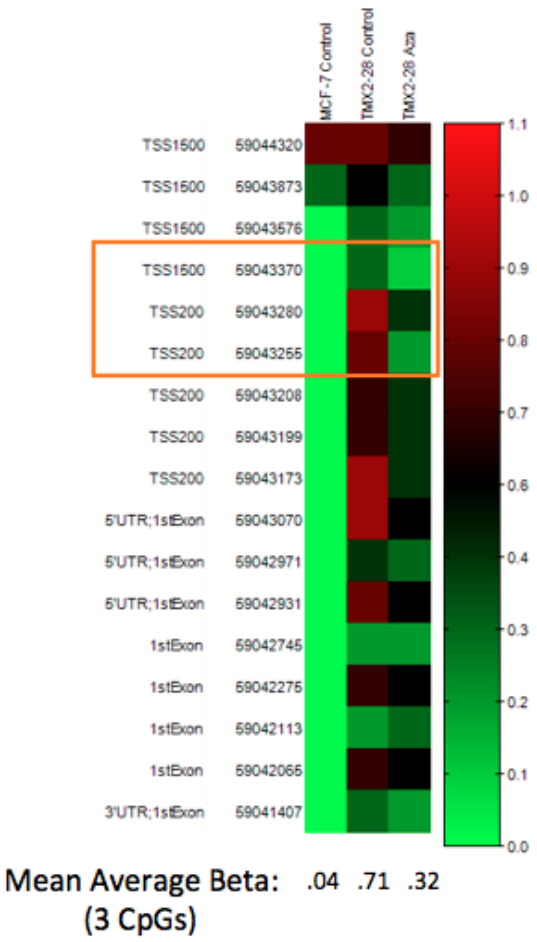
MCF-7 Control
TMX2-28 Control
TMX2-28 Aza
TSS1500 59044320
TSS1500 59043873
TSS1500 59043576
TSS1500 59043370
TSS200 59043280
TSS200 59043255
TSS200 59043208
TSS200 59043199
TSS200 59043173
5'UTR;1stExon 59043070
5'UTR;1stExon 59042971
5'UTR;1stExon 59042931
1stExon 59042745
1stExon 59042275
1stExon 59042113
1stExon 59042065
3'UTR;1stExon 59041407
1.1
1.0
0.9
0.8
0.7
0.6
0.4
0.3
0.2
0.1
0.0
Mean Average Beta: .04 .71 .32
(3 CpGs)

(Figure 2.8)

(B)

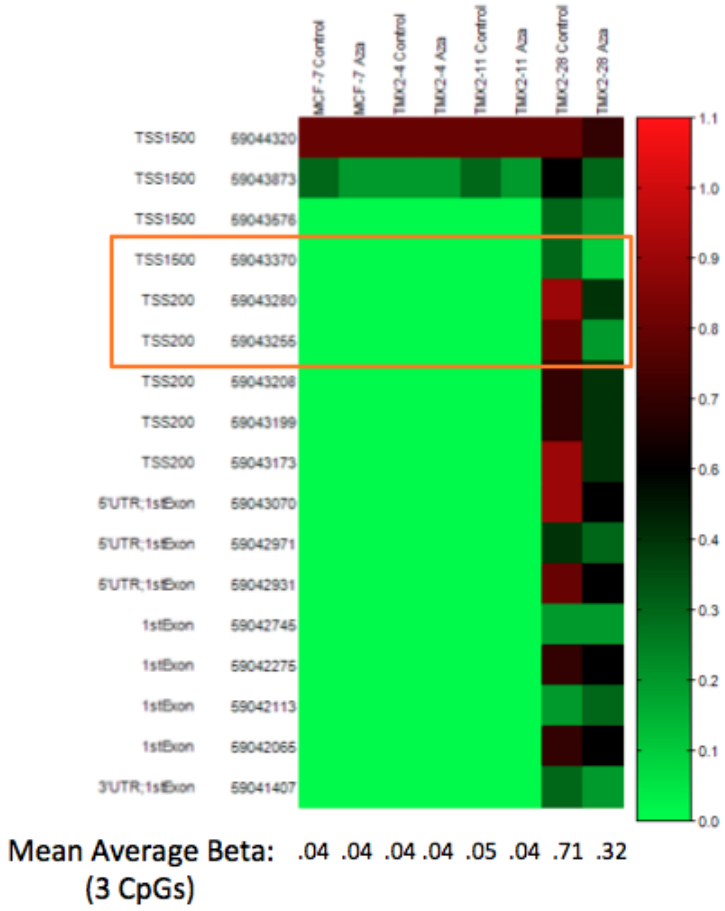

Figure 2.8: Methylation Patterns for *TACSTD2* in DMSO-Control and 5-Aza-2'-deoxycytidine-Treated Cell Lines. Heatmaps indicating methylation of CpG sites in *TACSTD2*, represented by average beta values (scale at right) for MCF-7-Control, TMX2-28-Control and TMX2-28-5-Aza-2'-deoxycytidine-treated cell lines (A) and all of the control- and 5-Aza-2'-deoxycytidine-treated cell lines (B). Left: Refgene Group location and MAPINFO number for each CpG site. Bottom: Mean average beta values for the 3 CpGs (orange box) identified as hypermethylated in TMX2-28 with decreased methylation in TMX2-28 after 5-Aza-2'-deoxycytidine treatment.

(A)

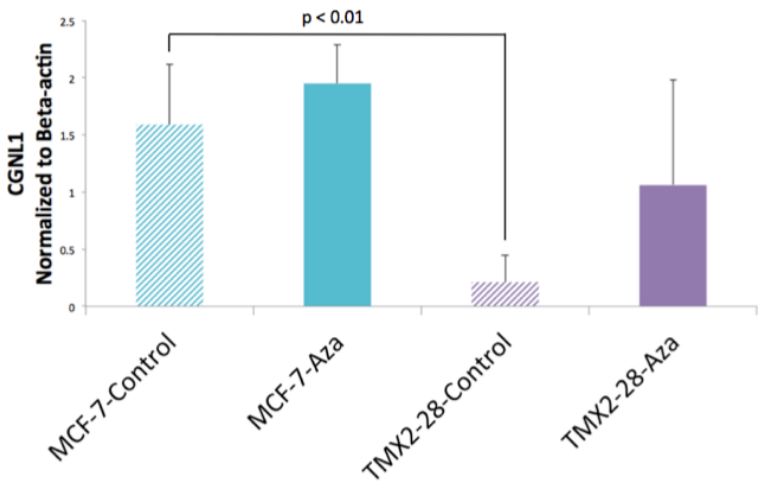
p < 0.01
CGNL1
Normalized to Beta-actin
2.5
2
1.5
1
0.5
0
MCF-7-Control
MCF-7-Aza
TMX2-28-Control
TMX2-28-Aza

(B)

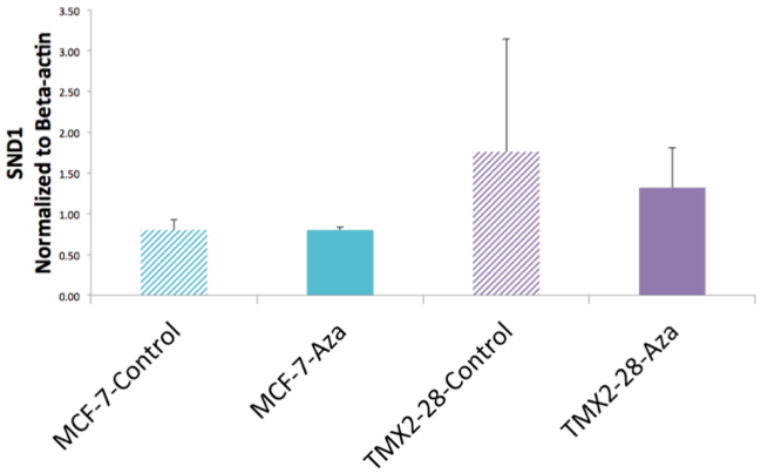
SND1
Normalized to Beta-actin
3.50
3.00
2.50
2.00
1.50
1.00
0.50
0.00
MCF-7-Control
MCF-7-Aza
TMX2-28-Control
TMX2-28-Aza

(Figure 2.9)

(C)

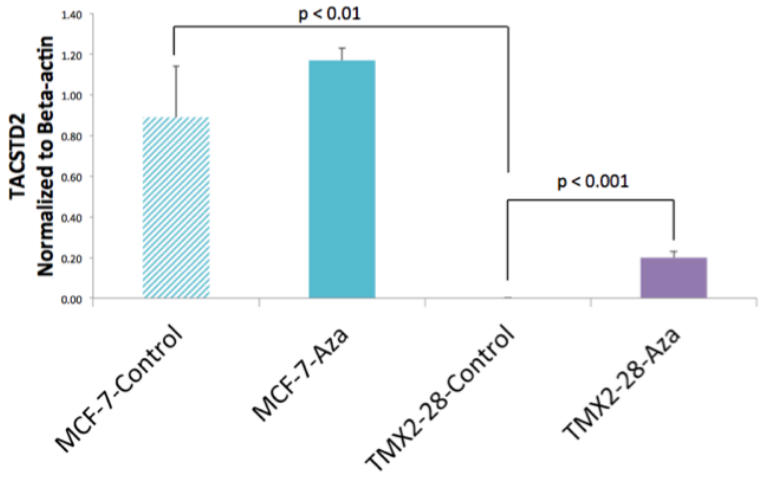

(D)

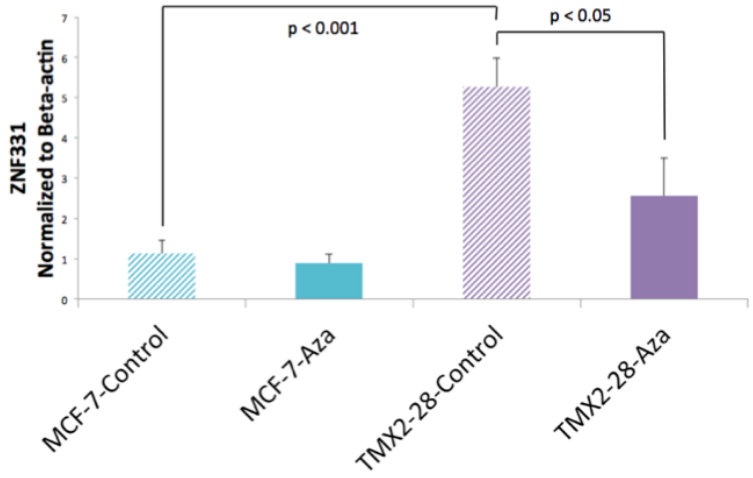

Figure 2.9: Relative mRNA Expression of Target Genes in DMSO-Control and 5-Aza-2'-deoxycytidine-Treated Cells. Relative mRNA expression of (A) CGNL1, (B) SND1, (C) *TACSTD2* and (D) ZNF331 determined by RT-PCR normalized to Beta-actin (n = 3).

CHAPTER 3

5-AZA-2'-DEOXYCYTIDINE INHIBITS PROLIFERATION, MIGRATION AND ADHESION IN TMX2-28

Introduction

Hanahan and Weinberg characterized the ability of cancer cells to maintain continuous proliferation and initiate invasion and metastasis as two of the six Hallmarks of Cancer.[7,8] These hallmarks are critical features of cancer cells required for facilitating tumor growth and metastasis. Specifically, tumor cells rely on growth factor signals and mitogenic signals (both paracrine and autocrine signaling) to promote uncontrolled cell growth. Cancer cells can achieve this deregulated signaling by several mechanisms: production of growth factor ligands to facilitate autocrine signaling, manipulation of normal cells to produce growth factors required by the cancer cells, overexpression of growth factor receptors at the cancer cell membrane, alterations in protein structure that result in ligand-independent signal activation or constitutive activation of members of the signaling pathways downstream of receptors. Somatic mutations can also facilitate proliferative signaling by activating pathways downstream of receptors, such as the MAPK and Akt/PKB signaling pathways. Cancer cells may also disrupt negative feedback mechanisms that suppress proliferation.[8] One or more of these means are often employed by cancer cells to sustain uncontrolled cell proliferation and promote tumorigenesis. Signaling pathways can be constitutively activated by mutations and or epigenetic changes. Cell cycle proteins known to have altered expression in

cancer may include Rb, cyclin dependent kinases (CDKs), and CDK inhibitors. The Wnt, IGF and PI3K/Akt signaling pathways are a few examples of pathways that are often constitutively active in cancer cells.[79]

Breast cancer cells can utilize a variety of mechanisms to facilitate uncontrolled cell proliferation. In some cell lines, overexpression of the ubiquitin ligase, Cullin7, can promote both proliferation and invasion by downregulating p53.[80] The tumor stroma and surrounding microenvironment can also contribute to sustained proliferative signaling. Cancer-associated fibroblasts in the mammary gland can produce growth factors such as, hepatocyte growth factor (HGF), epidermal growth factor (EGF), basic fibroblast growth factor (bFGF) and insulin-like growth factor (IGF), which can promote cancer cell proliferation by activating paracrine signaling networks.[81] The PI3K-AKT-mTOR pathway is a key signaling pathway that mediates extracellular and intracellular growth and survival signaling. It has been shown to play an important role in endocrine resistance and drugs that target components of this pathway have been successful in the clinical setting. The cell cycle can also be subject to aberrant regulation during breast cancer progression. Inhibitors of CDK4/6, which regulate the G1-S phase transition, are also being evaluated for use in the clinic.[82] Changes in these pathways, which lead to sustained proliferation, can arise due to genetic and/or epigenetic alterations.

Additionally during disease progression, cancer cells acquire the ability to invade local surrounding tissue, intravasate into neighboring blood and lymphatic vessels, survive in the blood system, extravasate into tissue at a distant site and colonize this secondary site by establishing micrometastases which eventually

develop into macroscopic tumors. This process is known as the invasion-metastasis cascade, which can be regulated by properties of the cancer cells themselves and also by recruitment of immune and stromal cells by the cancer cells to alter the extracellular matrix, making it easier for cancer cells to disseminate and colonize a distant site.[8]

Different types of tumors have distinct patterns of metastases. Breast cancer has a high propensity to metastasize to bone, while colorectal cancer spreads mainly to the liver, prostate cancer tends to metastasize to bone and kidney cancer prefers the lung. Breast cancer also has a high rate of lung and liver metastases.[83] Different breast cancer subtypes also exhibit preferential metastasis to various sites. Luminal and HER2-positive cancers tend to spread to the brain, liver and lung while basal-like tumors prefer brain, lung and distant lymph nodes.[84] ER-positive/PR-positive tumors metastasize mainly to bone, HER2-positive to the liver and triple-negative cancers to the lung and brain.[85] As reviewed by *Scully et al. 2012,*[3] the majority of breast cancer-related deaths occur due to metastasis to other sites within the body. Therefore, understanding how cancer cells escape from the primary tumor, survive in circulation and establish tumors at secondary sites is essential for identifying new therapeutic targets.

Scully and colleagues describe some of the key steps in breast cancer metastasis, which begins with tumor cells altering cell-cell adhesion and cell adhesion to the extracellular matric (ECM). Cell-cell adhesion is regulated by cadherins and adherence to the ECM is facilitated by integrins. Tumor cells utilize MMPs and the urokinase plasminogen activator system to degrade components of

the ECM and allow tumors cells to invade local tissue. Tumor cells can then migrate individually or collectively. Single cell migration is either protease-dependent (mesenchymal) or –independent (amoeboid-like). Mesenchymal single-cell migration is regulated by mechanisms governing the epithelial-to-mesenchymal transition (EMT), such as gain of expression of mesenchymal markers like vimentin, Snail, and Slug and also activation of TGFβ, WNT and PI3K/AKT signaling pathways. The tumor microenvironment and recruitment of macrophages is also important for proliferative signaling, invasion, angiogenesis and immune evasion.[3] Drugs that target the signaling molecules that regulate these processes are imperative for preventing deaths due to breast cancer metastasis.

The DNMT1 inhibitor, 5-Aza-2'-deoxycytidine, has potential as an epigenetic therapeutic for breast cancer. Inhibition of DNMT1 leads to decreased methylation and potentially re-expression of genes that have been silenced by promoter methylation during disease progression. Used alone or in combination with other cancer therapeutics, 5-Aza-2'-deoxycytidine may prove to be beneficial for treating tamoxifen-resistant breast cancer.

Treatment with 5-Aza-2'-deoxycytidine is known to inhibit cell growth and migration and induce re-expression of genes silenced by DNA methylation in certain cell lines. In the bladder cancer cell line, T24, 5-Aza-2'-deoxycytidine treatment results in re-expression of maspin, which is silenced by DNA promoter methylation. 5-Aza-2'-deoxycytidine treatment of T24 cells also inhibits proliferation, migration and invasion and results in increased apoptosis.[86] Treatment of the human multiple myeloma cell line, RPMI-8226, with 5-Aza-2'-deoxycytidine results in re-expression

of the tumor suppressor, DLC-1, and dose-dependent inhibition of growth and induction of apoptosis.[87] 5-Aza-2'-deoxycytidine is also known to inhibit growth of HeLa cells and re-express the apoptosis regulatory protein, APAF-1.[88]

Inhibition of DNMT1 by 5-Aza-2'-deoxycytidine is known to decrease methylation of genes and correspondingly increase gene expression in breast cancer cell lines as well. In the human breast cancer cell line, MRK-nu-1, 5-Aza-2'-deoxycytidine treatment decreases methylation of retinoic acid receptor beta 2 (RARβ2), resulting in increased gene expression. In addition, 5-Aza-2'-deoxycytidine induces cell-cycle arrest and inhibits proliferation.[89] A similar effect on cell-cycle arrest and proliferation was observed in MCF-7 cells treated with 5-Aza-2'-deoxycytidine, along with increased expression of APAF-1.[90] Decreased promoter methylation and increased expression of IGFBP-3 has been observed in MCF-7 and T47D breast cancer cell lines. Additionally, 5-Aza-2'-deoxycytidine inhibited growth and colony formation as well as increased cell death in these cell lines.[91] While these tissue culture experiments have identified genes with changes in methylation induced by 5-Aza-2'-deoxycytidine, the effect of 5-Aza-2'-deoxycytidine treatment on ER-negative, tamoxifen-resistant cell lines is not known. Investing this concept will provide insight as to whether 5-Aza-2'-deoxycytidine could be utilized as a valuable therapy for ER-negative, recurrent breast cancer after Tamoxifen treatment.

In addition to the growth inhibitory effects of 5-Aza-2'-deoxycytidine treatment on breast cancer cell lines,[89-91] 5-Aza-2'-deoxycytidine has also been shown to affect migration and invasion in other tissue culture experiments. The

bladder cancer cell line, T24, has reduced migration and invasion after 5-Aza-2'-deoxycytidine treatment.[86] Decreased promoter methylation and increased protein expression of maspin in extravillous trophoblast cells induced by treatment with 5-Aza-2'-deoxycytidine also results in inhibition of migration and invasion.[92] 5-Aza-2'-deoxycytidine has also been shown to decrease promoter methylation of miR495 in gastric cancer cell lines, resulting in increase expression of miR495. This microRNA then represses PRL-3 expression and inhibits migration and invasion.[93] Therefore, we wanted to test the hypothesis that changes in DNA methylation and gene expression induced by 5-Aza-2'-deoxycytidine may affect proliferation and migration in the ER-negative, tamoxifen-resistant cell line, TMX2-28, and could have potential as a therapeutic for Tamoxifen resistance in the clinic.

In order to determine the effect of 5-Aza-2'-deoxycytidine treatment on these biological processes, MCF-7 and TMX2-28 cells were treated with 2.5 μM 5-Aza-2'-deoxycytidine for 48 to 120 hours. Cell proliferation was determined using the colorimetric assay with the Cell Titer 96® Aqueous One Solution (Promega), adhesion to fibronectin was determined using pre-coated fibronectin plates and staining adherent cells with crystal violet, migration assay. Evaluating the effect of 5-Aza-2'-deoxycytidine on these biological processes provided a quantitative method for assessing whether this therapy might be effective for treatment of ER-negative, Tamoxifen-reistant disease.

Materials and Methods

Cell culture: MCF-7 cells were purchased from the American Type Culture Collection (ATCC). TMX2-4, TMX2-11 and TMX2-28 cells were provided by John Gierthy (Wadsworth Center Albany, NY). Cells were grown in Dulbecco's modified eagle medium (without phenol red). Medium was supplemented with 5% cosmic calf serum (Hyclone Cat. No. SH30087.03), 2.0 mM of L-glutamine, 0.1 mM of nonessential amino acids and 250 ng/mL of insulin. Cells were maintained at 37°C, 5% CO_2 in a humidified incubator and passaged at subconfluence or media exchanged every 2 days.

5-Aza-2'-deoxycytidine Treatment: Cells were seeded into plates or flasks and allowed to adhere overnight at 37°C, 5% CO_2. Cells were treated with either 0.1% DMSO (vehicle control) or 2.5 μM 5-Aza-2'-deoxycytidine (Aza or 5-Aza-CdR) (Sigma-Aldrich Cat. No. A3656) in 0.1% DMSO for 96 hours, with media exchanged every other day.

Proliferation Assay: Cells were seeded in a 96-well plate at 5,000 cells/well and treated with 2.5 μM Aza or DMSO (at 50% re-feed with 100 μL of growth media with Aza or DMSO) for 48 hrs. or 2,500 cells/well and treated with 2.5 μM Aza or DMSO for 120 hrs. At the time of the assay, 20 μL of Cell Titer 96® Aqueous One Solution (Promega, Madison, WI) was added to each well containing 100 μL of growth media. The plate was then incubated at 37°C, 5% CO_2 for 1 hr. 30 min. Absorbance at 490 nm was read on a VersaMax Tunable Microplate reader

(Molecular Devices, Sunnyvale, CA). Cell proliferation was quantified as a percentage of the control for each cell line.

Migration/Wound-healing Assay: TMX2-28 and MCF-7 cell cultures were treated in triplicate with 2.5 μM 5-Aza-2'-deoxycytidine (Aza) or vehicle control (DMSO) for 48 hours and allowed to reach 90% confluency. Then the monolayer was scratched with a pipette tip and washed with PBS to remove detached cells. The wound boundary was then imaged every 24 hours to monitor cell migration for 48 hours in the presence of Aza.

Cell Viability Assay: The viability of adherent and non-adherent cells was determined by counting cells stained with the membrane exclusion dye, trypan blue. Adherent cells were washed once with PBS and incubated in trypsin for 10 minutes. A single-cell suspension was formed by the addition of media and a 10 μL aliquot will be diluted 1:1 with trypan blue. Live and dead cells will be counted using a hemocytometer. Non-adherent cells will be pelleted, resuspended in PBS, stained and counted as described above.

Adhesion Assay (pre-coated plates): Cells were seeded in a 96-well plate pre-coated with human fibronectin (Corning, Bedford, MA) at 20,000 cells/well and incubated at 37°C, 5% CO_2 for 30 min. Shaking the plate on a plate shaker for 10-15 sec displaced non-adherent cells. The cell suspension was then removed and the wells were washed three times with 100 μL of wash buffer (0.1% BSA in serum-free media). The cells were fixed by incubating with 100 μL of 4% paraformaldehyde in PBS for 10-15 min. The wells were then washed with wash buffer and removed by dumping out and tapping the plate on the bench. The cells were stained with 5

mg/mL crystal violet in 2% ethanol for 10 min. The staining solution was removed and the plates were washed three times by submerging in water and discarding the wash. Excess water was removed by tapping the plate on the bench and the plate was dried for at least 24 hours. After the plate dried, 100 µL of 1% SDS was added to each well and incubated at room temperature for 30 min. Absorbance at 550 nm was read on a VersaMax Tunable Microplate reader (Molecular Devices, Sunnyvale, CA). Cell adhesion to fibronectin was quantified as a percentage of the control for each cell line.

Adhesion Assay (without pre-coated plates): A 96-well plate was coated with 50 µL of fibronectin (20 µg/mL, BD BioSciences, Cat. No. 354008) and incubated at 37 °C for 1 hour or at 4°C overnight. The plate was then washed two times with 150 µL of washing buffer (0.1% BSA in serum-free media) and incubated with 150 µL of blocking buffer (0.5% BSA in serum-free media) at 37 °C, 5% CO_2 for 1 hour. The plate was then washed with washing buffer two times and chilled on ice. Cells were counted and diluted to 200,000 cells/mL. Cells were seeded into the coated plate at 20,000 cells/well and incubated at 37°C, 5% CO_2 for 30 min. The plate was then washed and stained with crystal violet as described above.

Pyrosequencing: The EZ DNA Methylation-Lightning kit (Zymo, Cat. No. D5030) was used to bisulfite treat DNA. PCR primers were designed using the Pyromark Assay Design Software (Qiagen). Bisulfite treated DNA was then amplified using the EPIK Amplification kit (Bioline, Cat. No. BIO-66025). Gene-specific primers targeting the three CpG sites in the promoter region of *TACSTD2* (NM_002353) GRCh37 HG19 Map position (MAPINFO) Ch1 coordinates: 58815843,

58815868 and 58815958 analyzed by the BeadChip were designed. Primers for pyrosequencing: FWD Biot-5'-GGTTGGGGTTGGGAAAGAA-3', REV 5'-ACCCCACCTCCTACTACAAACCTA-3', SEQ 5'-GGAAAGAAAGAAAAGGGA-3'. The Pyromark vacuum prep tool (Biotage) was used to isolate single stranded products for pyrosequencing. The Pyromark Q24 system (Biotage) was used to perform pyrosequencing reactions according to manufacturer's protocol (Qiagen). Percent methylation at the interrogated CpG sites was determined using the Pyromark Q24 Software.

Data Analysis: Proliferation, methylation, adhesion assay and migration assay data was analyzed using a using an un-paired Student t test (StatPlus for Mac v. 5.8.2.0).

Results

5-Aza-2'-deoxycytidine Inhibits Proliferation in TMX2-28

Sustaining proliferative signals is one of the critical essential characteristics acquired by cancer cells.[7] One of the mechanisms employed by cancer cells to achieve this hallmark trait is by improper regulation of growth signaling pathways, such as MAPK pathway.[7]

Previous work in our lab indicated that 96-hour treatment with 5-Aza-2'-deoxycytidine inhibits proliferation of TMX2-28, but not the parental line, MCF-7 (*Kristin Williams, unpublished data*). Using a MTS assay, a colormetric assay that indicates metabolic activity, treatment with 5-Aza-2'-deoxycytidine for 96 hours decreased proliferation of TMX2-28 by approximately 30% (Figure 3.1).

Importantly, results from this initial study were confirmed by repeating the proliferation assay with MCF-7 and TMX2-28 cells treated with 5-Aza-2'-deoxycytidine for 120 hours (Figure 3.2). Treatment with 5-Aza-2'-deoxycytidine for 120 hours decreased proliferation in TMX2-28 by 39%.

5-Aza-2'-deoxycytidine Inhibits Cell Migration (Scratch/Wound) in TMX2-28

To determine whether 5-Aza-2'-deoxycytidine treatment affected migration, I conducted a wound-healing assay with a 48-hour 5-Aza-2'-deoxycytidine pre-treatment for triplicates of MCF-7 and TMX2-28 5-Aza-2'-deoxycytidine -treated and control. I found that 5-Aza-2'-deoxycytidine treatment increased migration in MCF-7, confirming what is known in the literature.[94] However, treatment of TMX2-28 with 5-Aza-2'-deoxycytidine inhibited migration (Figure 3.3). Over the course of this experiment while monitoring migration, I observed an increase in the number of floating, 5-Aza-2'-deoxycytidine-treated TMX2-28 cells (cells that had detached from the bottom of the well). In order to determine whether the scratch (i.e. wound to the monolayer) or 5-Aza-2'-deoxycytidine treatment was causing loss of adherence, I repeated the wound-healing assay with 48-hour 5-Aza-2'-deoxycytidine pre-treatment both with and without the scratch. Regardless of the scratch, the number of floating TMX2-28 cells increased with 5-Aza-2'-deoxycytidine treatment (Figure 3.4). Therefore, 5-Aza-2'-deoxycytidine treatment inhibits migration and adherence in TMX2-28.

To determine whether the detached TMX2-28 cells were viable, cells were pre-treated with 5-Aza-2'-deoxycytidine for 48 hours, then media containing either

the 5-Aza-2'-deoxycytidine-treated or control (3 wells each) TMX2-28 floating cells was transferred to a new well of a 6-well plate every 6 to 24 hours. After 8 days, the media containing the floating population was collected, cells were stained with the membrane exclusion dye, Trypan blue, and counted. The adherent cells (re-adherent population) were incubated with Trypsin, stained with Trypan blue and counted. Treatment with 5-Aza-2'-deoxycytidine decreased the viability of both the floating and re-adherent populations (Figure 3.5). Therefore, 5-Aza-2'-deoxycytidine treatment inhibits migration, adherence and viability of TMX2-28. Based on these preliminary results, 5-Aza-2'-deoxycytidine treatment may be an effective therapy for women with recurrent, ER-negative breast cancer after Tamoxifen treatment. We predict that treatment with Aza alters promoter methylation and therefore expression of genes identified in *Chapter 2* that may be involved in regulating these processes.

Optimization of Seeding Densities for Quantitative Adhesion Assay

After determining that 5-Aza-2'-deoxycytidine inhibits proliferation in TMX2-28 but not MCF-7, I wanted to determine what other biological properties might be affected by 5-Aza-2'-deoxycytidine treatment. Treatment with 5-Aza-2'-deoxycytidine seems to also promote detachment of TMX2-28 cells from the monolayer. However, the methods described previously to monitor cell detachment were not very accurate. Therefore, I switched to a more sensitive and quantitative method to monitor cell adhesion to fibronectin. Breifly, cells are given a certain amount of time to adhere to a fibronectin-coated plate, non-adherent cells are then

washed away and the cells that remain are fixed and stained with crystal violet which is then solubilized in SDS and an absorbance measurement is recorded.

First, I wanted to determine the optimum seeding density for the fibronectin adhesion assay. In order to determine the approximate number of cells that could be detected with the adhesion assay, I seeded 1:10 serial dilutions of cells onto a plate coated with fibronectin the day before (See Appendix B). I determined that the background staining needed to be reduced in order to have a more sensitive assay. After modifying the protocol by filtering the crystal violet staining solution and washing the plate by submerging it in water, the background staining was reduced considerably. I determined the optimum seeding density for the assay to be between 30,000 and 14,000 cells/well.

Variability With Initial Experiments and Switch to Pre-coated Fibronectin Plates

In order to determine whether cell adhesion to fibronectin was altered by 5-Aza-2'-deoxycytidine, cells were grown in flasks and treated with 5-Aza-2'-deoxycytidine. Treatments were staggered such that each would finish on the same day (Figure 3.6). Cells were then harvested, counted and diluted. Three experiments with the following treatments were conducted: 24-hour and 48-hour 5-Aza-2'-deoxycytidine -treatment adhesion assays with MCF-7 and TMX2-28. Based on previous observations, I predict that 5-Aza-2'-deoxycytidine treatment will result in decreased adhesion of TMX2-28 cells to fibronectin. However, the results from these first three experiments were variable (See Appendix B). Two of the three

showed an increase in absorbance indicating an increase in adhesion in 5-Aza-2'-deoxycytidine-treated TMX2-28 cells. There was also some variability in adhesion for MCF-7 cells. There are several possible explanations for this. First, there could be inconsistency with coating the plates by hand with fibronectin. Second, the cell counts obtained using a hemocytometer could be incorrect; therefore the dilutions and seeding densities would not be accurate. It is also possible that prior to seeding in the 96-well plate, there are two populations of cells in the flask (adherent and suspension) and each is behaving differently. Lastly, the inconsistency could simply be due to variability in response to short-term 5-Aza-2'-deoxycytidine treatment.

I then switched to using commercially available pre-coated fibronectin plates to minimize variability from coating and used an automated cell counter to minimize variability by counting with the hemocytometer. I also tested two longer treatments with 5-Aza-2'-deoxycytidine, 48- and 72-hours. Two experiments were conducted in parallel, one for which the adherent cells in the flask were trypsinized and used for the assay and the other for which the adherent cells in the flask were combined with any cells that may have already detached and were in suspension in the flask. Comparing the results between these two populations will indicate whether the detached cells are affecting the behavior of the cells that were adherent.

5-Aza-2'-deoxycytidine Inhibits Adhesion in TMX2-28

Because previous experiments showed that TMX2-28 cells treated with 5-Aza-2'-deoxycytidine detach from the monolayer, I wanted to see if there was a difference in adhesion between the adherent cells and the adherent cells combined

with those cells that were in suspension. For the first experiment, two replicate flasks were seeded for each treatment (see Appendix D). On the day of the adhesion assay, the adherent cells were trypsinzed, counted and seeded for the assay. For the second set, cells that were floating in the spent media were combined with adherent cells, counted and seeded for the assay. Cells were seeded on the pre-coated fibronectin plate at 15,400 cells/well (due to a limited number of cells in one of the samples). Remaining cell pellets from each treatment flask were divided into two and stored at -80°C for DNA and RNA isolation at a later date. Results from the adherent population only indicate that treatment with 5-Aza-2'-deoxycytidine inhibits adhesion of TMX2-28 cells to fibronectin, but does not affect adhesion of MCF-7 cells (Figure 3.7).

Importantly, results from this experiment were verified by a second experiment. Repeating the 48-hour and 72-hour 5-Aza-2'-deoxycytidine treatment and seeding the trypsinized cells at 30,000 cells/well using the pre-coated plate confirmed the results from the first experiment with the pre-coated fibronectin plate. (Remaining cell pellets from each treatment flask for this experiment were also divided into two and stored at -80°C for DNA and RNA isolation). Treatment with 5-Aza-2'-deoxycytidine did not alter MCF-7 adhesion to fibronectin. However, there was a step-wise decrease in TMX2-28 adhesion to fibronectin with 5-Aza-2'-deoxycytidine treatment. Treatment with 5-Aza-2'-deoxycytidine resulted in a 21% decrease in TMX2-28 adhesion to fibronectin compared to the control (Figure 3.8).

Validation of Changes in Methylation Identified on 450 BeadChip

In order to validate the changes in *TACSTD2* promoter methylation identified on the 450 BeadChip, DNA from the cells used for the 5-Aza-2'-deoxycytidine adhesion assay experiments (Figure 3.6) was isolated and promoter methylation was analyzed by pyrosequencing. The pyrosequencing assay was designed to include two of the three CpGs identified as differentially methylated on the 450 BeadChip (see Table 2.8). Treatment with 5-Aza-2'-deoxycytidine for 48 or 72 hours decreased promoter methylation by an average of 45 % ($p < 0.0001$) and 36 % ($p < 0.0001$), respectively compared to control DMSO treated TMX2-28 cells. There was no change in promoter methylation for MCF-7 cells after treatment with 5-Aza-2'-deoxycytidine. This assay was repeated twice with similar results. This confirms the results from the 450 BeadChip.

Discussion

Cancer can be considered a disease of both genetic and epigenetic abnormalities.[14] Histone modification and DNA methylation are epigenetic alterations known to be involved in cancer progression.[30] Aberrant DNA methylation and silencing of gene promoters with CpG islands occurs often in cancer.[20] Increased promoter methylation is recognized as an early and fundamental event in carcinogenesis and specifically in breast cancer.[13,16] Changes in DNA methylation are reversible and, based on these initial experiments, 5-Aza-2'-deoxycytidine seems to affect proliferation, migration and adhesion in the

tamoxifen-resistant cell line only, indicating that it may be an effective therapeutic for patients with acquired ER-negative tamoxifen-resistant tumors.

The primary objective of this study is to evaluate how changes in DNA methylation in response to the DNMT1 inhibitor, 5-Aza-2'-deoxycytidine, affect gene expression and cell behavior related to the Hallmarks of Cancer in the ER-negative model of tamoxifen-resistance. The results from this study will help determine whether 5-Aza-2'-deoxycytidine would be an effective therapeutic for tamoxifen-resistant breast cancer. To accomplish this, I first validated previous unpublished data from our lab demonstrating that 5-Aza-2'-deoxycytidine treatment inhibits proliferation in TMX2-28, but not the parental cell line, MCF-7. Next I determined that migration of TMX2-28 cells in a scratch/wound assay is inhibited by 5-Aza-2'-deoxycytidine treatment. However, 5-Aza-2'-deoxycytidine treatment increased migration in the parental cell line, MCF-7. Based on the observation during the scratch/wound experiment that 5-Aza-2'-deoxycytidine seemed to increase the number of floating cells for TMX2-28, simply counting cells from the adherent and suspension populations and staining with Trypan blue indicated that 5-Aza-2'-deoxycytidine treatment induced detachment and decreased viability of TMX2-28 cells. I then used the pre-coated fibronectin plates as a more precise and quantitative measure of cell adhesion to the ECM. I found that TMX2-28 cells treated with 5-Aza-2'-deoxycytidine for 48 or 72 hours had decreased adhesion to fibronectin, while MCF-7 adhesion to fibronectin was not affected by the treatment. These results indicate that changes in DNA methylation resulting from exposure to 5-Aza-2'-deoxycytidine cause changes in gene expression that decrease proliferation

and inhibit both migration and adhesion in TMX2-28. Treatment of MCF-7 cells with 5-Aza-2'-deoxycytidine seemed to promote migration. However, proliferation and adhesion of MCF-7 cells is not affected by 5-Aza-2'-deoxycytidine. These results are promising and indicate that women with ER-negative, tamoxifen-resistant disease who have methylation signatures similar to TMX2-28, may benefit from 5-Aza-2'-deoxycytidine therapy. However, based on the result that 5-Aza-2'-deoxycytidine promotes migration of MCF-7 cells, breast cancers similar to these cells should not be treated with 5-Aza-2'-deoxycytidine.

During the 1960's and early 1970's, 5-Aza-2'-deoxycytidine (decitabine) and 5-azacytidine were first synthesized and tested as cytotoxic chemotherapeutics.[95,96] However, their demethylating activity was unknown until 10-15 years later.[97] 5-azacytidine was approved in 2004 by the FDA as a therapy for myelodysplasia (MDS), a leukemia predisposition disorder, followed shortly thereafter by the approval of 5-Aza-2'-deoxycytidine in 2006. Both of these drugs are also an effective therapy for acute myeloid leukemia (AML).[13] As reviewed by *Visconte et al. 2014,*[98] MDS is a clonal stem cell malignancy characterized by cytopenia, inefficient hematopoiesis, dysplasia in one or more myeloid cell lineages and increased risk of development of AML. Aberrant methylation of tumor suppressor genes is known to occur in MDS along with altered patterns of DNA methylation and histone modifications. Genetic defects such as mutations, chromosomal aberrations and copy-number alterations are frequently observed in MDS. Some of these genetic defects affect genes that are involved in regulating DNA methylation or histone modifications. For example, mutations in DNMT3A are known to occur in a small

percentage of MDS patients. Loss of function mutations in TET2, a dioxygenase that catalyzes the conversion of 5-methylcytosine to 5-hydroxymethycytosine, occur in 20-25% of MDS patients. This leads to a decrease in 5-hydroxymethylcytosine levels and a corresponding increase in 5-methylcytosine, which contributes to DNA hypermethylation and gene silencing. Mutations in IDH1/2 are also known to occur in MDS, which may result in altered mitochondria function and lead to hypermethylation. Mutations in the polycomb group member, ASXL1, have also been found in MDS patients. These mutations lead to alterations in chromatin remodeling and homeotic gene repression. Finally, deletions of chromosome 7/7q, which contains the EZH2 gene, are known to occur in MDS. EZH2 is a histone methyltransferase factor and part of the catalytic component of polycomb repressive complex 2 (PRC2), which is responsible for modifying histones with the repressive mark, H3K27me3.[98] With these epigenetic factors that contribute to the development of MDS and ultimately progression to AML, it is clear why inhibition of DNMT's by 5-azacytidine or 5-Aza-2'-deoxycytidine leading to decreased methylation would be beneficial for MDS patients.

It is not clear why the tamoxifen-resistant TMX2-28 cells, exhibit more changes in methylation in response to 5-Aza-2'-deoxycytidine (Figure 2.3). One mechanism of inhibition of methylation by 5-Aza-2'-deoxycytidine results from the incorporation of the cytosine analog into DNA and formation of a covalent bond between the analog and DNMT1. This leads to enzyme degradation, loss of methylation with subsequent cell divisions and re-expression of genes silenced by promoter methylation.[70,71] However, this may not be the only mechanism by which

5-Aza-2'-deoxycytidine and 5-Aza-cytidine leads to decreased methylation. DNA methyltransferase activity is known to decrease faster than incorporation of 5-Aza-cytidine into DNA.[99] Additionally, gene expression profile analysis of colon cancer cells treated with 5-Aza-2'-deoxycytidine show that changes in gene expression occur independently of cell cycle and are not due entirely to incorporation of 5-Aza-2'-deoxycytidine into DNA.[100] Ghoshal and colleagues[101] demonstrated that DNMT1 undergoes rapid and selective degradation via the proteasomal pathway in response to 5-Aza-2'-deoxycytidine. They also found this process to occur in the nucleus, independent of DNA replication, and to require the conserved KEN box domain of DNMT1.[101] It is likely that the 5-Aza-2'-deoxycytidine-induced changes in DNA methylation, gene expression and behavior of TMX2-28 result from a combination of the processes described above. Therefore, cell-line specific changes in methylation in response to 5-Aza-2'-deoxycytidine may result from variations in expression levels of DNMT1 or components of the proteasomal pathway. It may be useful to determine expression levels of these proteins or the presence of genetic mutations that may dictate a patient's response to 5-Aza-2'-deoxycytidine therapy.

The 5-Aza-2'-deoxycytidine-induced inhibition of proliferation, migration and adhesion in TMX2-28 could be partially due to the dependence on or constitutive activation of regulatory signaling pathways in this cell line resulting from loss of ER expression or tamoxifen exposure. Decreased methylation and re-expression of genes in growth inhibitory or negative feedback mechanisms may be induced by 5-Aza-2'-deoxycytidine. Constitutive activation of alternative signaling pathways is one of the Hallmarks of cancer cells that leads to sustained

proliferation.[7,8] Cell culture models of tamoxifen resistance have indicated that breast cancer cells can utilize other pathways to overcome the inhibition of estrogen signaling, such as the GPER and IGF1R pathways.[24,28] Previous studies in our lab demonstrated that TMX2-28 cells overexpress the S-phase kinase-associated protein 2 (SKP2). SKP2 regulates the cell cycle by targeting the CDK inhibitor, p27, for degradation and promotes cell cycle progression in TMX2-28.[39] TMX2-28 cells also have high expression of the Ras Homolog Gene Family Member, A (RhoA), which may contribute to their invasive behavior.[38] However, these genes were not identified as having significant changes in methylation induced by 5-Aza-2'-deoxycytidine. But it is likely, that the expression of many genes is altered by treatment with 5-Aza-2'-deoxycytidine and a global measurement of changes in mRNA expression after treatment would be beneficial.

The specific role of TROP2 in regulating the response of TMX2-28 cells to treatment with 5-Aza-2'-deoxycytidine could be investigated further by knockdown and overexpression studies. Therefore, I will create a stable TMX2-28 cell line with increased expression of *TACSTD2*, which will mimic the effect of 5-Aza-2'-deoxycytidine treatment. I will also generate an MCF-7 cell line with decreased *TACSTD2* expression. I predict these cells will behave similar to TMX2-28 cells, which have low expression of TROP2 under normal growth conditions. These cell lines will help to further investigate the role of TROP2 in regulating proliferation, adhesion and migration in tamoxifen resistance.

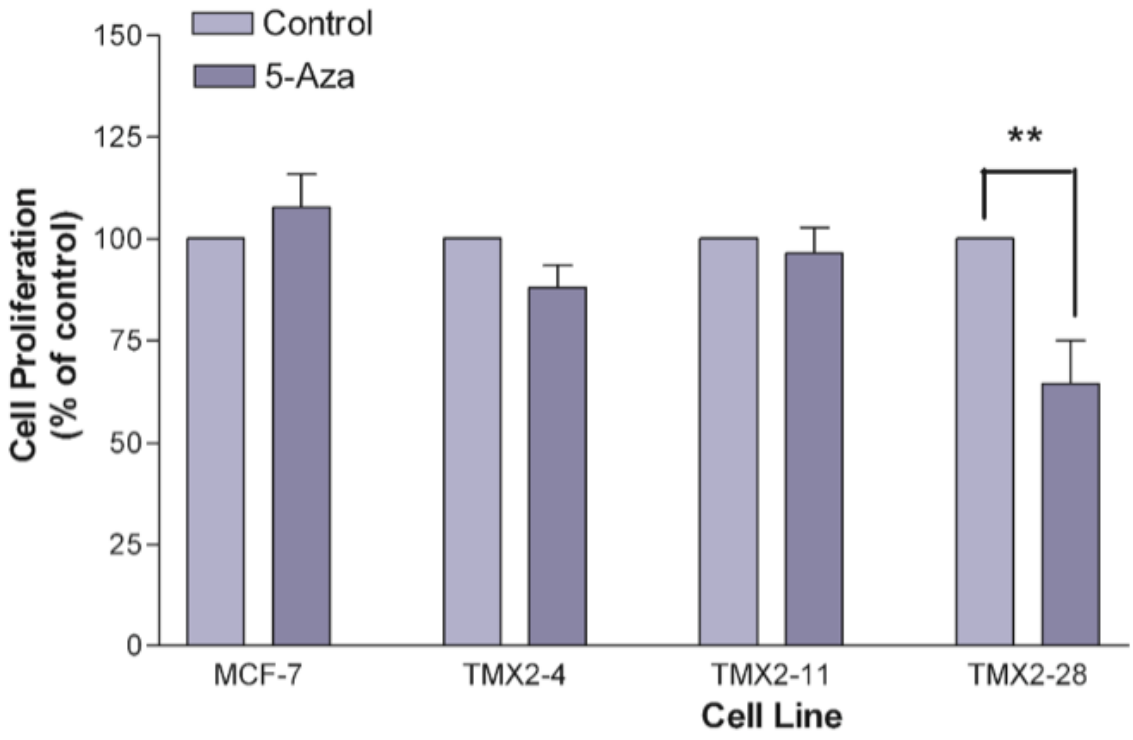

Figure 3.1: Treatment With 5-Aza-2'-deoxycytidine for 96 Hours Decreases Proliferation in TMX2-28. Cell proliferation in 96-hr. Aza treated cells, represented as percentage of control, determined by MTS assay for the parental cell line and each of the tamoxifen-resistant cell lines ($n = 3$, $p \leq 0.001$).[102]

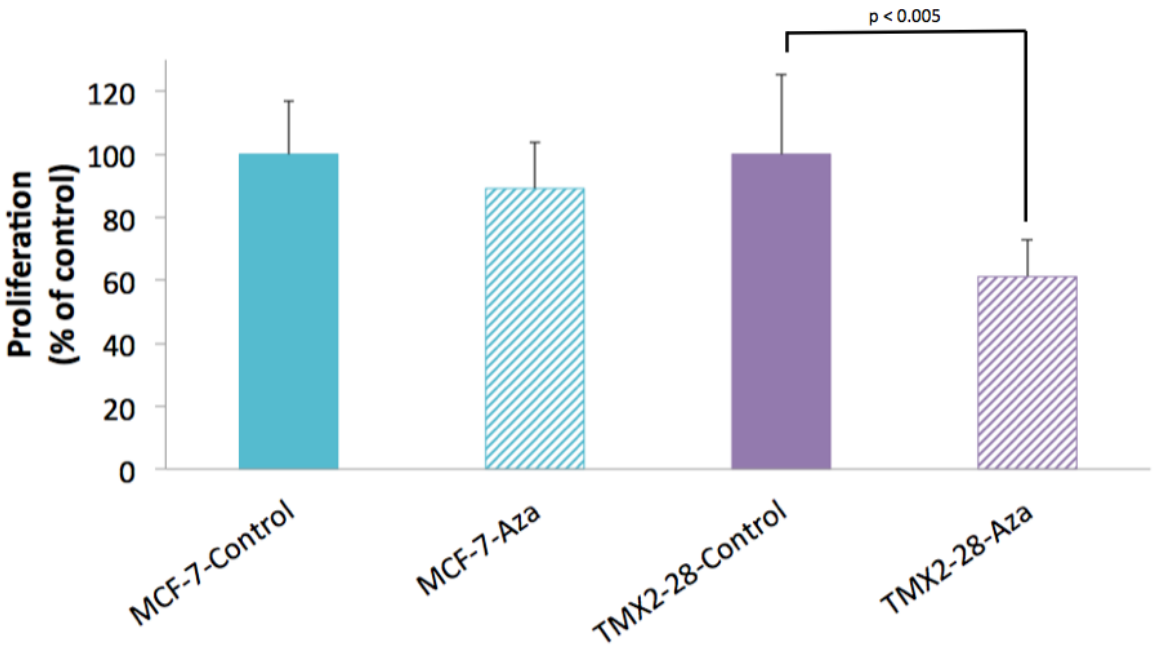

Figure 3.2: 5-Aza-2'-deoxycytidine Treatment Decreases Proliferation in TMX2-28. Proliferation, determined by MTS assay, in control and 120-hour 5-Aza-2'-deoxycytidine-treated cells (n = 8). Data represented as percentage of control, for the parental line, MCF-7, and the ER-Negative tamoxifen-resistant cell line, TMX2-28.

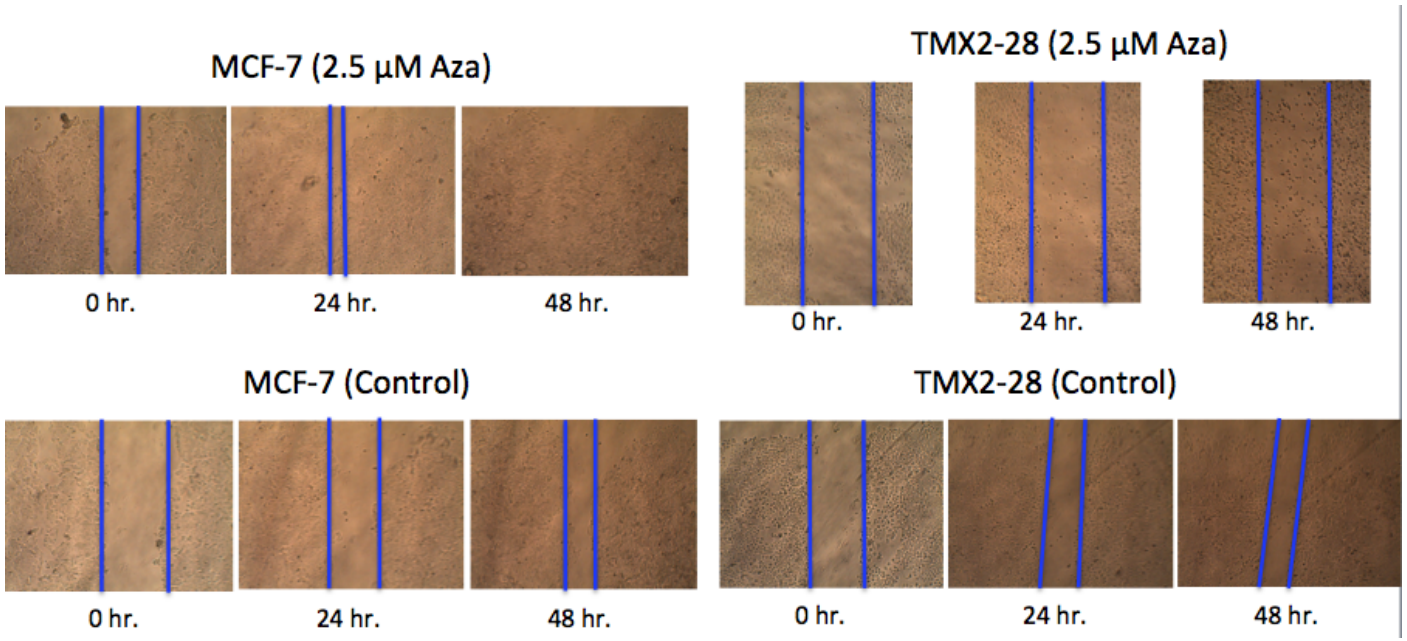

Figure 3.3: 5-Aza-2'-deoxycytidine Treatment Inhibits Migration in Scratch/Wound Assay in TMX2-28. Images from the MCF-7 (A) and TMX2-28 (B) Aza-treated and control wells at the time of the scratch (0 hrs.), 24 and 48 hrs. Wound boundaries are marked with vertical blue lines (cells are growing in a monolayer outside the lines, the center area between the lines is the location of the wound and is free of cells).

(A) **(B)**

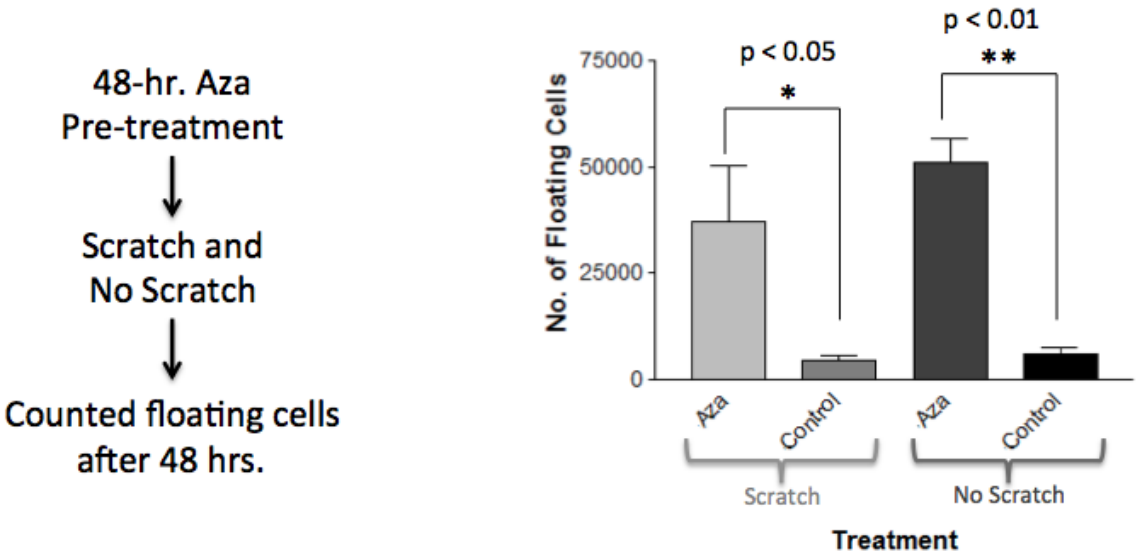

Figure 3.4: 5-Aza-2'-deoxycytidine Treatment Results in Detachment of Cells Independent of Scratch. Schematic of experimental design (A). Average number of floating TMX2-28 cells/well (n = 3) for control and Aza-treated cells either with or without the scratch, planned t-test (B).

(A) **(B)**

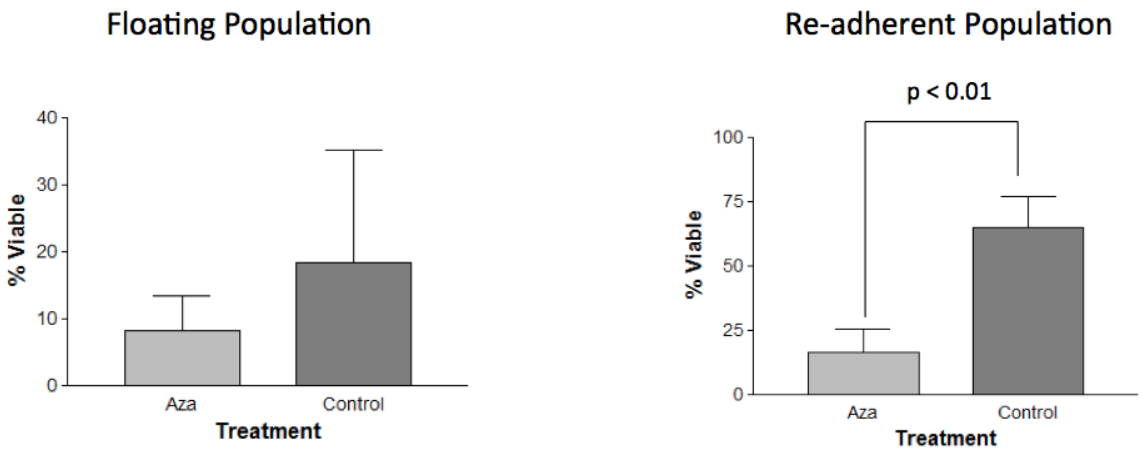

Figure 3.5: 5-Aza-2'-deoxycytidine Treatment Decreases Viability in TMX2-28. TMX2-28 cells were pre-treated with DMSO-control or 5-Aza-2'-deoxycytidine media for 48 hours. At 48 hours, the spent media, containing detached cells, from each well (n=3) was transferred to a new well. Cells were cultured for 8 days and the viability of cells that were capable of re-adhering and those that were floating was determined by staining with trypan blue. Percentage of viable TMX2-28 cells in the floating population (n = 3) (A) and the re-adherent populations (n = 3) (B), planned t-test.

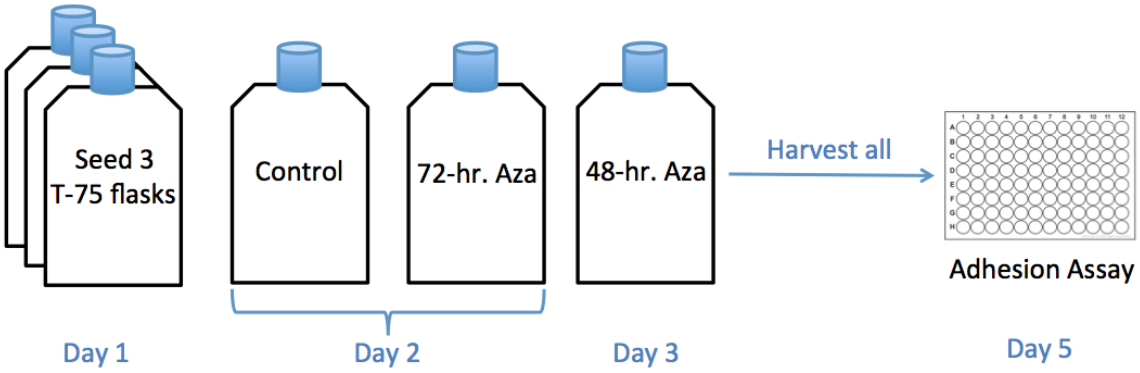

Figure 3.6: Schematic of Experimental Design for 5-Aza-2'-deoxycytidine Treatment and Adhesion Assay. Cells were seeded into three T-75 flasks (Day 1). The 72-hour treatment with vehicle control or 2.5 μM 5-Aza-2'-deoxycytidine began for two of the flasks on Day 2. On the following day (Day 3) the 48-hour treatment with 5-Aza-2'-deoxycytidine began for the third flask. Two days later (Day 5), cells from each flask were harvested, counted and seed into a 96-well fibronectin-coated plate at 20,000 cells/well. (Remaining cell pellets were saved and stored at -80°C). Cells were allowed to adhere to the fibronectin-coated plate for 30 minutes, washed and stained with crystal violet, as described previously.

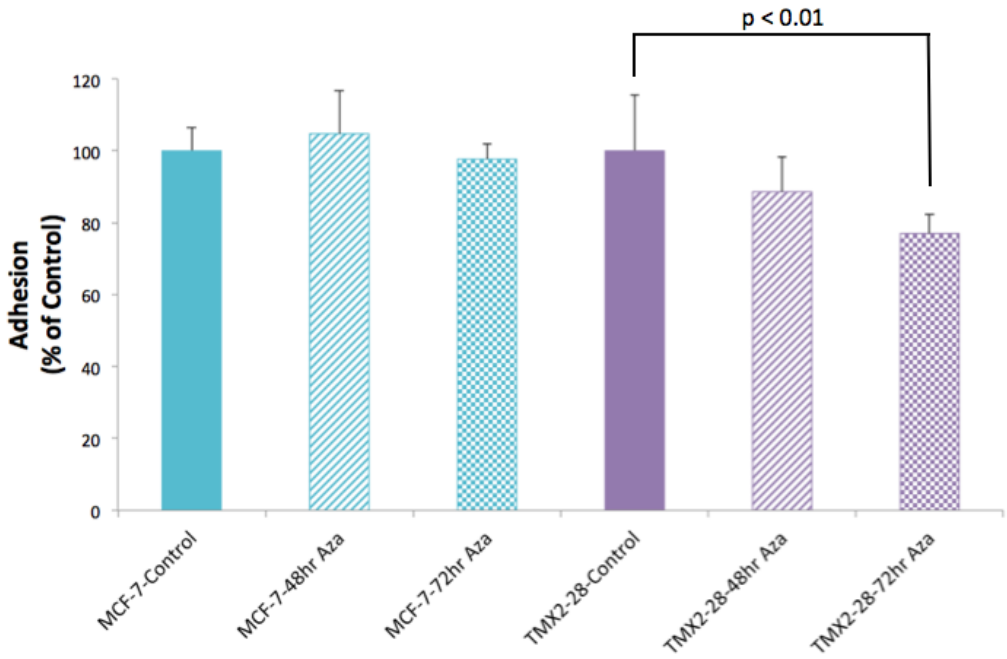

Figure 3.7: 5-Aza-2'-deoxycytidine Treatment Decreases Adhesion in TMX2-28. Adhesion to fibronectin-coated plate represented as percentage of control for MCF-7 and TMX2-28 control- and 5-Aza-2'-deoxycytidine-treated cells (n = 8), for adherent cells only.

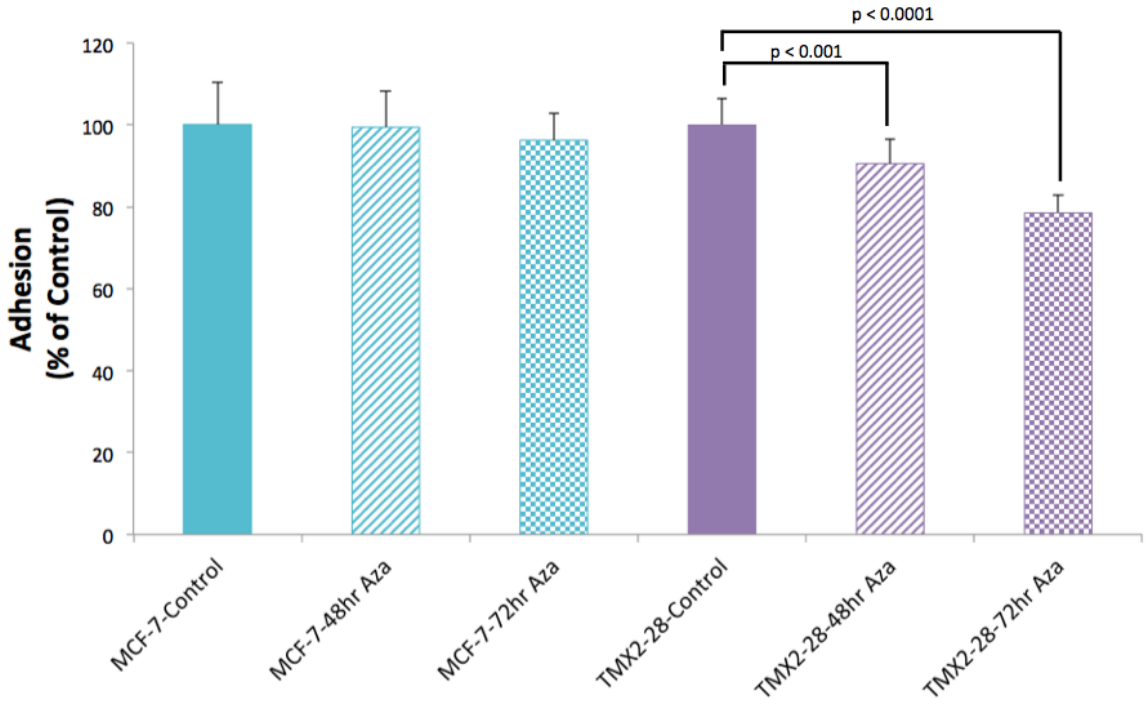

Figure 3.8: 5-Aza-2'-deoxycytidine Treatment Decreases Adhesion in TMX2-28 (n = 16). Adhesion to fibronectin-coated plate represented as percentage of control for MCF-7 and TMX2-28 treated with control DMSO or 5-Aza-2'-deoxycytidine for 48 or 72 hours (n = 16).

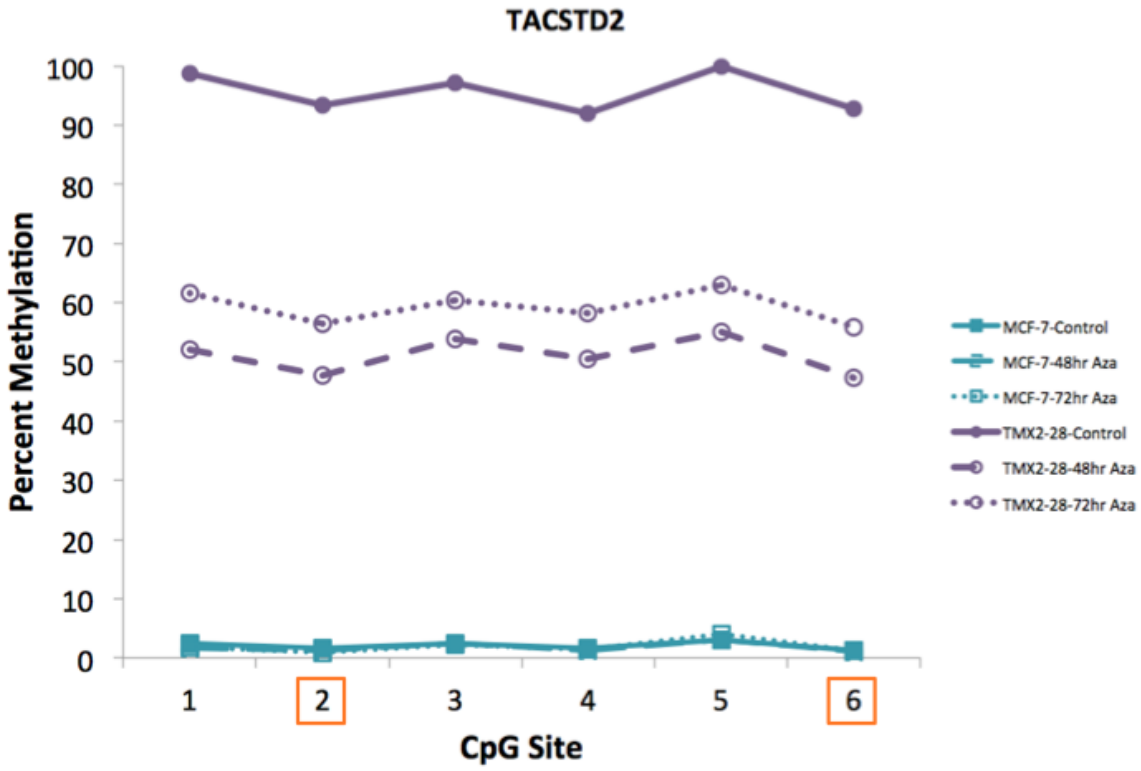

Figure 3.9: 5-Aza-2'-deoxycytidine Treatment Decreases Promoter Methylation of *TACSTD2*. DNA methylation of six CpG sites in the promoter region of *TACSTD2* determined by pyrosequencing for control and 5-Aza-2'-deoxycytidine treated cells from the adhesion assay experiment (see Figures 3.6 and 3.8). Orange boxes indicate CpG sites identified as differentially methylated on the HM450 BeadChip.

CHAPTER 4

THE ROLE OF TROP2 IN REGULATION OF ADHESION, MIGRATION AND PROLIFERATION IN TMX2-28

Introduction

According to the Human Methylation BeadChip, the *TACSTD2* promoter is hypermethylated in TMX2-28 (Table 2.8 and Figure 2.8) and correspondingly TROP2 expression is downregulated (Figure 2.9) indicating that promoter methylation may regulate gene expression in the ER-negative, tamoxifen-resistant cell line. Interestingly, *TACSTD2* expression is regulated by promoter methylation in lung adenocarcinoma.[61] The authors found that treatment of lung cancer cell lines with 5-Aza-2'-deoxycytidine decreased methylation and increased expression of TROP2 in lung cancer cell lines. They also observed *TACSTD2* methylation and low expression of TROP2 in lung adenocarcinoma tissue. Forced expression of TROP2 inhibited AKT and ERK activation, inhibiting proliferation and colony formation. *TACSTD2* also appears to be methylated in primary prostate tumors[103] and stomach cancer cell lines.[104] Therefore, I wanted to determine the extent to which expression of TROP2 in TMX2-28, induced by decreased promoter methylation, was responsible for the decrease in proliferation, adhesion and migration in 5-Aza-2'-deoxycytidine-treated TMX2-28 cells.

Previous studies in our lab have shown that, compared to the parental line, MCF-7, TMX2-28 cells have increased cell cycle progression, migration and invasion.[74,75] In my experiments with control DMSO- and 5-Aza-2'-deoxycytidine-

treated cells (Figure 3.8), both MCF-7 and TMX2-28-DMSO-treated cells have similar adhesion to fibronectin. However, in response to 5-Aza-2'-deoxycytidine, TMX2-28 cells have decreased proliferation, adhesion and migration (Figures 3.2, 3.3 and 3.4). While 5-Aza-2'-deoxycytidine affects only migration of MCF-7. MCF-7 cells treated with 5-Aza-2'-deoxycytidine have increased migration determined by scratch-wound assay (Figure 3.3). If the changes in proliferation, adhesion and migration in TMX2-28 that result from 5-Aza-2'-deoxycytidine treatment are caused by the increase in TROP2 expression, I predict that forced expression of TROP2 in TMX2-28 will inhibit proliferation, adhesion and migration (Table 4.1). Subsequently, I predict that knockdown of Trop2 in MCF-7 will increase proliferation, migration and adhesion.

Although TROP2 expression seems to inhibit cell growth and proliferation in lung cancer, [61] it promotes growth in other cell types. TROP2 overexpression increases growth of human colon and ovarian cancer cell lines and knockdown inhibits growth in MCF-7 and colon cancer cell lines. [64] TROP2 also appears to be involved in regulating cell adhesion and migration. As with the proliferation data in the literature, TROP2 seems to have a cell type-specific effect on adhesion and migration. In the developing mouse kidney, cells with high TROP2 expression have decreased adhesion to collagen-coated plates along with decreased motility. [105] However, TROP2 acts to promote detachment from the extracellular matrix (ECM) and increase migration in prostate cancer cells. [64,106] In these cells, TROP2 interacts with $\alpha_5\beta_1$ integrin, causing $\alpha_5\beta_1$ integrin and talin to relocalize from focal adhesions to the leading edge of the cell. This results in increased Ras-related C3 botulinum

toxin substrate 1 (Rac1) GTPase and p21 protein (Cdc42/Rac)-activated kinase 4 (PAK4) activity, which increases focal adhesion turnover and promotes migration.[64] Cell migration requires the cyclic assembly, maturation and disassembly of focal adhesions and involves a variety of proteins and signaling molecules, which facilitate integrin attachment to the ECM and the regulation of tension in the cytoskeleton.[107] TROP2 also appears to promote migration in the human laryngeal carcinoma cell line, Hep2, as knockdown inhibits migration and invasion.[108] TROP2 promotes migration and anchorage independent growth in mouse pancreatic cells.[59] Given the variable results in the literature, I wanted to determine how TROP2 affects proliferation, adhesion and migration in our model of tamoxifen resistance. Specifically, I wanted to test the hypothesis that increased TROP2 expression in TMX2-28, induced by 5-Aza-2'-deoxycytidine, was responsible for the decrease in proliferation, adhesion and migration.

To test this hypothesis, I first generated stable cells with either increased TROP2 expression or decreased TROP2 expression. Increasing TROP2 expression in TMX2-28, which has low endogenous TROP2 expression, should mimic the effect of 5-Aza-2'-deoxycytidine treatment, which increases TROP2 expression as a result of decreased promoter methylation. Knockdown of TROP2 in the parental cell line, MCF-7, will help to validate the role of TROP2 in regulating proliferation, adhesion and migration. Next, I quantifed proliferation, adhesion and migration in the overexpression, knockdown and control vector-transfected cell lines. I predicted that the TMX2-28 cell line with increased expression of TROP2 would have decreased proliferation, adhesion and migration while knockdown of TROP2

expression would increase proliferation, adhesion and migration in MCF-7 cells (Table 4.1).

Additionally, I examined *TACSTD2* methylation and TROP2 expression in clinical breast cancer samples. The results from the clinical samples will indicate whether the tissue culture model is an accurate representation of methylation and expression patterns in human disease. Human tissue samples were collected in collaboration with Baystate Medical Center (Springfield, MA) and analyzed on the Human Illumina 450 BeadChip for DNA methylation and formalin-fixed paraffin-embedded (FFPE) tumor blocks were analyzed for protein expression of hormone receptors (ER, PR and HER2), the proliferation marker, Ki67, and TROP2. Based on the methylation data for *TACSTD2* in the cell lines, I predict that ER-positive primary tumors that recur as ER-negative tumors will have methylation and expression of TROP2 similar to that of TMX2-28 (Table 4.2). This is because TMX2-28 cells were derived from the ER-positive, MCF-7 cell line, treated with tamoxifen and subsequently lost ER expression. If TROP2 expression is regulated by promoter methylation as seen in the ER-negative, tamoxifen-resistant cell line, TMX2-28, I predict samples with high promoter methylation will have low protein expression. Conversely, I predict samples will low promoter methylation will have high protein expression.

There is some evidence that TROP2 expression in clinical samples is associated with prognosis, tumor grade and proliferative index. In breast cancer, membrane localization of TROP2 (indicative of mature glycosylation) is associated with a poor prognosis.[65] In the same study, researchers found that intracellular

TROP2 localization was associated with a favorable prognosis.[65] A study that examined 32 breast cancer samples found that TROP2 expression was significantly higher in the ER-negative/HER2-positive tumors.[109] However, another study analyzing TROP2 expression in 423 breast cancer patients found TROP2 expression was associated with ER and HER2 expression. These authors also found TROP2 expression was correlated with expression of genes that promote cell cycle progression.[60] Similarly, high TROP2 expression is associated with high Ki-67 expression in the fetal rat lung[110] and human cervical cancer[111] and high grade gliomas.[112] Therefore, I predict tumors with high levels of Ki67 will have high expression of TROP2. Similarly, high TROP2 expression is linked to disease progression in colon cancer.[113] Analogously, a study examining TROP2 expression in invasive ductal carcinoma and adjacent normal tissue found high TROP2 expression was correlated with CyclinD1 expression, high tumor grade, lymph node metastasis and distant metastasis.[114] Similar studies in colon cancer found high TROP2 expression was associated with liver metastasis[115] and decreased survival.[116] Therefore, I predict the recurrent breast cancer samples will have increased expression of TROP2 while the non-recurrent samples should have decreased expression of TROP2. My predictions for the tumor samples based on the literature are outlined in Table 4.3.

Examination of *TACSTD2* methylation and expression patterns of TROP2 in clinical breast cancer samples will validate the tissue culture study experiments. This will help determine whether the same trends in our ER-negative, tamoxifen-resistant cell line model are also present in clinical samples. This will confirm

whether targeting TROP2 and *TACSTD2* methylation should be investigated as a therapeutic option for tamoxifen-resistant disease.

Materials and Methods

Cell culture: MCF-7 cells were purchased from the American Type Culture Collection (ATCC). TMX2-28 cells were provided by John Gierthy (Wadsworth Center Albany, NY). Cells were grown in Dulbecco's modified eagle medium (without phenol red). Medium was supplemented with 5% cosmic calf serum (Hyclone Cat. No. SH30087.03), 2.0 mM of L-glutamine, 0.1 mM of nonessential amino acids and 250 ng/mL of insulin. Cells transfected with the TROP2 knockdown or overexpression constructs were maintained in medium as described above supplemented with 300 µg/mL G418 disulfate salt (Sigma Aldrich, Cat no. A1720). Cells were maintained at 37°C, 5% CO_2 in a humidified incubator and passaged at subconfluence or media exchanged every 2 days.

Bacterial Transformation: The following vectors were received from the Alberti Lab: pSUPER (empty, control vector), hTrop-2siRNA#19 (knockdown construct), pΔEYFP-N1 (empty, control vector) and hTrop2 in pΔEYFP-N1 (overexpression construct). The vectors were reconstituted in 100 µL of TE buffer. One Shot TOP10 Chemically Competent *E. coli* (Invitrogen / Life Technologies, Carlsbad, CA) were transformed according to manufacturer's protocol. Briefly, cells were thawed on ice. 1 µL of DNA was added to 20 µL of competent cells and incubated on ice for 20 min. The cells were then heat shocked for 30 sec. at 42°C and incubated on ice for 2 min. 250 µL of pre-warmed S.O.C. medium was added to

each vial and the vials were incubated at 37°C in a shaking incubator for 30 min. 50-70 µL of transformation was plated on a pre-warmed selective plate and incubated overnight at 37°C. Single colonies were selected and grown in 2 mL LB broth supplemented with antibiotic overnight in a shaking incubator at 37°C. DNA was isolated using the STET Miniplasmid Prep Protocol.

STET Miniplasmid Prep: 1,500 µL of bacterial suspension was transferred to a new tube and centrifuged for 2 min. at 15,000 rpm. The supernatant was discarded and the pellet was resuspended in 140 µL of STET buffer (8% sucrose, 5% Triton-X, 50 mM EDTA and 50 mM Tris-HCl, pH8) and vortexed. 10 µL of lysozyme (Sigma-Aldrich, St. Louis, MO) (10mg/mL) was added and samples were boiled for 60 sec. Samples were then centrifuged for 10 min. at 15,000 rpm. A toothpick was used to remove and discard the pellet then 150 µL of isopropyl alcohol was added and vortexed. The samples were centrifuged for 10 min. at 15,00 rpm and the supernatant was discarded. The pellet was resuspended in 70% ethanol and centrifuged for 10 min. at 15,000 rpm. The supernatant was discarded and the pellet was resuspended in 30 µL of water.

Restriction Enzyme Digest and Gel Electrophoresis: A single restriction digest was used to determine the approximate size of the plasmid isolated from each bacterial colony. XbaI with NEB4 and BSA (New England Biolabs, Ipswich, MA) was used for pSUPER plasmids. StuI with NEB4 was used for pΔEYFP-N1 plasmids. 0.5 µL of RNaseA (20 mg/mL)(Invitrogen, Carlsbad, CA) or 1 µL of RNaseA (10 mg/mL)(Thermo Scientific, Waltham, MA) was added to each 50 µL sample after the

digest was complete. Products from the restriction enzyme digest were run on a 1% agarose gel at 100 V for 1 hr. 30 min.

TROP2 Knockdown/Overexpression: TMX2-28 or MCF-7 cells were seeded one day prior to the transfection in a 6-well plate such that they reached 40% confluence on the day of the transfection. MCF-7 cells were transfected with 5 μg of either pSUPER (empty, control vector) or hTrop2-siRNA#19 (knockdown construct) plus 200 ng of pΔEYFP-N1 (contains G418 selection marker). TMX2-28 cells were transfected with 2 μg of pΔEYFP-N1 (empty, control vector) or pΔEYFP-N1-hTrop2 with SuperFect (Qiagen no. 301305) per manufacturers instructions. Briefly, 2-5 μg of DNA were diluted in 100 μL serum-free media. SuperFect transfection reagent was then added to the DNA solution and vortexed for 10 sec., the solution was then incubated at room temperature for 5-10 min. to allow for complex formation. Then 600 μL of regular growth medium was added to the complex solution, mixed by pipetting up and down twice and transferred directly to the cells (which were rinsed with PBS prior to addition). The cells were incubated with the transfection complexes for 2-3 hours at 37°C, 5% CO_2 in a humidified incubator. Then fresh regular growth medium was added to each well and the cells were allowed to grow for 24 – 48 hours. After this time, the spent medium was exchanged with selective media containing 300 μg/mL of G418 disulfate salt (Sigma Aldrich, Cat no. A1720). Cells were maintained in G418 selection media until there was a sufficient amount to count and seed for colony isolation with the medium exchanged every 2-3 days.

Colony Isolation with Cloning Cylinders: Cells were seeded in a 6-well plate at a density of 1,000 – 2,000 cells/well and cultured in selective media until colonies

were a sufficient size to harvest and visible by eye (300+ cells). Desired colonies were isolated using cloning cylinders. Briefly, colonies were marked on the bottom of the plate with a marker and spent media from the well was aspirated, wells were rinsed with PBS. After rinsing and aspirating PBS, a cloning cylinder with vacuum grease on the edge was placed around the colony. Cells were harvested with trypsin and transferred to a single well of a 96-well plate containing 200 µL of selection media and cultured overnight at 37°C, 5% CO_2 in a humidified incubator. On the following day, the spent media was exchanged for fresh selective media and cells were cultured until confluent, with media exchanged as needed. Cells were then transferred to successively larger growth-area plates until there were enough cells to transfer to flasks for RNA isolation or cryopreservation.

RNA Isolation: RNA was isolated per manufacturers protocol using TriReagent (Molecular Research Center, Inc. Cat. No. TR118). Purified RNA was quantified using a NanoDrop 8000 (Thermo Scientific).

Two-Step Reverse Transcriptase PCR (RT-PCR): Changes in gene expression were confirmed by two-step RT-PCR. RNA was reverse transcribed using the High-Capacity cDNA Reverse Transcription Kit (Applied Biosytems) supplemented with the RNase Inhibitor, RNasin (Promega). cDNA was quantified using a NanoDrop 8000 (Thermo Scientific) and diluted to 50 ng/µL. Primers for RT-PCR were designed to span an exon-exon junction using Primer-BLAST (NIH) (Table 2.1). RT-PCR was conducted using the FastStart Universal SYBR Green Master (with Rox Reference Dye) (Roche) on the Stratagene MxPro (Mx3005P, Agilent). Relative

mRNA expression will be quantified using the Standard Curve Method normalized to beta-actin or by comparison of cycle thresholds.

Proliferation Assay: Cells were seeded in a 96-well plate at 5,000 cells/well. At the time of the assay, 20 μL of Cell Titer 96® Aqueous One Solution (Promega, Madison, WI) was added to each well containing 100 μL of growth media. The plate was then incubated at 37°C, 5% CO_2 for 1 hr. 30 min. Absorbance at 490 nm was read on a VersaMax Tunable Microplate reader (Molecular Devices, Sunnyvale, CA). Cell proliferation was quantified as a percentage of the control for each cell line.

Migration Assay: Cells (5×10^4 total, n = 3) were seeded in basal medium (DMEM) in the top chamber of the transwell inserts (BD 8 μm pore size PET track-etched membranes, Becton Dickinson, Franklin Lakes, NJ). Rich medium (DMEM supplemented with 10% FBS) was added to the bottom of the chamber as a chemoattractant. Cells were maintained for 28-30 hours at 37°C, 5% CO_2 in a humidified incubator. Media was removed from the top of the inserts and the inserts were washed by dunking in PBS twice. Non-migratory cells were removed from the top of the membrane insert using a Q-tip soaked in PBS, the stick-end of a Q-tip cut in half soaked in PBS and a dry Q-tip. The migratory cells on the bottom of the insert were then fixed for 10 min. in cold methanol at -20°C and washed by dunking in PBS twice. The cells were then stained with Hematoxylin QS (Vector Laboratories, Burlingame, CA, Cat. No. H-3404) for 8 min and washed by dunking in 3 separate beakers of tap water, leaving them in each one for a few seconds. The inserts were then allowed to dry for approximately 15 min. After 15 min., the membranes were carefully cut out using a razor blade and mounted to slides using

Cytoseal XYL (Thermo Fisher Scientific, Waltham, MA, Cat. No. 8312-4). Numbers of migratory cells were determined from four non-overlapping images of each membrane (10x objective).

Adhesion Assay (pre-coated plates): Cells were seeded in a 96-well plate pre-coated with human fibronectin (Corning, Bedford, MA) at 20,000 cells/well and incubated at 37°C, 5% CO_2 for 1 hour. Shaking the plate on a plate shaker for 10-15 sec displaced non-adherent cells. The cell suspension was then removed and the wells were washed three times with 100 µL of wash buffer (0.1% BSA in serum-free media). The cells were fixed by incubating with 100 µL of 4% paraformaldehyde in PBS for 10-15 min. The wells were then washed with wash buffer, which was removed by dumping out and tapping the plate on the bench. The cells were stained with 5 mg/mL crystal violet in 2% ethanol for 10 min. The staining solution was removed and the plates were washed three times by submerging in water and discarding the wash. Excess water was removed by tapping the plate on the bench and the plate was dried for at least 24 hours. After the plate dried, 100 µL of 1% SDS was added to each well and incubated at room temperature for 30 min. Absorbance at 550 nm was read on a VersaMax Tunable Microplate reader (Molecular Devices, Sunnyvale, CA). Cell adhesion to fibronectin was quantified as a percentage of the control for each cell line.

Immunohistochemistry (IHC): Cells were seeded on poly-L-lysine (PLL)-coated slides (Polysciences, Cat. No. 22247, Warrington, PA) at a density of approximately 2 x 10^5 cells/mL/slide. Cells were maintained at 37°C, 5% CO_2 in a humidified incubator overnight and fixed approximately 24 hours later. First, the

slides were rinsed with cold phosphate-buffered saline solution (PBS) twice and then fixed in ice cold 100% methanol for 10 min. The slides were then allowed to dry and stored at -20°C until stained. Immunohistochemical staining was performed at Baystate. The slides were stained for TROP2 (Human TROP-2 affinity purified polyclonal antibody, R&D Systems, Cat. No. AF650) using the HRP-DAB Cell and Tissue Staining kit (R&D Systems, Cat. No. CTS008).

Formalin-fixed paraffin-embedded (FFPE) tissue blocks were prepared from the breast tumor samples. The blocks were sectioned (5μm thick) and placed on slides. Using the UltraView Universal DAB Detection Kit on the BenchMark Ultra platform, the slides were stained for ER, PR and HER2. The slides were stained for TROP2 (Human TROP-2 affinity purified polyclonal antibody, R&D Systems, Cat. No. AF650) using the HRP-DAB Cell and Tissue Staining kit (R&D Systems, Cat. No. CTS008). Hematoxylin and eosin (H&E) slides were prepared and used for tumor verification. The antibodies used for ER, PR and HER2 were previously optimized: ER (Ventana anti-estrogen receptor SP1 rabbit monoclonal primary antibody), PR (Ventana anti-progesterone receptor 1E2 rabbit monoclonal primary antibody) and HER2 (Ventana PATHWAY anti-hER2/neu antibody 4B5 rabbit monoclonal antibody). Ethanol was used to dehydrate the slides followed by xylene post-staining and addition of coverslips. The Ki67 data were obtained from the pathology records.

Review of Pathology: Scoring of slides was conducted by one anatomic pathologist (Rahul Jawale). Slides were scored blindly for immunoreactivity of 5 antigens; approximate number of positive cells was recorded (%) and intensity of

immunoreactivity was reported. For ER and PR, Allred scored were recorded ranging from 0-8. Tumors with a score of 3 or greater were considered positive for receptor status and tumors were considered HER2 positive when 30% of the cells contained 3+ membrane staining. Ki67 scored ranged from 0-100% as the percentage of positive cells within the area of invasive cells. For TROP2, the scale for percent positive cells was 0: negative, 1: 1-33%, 2: 34-66% and 3:67-100% and the intensity was reported as a score from 0 (negative) to 3 (strong), this was recorded for both membrane-localized TROP2 and cytoplasmic TROP2. The overall score for membrane-localized TROP2 was determined by multiplying the percent positive score by the intensity score (range 0-9). Scoring of TROP2 was completed in one session with a single observer documenting records (SZ). One of the tumor samples was scored twice for TROP2 with similar results.

Results

Overexpression of TROP2 Alters Adhesion and Migration in TMX2-28, Not Proliferation

To mimic the effect of 5-Aza-2'-deoxycytidine treatment on TMX2-28 and increase TROP2 expression, a stable cell line with increased TROP2 mRNA expression (TMX2-28-Trop2) was generated as described above. A stable cell line expressing the control vector without the TROP2 coding sequence was also generated (TMX2-28-Control). As determined by RT-PCR, TROP2 mRNA expression increased by more than 100% in TMX2-28-Trop2 compared to TMX2-28-Control (Figure 4.1, A). TROP2 expression in the cloned cell lines was examined by IHC. As

predicted, the MCF-7-Control cell line has higher expression of TROP2 than the TMX2-28-Control cell line. Transfection of MCF-7 with the TROP2 knockdown construct resulted in decreased TROP2 expression in the MCF-7-Trop2-Knockdown (MCF-7-Trop2-Kd) cell line. While transfection of TMX2-28 with the TROP2 expression construct resulted in increased expression of TROP2 in the TMX2-28-Trop2 cell line (Figure 4.1, B and C). If TROP2 is involved in the phenotype in response to 5-Aza-2'-deoxycytidine treatment, I predict TMX2-28-Trop2 to have decreased proliferation, adhesion and migration compared to TMX2-28-Control. Proliferation, adhesion and migration assays were carried out as described above. TMX2-28-Trop2 proliferation is slightly lower than TMX2-28-Control, but the difference was not significant (Figure 4.2). This experiment was repeated two times with similar results, representative data shown. However, there was a significant difference in adhesion to fibronectin with increased TROP2 expression. The TMX2-28-Trop2 cell line has increased adhesion to fibronectin (26%) compared to TMX2-28-Control (Figure 4.3). This experiment was repeated three times with similar results, representative data shown. Next, a transwell migration experiment was used to determine whether TROP2 overexpression affects cell migration. The TMX2-28-Trop2 cell line has over 6 times more migratory cells per membrane than TMX2-28-Control (Figure 4.4). This experiment was repeated twice with a similar trend in results, representative data shown.

Knockdown of TROP2 in MCF-7 Alters Proliferation Only

To further examine the role of TROP2 in regulating proliferation, adhesion and migration, stable cell lines were generated as described above by transfecting MCF-7 cells with either a vector containing the scrambled control shRNA (MCF-7-Control) or the shRNA sequence targeting TROP2 (MCF-7-Trop2-Kd). As determined by RT-PCR, transfection with the shRNA vector against TROP2 resulted in an 80% knockdown of TROP2 mRNA compared to MCF-7-Control (Figure 4.1). The knockdown was approximately 50% compared to non-transfected MCF-7. Decreasing TROP2 expression in MCF-7 cells should cause them to behave similar to TMX2-28. Knockdown of TROP2 in MCF-7 increased proliferation (25%), compared to MCF-7-Control (Figure 4.5). This assay was repeated twice with similar results, representative data shown. TROP2 knockdown in MCF-7 had a variable result on adhesion to fibronectin. In two out of three of the experiments, MCF-7-Trop2-Kd had decreased adhesion to fibronectin compared to MCF-7-Control. However in the third experiment, MCF-7-Trop2-Kd had increased adhesion to fibronectin (Figure 4.6). Therefore, the results from these experiments are inconclusive. Knockdown of TROP2 did not affect migration of MCF-7 cells, as there were only two migratory cells in the MCF-7-Control and two in the MCF-7-Trop2-Kd samples (n = 3) (data not shown).

Analysis of *TACSTD2* Methylation and TROP2 Expression in Clinical Samples

Patient Demographics

A total of 86 human breast tumor samples were identified in the repository of the pathology department at Baystate Medical Center. There were 70 primary and recurrent tumor samples collected from patients where the isolated DNA passed the quality control tests and was analyzed for DNA methylation on the Human 450 BeadChip. Therefore, I will limit my analysis to the 70 tumor samples (34 primary tumors and 36 recurrent) for which we have methylation data. Patient demographics are summarized in Table 4.4. The average age of the women at the diagnosis of the primary tumor was 56.6 years and the average age at recurrence was 64.1 years, with the average time to recurrence being 67.8 months (approximately 5.5 years). Tumor blocks were sectioned for IHC analysis of hormone receptors (ER, PR and HER2), the proliferation marker, Ki67, and TROP2. The majority (76.5%) of primary tumors are ER-positive, while only 52.8% of recurrent tumors are ER-positive. PR and HER2 status are summarized in Table 4.4. Data on hormone therapy was available for 23 of the 34 (68%) primary tumor samples. Sixteen patients (69.5%) received anti-hormonal therapy. Of those women treated with anti-hormonal therapy, nine received either tamoxifen alone or tamoxifen in combination with an aromatase inhibitor.

The tumor samples were organized into four groups based on the ER status of their primary and recurrent tumors (Table 4.5). The women in the first group had primary tumors that were ER-positive and recurrent tumors that were also ER-positive. The second group contains patients whose primary tumor was ER-

negative and their recurrent tumor was also ER-negative. The next group consists of patients whose primary tumor was ER-positive and their recurrent tumor was ER-negative. There are 8 women who did not have a recurrence as of December 2015, 6 had ER-positive tumors and 2 had ER-negative tumors.

TACSTD2 Methylation in Clinical Samples

To determine whether the trend of increased *TACSTD2* methylation observed in the ER-negative, tamoxifen-resistant cell line, TMX2-28, was consistent in the clinical samples, I examined methylation of *TACSTD2* in the human tumor samples. Average beta values from the 450 BeadChip were obtained for the CpG sites in *TACSTD2*. If TMX2-28 is an accurate model of ER-negative, recurrent disease, I predict promoter methylation to be high in ER-negative recurrent tumors that were initially ER-positive primary tumors.

I first examined methylation for all *TACSTD2* CpG sites on the 450 BeadChip in all tumor samples. Comparing ER-positive tumors to ER-negative tumors, there is no difference in methylation. The mean beta values for all *TACSTD2* CpG sites in ER-positive tumors and ER-negative tumors is 0.183 and 0.180, respectively (Figure 4.7, A and Table 4.6). Because there was little difference in methylation of all *TACSTD2* CpG sites on the chip, I did the same comparison using only CpGs in the promoter of *TACSTD2* (TSS200 or TSS1500) (Figure 4.7, B and Table 4.6). There was no difference in *TACSTD2* promoter methylation between ER-positive and ER-negative tumors. The mean beta value for promoter CpGs in ER-positive tumors and ER-negative tumors is 0.206 and 0.200, respectively. Next I compared methylation of

all *TACSTD2* CpG sites and promoter CpG sites between primary and recurrent tumors. The mean beta value for all *TACSTD2* CpG sites in primary tumors and recurrent tumors is 0.183 and 0.181, respectively (Figure 4.8, A and Table 4.6). The mean beta value for promoter CpGs in primary tumors and recurrent tumors is 0.207 and 0.200, respectively (Figure 4.8, B and Table 4.6). Because there were no differences in methylation by ER status or primary vs. recurrent tumors, I examined methylation of only the 3 *TACSTD2* CpGs identified as differentially methylated and altered by 5-Aza-2'-deoxycytidine in the cell lines.

Based on the methylation data from the cells lines, I predict that *TACSTD2* promoter methylation will be low in ER-positive primary tumors and high in ER-negative recurrent tumors that were initially ER-positive. Specifically, I examined methylation of the 3 CpGs identified as differentially methylated between MCF-7 and TMX2-28 and altered by treatment with 5-Aza-2'-deoxycytidine in TMX2-28 (MAPINFO numbers 59043370: CpG 1, 59043280: CpG 2 and 59043255: CpG 3) in the tumor samples (see Tables 2.5 and 2.8). Although the average beta values for each site were much lower than those in the cell lines, mean methylation of each site in the recurrent tumor was higher than the mean methylation in the primary tumors for patients in this group (Figure 4.9, A). The difference in beta values was statistically significant for CpG 1(one-tail p-value = 0.047, two-tail p-value = 094). CpG sites 2 and 3 followed the same trend with the ER-negative recurrent tumor having a higher average beta value than the ER-positive primary tumor (one-tail p-values of 0.27 and 0.075, two-tail p-values of 0.53 and 0.15, respectively). For each of the three CpGs, the mean average beta values were higher in the ER-negative

recurrent tumor than the ER-positive primary tumor. This result is in agreement with my prediction based on DNA methylation in TMX2-28.

Interestingly, there was no difference in the mean average beta value of these three CpGs in the group with ER-positive primary tumors that recurred as ER-positive (Figure 4.9, B). Methylation was lower in the ER-positive recurrent tumor than the ER-positive primary tumor for CpG 1 however; the difference was not statistically significant. Mean beta values for CpGs 2 and 3 were similar between primary and recurrent tumors for this group.

TACSTD2 methylation values were also similar in the group with ER-negative tumors that recurred as ER-negative (Figure 4.9, C). The ER-negative recurrent samples had lower methylation than the ER-positive primary samples for CpG 3 however; the difference was not statistically significant (two-tail p-value = 0.064).

There were eight patients who did not have a recurrence. Six of these tumor samples were ER-positive and two were ER-negative. The mean average beta values for CpGs 1, 2 and 3 for the non-recurrent samples were 0.0856, 0.2229 and 0.1214, (standard deviations were 0.027, 0.080 and 0.046), respectively. Average beta values ranged from 0.054 to 0.11 for CpG 1, 0.10 to 0.31 for CpG 2 and 0.070 to 0.19 for CpG 3.

Expression of TROP2 in Clinical Samples and Correlation with Promoter Methylation

Protein expression and localization (cytoplasmic and/or membrane) of TROP2 was determined in the tumor samples by IHC. TROP2 IHC data was obtained

for 66 of the 70 tumor samples for which we also have methylation data. There was not enough tumor block to score the remaining four samples. Examples of cytoplasmic and membrane TROP2 staining from two patients are shown in Figure 4.10. Expression of membrane-localized TROP2 was detected in 59 (89%) of the samples. The membrane TROP2 scores ranged from 0 to 9 (mean, 5.1) (descriptive statistics are summarized in Table 4.7) (Figure 4.11, A). Cytoplasmic TROP2 was found in 65 (98%) of samples. The scores for cytoplasmic TROP2 ranged from 0 to 9 (mean, 4.3) (descriptive statistics are summarized in Table 4.8) (Figure 4.11, B). If methylation regulates expression of TROP2 in human tissue, I predict that tumor samples will have an inverse correlation between methylation and protein expression.

To determine whether promoter methylation of the 3 CpGs identified as differentially methylated in TMX2-28 and altered by 5-Aza-2'-deoxycytidine treatment was correlated with TROP2 expression, I examined the correlation between the mean average beta value of CpGs 1, 2 and 3 and membrane-localized TROP2 expression for all of the tumor samples. I chose to test membrane TROP2 only because there was greater variability in membrane TROP2 expression between tumor samples and because membrane-localized TROP2 has been shown to have prognostic value in breast cancer.[65] There was no linear relationship between mean methylation of the three CpGs and expression of membrane-localized TROP2 (R squared = 0.0006).

TROP2 Expression in Clinical Samples

Although there was no correlation between mean methylation of CpGs 1, 2 and 3 and membrane TROP2 expression, I know that the ER-negative recurrent tumors had increased methylation at these three CpGs compared to their ER-positive primary tumors (Figure 4.9, A). If TROP2 expression is regulated by promoter methylation, I would predict the ER-positive primary tumors in this group to have higher expression of TROP2 than the ER-negative recurrent tumors. Therefore, I wanted to determine whether expression of membrane-localized TROP2 was different between the ER-negative recurrent tumors and the ER-positive primary tumors for this group. However, there was no difference in expression of membrane-localized TROP2 between the ER-positive primary tumors and their ER-negative recurrent tumors (mean membrane TROP2 scores of 5 and 4.7, respectively) (Figure 4.12).

Next, I wanted to examine expression of membrane- and cytoplasmic-localized TROP2 by ER/HER2 status. A previous report found that ER-negative/HER2-positive breast tumors had higher expression of TROP2 than ER-positive/HER2-negative tumors.[109] They did not distinguish between membrane and cytoplasmic localization. Therefore, I predict that TROP2 expression will be high in tumors that are ER-negative/HER2-positive. First I categorized the samples into groups based on ER/HER2 status: ER-negative/HER2-negative (n = 18), ER-negative/HER2-positive (n = 5), ER-positive/HER2-negative (n = 37) and ER-postive/HER2-positive (n = 6). Then I compared membrane and cytoplasmic TROP2 scores separately between the groups using one-way ANOVA. As predicted,

the ER-negative/HER2-positive tumor samples had higher expression of membrane-localized TROP2 (mean membrane TROP2 score of 7.4 compared to 4.3, 5.3 and 4.3), however the results from the one-way ANOVA were not statistically significant (p-value = 0.28) (Figure 4.13, A). Because I predicted that ER-negative/HER2-positive tumors would have higher TROP2 expression than ER-positive/HER2-negative tumors, I compared the membrane TROP2 scores between these two groups using a student's t-test. There is a trend in the direction I predicted that the ER-negative/HER2-positive samples have higher membrane TROP2 expression than ER-positive/HER2-negative samples (one-tail p-value = 0.103). However, there was no difference in cytoplasmic TROP2 expression between the groups (one-way ANOVA p-value = 0.21) (Figure 4.13, B).

TROP2 Expression and Recurrence

Based on previous reports that TROP2 expression is associated with disease progression, [113] metastasis[115] and recurrence[116] in colon cancer, metastasis in breast cancer[114] and membrane-localized TROP2 indicates a poor prognosis in breast cancer, [65] I predict that recurrent samples will have increased TROP2 expression and strong expression of membrane-localized TROP2. I then wanted to determine whether TROP2 expression could be used to predict recurrence or earlier recurrence. First, I compared both membrane and cytoplasmic TROP2 expression in the non-recurrent tumor samples (n = 8) to the primary tumors that recur (n = 26). Surprisingly, expression of membrane-localized TROP2 was higher in the non-recurrent samples than in the primary samples that recur (mean membrane TROP2

score of 8.4 compared to 4.4, respectively, two-tail p-value < 0.01) (Figure 4.14, A). Meanwhile, there was no difference in cytoplasmic TROP2 score between the non-recurrent samples and the primary samples that recur (Figure 4.14, B).

Because there is a wide range of TROP2 scores in the primary samples that recur, I wanted to determine whether TROP2 expression levels were correlated with time to recurrence. Linear regression analysis shows that for all primary tumors that have a recurrence (n = 26), there is no correlation with membrane or cytoplasmic TROP2 expression and time to recurrence in months (R squared = 0.006 and 0.02, respectively). All of the patients without a recurrence were diagnosed in either 2008 or 2009 and have a time to recurrence (current through December 2015) ranging from 85 to 95 months. Interestingly, they have high membrane TROP2 expression (mean = 8.4) but moderate cytoplasmic TROP2 expression (mean = 4.6).

TROP2 Expression, Tumor Grade and Ki67 Status

Several published studies indicate that TROP2 expression may be correlated with high tumor grade and increased proliferation.[60,110-114] Therefore, I wanted to investigate the relationship between TROP2 expression and tumor grade and Ki67 status. For these analyses, I considered only membrane-localized TROP2 because there was more variability in membrane-localized TROP2 expression than cytoplasmic. First, I categorized membrane TROP2 expression as low (IHC score ≤ 3) or high (IHC score > 3) (Figure 4.15, A). Then I compared tumor grade (Figure 4.15, B) and Ki67 score (Figure 4.15, C) for the two categories of membrane TROP2

expression. There was no difference between tumors with low and high expression of membrane TROP2 according to tumor grade (n = 22 and 40, respectively) or Ki67 score (n = 25 and 41, respectively) (student's t-test p-values = 0.30 and 0.66, respectively).

Discussion

Sustaining proliferation, promoting migration and altering cell adhesion are important characteristics of cancer cells involved in promoting tumor growth and facilitating invasion and migration. TROP2 is known to regulate several aspects of these processes in various cell types. The primary objective of this study was to determine whether TROP2 is involved in regulating proliferation, adhesion and migration in our cell line model of tamoxifen resistance. To accomplish this, a stable TMX2-28 cell line was generated with increased expression of TROP2 and a stable MCF-7 cell line was generated with decreased TROP2 expression. Next, I quantified cell proliferation, adhesion to fibronectin and migration for each of these cell lines compared to their respective control vector transfected cell line. The results from these experiments will help determine whether TROP2 mediates the effects of 5-Aza-2'-deoxycytidine treatment. These experiments will also help determine whether treatment with 5-Aza-2'-deoxycytidine would be beneficial for women with tamoxifen resistant breast cancer, since 5-Aza-2'-deoxycytidine increases TROP2 expression in TMX2-28.

Increasing TROP2 expression in TMX2-28 is predicted to mimic the effect of treatment with 5-Aza-2'-deoxycytidine and therefore inhibit proliferation, adhesion

and migration. However, TROP2 overexpression did not affect proliferation (Figure 4.2), there was only a slight decrease in proliferation of TMX2-28-Trop2. This agrees somewhat with a 2012 paper stating that lung cancer cells had decreased proliferation as a result of decreased AKT and ERK activation in response to increased TROP2 expression.[61] Although, there was only a slight decrease in TMX2-28-Trop2 proliferation, this could indicate that TMX2-28-Trop2 cells have a slight decrease in AKT and ERK signaling. This however, is in contrast to several other papers in the literature that found increased TROP2 expression promotes growth and proliferation. Increased TROP2 expression has been shown to promote the growth of colon and ovarian cancer cell lines as well as fibroblasts isolated from the fetal rat lung.[64,110] Increased TROP2 expression was also found to promote cell cycle progression via phosphorylation of ERK1/2 in mouse pancreatic cancer cells and cervical cancer cell lines.[59,111] Overall the results from this experiment indicate that TROP2 and TROP2-induced signaling does not affect proliferation of TMX2-28. Therefore, the decreased proliferation of TMX2-28 in response to 5-Aza-2'-deoxycytidine is not due to increased expression of TROP2. This indicates that TMX2-28 cells utilize a mechanism that is independent of TROP2 signaling to sustain proliferative signals.

Opposite of predicted results, increased TROP2 expression promotes adhesion and migration of TMX2-28 cells (Figure 4.3 and 4.4). This indicates that TROP2 is not responsible for the decrease in adhesion and migration of TMX2-28 in response to 5-Aza-2'-deoxycytidine. The results do however agree with the majority of results in the literature. TROP2 is required for invasion of colon cancer

cells.[117] Similarly, TROP2 promotes migration of mouse pancreatic cancer cells,[59] fibroblasts isolated from fetal rat lung[62] and cervical cancer cells.[111] In prostate cancer cells TROP2 increases migration on fibronectin via interacting with β_1 integrin and increasing focal adhesion turnover.[57] It is not known whether TROP2 interacts with β_1 integrin in TMX2-28-TROP2 cells. However, a more recent paper found that knockdown of TROP2 in prostate cancer cells increases FAK signaling and turnover of focal adhesions.[118] Therefore, I would predict that increased TROP2 expression would inhibit FAK signaling and promote the formation of stable focal adhesions. TMX2-28-Trop2 cells do have increased adhesion to fibronectin, but also increased migration, which requires turnover of focal adhesions. The same authors also found that TROP2 was present in exosomes, endosomal vesicles that are involved in creating a favorable pre-metastatic niche by facilitating transfer of genetic material and signaling molecules. The TROP2-positive exosomes promote migration of cells that lack expression of TROP2.[118] However, it is not known whether TROP2 is recruited to exosomes in TMX2-28-Trop2 cells. Conflicting with this evidence that TROP2 promotes migration and invasion, there are a few cases where TROP2 is inhibitory. Expression of TROP2 in TROP2-negative prostate cancer cells inhibits adhesion to fibronectin.[106] Fetal mouse kidney cells with high expression of TROP2 have decreased adhesion to collagen and decreased motility compared to cells with low TROP2 expression.[105] Although TMX2-28-Trop2 cells have increased adhesion to fibronectin and increased migration. Therefore, it would be important to determine the mechanism by which TROP2 promotes adhesion and migration in TMX2-28-Trop2 cells and also in other tamoxifen-

resistant cell lines. It would also be valuable to determine whether TROP2 interacts with β_1 integrin to alter focal adhesion signaling and dynamics as well as whether TROP2 is present in exosomes in TMX2-28-Trop2 cells.

MCF-7 cells with low TROP2 expression were expected to behave similarly to TMX2-28 cells, which normally have low TROP2 expression. Our lab has established that compared to MCF-7, TMX2-28 cells have increased proliferation, migration and invasion.[74,75] Additionally, knockdown of TROP2 in lung cancer cells increases activation of AKT, promoting tumor growth.[61] Therefore, my prediction was that knockdown of TROP2 in MCF-7 would increase proliferation and migration. MCF-7-Trop2-Kd cells indeed had increased proliferation (Figure 4.5) however; there was no change in migration. I would therefore predict that MCF-7-Trop2-Kd cells have increased AKT activation. Contradictory to these results, there are several groups that present evidence that knockdown of TROP2 decreases proliferation. Previously, knockdown of TROP2 was found to inhibit growth of MCF-7 cells and colon cancer cells.[64] This is in direct contradiction to the results presented here and could be a result of differences in tissue culture conditions. The MCF-7 cells in their study were grown in RPMI-1640 growth medium and it is not clear whether the medium contained phenol red, which can have estrogenic activity. The growth medium used in the experiments presented here did not contain phenol red. Knockdown of TROP2 also decreases proliferation in fetal rat lung cells, cervical cancer cells and laryngeal carcinoma cells.[62,108,110,111] Therefore, it would be interesting to compare the activity of signaling molecules downstream of TROP2 in these cell types, such as AKT and ERK.[54]

In two out of three adhesion assay experiments, MCF-7-Trop2-Kd had decreased adhesion to fibronectin (Figure 4.6). However, knockdown of TROP2 in MCF-7 increased adhesion in the third experiment. Therefore, I conclude that the results were inconclusive and knockdown of TROP2 has variable results on adhesion of MCF-7 cells to fibronectin. Experiments in prostate cancer cells in which TROP2 expression is knocked down found the cells had increased adhesion to fibronectin, indicating that TROP2 inhibits adhesion.[106] Similarly, cells in the fetal mouse kidney with high TROP2 expression had low adhesion to collagen-coated plates.[105] Therefore, I predicted MCF-7-Trop2-Kd cells to have increased adhesion to fibronectin. However, my results indicate that TROP2 knockdown does not alter or has a variable effect on adhesion in MCF-7. TROP2 is also known to affect FAK signaling, which is involved in regulating focal adhesion turnover. However, knockdown of TROP2 in prostate cancer cells results in an increase in the number of FAK-containing focal adhesions but not the total number of focal adhesions.[118] Therefore, I would expect to find more FAK-containing focal adhesions in MCF-7-Trop2-Kd cells and therefore increased FAK signaling leading to increased focal adhesion turn-over and slight decrease in adhesion because the cells are more migratory. However, it is not known whether knockdown of TROP2 in MCF-7 results in an increase in the number of focal adhesions that contain FAK.

Although *TACSTD2* expression appears to be regulated by promoter methylation in the cell lines, expression of TROP2 does not appear to be regulated by promoter methylation in the tumor samples, as there was no correlation between promoter methylation and expression determined by IHC. However, similarly to the

methylation results from the cell line model, methylation of the three CpGs in the *TACSTD2* promoter identified in the cell line model was higher in the ER-negative recurrent tumors compared to their ER-positive primary tumors (Figure 4.9, A). Despite the small sample size of this study, the difference in methylation between the ER-positive primary tumors and their ER-negative recurrent tumors was significant for CpG 1. In general, *TACSTD2* methylation for the tumor samples is much lower than the methylation values seen in the cell lines. However, these low methylation values may still be important for regulating gene expression, as they are within the range of previously reported differentially methylated CpGs in breast cancer.[119,120] It would be important to confirm these findings with a larger sample size.

Expression of membrane- and cytoplasmic-localized TROP2 was detected in nearly all tumor samples (89% and 98%, respectively). Despite a previous report indicating that membrane localization of TROP2 was associated with a poor prognosis for breast cancer patients and intracellular TROP2 was associated with better survival,[65] this was not the case in our sample cohort. Non-recurrent tumors had higher levels of membrane TROP2 than primary tumors with a recurrence (Figure 4.13, A). There was no difference in cytoplasmic-localized TROP2 between these groups (Figure 4.13, B). However, the sample size in the present study was particularly small especially for the non-recurrent tumors. Therefore, it would be important to verify these findings in a larger sample size. It is also important to consider that the published study used different antibodies to recognize TROP2 post-translational modifications and therefore distinguish between membrane-

targeted and intracellular TROP2.[65] In the present study, we used one antibody and visually distinguished membrane versus cytoplasmic TROP2 expression when scoring the IHC samples.

In agreement with a previous report analyzing TROP2 expression in 32 breast cancer samples,[109] I found that ER-negative/HER2-positive tumors had higher expression of membrane TROP2 than ER-positive/HER2-negative tumors. Although the increase in TROP2 expression was not significant, it was in the direction predicted according to the results in the literature.

Several studies in other tissues found high TROP2 expression was associated with disease progression, migration, recurrence and increased proliferation.[110-113,115,116] This lead me to predict that tumor samples with high TROP2 expression would have increased proliferation, high tumor grade, and a shorter time to recurrence. However, I found no association between membrane TROP2 expression and tumor grade, Ki67 score or time to recurrence (Figures 4.14, B and C). This may be a reflection of a small sample size or it may indicate that TROP2 signaling is acting in a different way in breast cancer than other types of tissue.

The role of TROP2 in breast cancer could be further investigated by analyzing expression of downstream signaling components that may be associated with disease recurrence and drug resistance. Increased TROP2 expression had been shown to increase expression of growth regulatory proteins including NF-κβ, RB, STAT1 and STAT3.[60] I would predict that those tumor samples with high TROP2 expression would also have increased expression and activity of these downstream effectors. However, the expression levels of these proteins in the tumor samples

analyzed here are not known. Given the discrepancy between the results presented here and some of those in the literature, it appears that TROP2 may have tissue-specific roles in carcinogenesis. Therefore, it will be important in the future to determine not only the subcellular localization of TROP2 but also expression of other downstream signaling components that may act to promote growth signaling in cancer cells.

Table 4.1 Summary of Previous Results and Predictions					
			Results from Previous Experiments and Chp. 3		
Cell Line	***TACSTD2* Promoter Methylation**	**TROP2 mRNA Expression**	**Cell Cycle Progression/ Proliferation**	**Adhesion**	**Migration**
MCF-7	Low	High	Moderate	Similar to TMX2-28	Low
TMX2-28	High	Low	Increased	Similar to MCF-7	Increased
			Results from Chp. 3		
MCF-7-Aza	Low	High (no change)	No Change	n/a	(2D) Increase
TMX2-28-Aza	Low	High	Decrease	Decrease	(2D) Decrease
			Predictions		
MCF-7-Trop2-Kd	n/a	Low	Increase	Increase	Increase
TMX2-28-Trop2	n/a	High	Decrease	Decrease	Decrease
			Results from Chp. 4		
MCF-7-Trop2-Kd	n/a	Low	Increase	No change	No change
TMX2-28-Trop2	n/a	High	No change	Increase	Increase

Table 4.2 Predictions for Tumor Samples Based on Cell Line Data		
	ER + Primary	**ER - Recurrence**
Cell line model	MCF-7	TMX2-28
TACSTD2 promoter methylation	Low	High
TROP2 Expression	High	Low

Table 4.3 Predictions for Tumor Samples Based on Literature*			
	Non-Recurrent	**Recurrent**	**ER+/HER2+**
TROP2 Expression	Low	High	High
TROP2 Localization	Membrane absent	Membrane	Membrane
Ki67 Status	Low	High	High
Tumor Grade	Low	High	High

* Predictions based on [60,65,110-116]

Table 4.4 Patient and Tumor Characteristics		
Age (in years) mean (SD) range		
At Primary	56.6 (12.3), 37 - 84	
At Recurrence	64.1 (12.6), 39 - 90	
Menopausal n (%)		
At Primary	13 (38%)	
At Recurrence	21 (58%)	
TTR[1] (in months) mean (SD) range	67.8 (59.5) 10-252	
Tumors		
	Primary[2] **(34)**	**Recurrent (36)**
ER status n (%)		
+	26 (76.5)	19 (52.8)
-	8 (23.5)	17 (47.2)
PR status n (%)		
+	20 (58.8)	16 (44.4)
-	14 (41.2)	20 (55.6)
HER2 status n (%)		
+	5 (14.7)	9 (25)
-	29 (85.3)	27 (75)
Ki67 IHC n (%)		
low (≤15)	26 (76.5)	20 (55.6)
high (>15)	8 (23.5)	16 (44.4)
Tumor Grade n (%)[3]		
0	5 (15.1)	5 (15.1)
1	5 (15.1)	2 (6.1)
2	11 (33.3)	5 (15.1)
3	12 (36.3)	21 (63.6)
Tumor Type n (%)		
DCIS	5 (14.7)	5 (13.9)
IDC	23 (67.6)	26 (72.2)
ILC	4 (11.8)	4 (11.1)
IDLC	2 (5.9)	1 (2.8)
Location of Recurrence(s) n (%)[4]		
Ipsilateral to primary	NA	21 (60)
Contralateral to primary	NA	14 (40)
Tumor Size n (%)[3]		
≥20 mm	13 (48.2)	13 (52)
<20 mm	14 (51.8)	12 (48)
Anti-hormonal Therapy n (%)[3]		

No	7 (30.4)	NA
Yes, Tam	4 (17.4)	NA
Yes, AI	7 (30.4)	NA
Yes, Tam & AI	5 (21.8)	NA
Chemotherapy Type n (%)[3, 5]		
AC + paclitaxel	6 (23.1)	NA
AC + docetaxel	3 (11.6)	NA
Other	5 (19.2)	NA
None	12 (46.1)	NA

[1]TTR = time to recurrence
[2]Primary tumors include the 8 non-recurrent tumors
[3]Indicates that data are missing for some samples; percentages are calculated on the available data
[4]Includes second recurrences; missing laterality for one tumor
[5]AC = Adriamycin (doxorubicin) and C = cyclophosphamide
NA = not applicable
See text for scoring of ER, PR, HER2 and Ki67
Table from[102]

Table 4.5 TROP2 Staining in Breast Tumors

TROP2 Score mean (SD)	**Membrane TROP2**	**Cytoplasmic TROP2**
ER+ Primary to ER+ Recurrence		
ER+ Primary (n = 14)	3.9 (3.1)	4.8 (2.1)
ER+ Recurrence (n = 18)	4.9 (3.3)	4.3 (2.1)
ER- Primary to ER- Recurrence		
ER- Primary (n = 6)	5 (2.7)	3.7 (2.0)
ER- Recurrence (n = 8)	5 (3.8)	3.5 (2.8)
ER+ Primary to ER- Recurrence		
ER+ Primary (n = 6)	5 (4.5)	4.5 (1.6)
ER- Recurrence (n = 6)	4.7 (2.7)	4.6 (1.7)
Non-Recurrent		
ER+ (n = 6)	9 (0)	4.8 (1.8)
ER- (n = 2)	6.5 (3.5)	4 (2.8)
ER/HER2 status		
-/- (n = 18)	4.3 (2.8)	3.5 (2.2)
-/+ (n = 5)	7.4 (2.3)	5.1 (1.3)
+/- (n = 37)	5.3 (3.5)	4.5 (2.0)
+/+ (n = 6)	4.3 (3.8)	5 (1.5)
Non-Recurrent (n = 8)	8.4 (1.8)	4.6 (1.9)
Primaries that Recur (n = 26)	4.4 (3.3)	4.4 (2.0)

See text for scoring of TROP2

Table 4.6 Descriptive Statistics for Average Beta Values by ER Status				
All *TACSTD2* CpGs				
	ER-Positive Tumors	**ER-Negative Tumors**	**Primary Tumors**	**Recurrent Tumors**
Mean	0.183	0.180	0.183	0.181
Minimum	0.080	0.089	0.084	0.082
Maximum	0.706	0.651	0.697	0.678
Range	0.626	0.562	0.613	0.600
Variance	0.021	0.018	0.021	0.019
Standard Deviation	0.145	0.132	0.144	0.138
Median	0.139	0.135	0.145	0.130
25th Percentile	0.112	0.115	0.105	0.125
75th Percentile	0.206	0.205	0.209	0.199
Interquartile Range	0.095	0.090	0.105	0.074
***TACSTD2* Promoter CpGs**				
	ER-Positive Tumors	**ER-Negative Tumors**	**Primary Tumors**	**Recurrent Tumors**
Mean	0.206	0.200	0.207	0.201
Minimum	0.090	0.089	0.097	0.082
Maximum	0.706	0.651	0.697	0.678
Range	0.616	0.562	0.600	0.596
Variance	0.037	0.030	0.035	0.034
Standard Deviation	0.191	0.174	0.188	0.183
Median	0.152	0.146	0.150	0.149
25th Percentile	0.124	0.126	0.124	0.125
75th Percentile	0.203	0.204	0.207	0.199
Interquartile Range	0.079	0.078	0.083	0.074

Table 4.7 Descriptive Statistics for Membrane TROP2 Scores	
Mean	5.11
Minimum	0
Maximum	9
Range	9
Variance	10.94
Standard Deviation	3.31
Mode	9
Median	4.5
25^{th} Percentile	2.25
75^{th} Percentile	9
Interquartile Range	6.75

Table 4.8 Descriptive Statistics for Cytoplasmic TROP2 Scores	
Mean	4.33
Minimum	0
Maximum	9
Range	9
Variance	4.21
Standard Deviation	2.05
Mode	6
Median	3
25th Percentile	3
75th Percentile	6
Interquartile Range	3

(A)

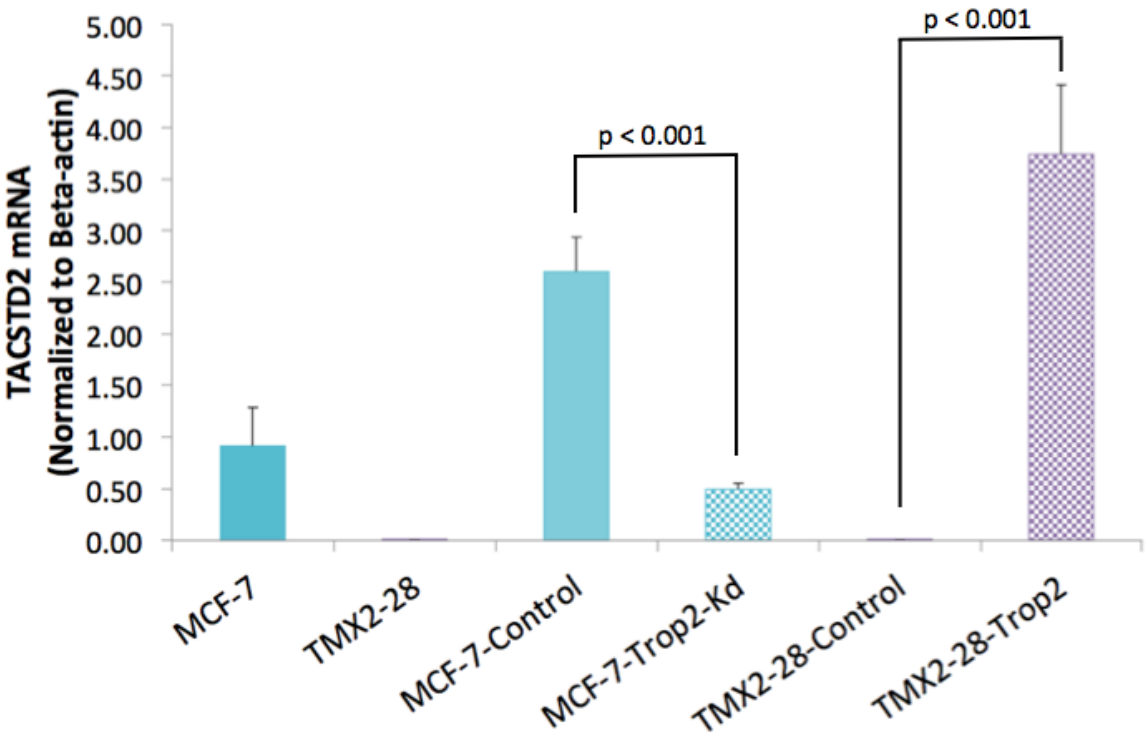
TACSTD2 mRNA
(Normalized to Beta-actin)
5.00
4.50
4.00
3.50
3.00
2.50
2.00
1.50
1.00
0.50
0.00
p < 0.001
p < 0.001
MCF-7
TMX2-28
MCF-7-Control
MCF-7-Trop2-Kd
TMX2-28-Control
TMX2-28-Trop2

(Figure 4.1)

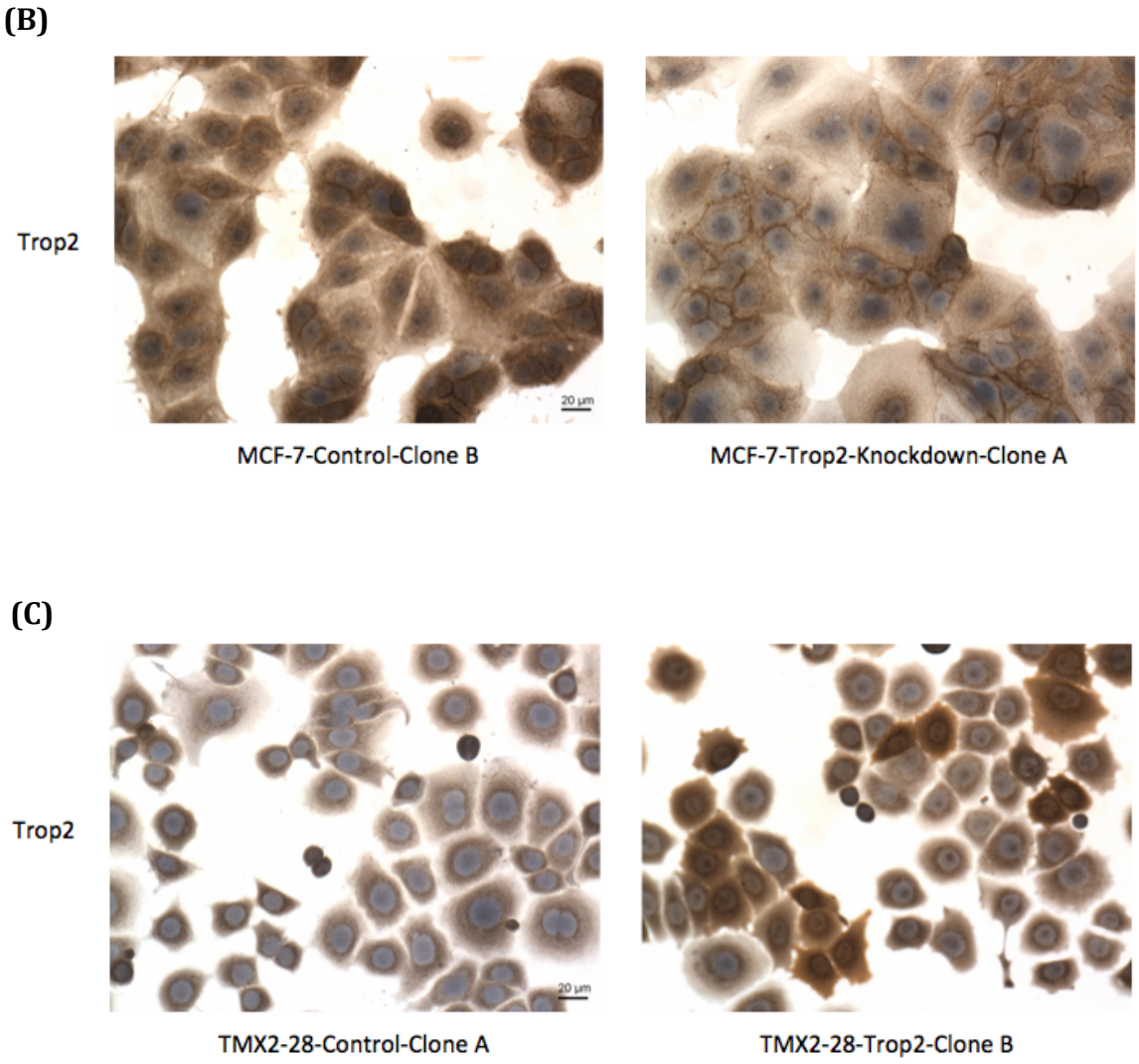

Figure 4.1: TROP2 Expression in the Cloned Cell Lines. TROP2 mRNA expression determined by RT-PCR run in technical triplicate for MCF-7 (non-transfected), MCF-7-Control, MCF-7-Trop2-Knockdown, TMX2-28 (non-transfected), TMX2-28-Control and TMX2-28-Trop2 cell lines (A). Expression of TROP2 determined by IHC for MCF-7-Control-Clone-B and MCF-7-Trop2-Knockdown-Clone-A (B). Expression of TROP2 determined by IHC for TMX2-28-Control-Clone-A and TMX2-28-Trop2-Clone-B (C). Magnification = 200X.

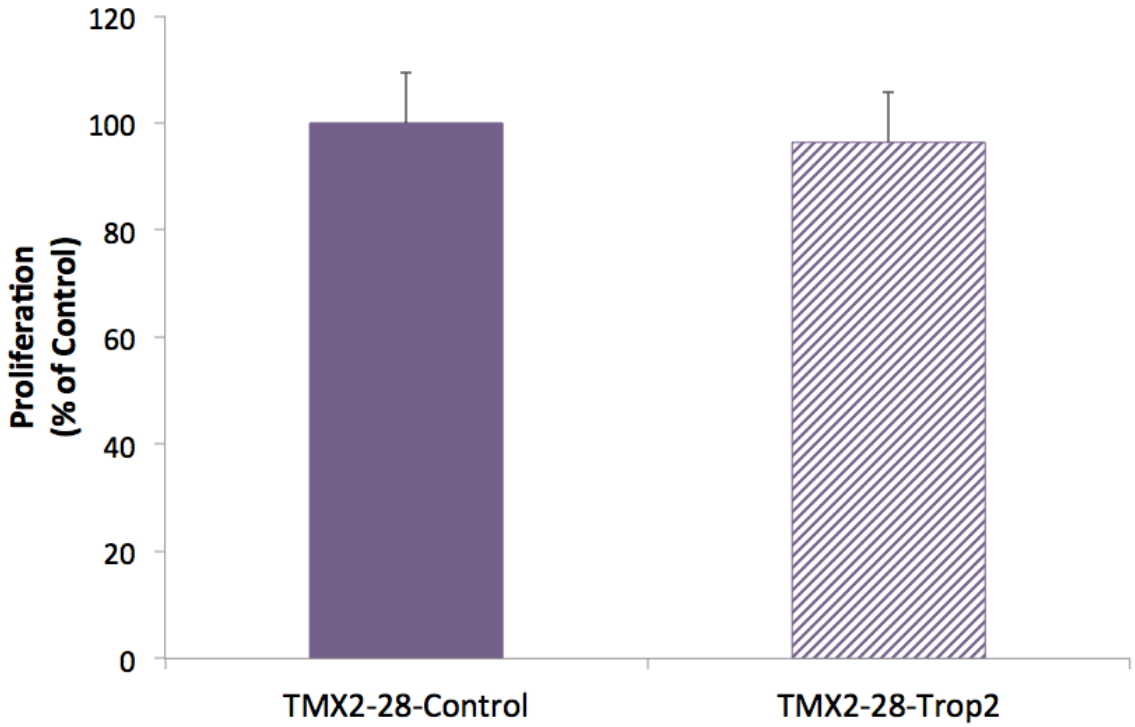

Figure 4.2: TROP2 Overexpression Does Not Affect Proliferation in TMX2-28. Cell proliferation determined by MTS assay represented as percent of control for TMX2-28-Control and TMX2-28-Trop2 cell lines (n = 16, p = 0.29).

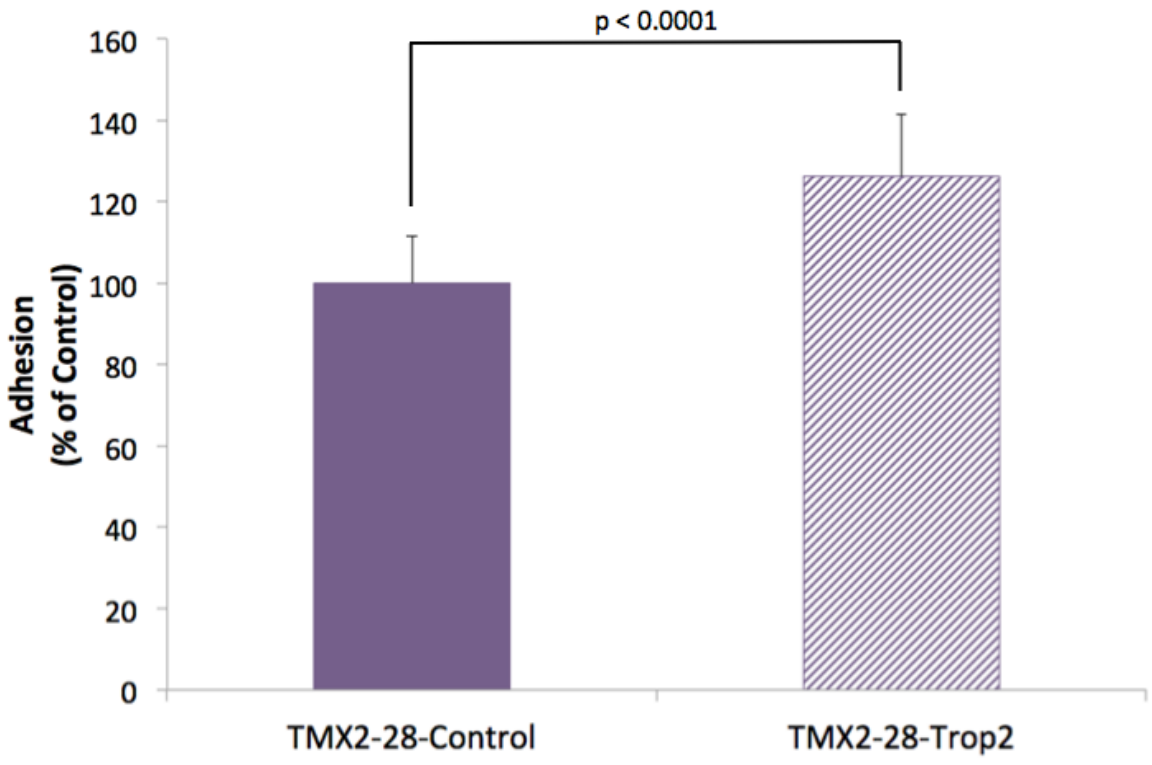

Figure 4.3: TROP2 Increases Adhesion to Fibronectin in TMX2-28. Adhesion to fibronectin represented as percent of control for TMX2-28-Control and TMX2-28-Trop2 cell lines (n = 16, $p < 0.0001$).

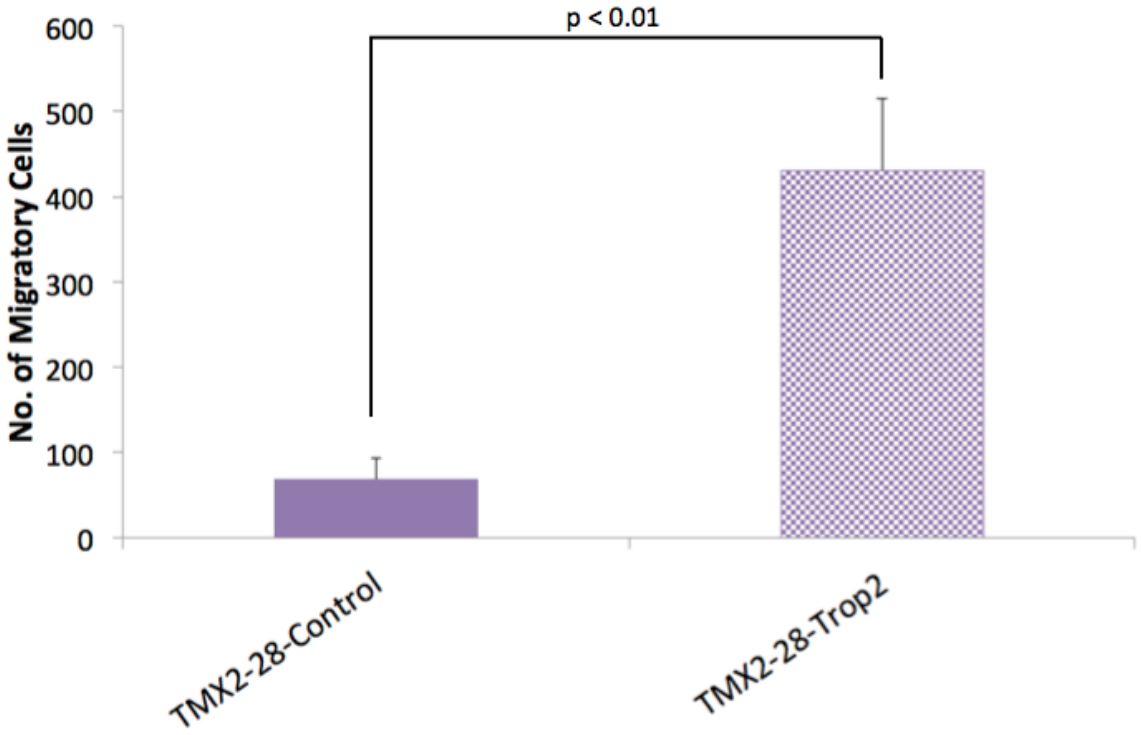

Figure 4.4: TROP2 Promotes Migration of TMX2-28. Number of migratory cells per transwell membrane determined from four non-overlapping images per sample (n = 3).

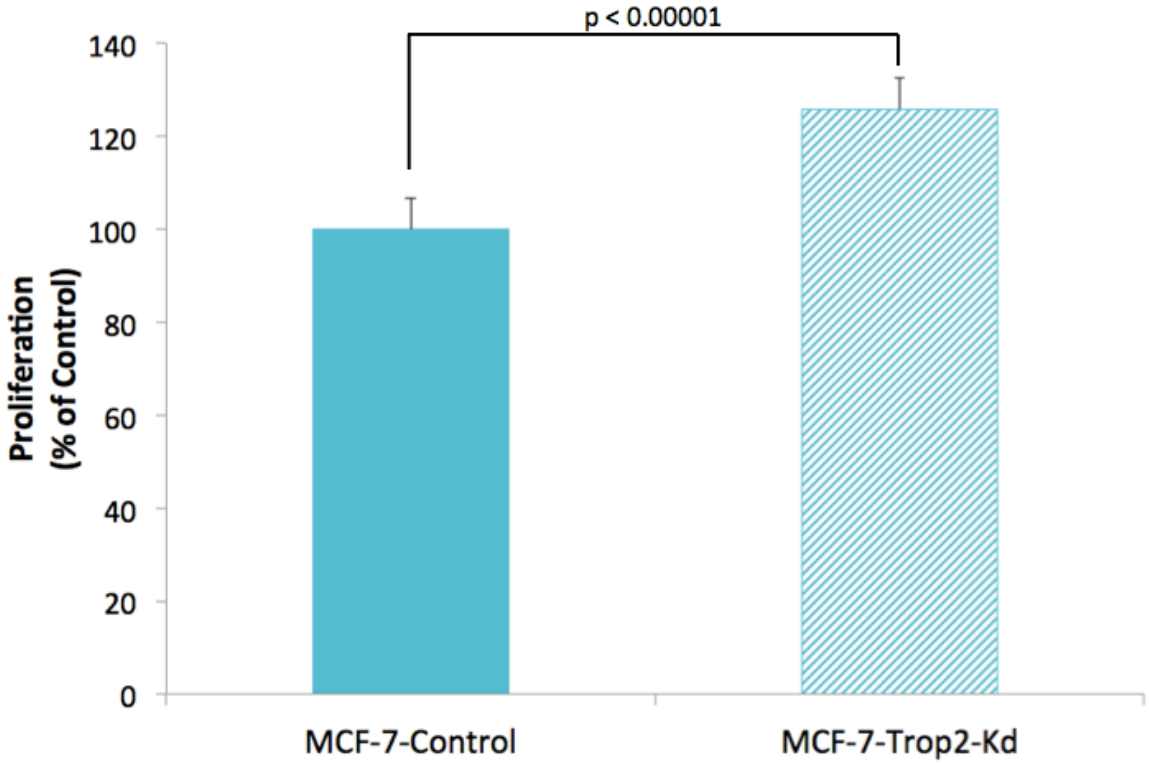

Figure 4.5: Knockdown of TROP2 in MCF-7 Increases Proliferation. Cell proliferation determined by MTS assay represented as percent of control for MCF-7--Control and MCF-7-Trop2-Kd cell lines (n = 16, p < 0.00001).

(A)

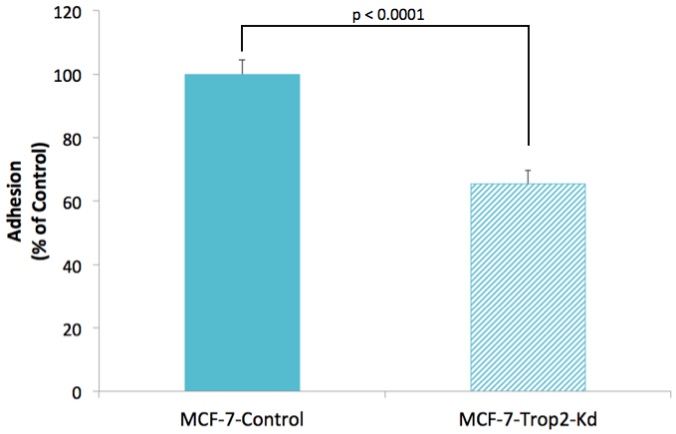

(B)

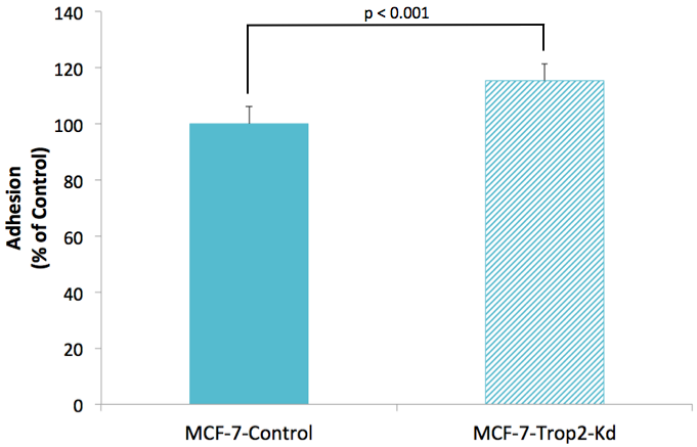

(C)

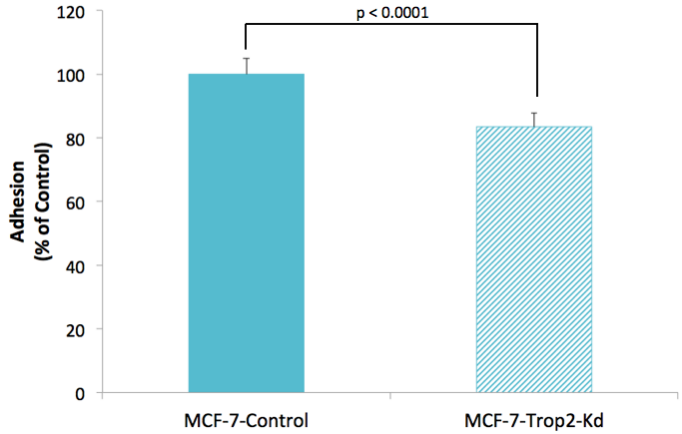

(Figure 4.6)

Figure 4.6: TROP2 Knockdown Has Variable Results on MCF-7 Adhesion to Fibronectin. Adhesion to fibronectin represented as percent of control for MCF-7-Control and MCF-7-Trop2-Kd cell lines for three separate experiments (A) n = 16, (B) n = 8 and (C) n = 16. A significant decrease in adhesion to fibronectin in MCF-7-Trop2-Kd was observed in two out of the three experiments.

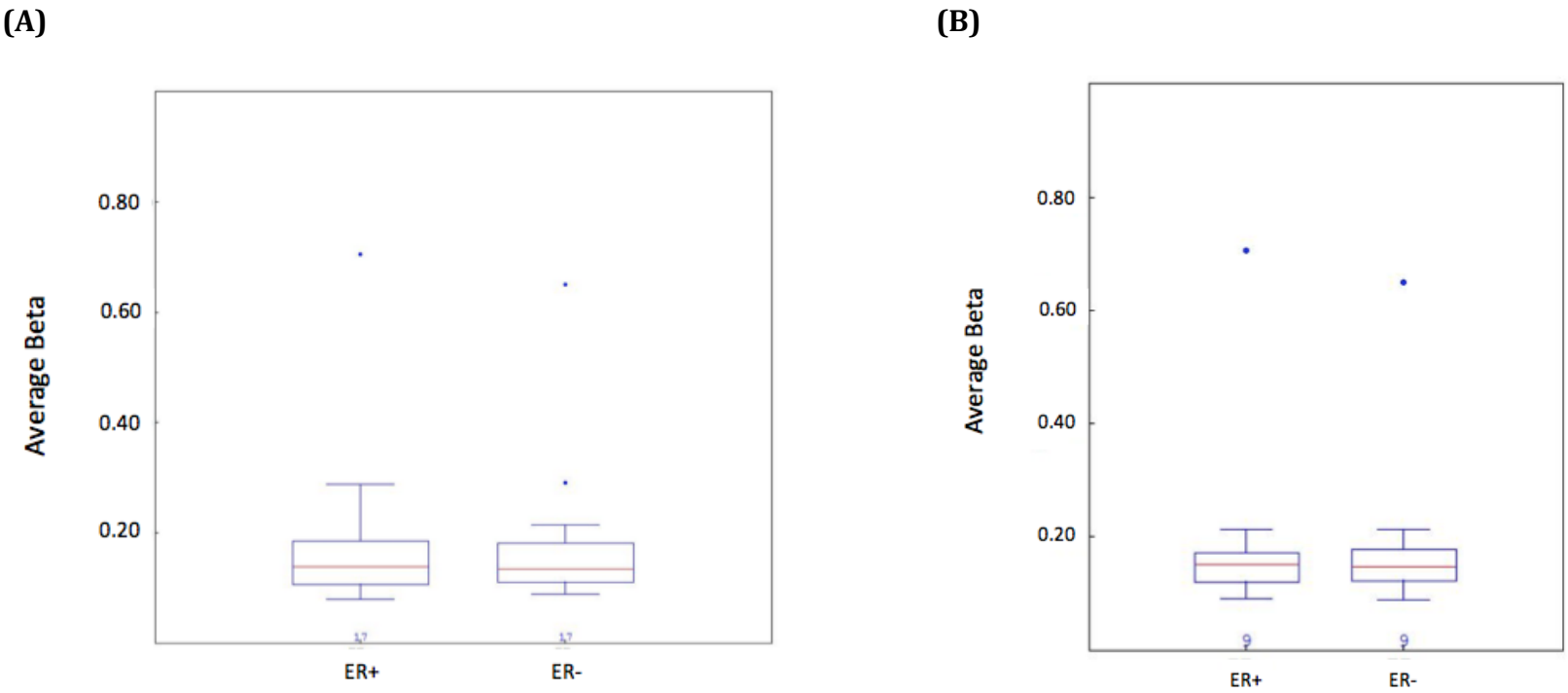

Figure 4.7: Average Methylation for *TACSTD2* in Tumor Samples by ER status. Boxplots indicating average beta values for all *TACSTD2* CpGs on the 450 BeadChip for the tumor samples by ER status (ER-positive v. ER-negative) (A) and CpGs located in the promoter only (TSS200 or TSS1500) (B). Boxplots generated in Genome Studio.

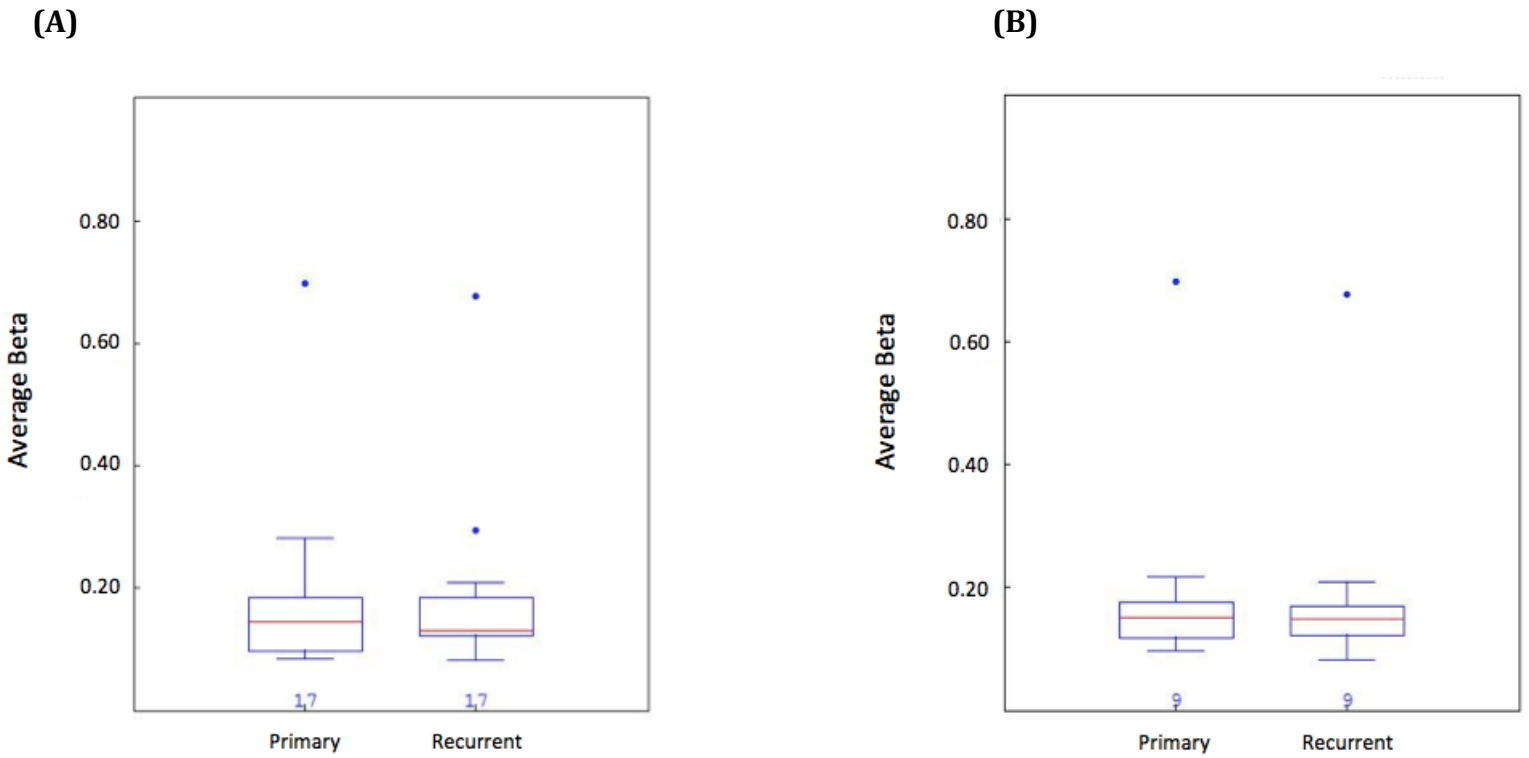

Figure 4.8: Average Methylation for *TACSTD2* in Primary and Recurrent Tumor Samples. Boxplots indicating average beta values for all *TACSTD2* CpGs on the 450 BeadChip for primary and recurrent tumor samples (A) and CpGs located in the promoter only (TSS200 or TSS1500) (B). Boxplots generated in Genome Studio.

(A)

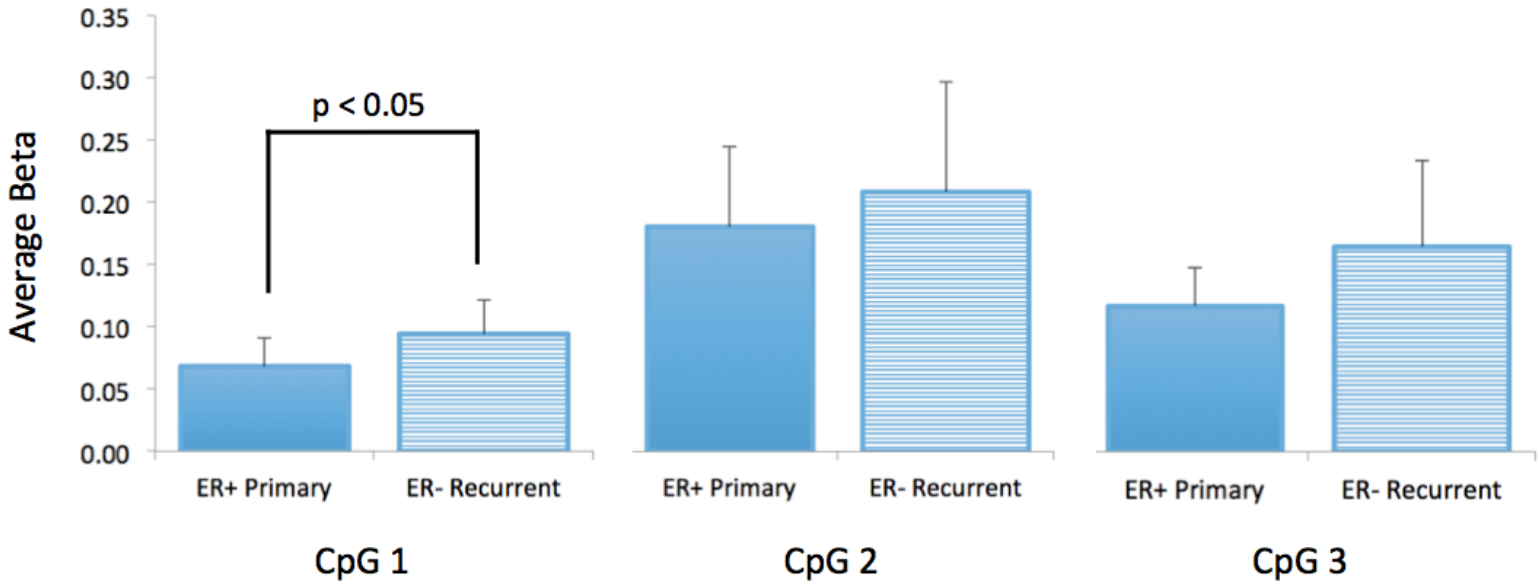
0.35
0.30
0.25
0.20
0.15
0.10
0.05
0.00
Average Beta
p < 0.05
ER+ Primary
ER- Recurrent
ER+ Primary
ER- Recurrent
ER+ Primary
ER- Recurrent
CpG 1
CpG 2
CpG 3

(Figure 4.9)

(B)

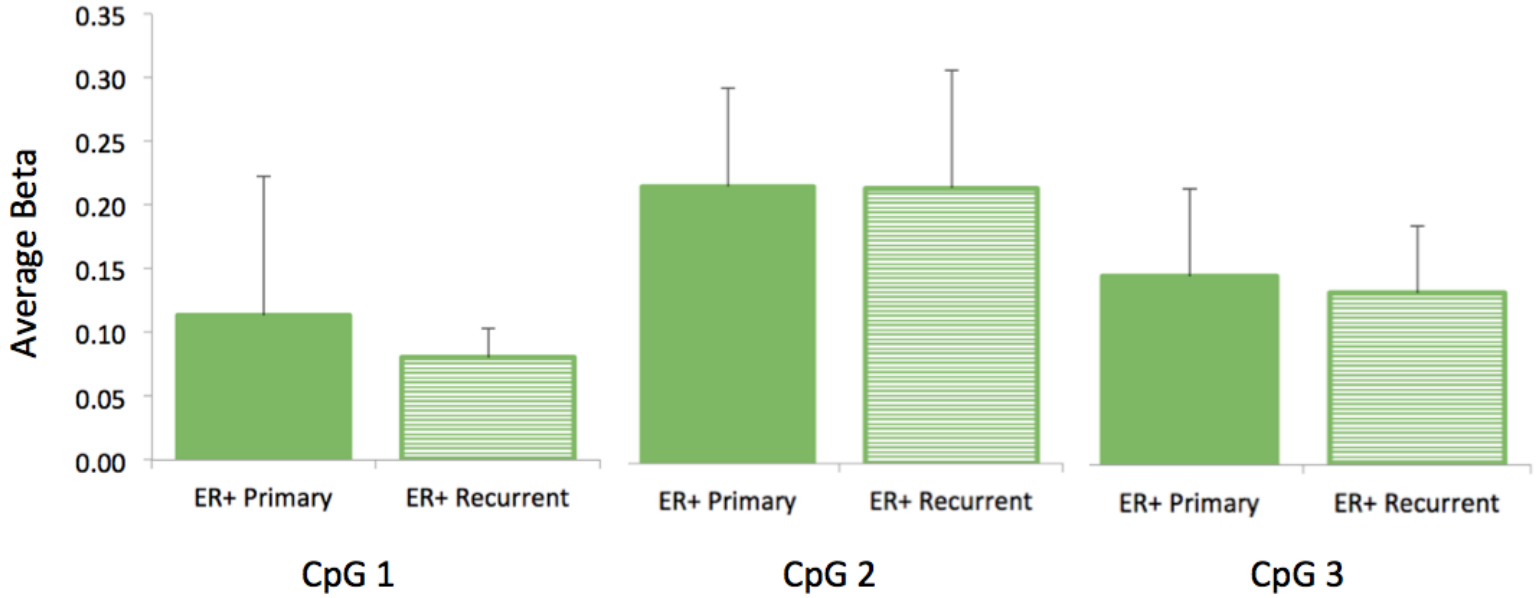
Average Beta
0.35
0.30
0.25
0.20
0.15
0.10
0.05
0.00
ER+ Primary
ER+ Recurrent
ER+ Primary
ER+ Recurrent
ER+ Primary
ER+ Recurrent
CpG 1
CpG 2
CpG 3

(Figure 4.9)

(C)

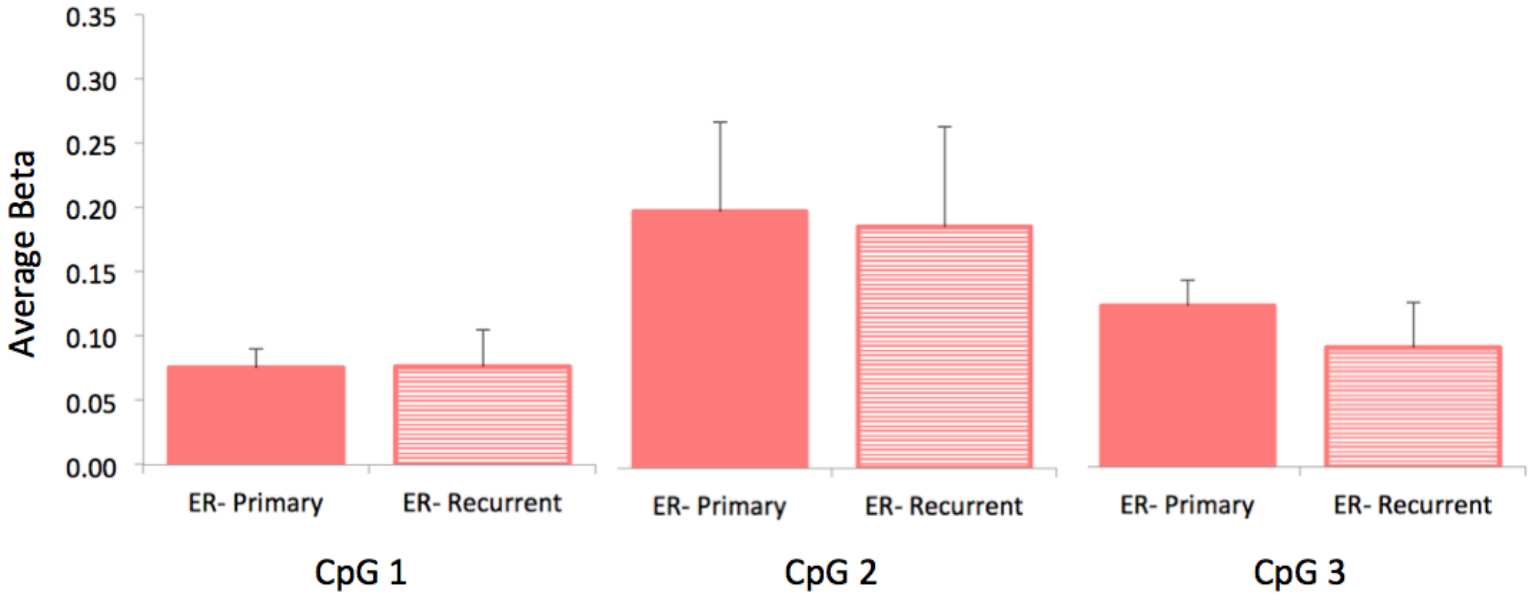

Figure 4.9: *TACSTD2* Methylation in Tumor Samples. Average beta values for the three *TACSTD2* CpGs identified as differentially methylated in the cell lines (CpG 1, CpG2 and CpG 3) in the tumor samples by group; ER-positive primary (n = 6) to ER-negative recurrent tumors (n = 7) (A), ER-positive primary (n = 14) to ER-positive recurrent (n = 20) (B), ER-negative primary (n = 6) to ER-negative recurrent (n = 9)(C).

(A)

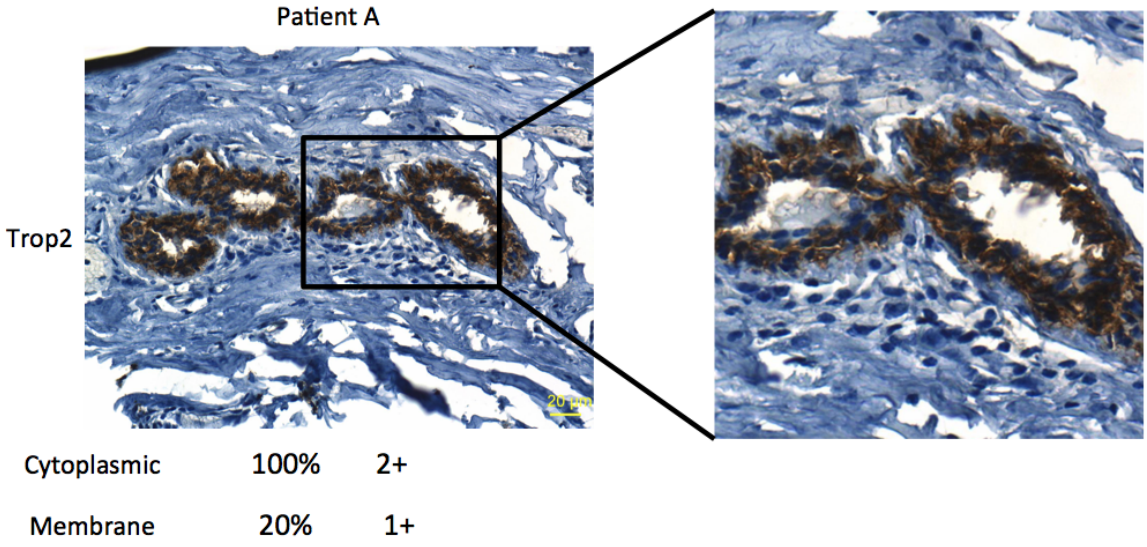

(B)

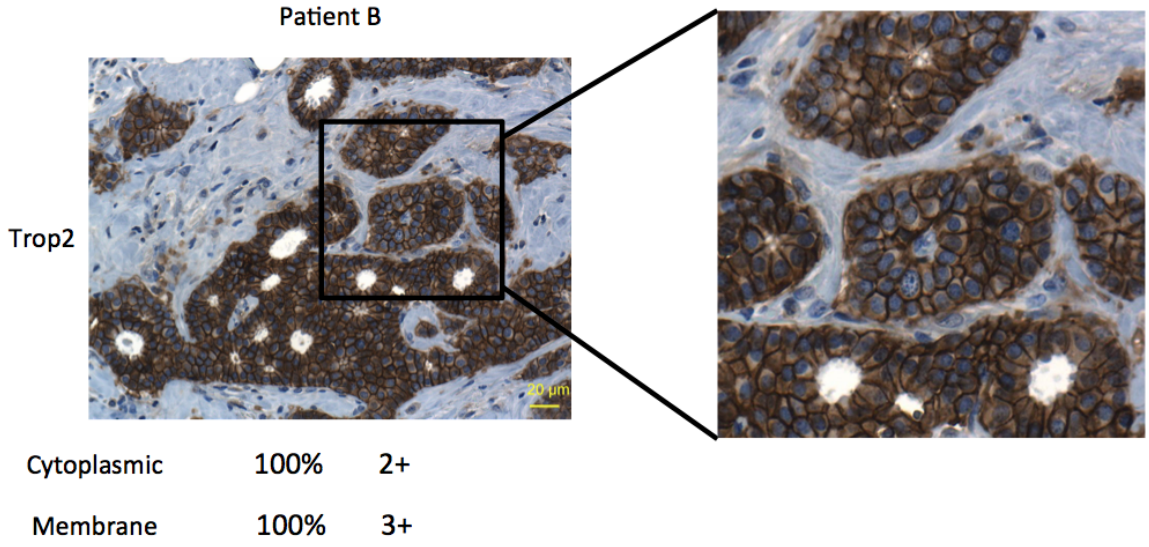

Figure 4.10: TROP2 IHC Scoring in Tumor Samples. Images of two different tumor samples (Patient A and Patient B) showing examples of diffuse (100%), moderate (2+) staining for cytoplasmic TROP2 (A, see inset) and diffuse (100%), strong staining for membrane TROP2 (B, see inset). Magnification = 200X.

(A)

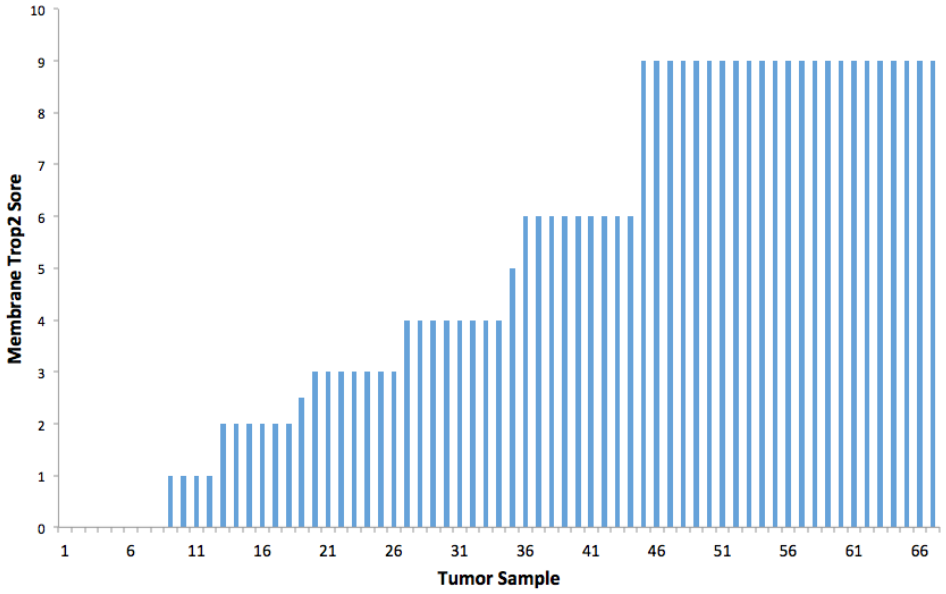

(B)

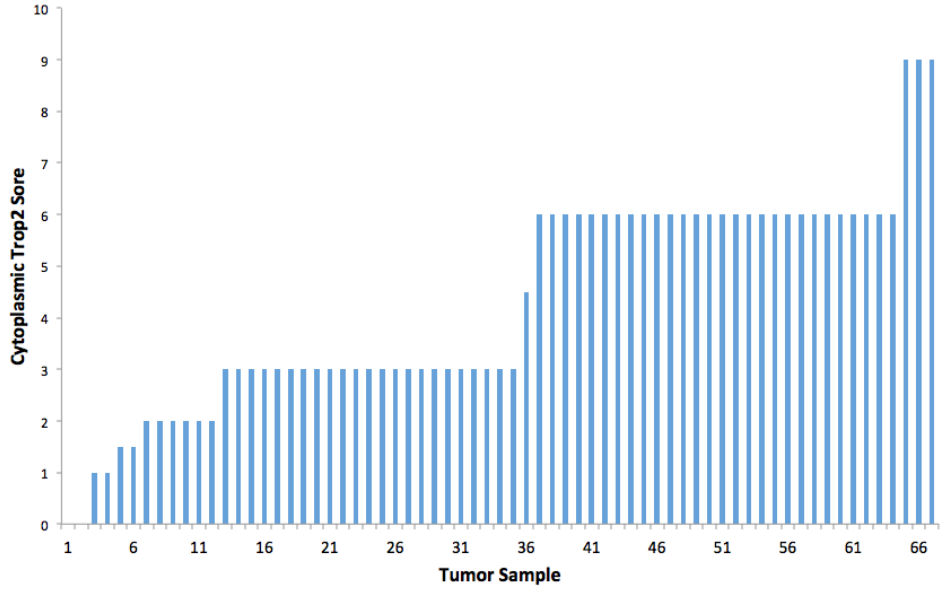

Figure 4.11: Summary of Membrane and Cytoplasmic TROP2 IHC Scoring in Tumor Samples. Distribution of IHC scores (scored as previously described) for membrane (A) and cytoplasmic (B) TROP2 in the tumor samples.

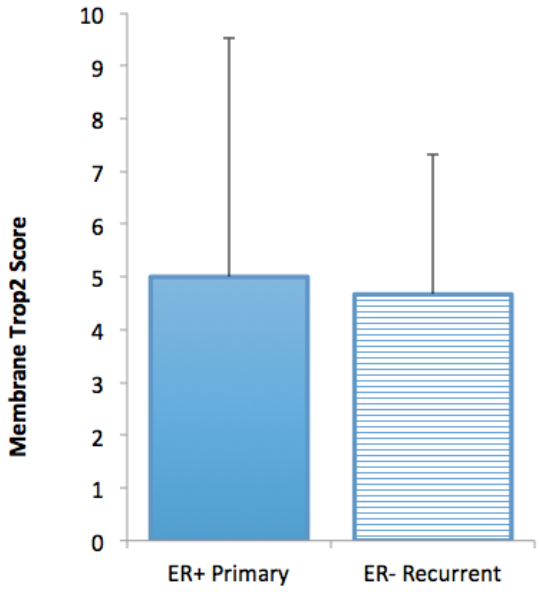

Figure 4.12: Expression of Membrane TROP2 in ER-Positive Primary Tumors that Recur as ER-Negative. Mean membrane TROP2 scores determined by IHC for the ER-positive primary tumors (n = 6) that recur as ER-negative tumors (n = 6) (one-tail p-value = 0.44, two-tail p-value = 0.88).

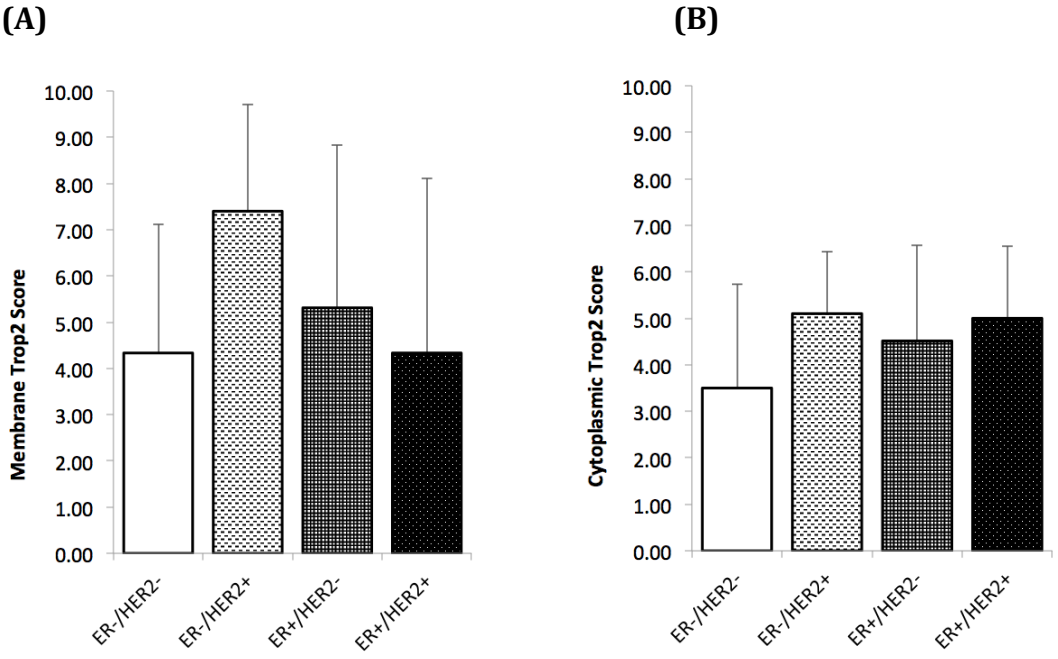

Figure 4.13: Expression of TROP2 in Tumor Samples by ER/HER2 Status. Mean membrane (A) and cytoplasmic (B) TROP2 scores determined by IHC for the tumor samples grouped by ER/HER2 status (ER-negative/HER2-negative: n = 18, ER-negative/HER2-positive, n = 5, ER-positive/HER2-negative, n = 37, and ER-positive/HER2-postitive, n = 6). (One-way ANOVA p-values for membrane and cytoplasmic TROP2 equal 0.28 and 0.21, respectively).

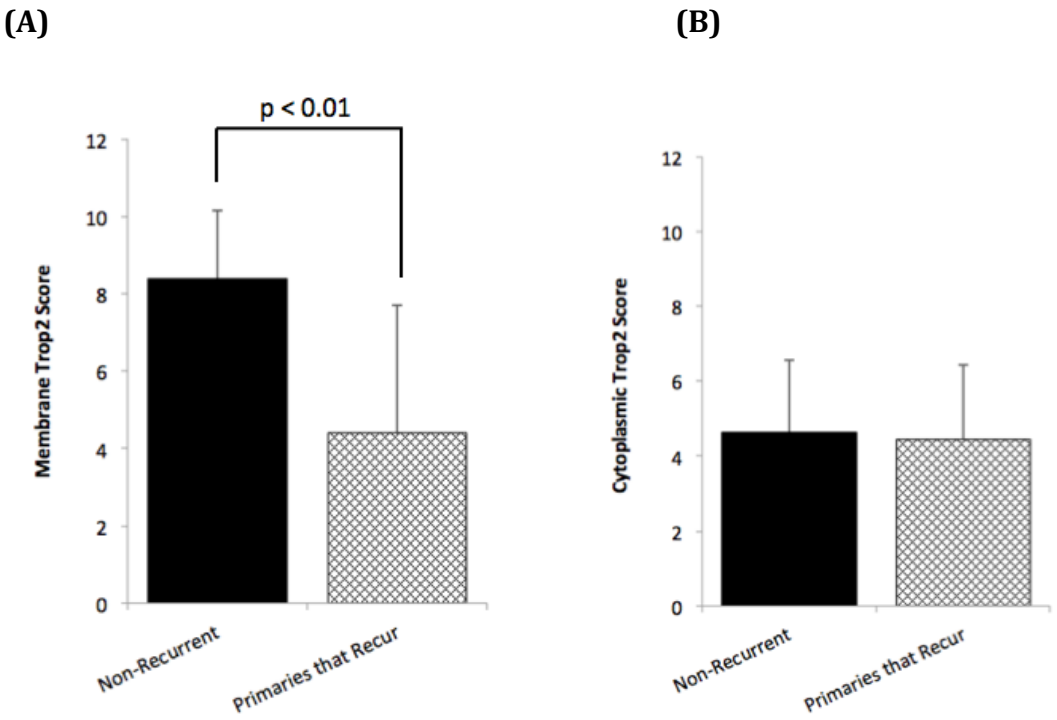

Figure 4.14: Expression of TROP2 in Non-Recurrent Samples and Primary Samples that Recur. Mean membrane (A) and cytoplasmic (B) TROP2 scores determined by IHC for the tumor samples grouped by non-recurrent (n = 8, students t-test $p < 0.01$) and primary samples that recur (n = 26, students t-test $p = 0.82$).

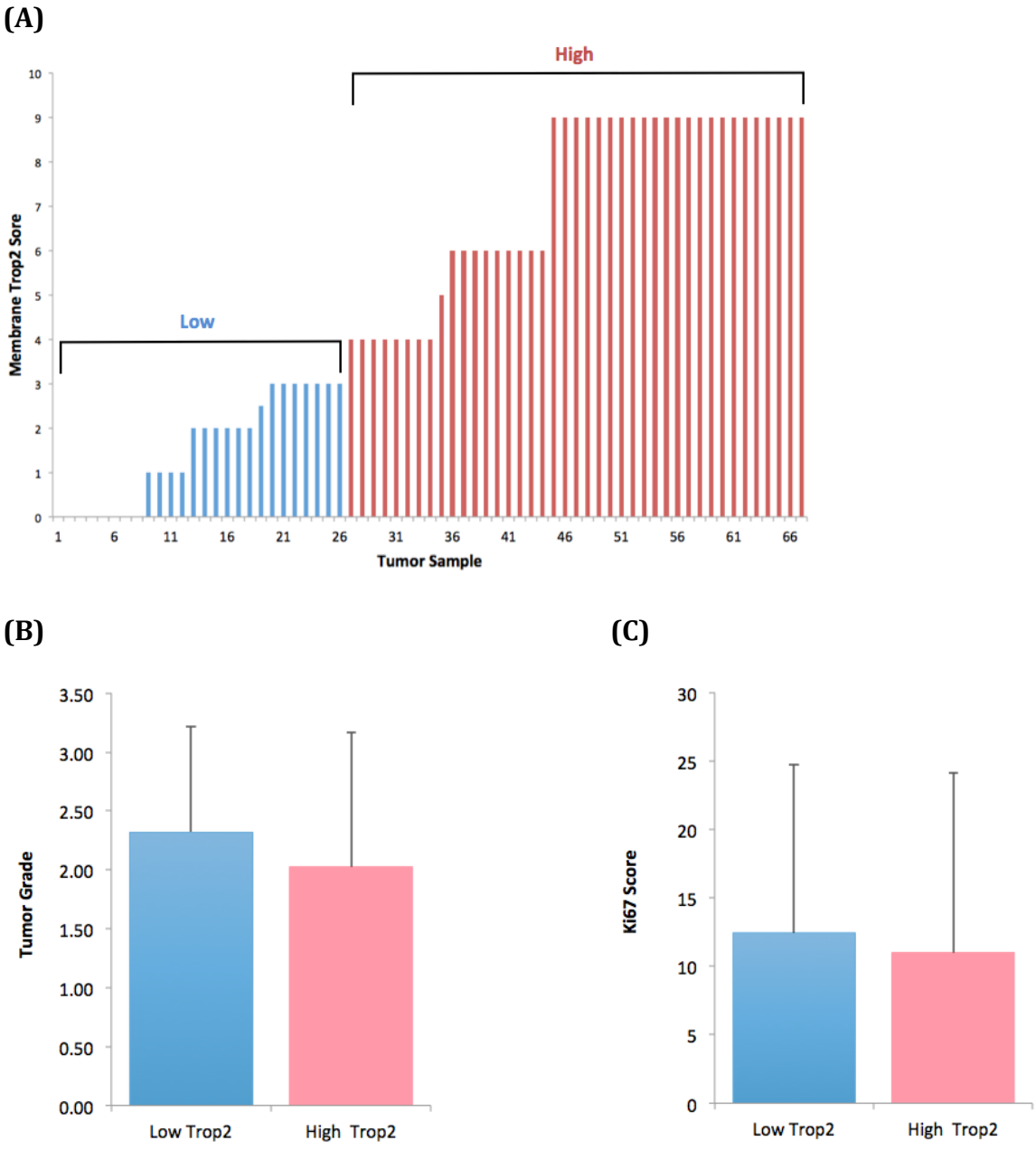

Figure 4.15: Tumor Grade and Ki67 Score by Expression Level of Membrane TROP2. Categorized membrane TROP2 expression levels (low: IHC score ≤ 3 or high: IHC score > 3) (A). Differences in tumor grade (n = 62) (B) and Ki67 score (n = 66) (C) between tumors with low and high expression of membrane TROP2 (students t-test p-value = 0.30 and 0.66, respectively).

CHAPTER 5

FURTHER CHARACTERIZATION OF TAMOXIFEN-RESISTANT BREAST CANCER CELL LINES BY KERATIN EXPRESSION

Introduction

As reviewed by Karantza, [121] the cytoskeleton is composed of three types of cytoskeletal filaments: microfilaments, intermediate filaments and microtubules (Figure 5.1). Microfilaments (also called actin filaments) are made of interlaced actin chains (6nm in diameter). They function to maintain cellular shape, resist tension, form cytoplasmic protrusions and are involved in cell-cell and cell-matrix interactions. Intermediate filaments (10 nm in diameter) are slightly larger and stronger than actin filaments. They help maintain the internal cell structure by preserving shape and bearing tension. Microtubules are 23 nm in diameter and are hollow cylinders made of 13 protofilaments (polymers of alpha- and beta- tubulin). Microtubules form the mitotic spindle and are important for intracellular transport. Keratins are a type of intermediate filament classified according to the amino acid sequence of their rod-domain. Expression of keratins has a tissue- and differentiation-state-specific pattern. [121] Therefore, keratin expression patterns are often used to identify tumor cells from carcinomas that have metastasized or circulating tumor cells.[122]

Keratins (also known as cytokeratins) are classified based on 2D isoelectric focusing and SDS-polyacrylamide gel electrophoresis. Moll and colleagues initially characterized and categorized keratins from human cell lines, normal epithelia and

tumors in this manner.[123] Keratins make up two of the six types of intermediate filaments.[121,124] Type I (acidic) and Type II (basic or neutral) keratins are typically expressed in epithelial cells. Keratin filaments are composed of heterotypic pairs of Type I and Type II proteins. They help protect epithelial cells from both mechanical and non-mechanical stress. In addition, keratins are involved in regulating apico-basal polarity, determining cell size, spacing of organelles, targeting of membrane proteins and controlling protein translation.[121] Throughout tumorigenesis, cancer cells generally maintain their original keratin expression profile.[124] Therefore, pathologists and oncologists utilize keratins as a diagnostic tool in epithelial cancers by using their expression pattern to classify adenocarcinomas by tissue of origin and to help determine the best treatment options for the patient.[121]

There are variable results regarding keratin expression in breast cancers in the literature, depending on sample size and antibodies used. In the normal breast, CK5 and CK14 are expressed in myoepithelial cells while CK7, CK8, CK18 and CK19 are expressed in ductal cells.[124] However, most adenocarcinomas (epithelial cancer that develops in glandular tissues) express the following keratins: CK8, CK18 and CK19 while expression of CK7 and CK20 is variable. A large number of breast adenocarcinomas including ductal and lobular express CK7, CK8, CK18 and CK19. Ductal adenocarcinomas typically have positive peripheral CK8 staining while lobular adenocarcinomas have perinuclear CK8 staining.[121] However, primary breast cancers can undergo changes in keratin expression during metastasis.[122]

As reviewed by Gusterson and colleagues, heterogeneity is observed in all aspects of breast cancer including morphology, response to therapy and clinical

outcome. In the anatomy of normal breast tissue, there are inner luminal cells, a distinct outer cell layer next to the basement membrane (myoepithelium) and a basement membrane or basal cell layer (Figure 1.1). Myoepithelial cells are cells that possess both epithelial and basal or contractile properties. Throughout the basal cell layer there is morphological heterogeneity where some cells are spindle-like and some are cuboidal. Cell morphology is dependent on their location within the branched ductal network of the breast and on the hormone or menopause status of the tissue. This basal layer in the breast differs from basal cells of stratified squamous epithelium by expression of smooth muscle actin (SMA), myosin and neutral endopeptidase (CD10).[125] Basal cells were initially characterized as cells that express high molecular weight cytokeratins such as CK5 and CK14.[123,125] In normal glandular epithelia, CK5 and CK14 are expressed in cells that are adjacent to the basement membrane and in a basal position from the ducts to the acini. Therefore, in most tissues, "basal position" and cells that express "basal keratins" refers to the same population of cells. However, in the breast, cell types other than myoepithelial cells can express CK5, CK14 and CK17, such as luminal cells located in the terminal duct lobular unit. Expression of CK8 and CK18 is only found in luminal cells. However, luminal cells have also been found to express basal cytokeratins, CK5, CK14 and CK17. Therefore the term "basal" can be defined as either myoepithelium or the subpopulation of cells expressing basal cytokeratins, which can be located in either a luminal or basal location in normal glands. Expression of CK5, CK14 and CK17 in myoepithelial cells of *in situ* breast lesions is associated with a poor prognosis. High-grade tumors expressing keratins of stratified epithelium

(CK4, CK14 and/or CK17) have a poor prognosis and generally lack expression of ER. While tumors of grade 1 and 2 generally express simple epithelial (or luminal) keratins. Most breast tumors express simple epithelial cytokeratins (CK7, CK8, CK18 or CK19). Expression of CK5/6 is associated with ER-negative and PR-negative tumors, which have high expression of p53, EGFR and a high proliferative index. Identifying differences between luminal and basal breast cancers helps determine the best therapeutic option and may affect response to chemotherapy.[125]

Another protein which may help to distinguish basal and luminal cells is p63, a transcription factor in the p53 gene family.[126,127] The p63 protein is important for development and homeostasis of ectodermal and epidermal tissues.[126] It is critical for the maturation of stratified epithelia such as limb buds, skin and mammary glands and is highly expressed in adult skin basal stem cells. P63 can regulate proliferation, differentiation and maintenance of stem cell populations and is required for development of the fetal mammary gland.[127] There are two major isoforms of p63. Tap63 contains the N-terminal transactivation (TA) domain, while ΔNp63 is missing the N-terminal TA domain but has a second internal TA domain.[127] In human and murine breast cancer samples, there is high expression of ΔNp63 in basal myoepithelial cells and TAp63 is expressed in some luminal cells. The ΔNp63 isoform promotes cell survival by suppressing transcription of pro-apoptotic genes and activating transcription of anti-apoptotic genes.[127] Sonic Hedgehog signaling, which promotes self-renewal of mammary stem cells, is also promoted by ΔNp63.[128] TAp63 regulates responses to DNA damage by inducing cell cycle arrest or apoptosis and can also suppress TGFβ signaling, which is important for

metastasis.[126] Therefore, it is important to determine expression levels of p63 in our tissue culture model.

The objective of this study was to better characterize our cell line models of tamoxifen resistance by examining expression of several basal and luminal keratins. Keratin expression will be determined by immunohistochemistry (IHC) for the parental cell line, MCF-7, and the tamoxifen resistant cell lines, TMX2-4, TMX2-11 and TMX2-28. Expression of basal cytokeratins (CK5, CK5/6, CK14 and the cocktail 34βE12) and luminal cytokeratins (CK8, CK17, CK18 and CK20) as well as the transcription factor p63 and its isoform, ΔNp63 (p40), will be determined by IHC. The CK34βE12 antibody recognizes the basal cytokeratins CK1, CK5, CK10 and CK14. Additionally, methylation of the cytokeratins and transcription factors will be examined in the control DMSO-treated cell lines (see Chapter 2). Determining methylation levels from the 450K BeadChip array will indicate whether expression of these genes might be regulated by promoter methylation. Characterizing the keratin expression profile in our cell line model of tamoxifen resistance will provide a better understanding of the changes that may occur during the development of tamoxifen resistant disease.

Materials and Methods

Cell Culture: As previously described, MCF-7 cells were purchased from the American Type Culture Collection (ATCC). TMX2-4, TMX2-11 and TMX2-28 cells were provided by John Gierthy (Wadsworth Center Albany, NY). Cells were grown in Dulbecco's modified eagle medium (without phenol red). Medium was

supplemented with 5% cosmic calf serum (Hyclone Cat. No. SH30087.03), 2.0 mM of L-glutamine, 0.1 mM of nonessential amino acids and 250 ng/mL of insulin. Cells were maintained at 37°C, 5% CO_2 in a humidified incubator and passaged at subconfluence or media exchanged every 2 days.

Immunohistochemistry (IHC): Cells were seeded on poly-L-lysine (PLL)-coated slides (Polysciences, Cat. No. 22247, Warrington, PA) at a density of approximately 2 x 10^5 cells/mL/slide. Cells were maintained at 37°C, 5% CO_2 in a humidified incubator overnight and fixed approximately 24 hours later. First, the slides were rinsed with cold phosphate-buffered saline solution (PBS) twice and then fixed in ice cold 100% methanol for 10 min. The slides were then allowed to dry and stored at -20°C until stained. Immunohistochemical staining was performed at Baystate using the ADVANCE HRP System (Dako Cat. No. K4067, Carpinteria, CA) with the following primary antibodies: TP63 (Dako Cat. No. M7247, Carpinteria, CA), CK 34βE12 (Enzo, Cat. No. ENZ-C34903, Farmingdale, NY), CK 5 (Vector, Cat. No. VP-C400, Burlingame, CA), CK 8 (Vector, Cat. No. VP-C404, Burlingame, CA), CK 17 (Vector, Cat. No. VP-C413, Burlingame, CA), CK 18 (Vector, Cat. No. VP-C414, Burlingame, CA) and CK 20 (Dako, Cat. No. M7019, Carpinteria, CA). The UltraView Universal DAB Detection kit (Ventana Medical Systems, Inc., Cat. No. 760-500) was used with the following primary antibodies: CK 5/6 (Ventana Medical Systems, Inc., Cat. No. 790-4554, Tucson, AZ), CK 14 (Ventana Medical Systems, Inc., Cat. No. 760-4251, Tucson, AZ), and TP40 (Biocare, Cat. No. ACI3066, Concord, CA).

Appropriate negative (no primary antibody) and positive controls were used to optimize antibody performance in addition to testing a dilution series including the dilutions recommended by the manufacturer.

Review of Pathology: Scoring of slides was conducted by one anatomic pathologist (Rahul Jawale). Slides were scored for immunoreactivity of 10 antigens; approximate number of positive cells was recorded (%) and intensity of immunoreactivity was reported on a scale of 0 (negative), 1+ (weak), 2+ (moderate), 3+ (strong). Scoring was completed in one session with a single observer documenting records (SZ).

Illumina Human Methylation 450 BeadChip: Methylation of the genes encoding the cytokeratins was investigated in the DMSO-control and 5-Aza-2'-deoxycytidine treated cell lines as previously described (Chapter 2) using the 450K array.

Data Analysis: The methylation data obtained from the HM450 BeadChip was analyzed using Genome Studio Methylation Module (v.1.9.0). Detection p-values of < 0.01 were used to select statistically significant CpG site data. Methylation data was exported from Genome Studio and averages were calculated in Excel.

Results

TMX2-28 Cells Have a Mixed Cytokeratin Expression Profile

None of the cell lines expressed the transcription factors or CK 20 (Table 5.1). There was also no protein expression detected with the CK 34βE12 or CK 5/6 antibodies. All cell lines express high levels of the low molecular weight, luminal

markers, CK 8 and 18. However, TMX2-28 had increased expression of the high molecular weight, basal cytokeratins, CK5 and CK14, compared to the parental cell line, MCF-7. Interestingly, TMX2-28 also expressed higher levels of the luminal marker, CK17, compared to the parental cell line. The cytokeratin protein expression determined by IHC for TMX2-28 and MCF-7 agree with previously published mRNA data from our lab. In the 2007 paper, the trends in mRNA expression of CK 5, CK 14, CK 8, CK 17 and CK18 are in alignment with the protein expression results presented here. However, Gozgit and colleagues found MCF-7 cells express high levels of CK 20 mRNA.[75] While the IHC results indicate that MCF-7 do not express CK20 protein.

Expression of Several Cytokeratins and p40 May Be Regulated by Promoter Methylation

Expression of p40 May Be Regulated by Promoter Methylation

To determine whether DNA methylation may be regulating expression of the cytokeratins or transcription factors, I utilized the 450K BeadChip array data from the DMSO control-treated cell lines. I generated heatmaps to visualize the differences in methylation between the cells. The p40 antibody recognizes the ΔNp63 isoform of the TP63 gene. Filtering the methylation array data for CpG sites corresponding to the ΔNp63 isoform (accession numbers NM_001114980, NM_001114982 and NM_001114983), methylation of these CpG sites is high. The mean average beta values for all CpGs in the ΔNp63 isoform for each cell line range from 0.71 – 0.80 (Figure 5.2, A). This inverse relationship between promoter

methylation and protein expression indicates that ΔNp63 expression may be repressed by promoter methylation. The CpG sites on the chip included loci in the TSS200 (200 base pairs upstream from transcription start site), TSS1500, body and 3'UTR (3' untranslated region) of the three p40 transcripts. It is also interesting that treatment with 5-Aza-2'-deoxycytidine, decreased methylation throughout the gene in TMX2-28 cells only, indicating that this transcript may be re-expressed in TMX2-28 upon treatment with 5-Aza-2'-deoxycytidine. The mean average beta value for the ΔNp63 CpGs for TMX2-28-5-Aza-2'-deoxycytidine-treated is 0.51, a decrease of 20% compared to TMX2-28-Control (Figure 5.2, B).

Expression of Basal Cytokeratins, CK5 and CK14, May Be Regulated by Promoter Methylation

Protein expression of CK5 is increased in TMX2-28 (Table 5.1) compared to the other cell lines. The gene encoding CK5, KRT5, has decreased methylation in three CpG sites (MAPINFO no.52914409, 52914330 and 52914229) in the TSS200 or first exon/5'UTR compared to the three other cell lines (Figure 5.3, A). The mean average beta value for these 3 CpGs in TMX2-28 is 0.47 compared to 0.75 in MCF-7. Decreased methylation at these loci along with an increase in protein expression, may indicate that methylation of these CpG sites is important for regulating gene expression. Treatment with 5-Aza-2'-deoxycytidine further decreased mean methylation of the CpGs for the CK5 gene in TMX2-28 from 0.57 to 0.42 (Figure 5.3, B). Therefore, I would predict increased expression of CK5 in 5-Aza-2'-deoxycytidine-treated TMX2-28 cells.

Despite the mean average beta values for all KRT14 loci being similar for each cell line, the mean average beta values of the CpGs in the KRT14 promoter (MAPINFO numbers: 39744055, 39743427, 39743273, 39743241, 39743164)) are different. The mean average beta value for these sites in the KRT14 promoter for TMX2-28 is 62%, which is lower than promoter methylation for MCF-7, which is 76%. This decrease of 14% may be responsible for the corresponding increase in CK14 expression in TMX2-28. This is consistent with the idea that promoter methylation may be regulating gene expression of KRT14 in TMX2-28. There is also a decrease in promoter methylation between TMX2-4 and MCF-7. However, this change in promoter methylation does not appear to be regulating gene expression in TMX2-4 because there is no increase in protein expression (Figure 5.4, A). Treatment with 5-Aza-2'-deoxycytidine resulted in decreased KRT14 promoter methylation in each cell line relative to the control (Figure 5.4, B). Therefore, I would predict that treatment with 5-Aza-2'-deoxycytidine would result in increased CK14 expression in each cell line.

Expression of Luminal Cytokeratins, CK8, CK17, CK18 and CK20, May Be Regulated by Promoter Methylation

The parental cell line, MCF-7, and all three tamoxifen-resistant cell lines, TMX2-4, TMX2-11 and TMX2-28, have high expression of the luminal cytokeratin, CK8. Each cell line also has low methylation for each KRT8 loci represented on the 450 BeadChip. The mean average beta values for each cell line for all KRT8 loci range from 0.11 – 0.15 (Figure 5.5, A). Low methylation of CpGs in the promoter

along with high protein expression may indicate that promoter methylation is involved in regulating gene expression of KRT8. Treatment of each cell line with 5-Aza-2'-deoxycytidine did not alter methylation of KRT8 (Figure 5.5, B).

Expression of CK17 determined by IHC is higher in TMX2-28 compared to the parental cell line, MCF-7. Interestingly methylation of 3 CpGs in the promoter region (MAPINFO no. 39781130, 39781108 and 39781055) have decreased methylation in TMX2-28 (mean average beta of 0.35) compared to MCF-7 (mean average beta of 0.62) (Figure 5.6, A). There was also a decrease in methylation in TMX2-4 and TMX2-11. An increase in CK17 expression was observed in TMX2-11 but not TMX2-4 (Figure 5.6, C). This inverse relationship between DNA promoter methylation and protein expression may indicate that promoter methylation regulates expression of CK17 in TMX2-11 and TMX2-28. A different mechanism may be responsible for regulating expression of CK17 in TMX2-4. Additionally, the mean average beta values for KRT17 loci for each cell line decreased with 5-Aza-2'-deoxycytidine. Mean Methylation of KRT17 loci in TMX2-28 had the largest change after 5-Aza-2'-deoxycytidine treatment, decreasing from 0.51 to 0.39 (Figure 5.6, B). Therefore, I would predict a corresponding increase in CK17 expression in 5-Aza-2'-deoxycytidine-treated TMX2-28.

The majority of CpGs in the promoter of KRT18 have low methylation (with the exception of 2 CpGs MAPINFO numbers: 53341686 and 53342553) for MCF-7, TMX2-4, TMX2-11 and TMX2-28. The mean average beta values for all KRT18 loci for the four cell lines range from 0.18 – 0.20 and all four cell lines have high expression of CK18 (Figure 5.7, A). Low promoter methylation along with high

protein expression suggests possible regulation of gene expression by promoter methylation. It is also interesting to note that for CpG sites MAPINFO numbers 53341319, 53341686, 53341805 and 53342553, the methylation pattern for MCF-7 is similar to that of TMX2-11 while the methylation pattern for TMX2-4 is more similar to TMX2-28 than the other cell lines. Treatment with 5-Aza-2'-deoxycytidine had little effect on KRT18 methylation, as the mean average beta values ranged from 0.16 – 0.20 (Figure 5.7, B).

The IHC staining shows no expression of the luminal cytokeratin, CK20, in MCF-7, TMX2-4, TMX2-11 or TMX2-28. Interestingly, the majority of the CpG sites for the KRT20 gene represented on the 450 BeadChip are either in the TSS1500 or first exon and have high methylation (mean average beta values range from 0.61 – 0.74) with the exception of CpG site MAPINFO number 39041602 having low methylation in each cell line (Figure 5.8, A). As with the methylation pattern observed for KRT18, the methylation patterns for MCF-7 and TMX2-11 are more similar to each other than the other cell lines, while the methylation patterns for TMX2-4 and TMX2-28 are more similar to each other than the other cell lines. Interestingly, treatment with 5-Aza-2'-deoxycytidine decreased the mean average beta value for KRT20 loci in MCF-7, TMX2-11 and TMX2-28. TMX2-28 had the greatest decrease in mean average beta value from 0.61 in the control to 0.46 in the 5-Aza-2'-deoxycytidine-treated cells (Figure 5.8, B). I would predict CK20 expression to increase after 5-Aza-2'-deoxycytidine treatment in MCF-7, TMX2-11 and TMX2-28 with 5-Aza-2'-deoxycytidine-treated TMX2-28 having the highest expression of CK20.

Expression of the Basal Cytokeratins, CK1, CK6 and CK10, the Luminal Cytokeratin, CK17, and p63 Does Not Appear to Be Regulated by Promoter Methylation

KRT1 and KRT10 Expression is Not Regulated by Promoter Methylation

There is no protein expression of the basal cytokeratins CK1, CK6 or CK10 (recognized by the 34βE12 antibody) in MCF-7, TMX2-4, TMX2-11 or TMX2-28 (Table 5.1). Methylation of the promoter CpG sites represented on the 450 BeadChip for the KRT1 gene are approximately 0.20 for each of the four cell lines (mean average beta values for all KRT1 cites are higher and range from 0.42 – 0.55) (Figure 5.9, A). Treatment with 5-Aza-2'-deoxycytidine decreased KRT1 methylation in each cell line except TMX2-4. TMX2-28 was most affected by 5-Aza-2'-deoxycytidine treatment with a decrease of 12% in methylation (Figure 5.9, B). It would be interesting to determine whether this change in methylation would result in increased expression of CK1.

There are three transcripts of the CK6 gene represented on the 450 BeadChip, KRT6A, KRT6B and KRT6C. Because Ventana does not disclose which one the CK5/6 antibody recognizes, I examined DNA methylation in all three transcripts. DNA methylation in the cell lines is similar for all three transcripts (Figure 5.10, A, B and C) and treatment with 5-Aza-2'-deoxycytidine decreases the mean average beta value for each cell line, except TMX2-4 (Figure 5.10, D, E and F). The CK5/6 antibody should detect protein expression of CK5 and CK6. However, none of the cell lines had positive staining with the CK5/6 antibody yet 20% of TMX2-28 cells

were positive for CK5 determined by IHC staining with the individual antibody against CK5 (Figure 5.3). It would be interesting to examine CK6 expression with an individual antibody to determine whether CK5/6 staining is an accurate representation of protein expression.

Methylation of KRT10 is low and similar for MCF-7, TMX2-4, TMX2-11 and TMX2-28 (mean average beta values range from 0.40 – 0.47). Methylation of several CpGs in the promoter region is decreased in TMX2-28 compared to MCF-7. However, there is no protein expression of CK10 determined by 34βE12 antibody staining for any of the cell lines (Figure 5.11, A). As observed previously, treatment with 5-Aza-2'-deoxycytidine treatment has the greatest effect on methylation of KRT10 in TMX2-28, resulting in a decrease of 8% (Figure 5.11, B). However, it is not known whether this small decrease in methylation would result in an increase in protein expression.

IHC Results from the 34βE12 Antibody are Inconclusive

The other basal cytokeratins recognized by the 34βE12 antibody are CK5 and CK14. Although protein expression of CK5 and CK14 was detected in TMX2-28 with the individual antibody against each, there was no expression detected in any of the cell lines with the 34βE12 antibody (Table 5.1). Expression of CK5 and CK14 both seem to be regulated by promoter methylation in TMX2-28 (Figures 5.3 and 5.4). However the IHC results obtained with the individual antibodies do not agree with those from the 34βE12 antibody (Figure 5.12), therefore it would be best to examine the expression of CK1, CK6 and CK10 with individual antibodies as well.

Expression of p63 is Not Regulated by Promoter Methylation

According to the IHC results (Table 5.1), there is no expression of p63 in MCF-7, TMX2-4, TMX2-11 or TMX2-28. Looking at the CpG sites on the 450 BeadChip which correspond to the TP63 gene (filtering CpG sites by Refgene name has NM_001114978, NM_001114979, or NM_003722, which also contains some of the CpG sites for the ΔNp63 isoform of TP63 (p40, see Figure 5.2), most of the CpGs located in the promoter of TP63 are highly methylated in MCF-7, TMX2-4 and TMX2-11 (Figure 5.13, A). While several of these sites have decreased methylation in TMX2-28, there is not a corresponding increase in protein expression in TMX2-28. Treatment with 5-Aza-2'-deoxycytidine decreased methylation in each cell line except TMX2-4, as observed with several of the cytokeratin genes. TMX2-28 had the largest decrease in methylation with a mean average beta value of 0.65 in TMX2-28-Control and 0.49 in 5-Aza-2'-deoxycytidine-treated TMX2-28 (Figure 5.13, B). It would be interesting to determine whether 5-Aza-2'-deoxycytidine treatment increased p63 expression in the cell lines.

Discussion

According to the methylation status determined by the 450 BeadChip and protein expression determined by IHC for the parental cell line and the three tamoxifen-resistant cell lines, promoter methylation seems to play a role in regulating expression of p40, the basal cytokeratins CK5 and CK14, and the luminal cytokeratins CK8, CK17, CK18 and CK20. This is because the patterns in methylation observed among the four cell lines along with the IHC results are

consistent with the idea that promoter methylation decreases gene expression. However, promoter methylation does not appear to regulate expression of p63, or the basal cytokeratins, CK1, CK6, CK10. In the literature little is known about the role of promoter methylation and regulation of gene expression of p40, p63 and cytokeratins in breast cancer.

Interestingly methylation has been shown to play a role in regulating expression of p40, p63, CK8, CK17, CK18 in other types of cancers. Hypermethylation of a 5'-flanking CpG region of p51 or p63 was observed in hematological cancer cell lines lacking expression of p63.[129] TP63 is also methylated in b-cell lymphoma lines.[130] There is also evidence that p63 and ΔNp63 (p40) expression is regulated by methylation in bladder cancer cell lines. Treatment of some bladder cell lines with 5-Aza-2'-deoxycytidine increased expression of p63 and ΔNp63.[131] This finding is consistent with the results presented here, that p40 methylation is high in all four cell lines with no protein expression (Figure 5.2). Treatment with 5-Aza-2'-deoxycytidine decreases methylation in TMX2-28 and I would predict this results in increased protein expression of p40. However p40 protein expression after treatment with 5-Aza-2'-deoxycytidine was not quantified. In the present study, p63 expression does not seem to be regulated by promoter methylation as methylation is generally high in MCF-7, TMX2-4 and TMX2-11, but lower in TMX2-28 yet none of the cell lines have protein expression (Figure 5.12). Treatment with 5-Aza-2'-deoxycytidine decreases p63 methylation in TMX2-28 and I would predict this results in increased protein expression. However, Park and colleagues also found that certain bladder cancer cell lines had ***decreased***

expression of p63 and p40 after 5-Aza-2'-deoxycytidine treatment.[131] To date it is not known whether p40 or p63 protein expression increases in breast cancer cells after treatment with 5-Aza-2'-deoxycytidine.

There is some evidence in the literature indicating that methylation may play a role in regulating expression of CK8. Certain squamous cell carcinoma lines have increased methylation and corresponding decreased expression of CK8.[132] The gene encoding CK8, KRT8, was found to by hypomethylated with increased expression in samples of breast cancer brain metastases.[133] Similarly, treatment of mouse utricle epithelia-derived progenitor cells (MUCs), which are stem-cell like cells similar to prosensory cells which become inner ear epithelial hair cells and supporting cells during development, with 5-Aza-2'-deoxycytidine resulted in increased expression of CK8 amongst other genes as well as decreased global methylation.[134] Another study found 13 of 20 interrogated CpG sites in KRT8 to be hypermethylated, which was correlated with decreased expression in mouse colon cells.[135] These findings agree with the results presented here, as promoter methylation of KRT8 is low and expression of CK8 is high in all cell lines (Figure 5.5).

Methylation is also thought to regulate expression of CK18. In rat small intestine cells, KRT18 is hypermethylated and gene expression is downregulated.[135] Similarly, treatment of MUCs with 5-Aza-2'-deoxycytidine decreases global methylation and increases expression of KRT18.[134] With all four of the cell lines utilized in this project, the majority of CpG sites on the 450 BeadChip for KRT18 have low methylation and each cell line has high expression of CK18 (Figure 5.7).

Therefore, the results presented here are congruent with previously published findings.

The luminal cytokeratin CK17 has very low expression in MCF-7 and TMX2-4. However, 10-15% of TMX2-11 cells stained positive for CK17 and 20-25% of TMX2-28 cells were positive for CK17 (Figure 5.6). High CK17 expression is associated with a poor prognosis for cervical cancer patients. In human cervix, breast and pancreatic cancer cells, CK17 can be released from intermediate filaments and translocate to the nucleus. CK17 then binds the cyclin dependent kinase inhibitor, p27, and facilitates nuclear export of p27 and subsequent degradation. This contributes to sustaining proliferation and tumorigenesis. Expression of CK17 and p27 are inversely correlated in clinical cervical cancer samples.[136] Interestingly, previous work in our lab has shown that TMX2-28 cells express high levels of S-phase kinase-associated protein 2(SKP2), which also targets p27 for degradation by phosphorylating p27 at Thr187. SKP2 therefore promotes entry into S-phase of the cell cycle. Although TMX2-28 cells overexpress SKP2, they do not have reduced levels of p27. However, knockdown of SKP2 in TMX2-28 prevents phosphorylation of p27 at Ser10 and inhibits proliferation.[39] Therefore, because TMX2-28 do not have reduced p27 expression and CK17 contributes to p27 degradation, I would predict low expression of CK17 in TMX2-28. According to the IHC results (Table 5.1), 20-25% of TMX2-28 cells express a high level of CK17. This percentage of CK17-positive cells is greater for TMX2-28 than for MCF-7, TMX2-4 or TMX2-11. I would predict this subpopulation of TMX2-28 cells, which express CK17, to have low expression of p27 and therefore increased proliferation. Perhaps the high level of

CK17 in this subpopulation of TMX2-28 contributes to degradation of p27 and promotes proliferation.

Despite a small portion (20%) of TMX2-28 cells staining positive for CK5, there was no positive staining with the CK5/6 antibody (Table 5.1). The CK5/6 antibody can distinguish between cancerous and non-cancerous ductal proliferation.[137] However, the sensitivity and intensity of individual CK5 antibody staining is higher than that of CK5/6 antibody cocktails.[138] The cell line slides for IHC were fixed in methanol, a non-cross-linking fixative. Fixation with methanol removes water and disrupts hydrophobic bonds and hydrogen bonds, which causes protein unfolding. This denaturation may affect immunoreactivity depending on the nature of the antigen or antibody in this case.[139] The sensitivity of the detection kit also may have contributed to the discrepancy as different detection kits were used for the CK5 and CK5/6 antibody. This same reasoning may also explain the inconsistency between staining with the 34βE12 antibody and the individual CK5 and CK14 antibodies. The 34βE12 antibody should recognize the basal cytokeratins, CK1, CK5, CK10 and CK14. Neither MCF-7, TMX2-4, TMX2-11 nor TMX2-28 cells had positive staining with the 34βE12 antibody (Table 5.1). However, a small population of TMX2-28 cells stained positive for the individual antibodies against CK5 and CK14. This could be attributed to variations in the antibody recognition site between antibodies, denaturation of antigen or differences in sensitivity of the antibodies or detection kits.

The results presented here with regard to cytokeratin expression indicate that MCF-7, TMX2-4 and TMX2-11 express luminal (low molecular weight)

cytokeratins while TMX2-28 express a combination of luminal and basal cytokeratins. These new IHC data are consistent with previously published work from our lab[75] and demonstrate that TMX2-28 have a mixed basal-luminal phenotype. The data from the 450 BeadChip indicate that DNA promoter methylation may be involved in regulating expression of p40, CK5, CK14, CK8, CK17, CK18 and CK20 in breast cancer cells. The role of methylation in regulation of gene expression could be verified by examining protein expression in cells treated with 5-Aza-2'-deoxycytidine or a demethylating agent and confirming the degree of DNA methylation by pyrosequencing. DNA methylation of cytokeratin genes may be useful as an alternative indication of tumor subtype. Furthermore, analysis of methylation patterns in patient samples would further validate the use of these cell lines to study drug resistant breast cancer.

Table 5.1 Cytokeratin, p40 and p63 Expression Determined by IHC for Cell Lines

		MCF-7		TMX2-4		TMX2-11		TMX2-28	
		%	Intensity	%	Intensity	%	Intensity	%	Intensity
	p40	0	n/a	0	n/a	0	n/a	0	n/a
	p63	0	n/a	0	n/a	0	n/a	0	n/a
High molecular weight (basal)	34βE12*	0	n/a	0	n/a	0	n/a	0	n/a
	CK 5	0	n/a	< 1%	1+	0	n/a	20%	2+
	CK 5/6	0	n/a	0	n/a	0	n/a	0	n/a
	CK 14	0	n/a	0	n/a	0	n/a	10%	2+ (majority) (some 3+)
Low molecular weight (luminal)	CK 8	100%	2+	100%	2+	100%	2+	100%	2+
	CK 17	2-3%	2+	< 1%	2+	10-15%	2+ (majority) (occasional 3+)	20-25%	3+
	CK 18	100%	3+	100%	3+	100%	3+	100%	3+
	CK 20	0	n/a	0	n/a	0	n/a	0	n/a

*34βE12 antibody recognizes CK1, CK5, CK10 and CK14

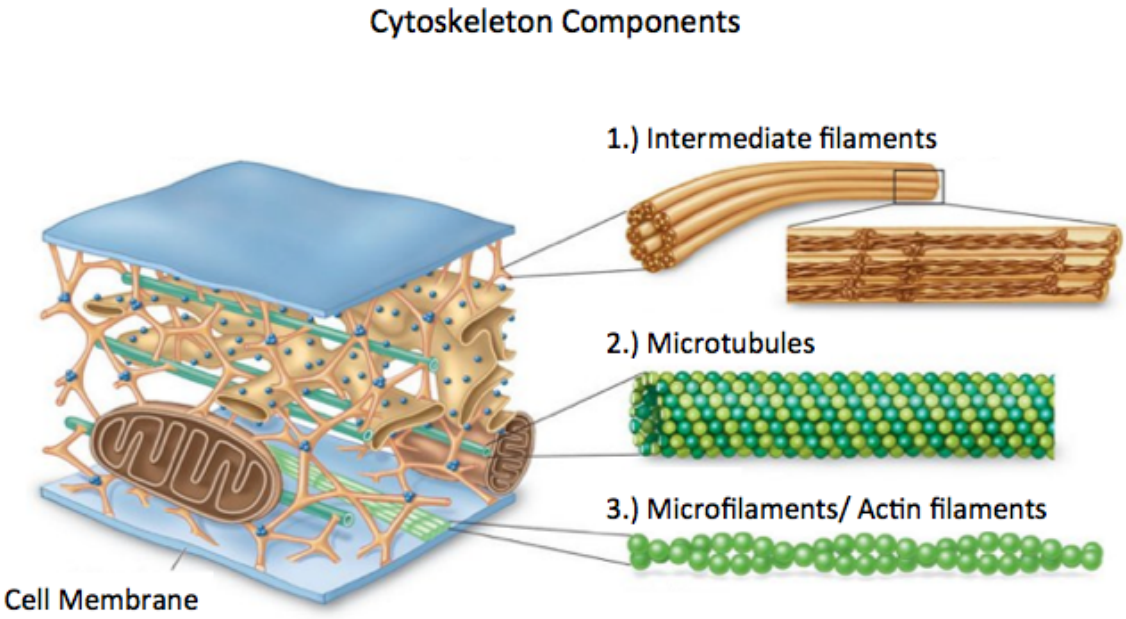

Figure 5.1: Components of the Cytoskeleton. Three-dimensional cross section view of a cell showing the three components of the cytoskeleton; intermediate filaments, microtubules and microfilaments/ actin filaments. Intermediate filaments are composed of specific fibrous proteins such as keratins and desmins. Microtubules are hollow tubes made up of alpha- and beta- tubulin assembled into protofilaments. Microfilaments or actin filaments are made of interlaced actin chains. Image modified from [140].

(A)

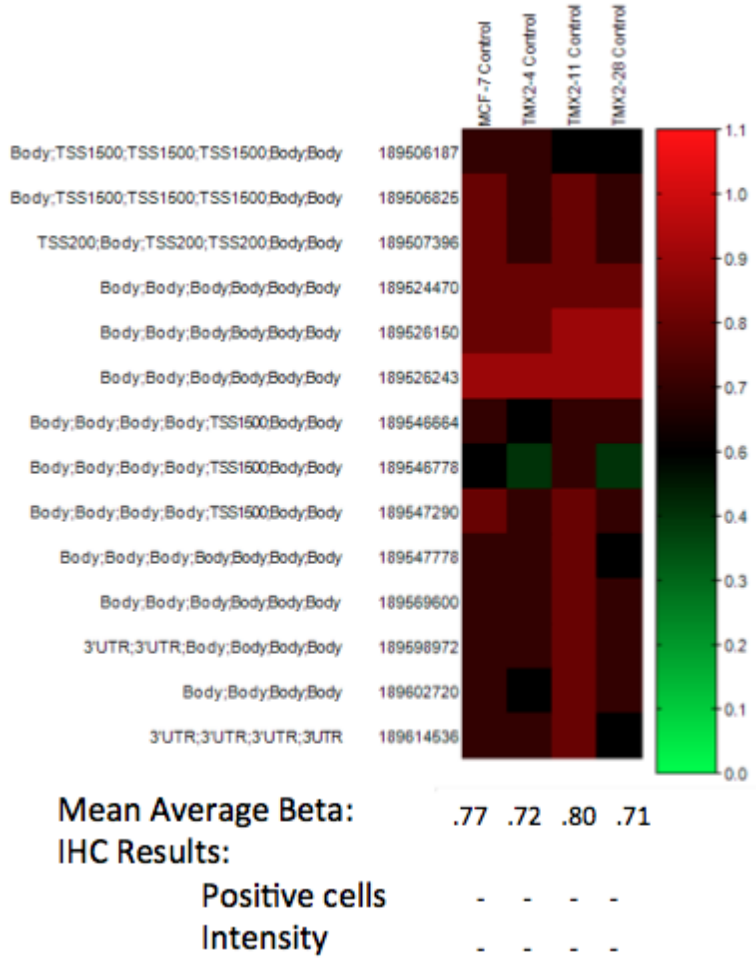
MCF-7 Control
TMX2-4 Control
TMX2-11 Control
TMX2-28 Control
Body;TSS1500;TSS1500;TSS1500;Body;Body 189506187
Body;TSS1500;TSS1500;TSS1500;Body;Body 189506825
TSS200;Body;TSS200;TSS200;Body;Body 189507396
Body;Body;Body;Body;Body;Body 189524470
Body;Body;Body;Body;Body;Body 189526150
Body;Body;Body;Body;Body;Body 189526243
Body;Body;Body;Body;TSS1500;Body;Body 189546664
Body;Body;Body;Body;TSS1500;Body;Body 189546778
Body;Body;Body;Body;TSS1500;Body;Body 189547290
Body;Body;Body;Body;Body;Body;Body 189547778
Body;Body;Body;Body;Body;Body 189569600
3'UTR;3'UTR;Body;Body;Body;Body 189598972
Body;Body;Body;Body 189602720
3'UTR;3'UTR;3'UTR;3'UTR 189614536
1.1
1.0
0.9
0.8
0.7
0.6
0.4
0.3
0.2
0.1
0.0
Mean Average Beta: .77 .72 .80 .71
IHC Results:
Positive cells - - - -
Intensity - - - -

(Figure 5.2)

(B)

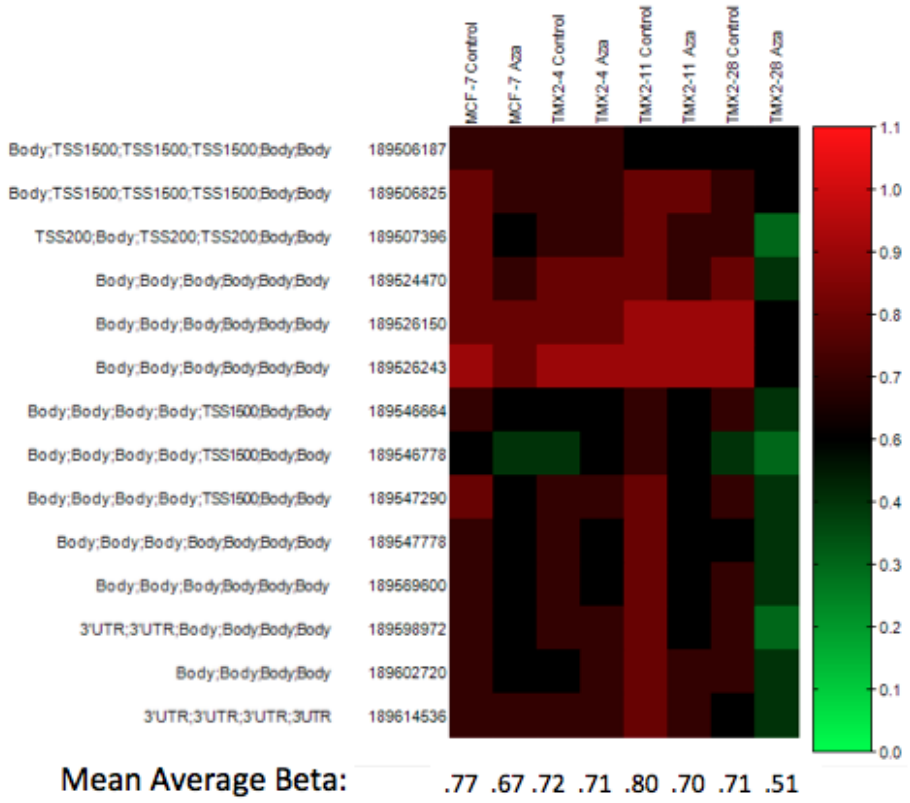

Figure 5.2: p40 is Highly Methylated in All Cell Lines. Heat map indicating average beta values of CpG sites on the 450K BeadChip for the ΔNp63 isoform of the TP63 gene (recognized by the p40 antibody) for each cell line (A) and the 5-Aza-2'-deoxycytidine-treated cell lines (B). Average beta value is represented by the scale, highest methylation value (1) in red and lowest methylation value (0) in green (see scale at right). Refgene group and MAPINFO number for each CpG site are listed to the left of each heat map. Mean average beta values of all CpG sites for each cell line are listed under the corresponding columns. IHC results are also listed for each cell line under the corresponding columns as percentage of positive cells and intensity (-: no staining).

(A)

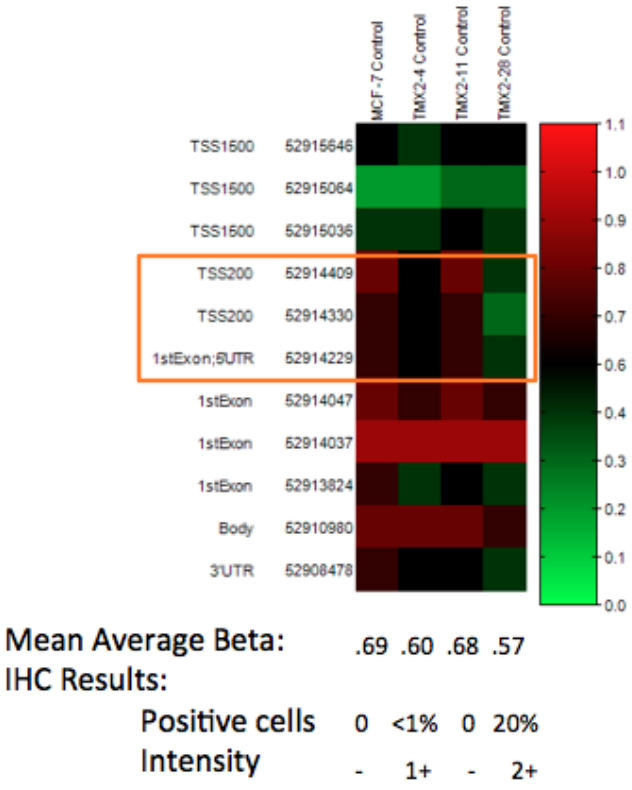
MCF-7 Control
TMX2-4 Control
TMX2-11 Control
TMX2-28 Control
TSS1500 52915646
TSS1500 52915064
TSS1500 52915036
TSS200 52914409
TSS200 52914330
1stExon;5'UTR 52914229
1stExon 52914047
1stExon 52914037
1stExon 52913824
Body 52910980
3'UTR 52908478
1.1
1.0
0.9
0.8
0.7
0.6
0.4
0.3
0.2
0.1
0.0
Mean Average Beta: .69 .60 .68 .57
IHC Results:
Positive cells 0 <1% 0 20%
Intensity - 1+ - 2+

(Figure 5.3)

(B)

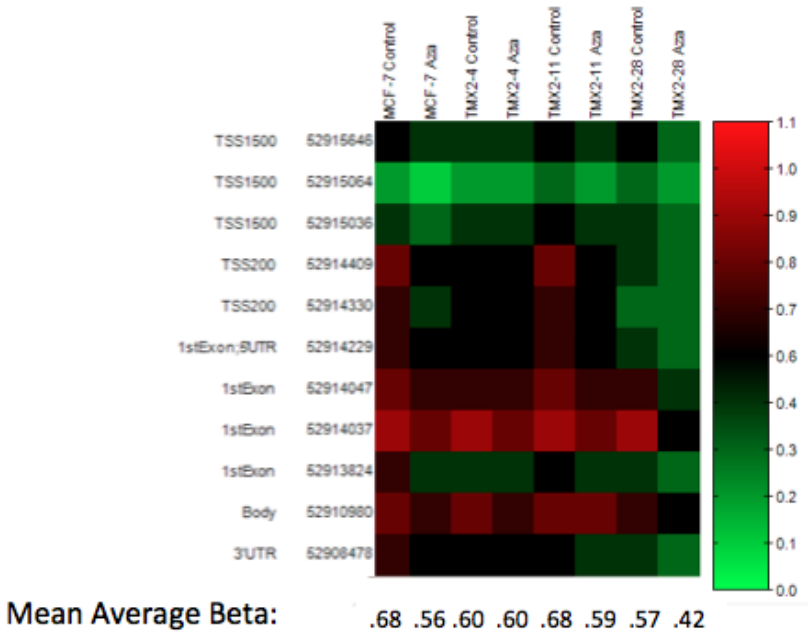

Figure 5.3: CK5 Expression May Be Regulated by Promoter Methylation in TMX2-28. Heatmap indicating average beta values of CpG sites in the KRT5 gene for each cell line (A) and the 5-Aza-2'-deoxycytidine-treated cell lines (B). Average beta value is represented by the scale, highest methylation value (1) in red and lowest methylation value (0) in green (see scale at right). Refgene group and MAPINFO number for each CpG site are listed to the left of each heat map. Mean average beta values of all CpG sites for each cell line are listed under the corresponding columns. IHC results are also listed for each cell line under the corresponding columns as percentage of positive cells and intensity (-: no staining).

(A)

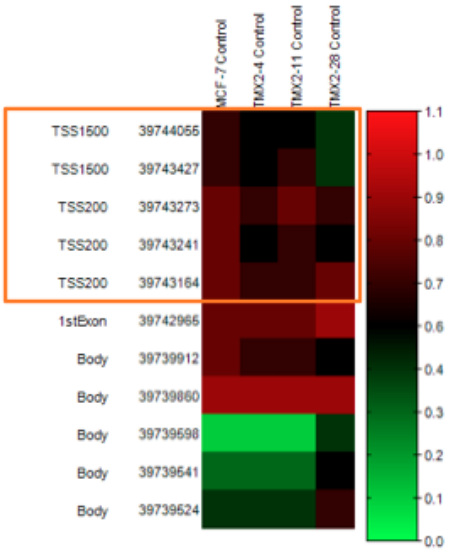

Mean Average Beta:	.67	.61	.65	.66
Promoter Mean Average Beta:	.76	.66	.72	.62
IHC Results:				
Positive cells	0	0	0	10%
Intensity	-	-	-	2+

(B)

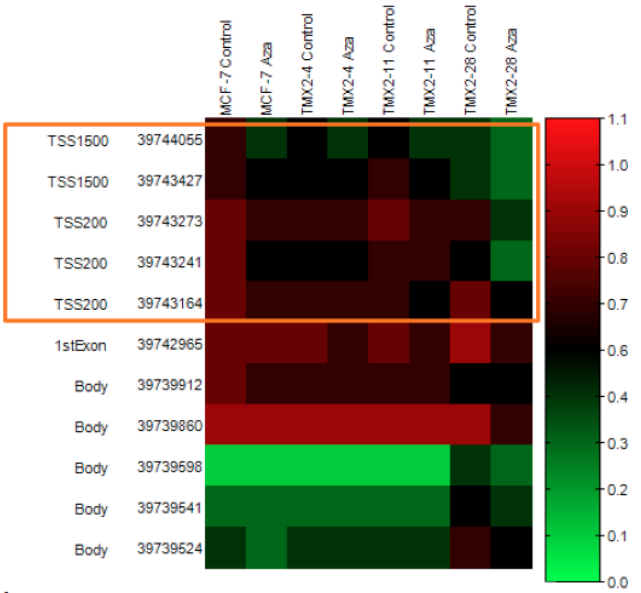

Mean Average Beta:	.67	.59	.61	.60	.65	.58	.66	.53
Promoter Mean Average Beta:	.76	.63	.66	.63	.71	.62	.62	.47

(Figure 5.4)

Figure 5.4: CK14 Expression May Be Regulated by Promoter Methylation.
Heatmap indicating methylation of CpG sites in KRT14 gene, represented by average beta values (scale at right), and corresponding protein expression determined by IHC for each cell line (A) and the 5-Aza-2'-deoxycytidine-treated cell lines (B). Orange box indicates CpGs located in the promoter. Left: Refgene Group location and MAPINFO number for each CpG site. Bottom: Mean average beta values for all CpGs, mean average beta values for CpGs in the promoter, percent positive cells and intensity determined from IHC scoring (-: negative staining).

(A)

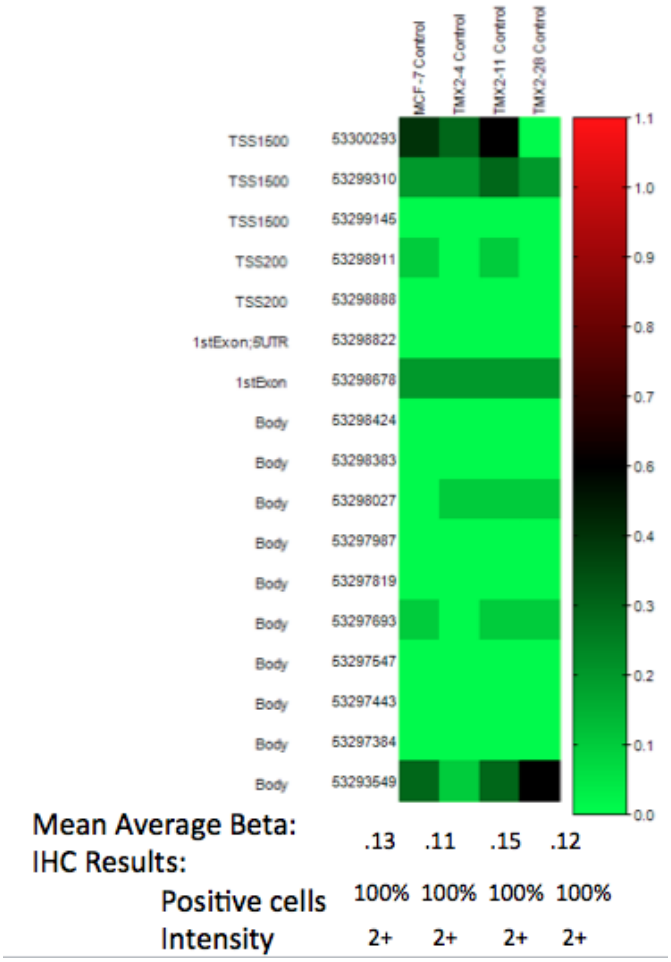
MCF-7 Control
TMX2-4 Control
TMX2-11 Control
TMX2-28 Control
TSS1500 53300293
TSS1500 53299310
TSS1500 53299145
TSS200 53298911
TSS200 53298888
1stExon;5UTR 53298822
1stExon 53298678
Body 53298424
Body 53298383
Body 53298027
Body 53297987
Body 53297819
Body 53297693
Body 53297547
Body 53297443
Body 53297384
Body 53293549
1.1
1.0
0.9
0.8
0.7
0.6
0.4
0.3
0.2
0.1
0.0
Mean Average Beta: .13 .11 .15 .12
IHC Results:
Positive cells 100% 100% 100% 100%
Intensity 2+ 2+ 2+ 2+

(Figure 5.5)

(B)

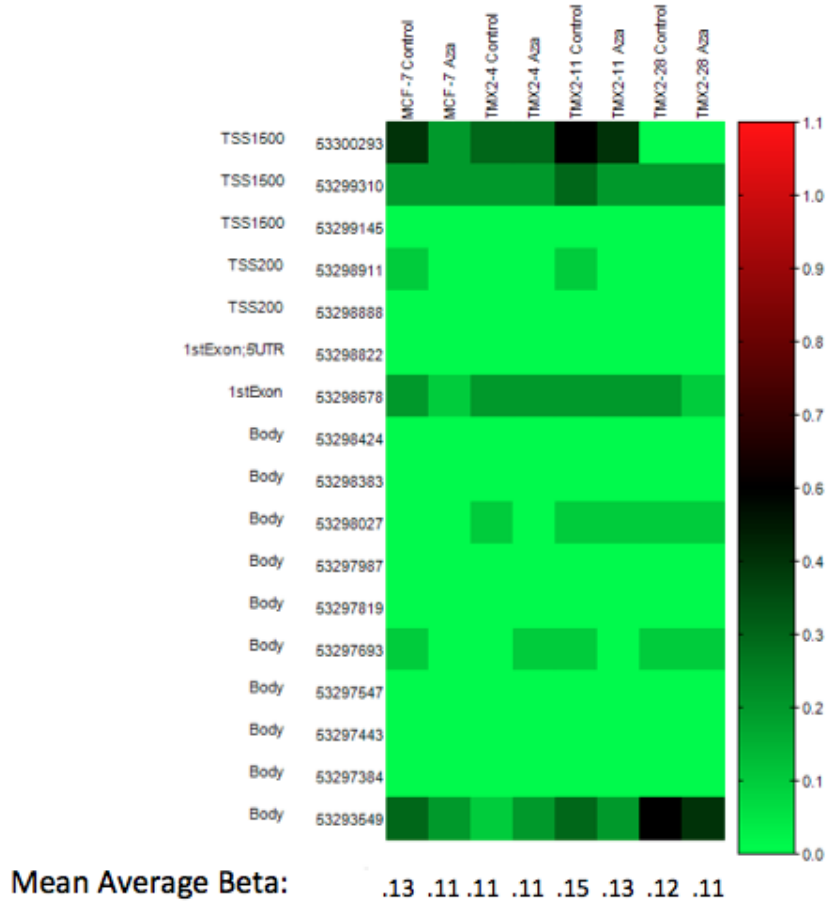

Figure 5.5: CK8 Expression May Be Regulated by Promoter Methylation. Heatmap indicating methylation of CpG sites in KRT8 gene, represented by average beta values (scale at right), and corresponding protein expression determined by IHC for each cell line (A) and the 5-Aza-2'-deoxycytidine-treated cell lines (B). Left: Refgene Group location and MAPINFO number for each CpG site. Bottom: Mean average beta values for all CpGs and percent positive cells and intensity determined from IHC scoring.

(A)

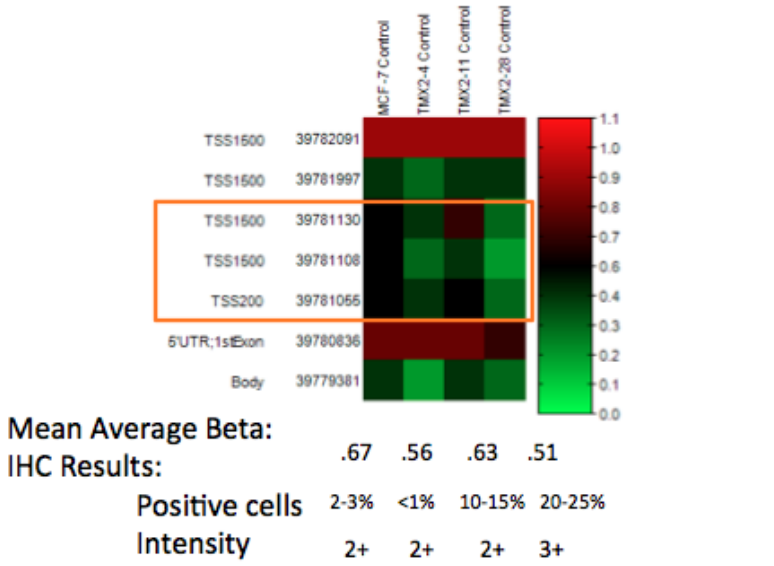
MCF-7 Control
TMX2-4 Control
TMX2-11 Control
TMX2-28 Control
TSS1500 39782091
TSS1500 39781997
TSS1500 39781130
TSS1500 39781108
TSS200 39781055
5'UTR;1stExon 39780836
Body 39779381
1.1
1.0
0.9
0.8
0.7
0.6
0.4
0.3
0.2
0.1
0.0
Mean Average Beta: .67 .56 .63 .51
IHC Results:
Positive cells 2-3% <1% 10-15% 20-25%
Intensity 2+ 2+ 2+ 3+

(B)

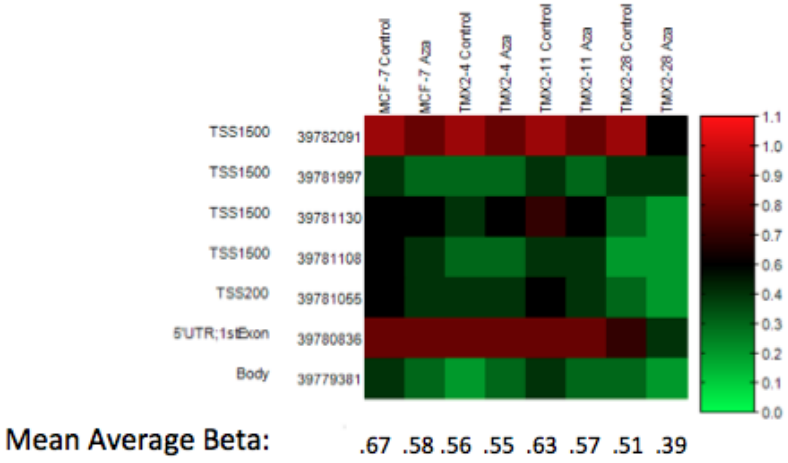
MCF-7 Control
MCF-7 Aza
TMX2-4 Control
TMX2-4 Aza
TMX2-11 Control
TMX2-11 Aza
TMX2-28 Control
TMX2-28 Aza
TSS1500 39782091
TSS1500 39781997
TSS1500 39781130
TSS1500 39781108
TSS200 39781055
5'UTR;1stExon 39780836
Body 39779381
1.1
1.0
0.9
0.8
0.7
0.6
0.4
0.3
0.2
0.1
0.0
Mean Average Beta: .67 .58 .56 .55 .63 .57 .51 .39

(Figure 5.6)

(C)

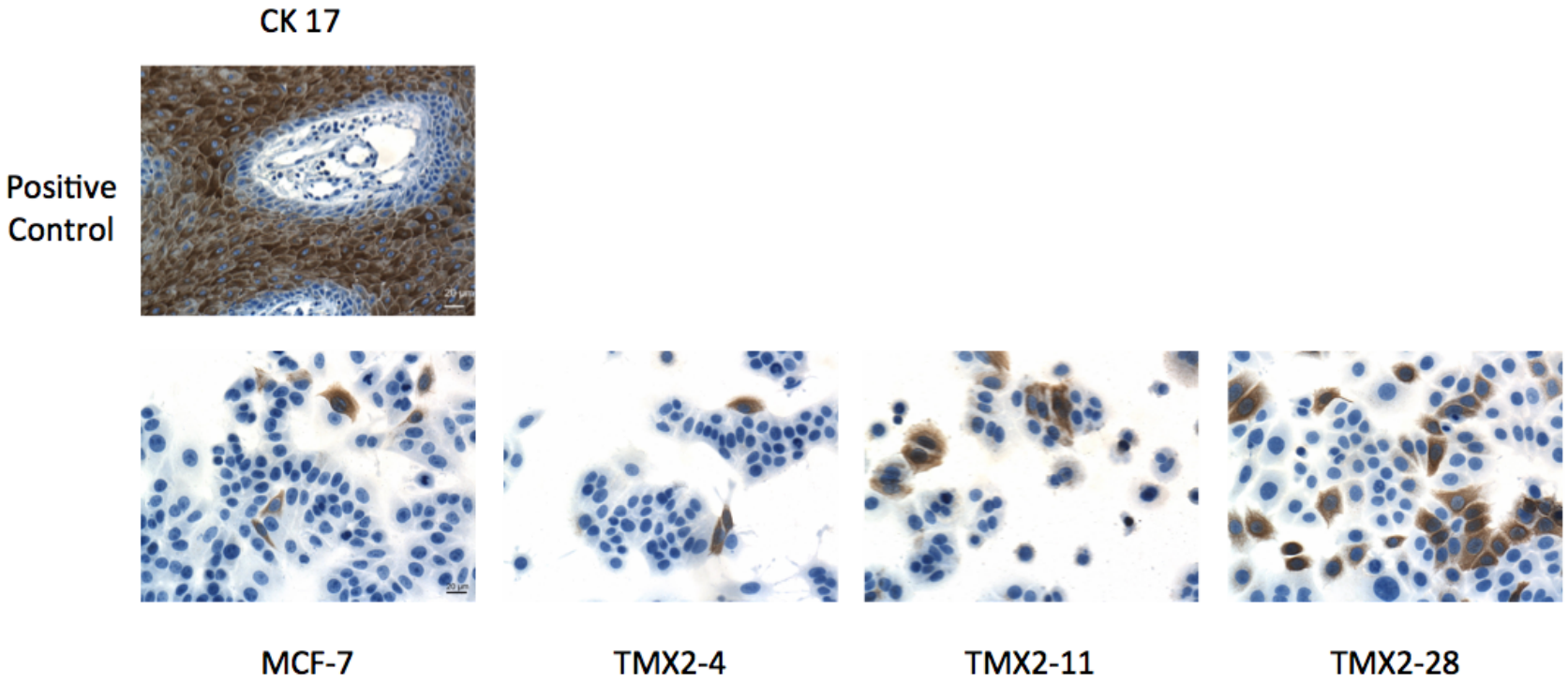

(Figure 5.6)

Figure 5.6: CK17 Expression May Be Regulated by Promoter Methylation. Heatmap indicating methylation of CpG sites in KRT17 gene, represented by average beta values (scale at right), and corresponding protein expression determined by IHC for each cell line (A) and the 5-Aza-2'-deoxycytidine-treated cell lines (B). Orange box indicates three CpGs in the promoter with decreased methylation in TMX2-28 compared to MCF-7. Left: Refgene Group location and MAPINFO number for each CpG site. Bottom: Mean average beta values for all CpGs and percent positive cells and intensity determined from IHC scoring. Representative images of IHC slides stained for CK17 in the positive control and MCF-7, TMX2-4, TMX2-11 and TMX2-28 (C). Magnification = 200X.

(A)

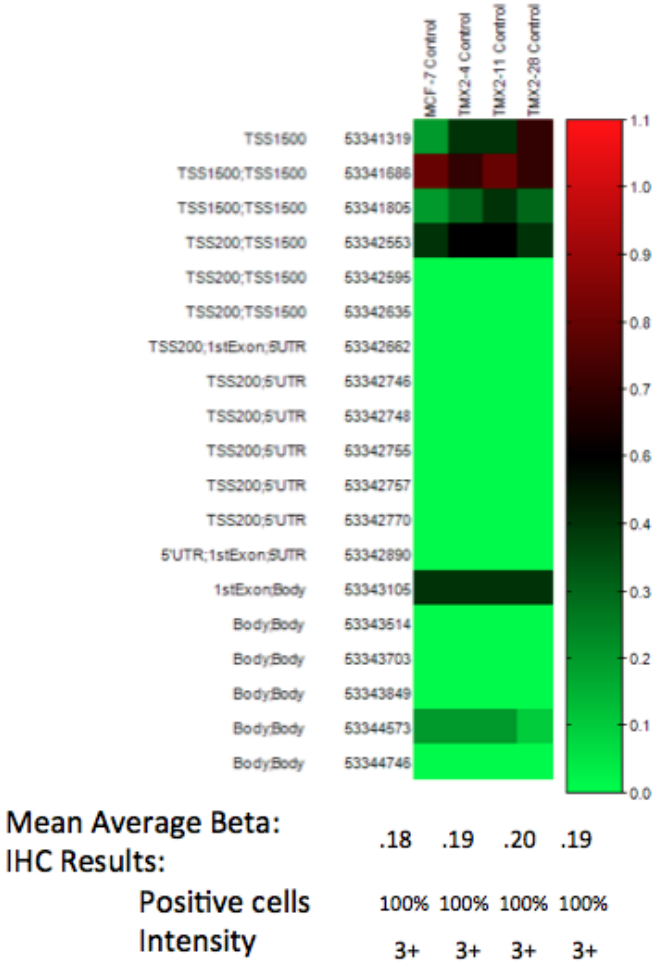
MCF-7 Control
TMX2-4 Control
TMX2-11 Control
TMX2-28 Control
TSS1500 53341319
TSS1500;TSS1500 53341686
TSS1500;TSS1500 53341805
TSS200;TSS1500 53342553
TSS200;TSS1500 53342595
TSS200;TSS1500 53342635
TSS200;1stExon;5'UTR 53342662
TSS200;5'UTR 53342746
TSS200;5'UTR 53342748
TSS200;5'UTR 53342755
TSS200;5'UTR 53342757
TSS200;5'UTR 53342770
5'UTR;1stExon;5'UTR 53342890
1stExon;Body 53343105
Body;Body 53343514
Body;Body 53343703
Body;Body 53343849
Body;Body 53344573
Body;Body 53344746
1.1
1.0
0.9
0.8
0.7
0.6
0.4
0.3
0.2
0.1
0.0
Mean Average Beta: .18 .19 .20 .19
IHC Results:
Positive cells 100% 100% 100% 100%
Intensity 3+ 3+ 3+ 3+

(Figure 5.7)

(B)

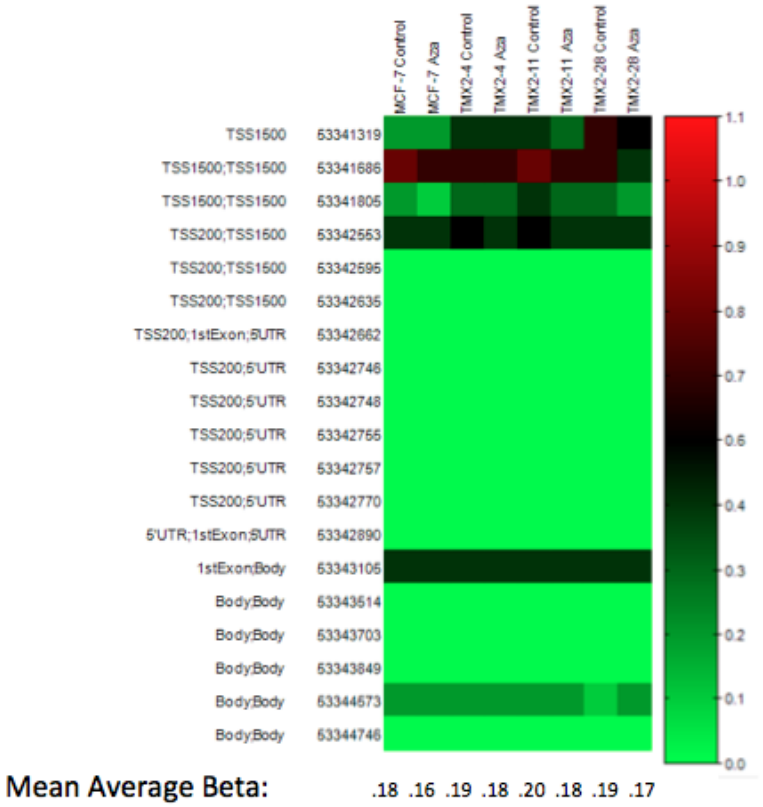

Figure 5.7: CK18 Expression May Be Regulated by Promoter Methylation. Heatmap indicating methylation of CpG sites in KRT18 gene, represented by average beta values (scale at right), and corresponding protein expression determined by IHC for each cell line (A) and the 5-Aza-2'-deoxycytidine-treated cell lines (B). Left: Refgene Group location and MAPINFO number for each CpG site. Bottom: Mean average beta values for all CpGs and percent positive cells and intensity determined from IHC scoring.

(A)

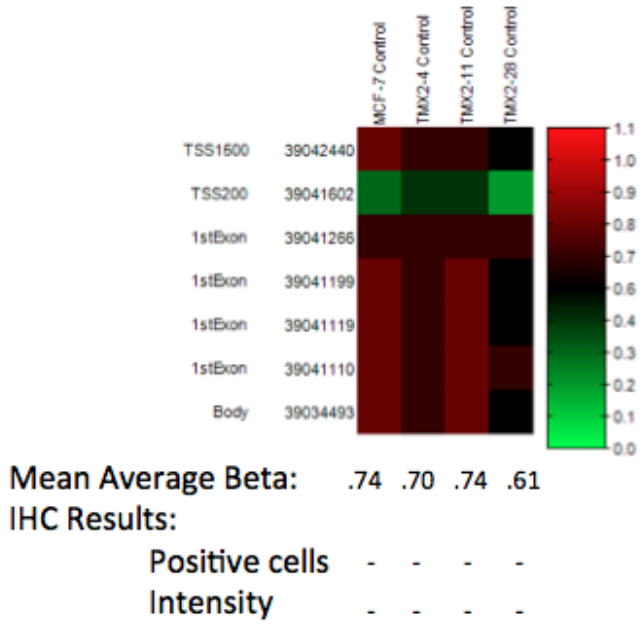

(B)

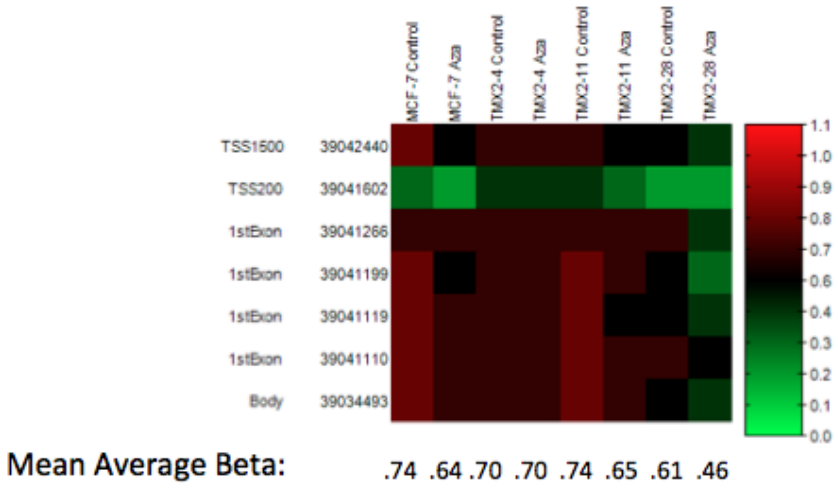

Figure 5.8: CK20 Expression May Be Repressed by Promoter Methylation. Heatmap indicating methylation of CpG sites in KRT20 gene, represented by average beta values (scale at right), and corresponding protein expression determined by IHC for each cell line (A) and the 5-Aza-2'-deoxycytidine-treated cell lines (B). Left: Refgene Group location and MAPINFO number for each CpG site. Bottom: Mean average beta values for all CpGs and percent positive cells and intensity determined from IHC scoring (-: no staining).

(A)

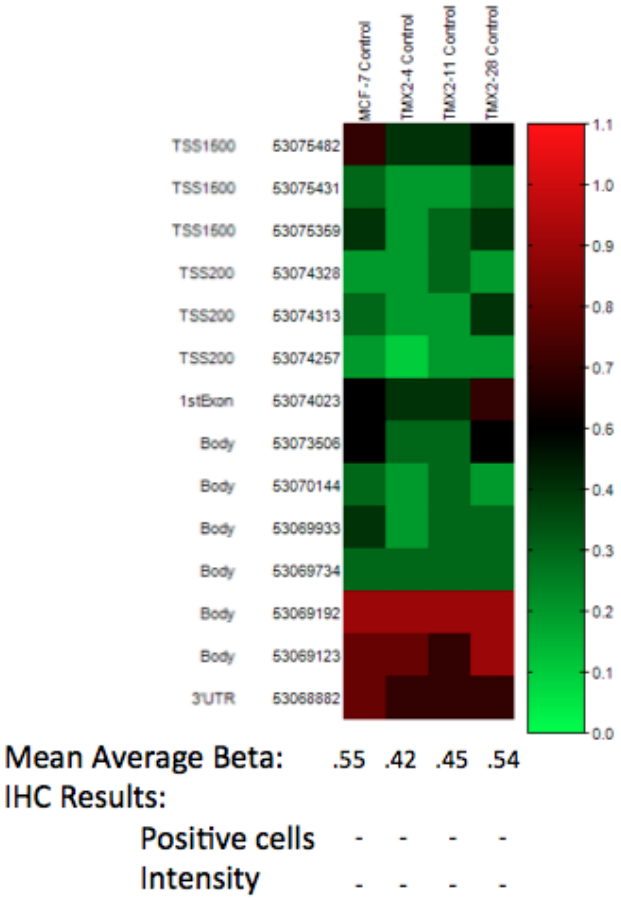
MCF-7 Control
TMX2-4 Control
TMX2-11 Control
TMX2-28 Control
TSS1500 53075482
TSS1500 53075431
TSS1500 53075359
TSS200 53074328
TSS200 53074313
TSS200 53074257
1stExon 53074023
Body 53073506
Body 53070144
Body 53069933
Body 53069734
Body 53069192
Body 53069123
3'UTR 53068882
1.1
1.0
0.9
0.8
0.7
0.6
0.4
0.3
0.2
0.1
0.0
Mean Average Beta: .55 .42 .45 .54
IHC Results:
Positive cells - - - -
Intensity - - - -

(Figure 5.9)

(B)

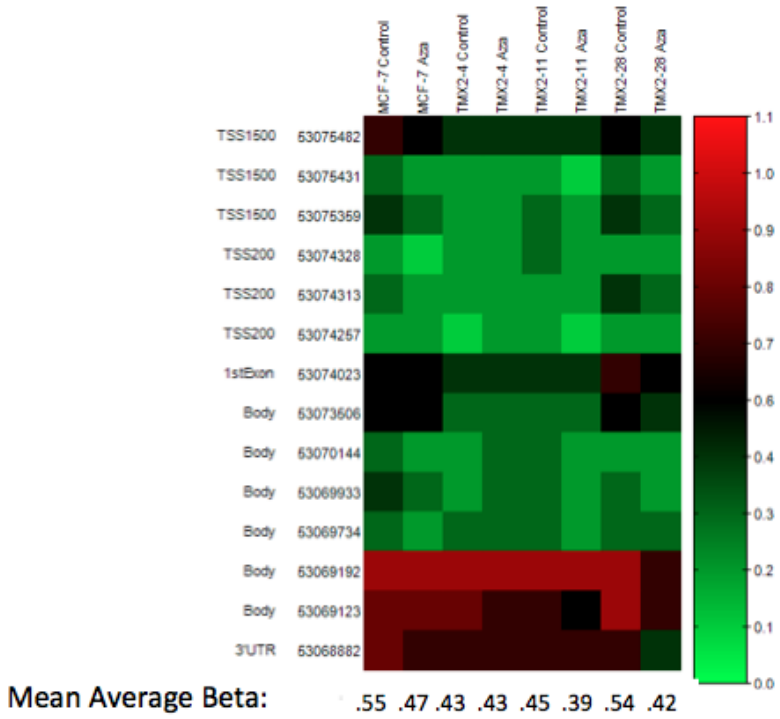

Figure 5.9: Expression of CK1 Does Not Appear to be Regulated by Promoter Methylation. Heatmap indicating methylation of CpG sites in KRT1 gene, represented by average beta values (scale at right), and corresponding protein expression determined by IHC for each cell line (A) and the 5-Aza-2'-deoxycytidine-treated cell lines (B). Left: Refgene Group location and MAPINFO number for each CpG site. Bottom: Mean average beta values for all CpGs and percent positive cells and intensity determined from IHC scoring (recognized by the 34βE12 antibody, -: no staining).

(A)

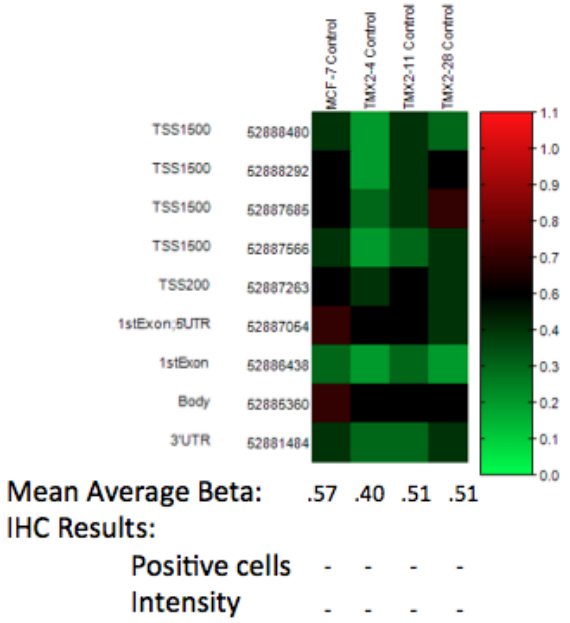

(B)

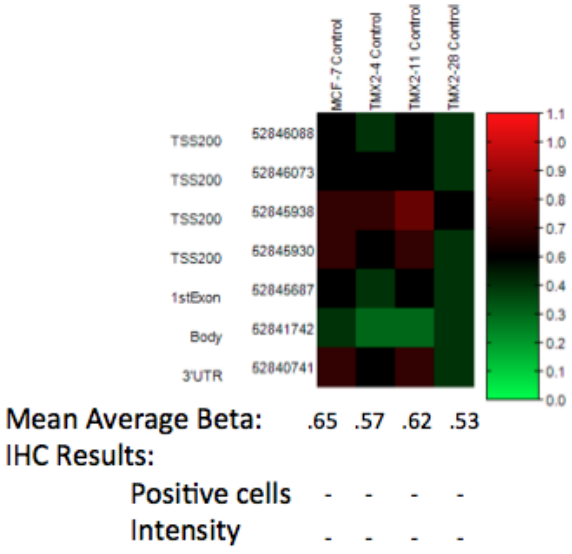

(Figure 5.10)

(C)

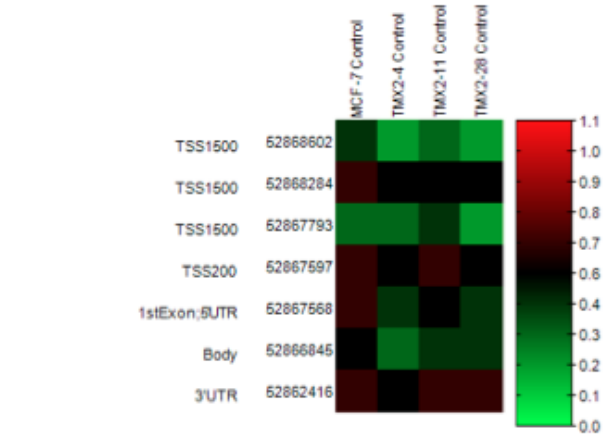

Mean Average Beta: .61 .50 .57 .50

IHC Results:

Positive cells - - - -

Intensity - - - -

(D)

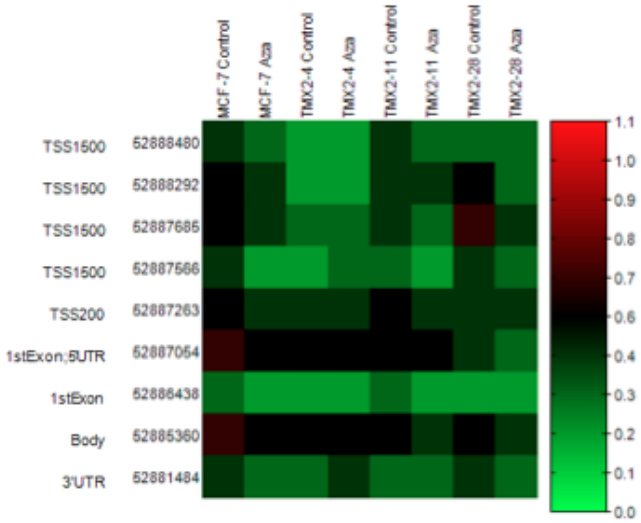

Mean Average Beta: .57 .46 .40 .43 .51 .44 .51 .41

(Figure 5.10)

(E)

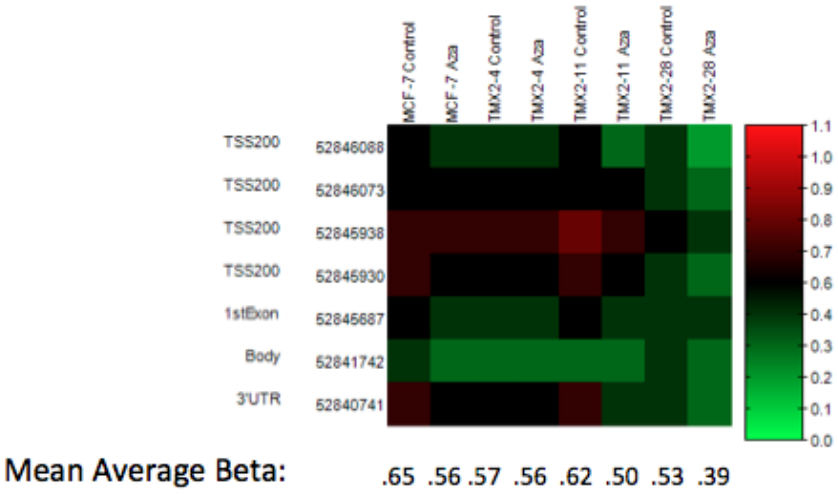

(F)

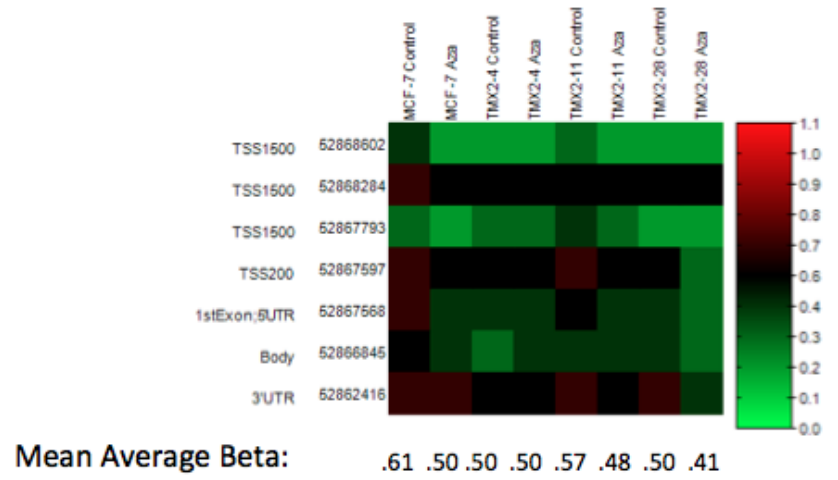

(Figure 5.10)

Figure 5.10. CK6 Expression Does Not Appear to be Regulated by Promoter Methylation. Heatmap indicating methylation of CpG sites in KRT6A (A), KRT6B (B) and KRT6C (C) gene, represented by average beta values (scale at right), and corresponding protein expression determined by IHC for each cell line and the 5-Aza-2'-deoxycytidine-treated cell lines for KRT6A (D), KRT6B (E) and KRT6C (F). Left: Refgene Group location and MAPINFO number for each CpG site. Bottom: Mean average beta values for all CpGs and percent positive cells and intensity determined from IHC scoring (recognized by the 34βE12 antibody, (-: no staining).

(A)

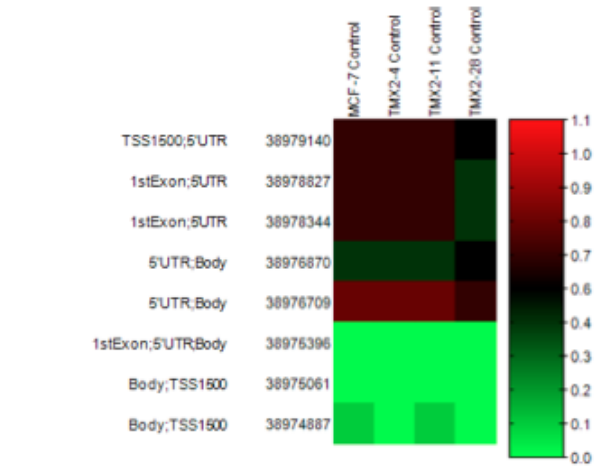

Mean Average Beta: .47 .46 .46 .40

IHC Results:

Positive cells - - - -

Intensity - - - -

(B)

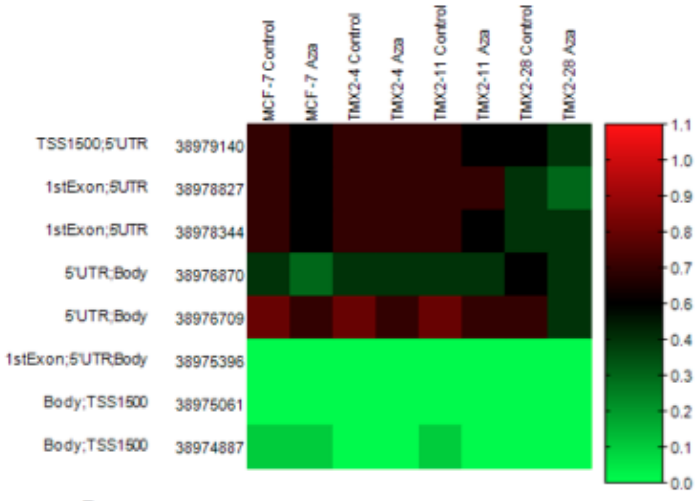

Mean Average Beta: .47 .41 .46 .45 .46 .42 .40 .32

(Figure 5.11)

Figure 5.11: Expression of CK10 Does Not Appear to be Regulated by Promoter Methylation. Heatmap indicating methylation of CpG sites in KRT10 gene, represented by average beta values (scale at right), and corresponding protein expression determined by IHC for each cell line (A) and the 5-Aza-2'-deoxycytidine-treated cell lines (B). Left: Refgene Group location and MAPINFO number for each CpG site. Bottom: Mean average beta values for all CpGs and percent positive cells and intensity determined from IHC scoring (recognized by the 34βE12 antibody, (-: no staining).

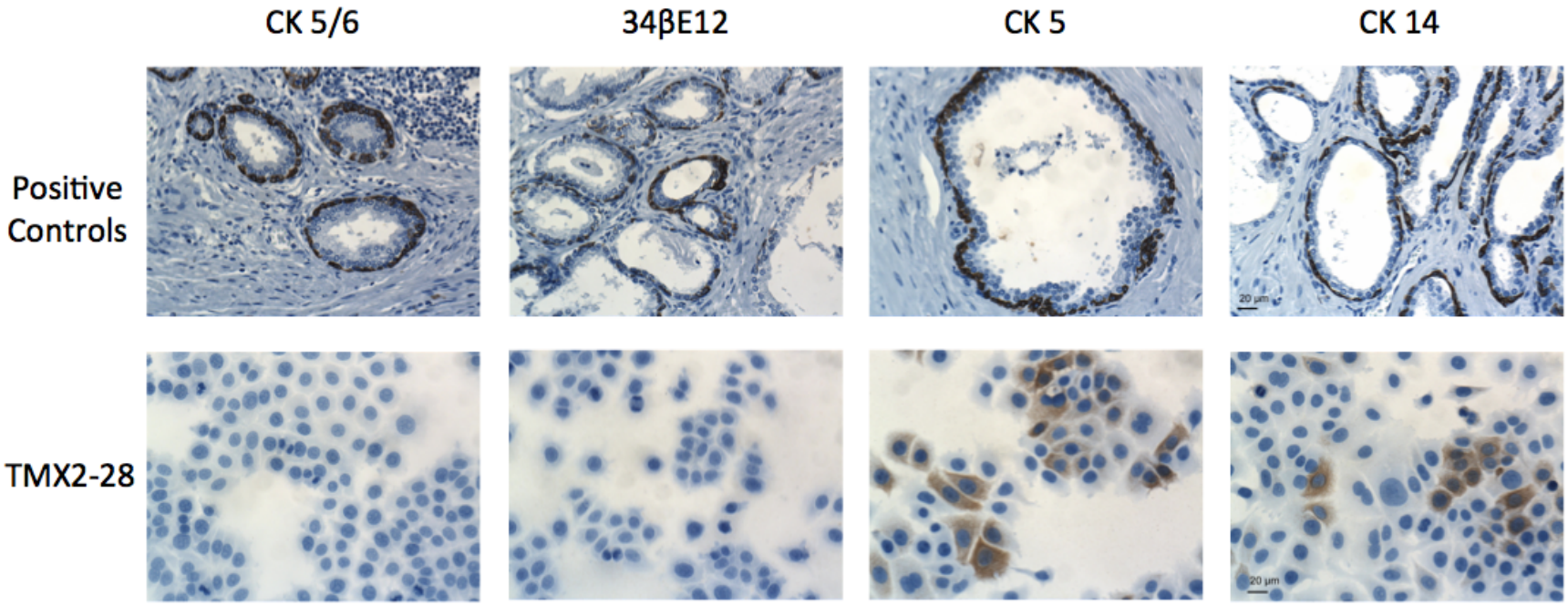

Figure 5.12: IHC Staining with Pan Cytokeratin Antibodies and Individual CK Antibodies. Representative images for staining of positive controls and TMX2-28 with the 34βE12 antibody and the antibodies recognizing CK5/6, CK5 and CK14. Magnification = 200X.

(A)

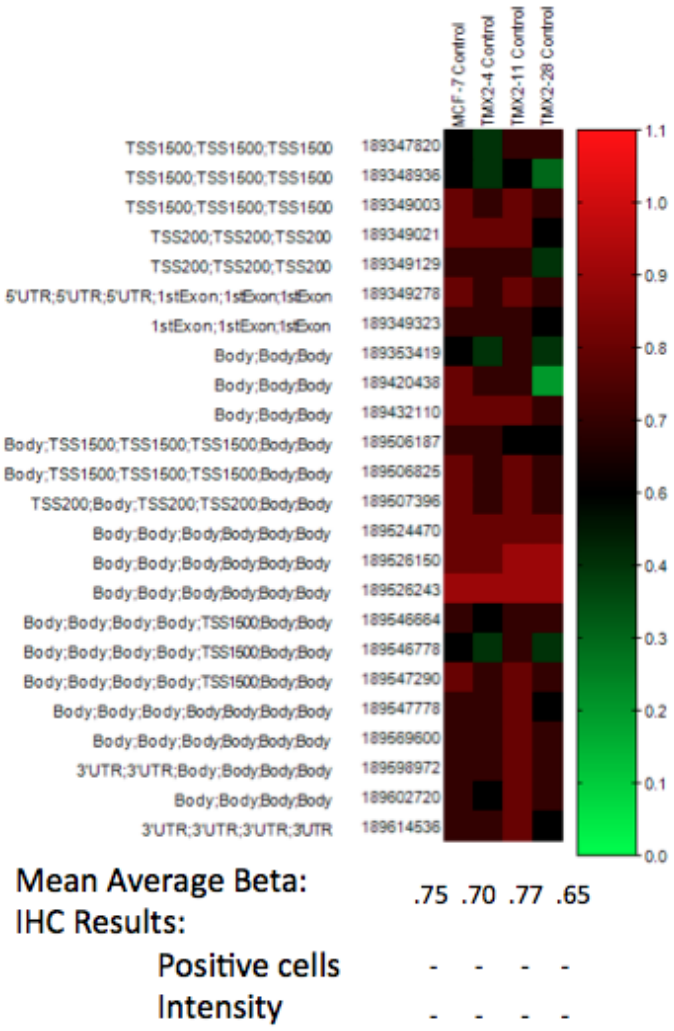
MCF-7 Control
TMX2-4 Control
TMX2-11 Control
TMX2-28 Control
TSS1500;TSS1500;TSS1500 189347820
TSS1500;TSS1500;TSS1500 189348936
TSS1500;TSS1500;TSS1500 189349003
TSS200;TSS200;TSS200 189349021
TSS200;TSS200;TSS200 189349129
5'UTR;5'UTR;5'UTR;1stExon;1stExon;1stExon 189349278
1stExon;1stExon;1stExon 189349323
Body;Body;Body 189353419
Body;Body;Body 189420438
Body;Body;Body 189432110
Body;TSS1500;TSS1500;TSS1500;Body;Body 189506187
Body;TSS1500;TSS1500;TSS1500;Body;Body 189506825
TSS200;Body;TSS200;TSS200;Body;Body 189507396
Body;Body;Body;Body;Body;Body 189524470
Body;Body;Body;Body;Body;Body 189526150
Body;Body;Body;Body;Body;Body 189526243
Body;Body;Body;Body;TSS1500;Body;Body 189546664
Body;Body;Body;Body;TSS1500;Body;Body 189546778
Body;Body;Body;Body;TSS1500;Body;Body 189547290
Body;Body;Body;Body;Body;Body;Body 189547778
Body;Body;Body;Body;Body;Body 189569600
3'UTR;3'UTR;Body;Body;Body;Body 189598972
Body;Body;Body;Body 189602720
3'UTR;3'UTR;3'UTR;3'UTR 189614536
1.1
1.0
0.9
0.8
0.7
0.6
0.4
0.3
0.2
0.1
0.0
Mean Average Beta: .75 .70 .77 .65
IHC Results:
Positive cells - - - -
Intensity - - - -

(Figure 5.13)

(B)

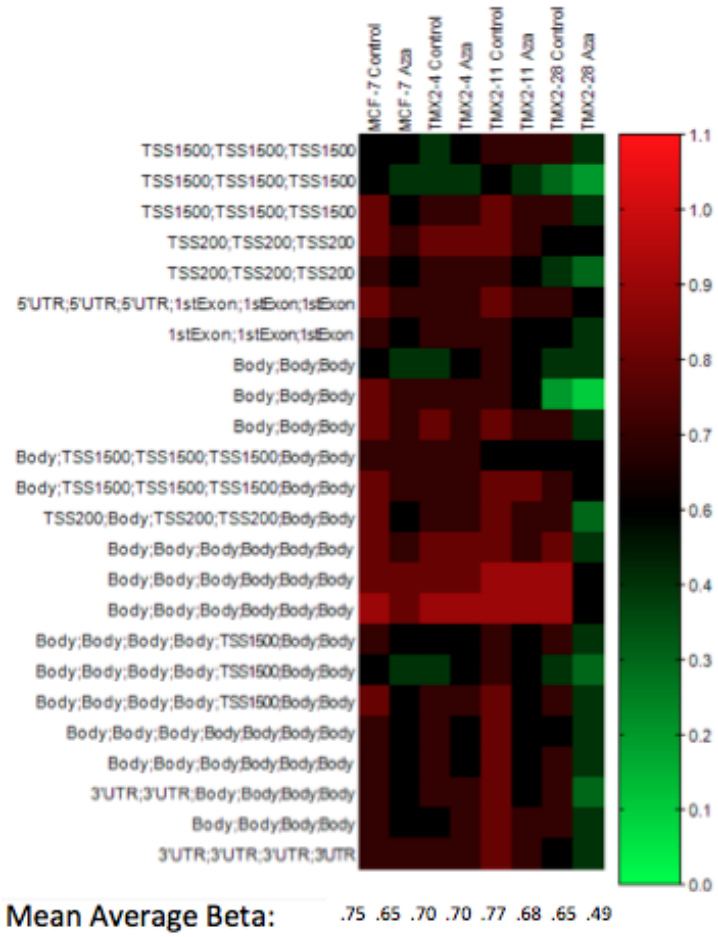

Figure 5.13: Expression of p63 is Not Regulated by Promoter Methylation. Heatmap indicating methylation of CpG sites for TP63 (filtering in Genome Studio for CpG sites that have Refgene name equal to NM_001114978, NM_001114979, or NM_003722, this overlaps with some of the CpG sites contained in the ΔNp63 isoform) represented by average beta values (scale at right) for each cell line (A) and the 5-Aza-2'-deoxycytidine-treated cell lines (B). Left: Refgene Group location and MAPINFO number for each CpG site. Bottom: Mean average beta values for all CpGs and percent positive cells and intensity determined from IHC scoring (recognized by the 34βE12 antibody, (-: no staining).

CHAPTER 6

DISCUSSION AND FUTURE DIRECTIONS

Introduction

Breast cancer is a heterogeneous disease and affects women of all ages. Approximately one of eight women will develop breast cancer throughout their lifetime.[2] During carcinogenesis breast cancer cells acquire certain characteristics that allow for escape of normal cell regulatory processes. These traits, also known as hallmarks of cancer, apply to every type of cancer and allow cancer cells to, for example, sustain growth signaling, evade the immune system and disseminate to other parts of the body.[7,8]

Expression of hormone receptors is one of the most important aspects in terms of identifying breast cancer subtypes, determining prognosis and predicting response to therapy. About 70% of breast cancers express estrogen receptor alpha (ER) and can be treated with the antiestrogen tamoxifen.[23] However, about one-third of women treated with tamoxifen for 5 years will have a recurrence.[26] This presents a huge clinical obstacle because these patients have limited treatment options. Changes in DNA methylation and epigenetics are implicated in cancer development and specifically tamoxifen resistance. Aberrant DNA methylation is an early event in carcinogenesis[13] and is known to occur in breast cancer.[16] Alterations in DNA methylation occur in ER-positive, tamoxifen-resistant cell lines.[25,27,31] However, the role of DNA methylation in ER-negative, tamoxifen-resistant disease is not well understood. The goal of this project was to evaluate the role of DNA

methylation in ER-negative, tamoxifen-resistant disease and the use of the DNMT1-inhibitor, 5-Aza-2'-deoxycytidine, as a potential epigenetic therapy for ER-negative recurrent disease.

In this study, I use three tamoxifen-resistant cell lines, TMX2-4, TMX2-11 and TMX2-28, selected from the parental cell line, MCF-7, after exposure to tamoxifen for 6 months. TMX2-4 and TMX2-11 cells express ER, but are resistant to tamoxifen, while TMX2-28 cells lost expression of ER.[37] Using the Illumina Human Methylation 450 BeadChip, I confirmed results of a previous study[31] indicating that TMX2-11 and TMX2-28 are differentially methylated with respect to the parental cell line, MCF-7. TMX2-4 cells also exhibit differential methylation compared to MCF-7. Additionally, I found MCF-7 cells and the three tamoxifen-resistant cell lines each respond differently to treatment with 5-Aza-2'-deoxycytidine. Also in agreement with previous work,[75] expression of a mixed basal and luminal cytokeratin profile was confirmed in TMX2-28 by immunohistochemistry (IHC).

DNA Methylation Patterns Differ Between the Parental and Tamoxifen-resistant Cell Lines

DNA methylation is an epigenetic modification that can be altered in cancer cells. CpG sites are found throughout the genome and are typically methylated. Normally CpG islands located in gene promoters are unmethylated. However, CpG islands are frequently methylated in cancer and prevent transcription.[20,30] Methylation patterns in non-promoter regions and gene body regions may also play a role in regulating transcription along with histone modifications.[14,20,30] Global

hypomethylation is more common in breast cancer than other types of cancer.[30] Methylation of gene panels and CpG signature loci have been associated with breast cancer development and disease progression.[141-143] Although ER-positive breast cancers have been shown to have higher frequencies of methylation than ER-negative cancers, hypermethylated CpG sites in ER-negative cancers are usually closer to gene promoters.[119] Changes in DNA methylation have been found in ER-positive, tamoxifen-resistant cell lines.[25,27,31] However, little is known about the role of methylation in ER-negative, tamoxifen-resistant breast cancer.

I first confirmed results from a previous study in our lab[31]indicating that TMX2-28 are hypermethylated compared to MCF-7. The results from the Illumina Human Methylation 450 BeadChip confirmed that TMX2-4, TMX2-11 and TMX2-28 have different methylation profiles than the parental line, MCF-7 (Figure 2.3). This indicates that DNA methylation could be involved in resistance to tamoxifen in these cell lines. Next, I investigated changes in DNA methylation induced by treatment with 5-Aza-2'-deoxycytidine. Treatment with 5-Aza-2'-deoxycytidine caused cell line-specific changes in DNA methylation, with TMX2-28 being the most sensitive cell line to the DNMT1-inhibitor (Figure 2.4). I also found global differences in mRNA expression between MCF-7 and TMX2-28 (Figure 2.5). I hypothesized that differences in mRNA expression between TMX2-28 and MCF-7 were caused by differences in promoter methylation, which alter gene transcription.

To identify genes with altered expression after 5-Aza-2'-deoxycytidine treatment in TMX2-28, I utilized DNA methylation data from the 450 BeadChip. I identified a set of 27 genes with increased methylation in TMX2-28 compared to

MCF-7 that also had decreased methylation in the promoter after treatment with 5-Aza-2'-deoxycytidine (Table 2.8). I predicted that the behavior of TMX2-28 in response to 5-Aza-2'-deoxycytidine was the result of changes in gene expression due to changes in promoter methylation.

5-Aza-2'-deoxycytidine Alters DNA Methylation, Proliferation, Migration and Adhesion in TMX2-28

Preliminary studies in our lab indicated that 5-Aza-2'-deoxycytidine inhibited proliferation in the ER-negative, tamoxifen-resistant cell line, TMX2-28 (Figures 3.1). I predicted that the behavior of TMX2-28 in response to 5-Aza-2'-deoxycytidine was the result of changes in gene expression due to changes in promoter methylation. I also investigated whether 5-Aza-2'-deoxycytidine affected other aspects of cell behavior related to the hallmarks of cancer. First I verified previous results from our lab indicating that treatment with 5-Aza-2'-deoxycytidine decreased proliferation in TMX2-28, but not the parental cell line, MCF-7 (Figure 3.2). Then I wanted to determine whether 5-Aza-2'-deoxycytidine affects migration of TMX2-28, which have been shown to be more migratory and invasive than MCF-7 cells.[38,74] The 2-dimensional scratch-wound assay showed that 5-Aza-2'-deoxycytidine inhibits the migratory ability of TMX2-28 while promoting migration in MCF-7 (Figure 3.5). This experiment also indicating that 5-Aza-2'-deoxycytidine treatment promotes TMX2-28 detachment from the monolayer (Figure 3.4) and decrease TMX2-28 cell viability (Figure 3.5). Further experiments confirmed that treatment of TMX2-28 with 5-Aza-2'-deoxycytidine inhibits cell adhesion to

fibronectin. However, 5-Aza-2'-deoxycytidine does not affect adhesion of MCF-7 cells to fibronectin (Figures 3.7 and 3.8).

Based on these results and the genes identified from the methylation analysis, TROP2 was identified as a candidate for regulating the behavior of TMX2-28 in response to 5-Aza-2'-deoxycytidine treatment. TROP2, the protein encoded by the *TACSTD2* gene, is silenced by DNA methylation in lung adenocarcinoma. Furthermore, treatment of lung cancer cell lines with 5-Aza-2'-deoxycytidine decreased promoter methylation and increased TROP2 expression. Forced expression of TROP2 in lung cancer cell lines inhibits proliferation and colony formation by decreasing AKT and ERK activation. The authors found that TROP2 inhibits IGF-1R signaling and loss of TROP2 in lung cancer via hypermethylation or loss of heterozygosity increases IGF-1R signaling and promotes cancer cell proliferation via AKT and MAPK signaling.[61] Interestingly, TROP2 is also known to inhibit adhesion of prostate cancer cells to fibronectin by promoting focal adhesion turnover.[106] However, TROP2 seems to have a tissue-specific function as TROP2 expression promotes growth in other cell types.[59,64,117] Therefore, I wanted to investigate the role of Trop in the ER-negative, tamoxifen-resistant cell line, TMX2-28. I confirmed the data from the 450 BeadChip by pyrosequencing. Indeed treatment with 5-Aza-2'-deoxycytidine decreases *TACSTD2* promoter methylation in TMX2-28 but does not affect methylation in MCF-7 (Figure 3.9). I then tested the hypothesis that increased TROP2 expression in TMX2-28 due to decreased promoter methylation was involved in regulating the decrease in proliferation, migration and adhesion in response to 5-Aza-2'-deoxycytidine treatment.

Role of TROP2 in Regulation of Proliferation, Migration and Adhesion in Cell Line Model

To determine the role of TROP2 in regulating proliferation, migration and adhesion, I generated a stable MCF-7 cell line with decreased expression of TROP2 (MCF-7-Trop2-Kd) and a stable TMX2-28 cell line with increased expression of TROP2 (TMX2-28-Trop2) (Figure 4.1). MCF-7 has low *TACSTD2* promoter methylation and high TROP2 expression while TMX2-28 has high *TACSTD2* promoter methylation and low expression. This is consistent with the hypothesis that promoter methylation is regulating gene expression. Treatment of TMX2-28 with 5-Aza-2'-deoxycytidine decreases *TACSTD2* promoter methylation and increases mRNA expression. Treating TMX2-28 cells with 5-Aza-2'-deoxycytidine decreases proliferation and 2-dimensional migration and inhibits cell adhesion to fibronectin. Based on the changes in cell behavior of TMX2-28 in response to 5-Aza-2'-deoxycytidine treatment and results in the literature regarding TROP2, [61,106] I predicted that forced expression of TROP2 in TMX2-28 would result in decreased proliferation, migration and cell adhesion.

Contrary to my prediction, TMX2-28-Trop2 cells had no change in proliferation and had increased adhesion to fibronectin and increased migration compared to the TMX2-28-Control cell line (Figures 4.2, 4.3 and 4.4). This indicates that the decrease in proliferation, adhesion and migration of TMX2-28 in response to treatment with 5-Aza-2'-deoxycytidine is not due to TROP2 expression. Although increased TROP2 expression has been shown to promote cell growth and

proliferation, which is in some instances due to increased phosphorylation of ERK1/2, [59,64,110,111] this is not the case in TMX2-28. This suggests that TMX2-28 utilize a mechanism that is independent of TROP2 to promote growth signaling. TMX2-28 cells are known to overexpress S-phase kinase-associated protein 2 (SKP2), a component of the SCF^{SKP2} complex, which targets CDK inhibitors, such as p27, for degradation. However, TMX2-28 cells have high expression of p27. [39] Therefore, if SKP2 overexpression is the predominant mechanism by which TMX2-28 cells sustain proliferative signaling I predict the expression of other CDK inhibitors, such as p16 or p21, to be low in TMX2-28. Cancer cells are thought to rely on more than one growth signaling pathway or combination of pathways to promote tumor growth. [7,8] This is likely the case in TMX2-28. However, it is not known which pathway is affected by 5-Aza-2'-deoxycytidine in TMX2-28. This could be determined, for example, by examining the phosphorylation patterns of cell cycle regulatory proteins in both control and 5-Aza-2'-deoxycytidine-treated TMX2-28 cells.

Knockdown of TROP2 in MCF-7 increased proliferation (Figure 4.5). This indicates that TROP2 acts to suppress proliferation in MCF-7. This could be related to the ability of TROP2 to bind IGF-1 and inhibit IGF-1R signaling.[61] Expression of IGF-1R was not examined in the present study, however it is known that MCF-7 cells express IGF-1R and respond to stimulation with IGF-1. [144] TROP2 may act to suppress some IGF-1R signaling in MCF-7 by binding IGF-1. Therefore, I predict MCF-7-Trop2-Kd cells would have increased IGF-1R signaling and AKT activation. In the future, this hypothesis could be examined by immunoblotting with phosphor-

specific antibodies for downstream signaling proteins in the IGF-1R pathway, such as AKT.

I also quantified adhesion to fibronectin in the stable cell lines. Fibronectin is a component of the extracellular matrix (ECM), which is produced during involution and breast cancer development; it is important for remodeling the ECM and forming the pre-metastatic niche.[145,146] TMX2-28-Trop2 cells had increased adhesion to fibronectin, which was opposite of my prediction (Figure 4.3). The results from the adhesion experiments in the MCF-7-Trop2-Kd cells were inconclusive (Figure 4.6). There is also evidence in the literature suggesting that increased TROP2 expression inhibits adhesion. Fetal mouse kidney cells with high TROP2 expression have decreased adhesion to collagen.[105] Forced expression of TROP2 in prostate cancer cells inhibits adhesion to fibronectin. This is probably due to relocalization of RACK1 to the membrane, increased phosphorylation of Src and FAK, which results in increased turnover of focal adhesions.[106] However, TROP2 can also promote migration of prostate cancer cells on fibronectin. Authors found this to be dependent on β1 integrins. Interaction of TROP2 with α5β1 integrin and talin causes α5β1 relocalization to the leading edge of the cell and increases Rac1 GTPase acivity. TROP2 can also activate PAK4, which results in increased focal adhesion turnover.[57] The TMX2-28-Trop2 cell line had increased adhesion to fibronectin and therefore stable focal adhesions. However the localization and activation of focal adhesion signaling proteins was not examined in this study. I predict decreased phosphorylation of signaling proteins and absence of RACK1 at the cell membrane. This could be examined by western blotting with phosphor-specific antibodies and

immunofluorescence microscopy. It would also be important to determine expression levels of β1 integrins in TMX2-28-Trop2. I predict TMX2-28-Trop2 would have low expression of α5β1 integrin.

It is also important to consider that the adhesion experiments in the present study examined how well cells adhere to fibronectin-coated tissue culture plates in a short time frame. The strength of cell adhesion could also be quantified by examining the time frame for detachment or the force required to detach cells. Fibronectin is just one component of the ECM, other components such as collagen or combinations of components could be examined in a 2- or 3-dimensional tissue culture setting. This may provide a more physiologically accurate setting to quantify adhesion.

If TMX2-28-Trop2 cells have stable focal adhesions, it is surprising that they had increased migration in the transwell assay (Figure 4.4) because migration requires focal adhesion turnover. Meanwhile, there was no change in migration of the MCF-7-Trop2-Kd cells. Perhaps TROP2 altered subcellular localization of a portion of molecules involved in focal adhesion signaling, allowing them to be poised for activation when needed. This hypothesis could be examined by immunoblotting or immunofluorescence microscopy using phosphor-specific antibodies. Increased TROP2 expression is known to promote invasion in other cell line models.[59,111,117] This agrees with results presented here that TMX2-28-Trop2 cells have increased migration. Correspondingly in the literature, knockdown of TROP2 has been shown to inhibit invasion and migration in tissue culture models.[108,117,147] Perhaps there was no effect on migration when knocking down

TROP2 expression in MCF-7 cells because of the inherent non-invasive characteristics of this cell line. Therefore, it would be important in the future to investigate the effect of TROP2 overexpression and knockdown in other breast cancer cell lines.

TACSTD2 Methylation and TROP2 Expression in Clinical Samples

TACSTD2 methylation was examined in clinical breast cancer samples using the Illumina Human Methylation 450 BeadChip and TROP2 protein expression was examined by IHC. Despite my predictions from the TMX2-28 cell line model, there was no inverse correlation between methylation and TROP2 expression in the breast cancer samples. There was, however, a change in methylation of the 3 *TACSTD2* CpG cites identified in TMX2-28 (Chapter 2) in the predicted direction for the group of ER-positive primary tumors that recur as ER-negative. In this group, methylation for each of the 3 CpGs was higher in the ER-negative recurrent tumor than the ER-positive primary tumor (Figure 4.9, A). The difference in methylation was only significant for CpG 1 however, the sample size was small with only 6 ER-positive primary tumors and 7 ER-negative recurrent tumors for this group. Regardless of this increase in methylation, there was no difference in expression of membrane TROP2 between the ER-positive primary tumors that recur as ER-negative tumors. However, the sample size is so small that if methylation and protein expression were examined in a larger sample size, there may be a corresponding decrease in protein expression with increased methylation. It would also be interesting to examine DNA methylation for breast cancer samples in the

literature for which there is TROP2 expression data available.[60,65,109,114] In agreement with previous findings in the literature,[109] the ER-negative/HER-positive tumors in the current study had higher expression of membrane TROP2 than the other tumors grouped by ER/HER2 status (Figure 4.13, A). However, the increase was not statistically significant and there was no difference in cytoplasmic TROP2 expression according to ER/HER2 status (Figure 4.13, B). Contrary to a previous report that found membrane-localized TROP2 was associated with poor survival,[65] expression of membrane-localized TROP2 in the present study was high in non-recurrent tumors (Figure 4.14, A). This could simply be a reflection of the small sample size here (n = 66) compared to their study (n = 702). Also contradictory to predictions based on results from the literature, I found no difference in membrane TROP2 expression according to tumor grade or Ki67 score (Figure 4.15, A and B). In the future, it would be important to examine TROP2 expression in clinical samples with a larger sample size. It may also be beneficial to use a specific antibody, which recognizes either cytoplasmic or membrane-bound TROP2 exclusively, to avoid ambiguity of pathological scoring.

Given the high percentage of clinical samples with expression of cytoplasmic (98%) or membrane-localized TROP2 (89%), TROP2 may be useful marker for targeted delivery of therapeutics in breast cancer. Antibodies against TROP2 have been used in cell lines to target epithelial cells and deliver drug conjugates.[148-152] A clinical trial using a TROP2 antibody-topoisomerase-I inhibitor conjugate was conducted and included 4 patients with triple negative breast cancer with promising results. Treatment increased the time-to-progression, determined by measuring

response evaluation criteria in solid tumors (RECIST), in 3 of the 4 patients.[153] The data presented here indicate that a large number of breast tumors express membrane-localized TROP2 and support the idea of its use for targeted drug delivery.

The data presented here provide insight into the role of DNA methylation and regulation of gene expression in ER-negative, tamoxifen-resistant breast cancer. Cell behavior and changes in DNA methylation in response to 5-Aza-2'-deoxycytidine were also evaluated. This study indicates that DNA methylation in cell line models may be applicable to clinical samples. However, further studies are needed to determine whether DNA methylation is correlated to gene expression and to determine the role of TROP2 signaling in ER-negative, tamoxifen-resistant breast cancer.

APPENDICES

APPENDIX A

COMPARISON OF CELL LINE REPLICATES ON 450 BEADCHIP

In order to examine the reproducibility and reliability of methylation data from the 450 BeadChip, I compared global methylation (all CpG sites on the array) for cell line replicates. First, I compared methylation from the initial 450 BeadChip experiments in our lab[31] to the DMSO-control-treated cells in the 5-Aza-2'-deoxycytidine treatment experiments (see Chapter 2) for MCF-7, TMX2-11 and TMX2-28 (TMX2-4 was not included in the initial 450 BeadChip study). As expected, R^2 is close to one for each cell line (Figure A.1). Some variability was expected, as the cells in the initial experiment were not exposed to DMSO.

Next, I wanted to compare methylation between the two 5-Aza-2'-deoxycytidine treated cell line replicates that were analyzed using the Human 450 BeadChip. For these biological replicates, r^2 ranged from 0.95 to 0.99 (Figure A.2). This data along with the data from Figure A.1 confirm that the data from the Human 450 Methylation BeadChip is reproducible and reliable.

(A)

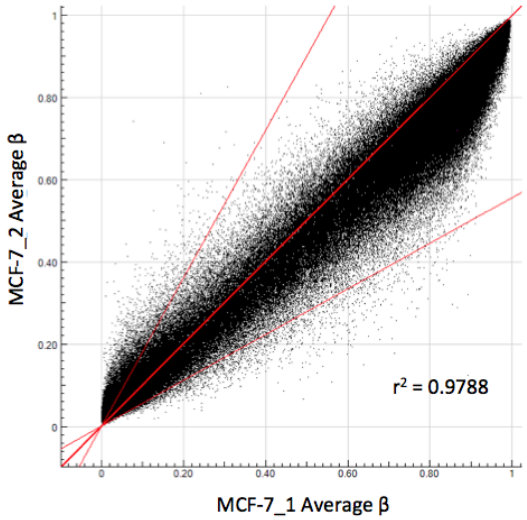

(B)

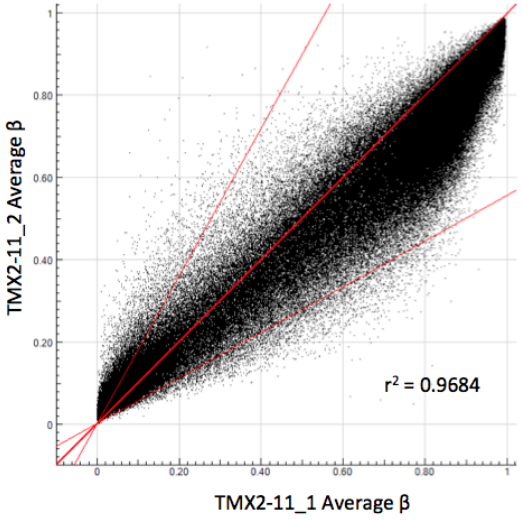

(C)

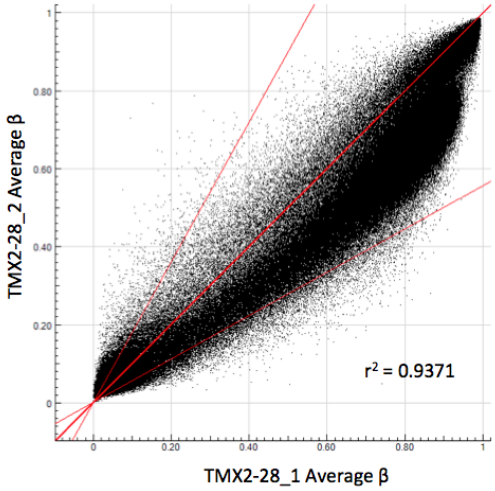

(Figure A.1)

Figure A.1: Scatter Plots Comparing DNA Methylation in Cell Line Replicates. Scatter plots indicating genome-wide methylation differences between cell lines from the initial experiment in our lab[31] ("…_1") and the DMSO-control-treated cells from the 5-Aza-2'-deoxycytidine experiment ("…_2") for (A) MCF-7, (B) TMX2-11 and (C) TMX2-28. Each black dot on the plot represents a CpG site analyzed on the Human Methylation 450 BeadChip. Center red line represents equal average beta values in the two samples and outer red lines indicate a 1.8-fold change in average beta values. Value of r^2 from Genome Studio represents goodness-of-fit of linear regression.

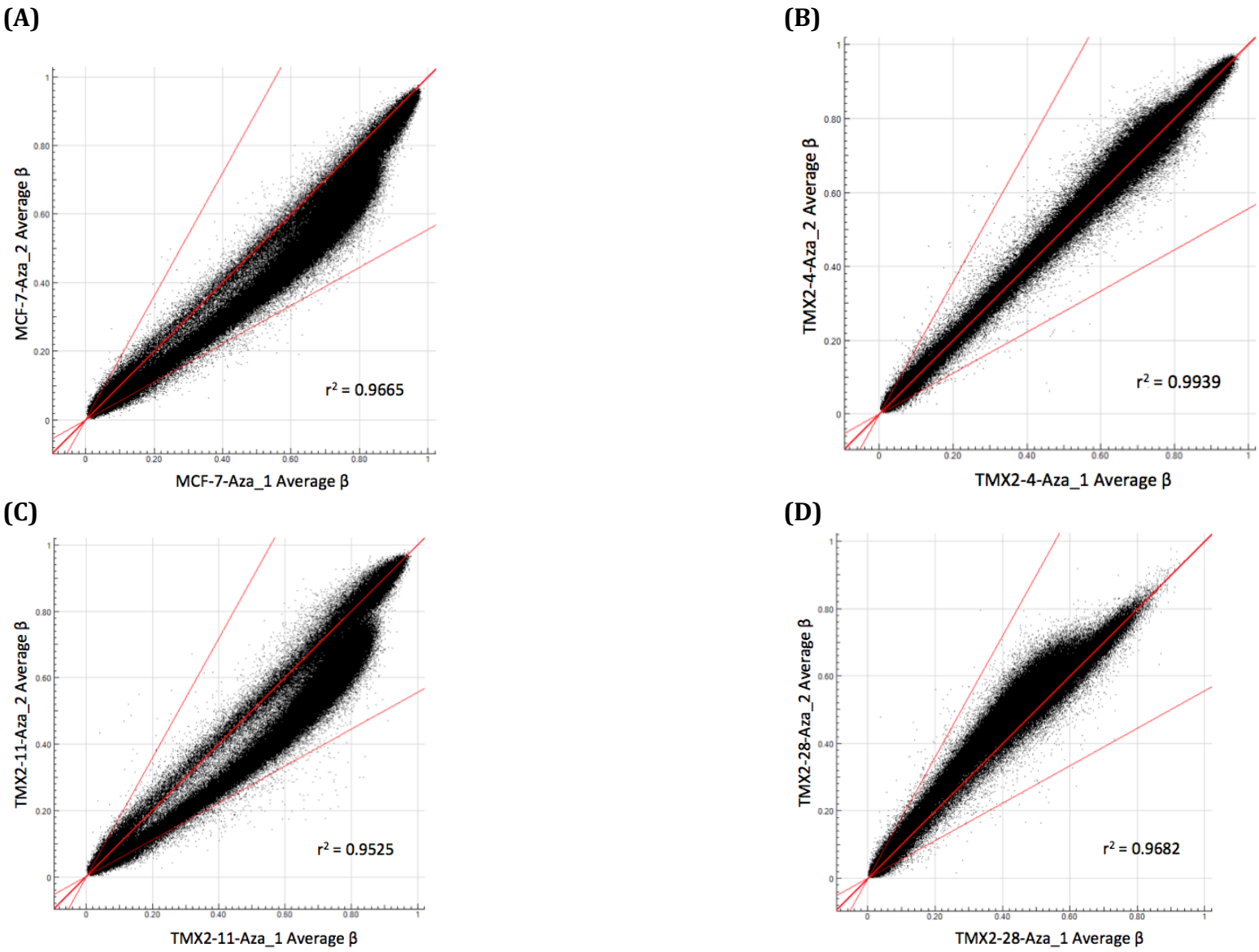
(A)
MCF-7-Aza_2 Average β
MCF-7-Aza_1 Average β
r² = 0.9665
(B)
TMX2-4-Aza_2 Average β
TMX2-4-Aza_1 Average β
r² = 0.9939
(C)
TMX2-11-Aza_2 Average β
TMX2-11-Aza_1 Average β
r² = 0.9525
(D)
TMX2-28-Aza_2 Average β
TMX2-28-Aza_1 Average β
r² = 0.9682

(Figure A.2)

Figure A.2: Scatter Plots Comparing DNA Methylation in Cell Line Replicates from the 5-Aza-2'-deoxycytidine Experiment. Scatter plots indicating genome-wide methylation differences between cell lines replicates from the 5-Aza-2'-deoxycytidine experiment from Chapter 2 ("…-Aza_1") and ("…-Aza_2") for (A) MCF-7, (B) TMX2-4, (C) TMX2-11 and (D) TMX2-28. Each black dot on the plot represents a CpG site analyzed on the Human Methylation 450 BeadChip. Center red line represents equal average beta values in the two samples and outer red lines indicate a 1.8-fold change in average beta values. Value of r^2 from Genome Studio represents goodness-of-fit of linear regression.

APPENDIX B

OPTIMIZATION OF SEEDING DENSITIES FOR ADHESION ASSAY

In order to determine the appropriate seeding density for the adhesion assay, MCF-7 and TMX2-28 cells were seeded in a 96-well plate coated with fibronectin one day before in various densities (n = 6), the top two rows of the plate were left uncoated as a negative control. To determine the limit of detection, a two-tailed Student's t-test was used to determine if the absorbance readings for 20,000 cells/well were different than the absorbance readings for each of the other cell densities. There was no difference between the absorbance readings for 20,000 and 10,000 cells/well. Therefore, the assay cannot distinguish absorbance values for 10,000 or fewer cells/well. There was a difference between readings between 20,000 cells/well and the 3 other densities tested. However, the background staining was very high in the wells without cells (Figure A.1). Therefore, I need to minimize the background staining in order to have a more sensitive assay.

To minimize background staining, the crystal violet staining solution was filtered through Whatman filter paper by gravity. After staining, the plate was rinsed by submerging it in water instead of pipetting water into the wells as the initial protocol indicated. The adhesion assay was repeated with MCF-7 cells and a higher initial cell density of 56,000 cells/well (n = 12). The differences in absorbance readings were analyzed using a Student's t-test. This time, the background staining (absorbance values for wells coated with fibronectin, but not

containing cells) was low. The absorbance readings for each seeding density were different than next lowest density (Figure A.2). Therefore, I decided the optimal seeding density for future adhesion assays should be between 30,000 and 14,000 cells/well, less than the highest density tested.

(A)

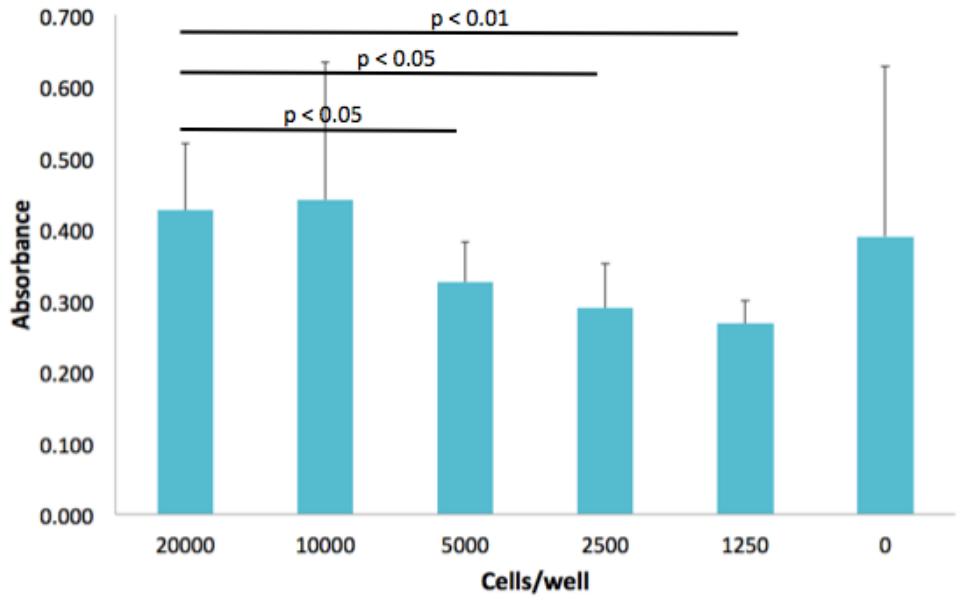

(B)

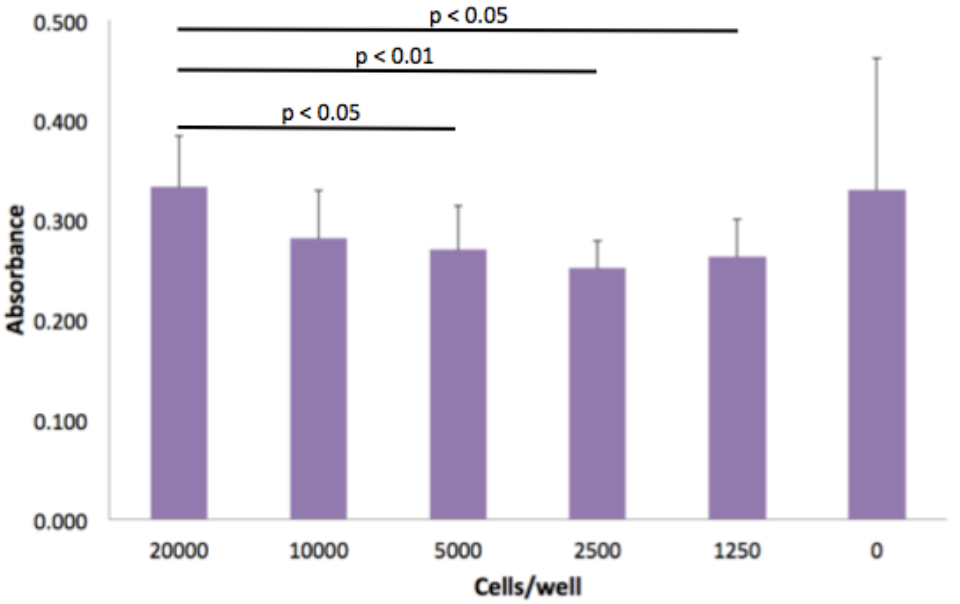

Figure B.1: Serial Dilution to Determine Seeding Density for Adhesion Assay. Absorbance readings for MCF-7 (A) and TMX2-28 (B) seeded in a 96-well plate coated with fibronectin (n = 6).

(A)

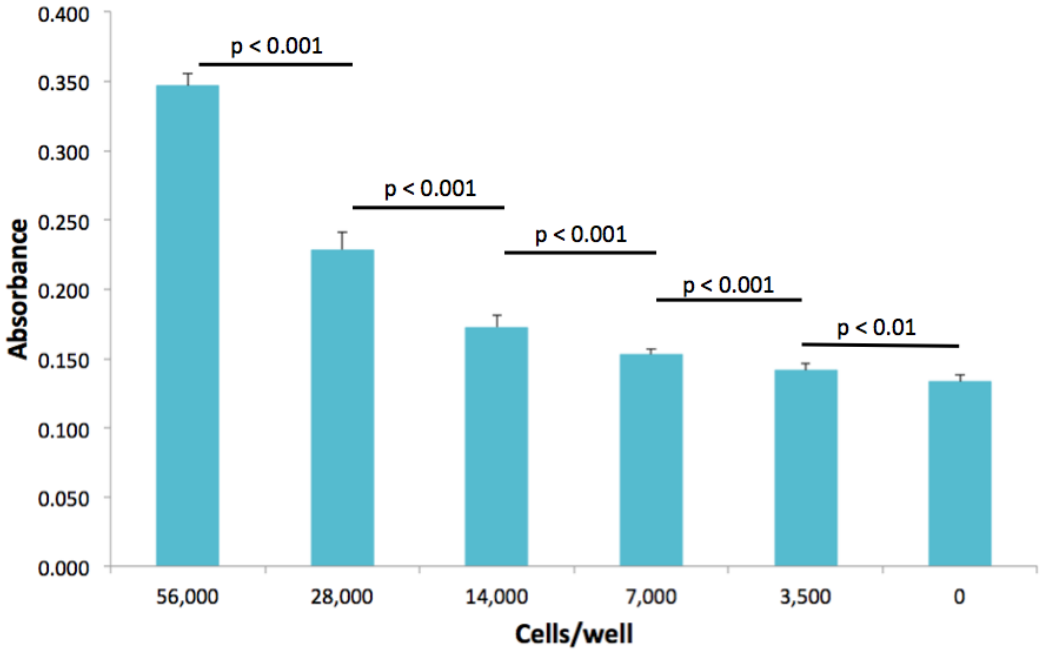

(B)

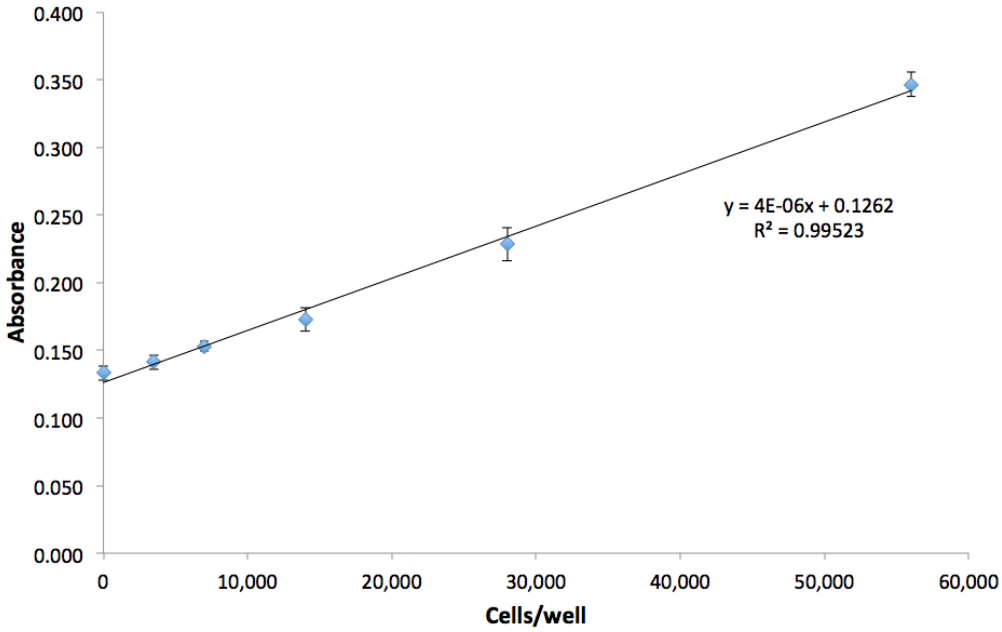

Figure B.2: Adhesion Assay Standard Curve with MCF-7. Absorbance values for MCF-7 cells (A) seeded at indicated densities in a 96-well plate coated with fibronectin (n = 12). Standard curve (B) with linear trend line for data from (A).

APPENDIX C

INNITIAL ADHESION ASSAY EXPERIMENTS

The first three adhesion assays were conducted using plates that were coated with fibronectin by hand. MCF-7 and TMX2-28 cells were treated with 5-Aza-2'-deoxycytidine for 24- and 48-hours. The adhesion assay was then conducted as described in Chapter 3 Materials and Methods. Based on previous observations, I predict that TMX2-28 will have decreased adhesion to fibronectin after treatment with 5-Aza-2'-deoxycytidine. A decrease in absorbance values, indicating decreased adhesion, compared to TMX2-28-Control was observed for TMX2-28-48-hour 5-Aza-2'-deoxycytidine-treated in the first experiment. However, in subsequent experiments, 5-Aza-2'-deoxycytidine treatment resulted in increased adhesion in TMX2-28 (Figure C.1). There was also variability in the absorbance values of 5-Aza-2'-deoxycytidine-treated MCF-7 cells. This variability could be due to inconsistent coating of the plates with fibronectin, inaccurate cell counts (and dilutions) or variable response to short-term 5-Aza-2'-deoxycytidine treatment.

(A)

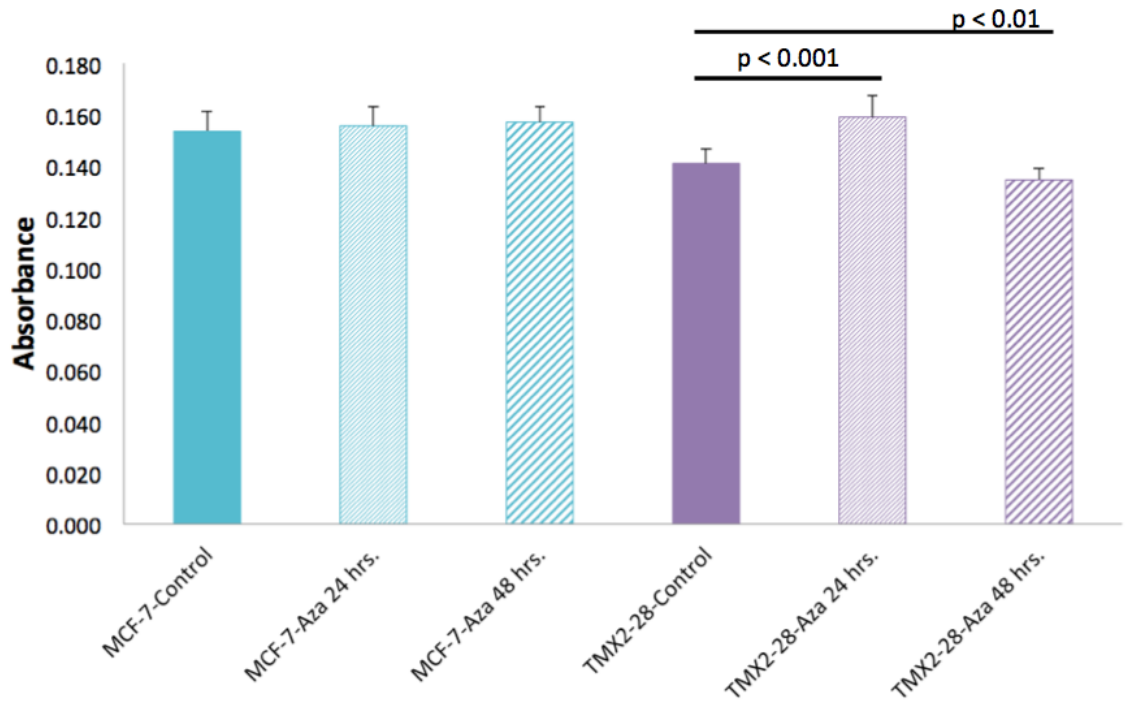
p < 0.01
p < 0.001
Absorbance
0.180
0.160
0.140
0.120
0.100
0.080
0.060
0.040
0.020
0.000
MCF-7-Control
MCF-7-Aza 24 hrs.
MCF-7-Aza 48 hrs.
TMX2-28-Control
TMX2-28-Aza 24 hrs.
TMX2-28-Aza 48 hrs.

(B)

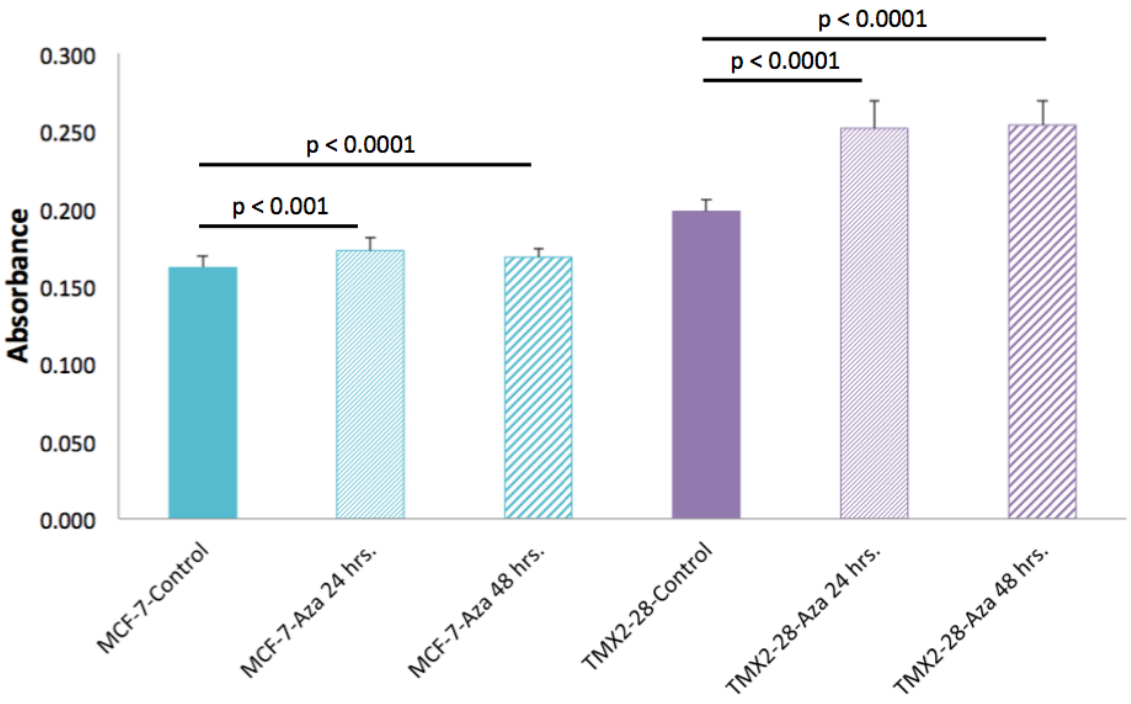
p < 0.0001
p < 0.0001
p < 0.0001
p < 0.001
Absorbance
0.300
0.250
0.200
0.150
0.100
0.050
0.000
MCF-7-Control
MCF-7-Aza 24 hrs.
MCF-7-Aza 48 hrs.
TMX2-28-Control
TMX2-28-Aza 24 hrs.
TMX2-28-Aza 48 hrs.

(Figure C.1)

(C)

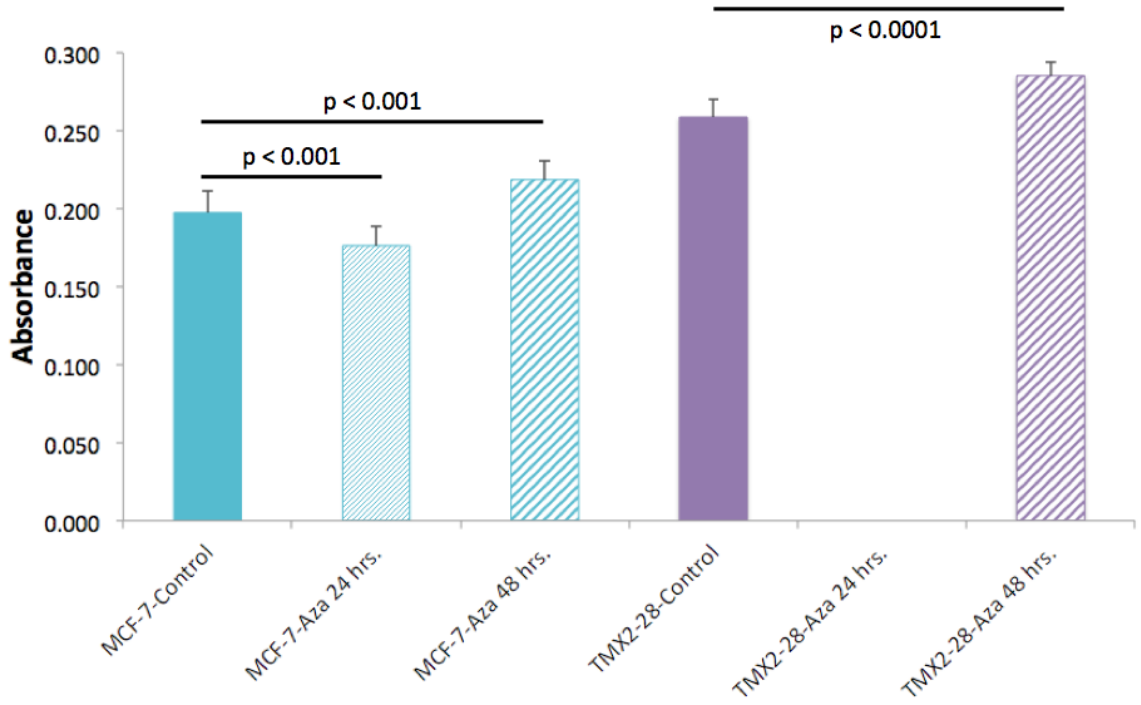

Figure C.1: Variability in Initial Adhesion Assay Experiments. Absorbance values for first (A), second (B) and third (C) experiments for 24- and 48-hour 5-Aza-2'-deoxycytidine-treated MCF-7 and TMX2-28 cells. Experiments were conducted with 96-well plates coated with 20 µg/mL fibronectin by hand prior to the experiment (n = 12). (The TMX2-28-Aza 24 hrs. sample was lost in the third experiment).

APPENDIX D

ADHESION OF ADHERENT AND FLOATING CELL POPULATIONS TREATED WITH 5-AZA-2'-DEOXYCYTIDINE

Because previous experiments showed that TMX2-28 cells treated with 5-Aza-2'-deoxycytidine detach from the monolayer, I wanted to determine if there was a difference in adhesion between the adherent cells and the adherent cells combined with those cells that were in suspension. For the first experiment, two replicate flasks were seeded for each treatment. On the day of the adhesion assay, the adherent cells were trypsinzed, counted and seeded for the assay. For the second set, cells that were floating in the spent media were combined with adherent cells, counted and seeded for the assay. Cells were seeded on the pre-coated fibronectin plate at 15,400 cells/well (due to limited number of cells in one of the samples) (Figure D.1). Remaining cell pellets from each treatment flask were divided into two and stored at -80°C for DNA and RNA isolation at a later date.

Differences among cell lines and treatment were analyzed by two-way ANOVA and post-hoc t-tests. The two-way ANOVA examined the effect of cell line and treatment on adhesion. The interaction between cell line and treatment approached significance ($F = 2.21$, $p = 0.05$). There was a significant effect of cell line on adhesion ($F = 8.23$, $p < 0.0001$) and treatment on adhesion ($F = 23.11$, $p < 0.0001$) (Figure D.1, A). There was a time-dependent decrease in adhesion with 5-Aza-2'-deoxycytidine treatment. Additionally, differences in adhesion between treatment for MCF-7 and TMX2-28 cell lines were analyzed by student's t-test. For

the adherent populations, there was no difference in adhesion of MCF-7 with 5-Aza-2'-deoxycytidine treatment, compared to control. There was however, a decrease in adhesion of TMX2-28 after treatment with 5-Aza-2'-deoxycytidine for 72 hours, compared to control (Figure D.1, B). Combining the floating population with the adherent population decreased adhesion in MCF-7 after 72-hour treatment with 5-Aza-2'-deoxycytidine, compared to control. The combined TMX2-28-72 hr Aza population also had decreased adhesion, compared to control (Figure D.1, C). However, adhesion of TMX2-28-72 hr Aza Combined was statistically higher than TMX2-28-72 hr Aza Adherent ($p < 0.01$).

These results indicate that treatment with 5-Aza-2'-deoxycytidine for 72 hours inhibits adhesion to fibronectin of TMX2-28, but does not affect adhesion of MCF-7. The results with the combined population for MCF-7 indicate that the addition of the floating population inhibits adhesion to fibronectin. The TMX2-28 combined population also had decreased adhesion to fibronectin, compared to control, however the percent adhesion is slightly higher than that of TMX2-28-72hr Aza-Adherent only population. This indicates that some of the floating TMX2-28 5-Aza-2'-deoxycytidine-treated cells are capable of adhering to fibronectin. This result is in agreement with a previous experiment in which I observed that floating TMX2-28 cells after treatment with 5-Aza-2'-deoxycytidine were capable of re-adhering when transferred to a new plastic tissue culture plate (Figure 3.5).

(A)

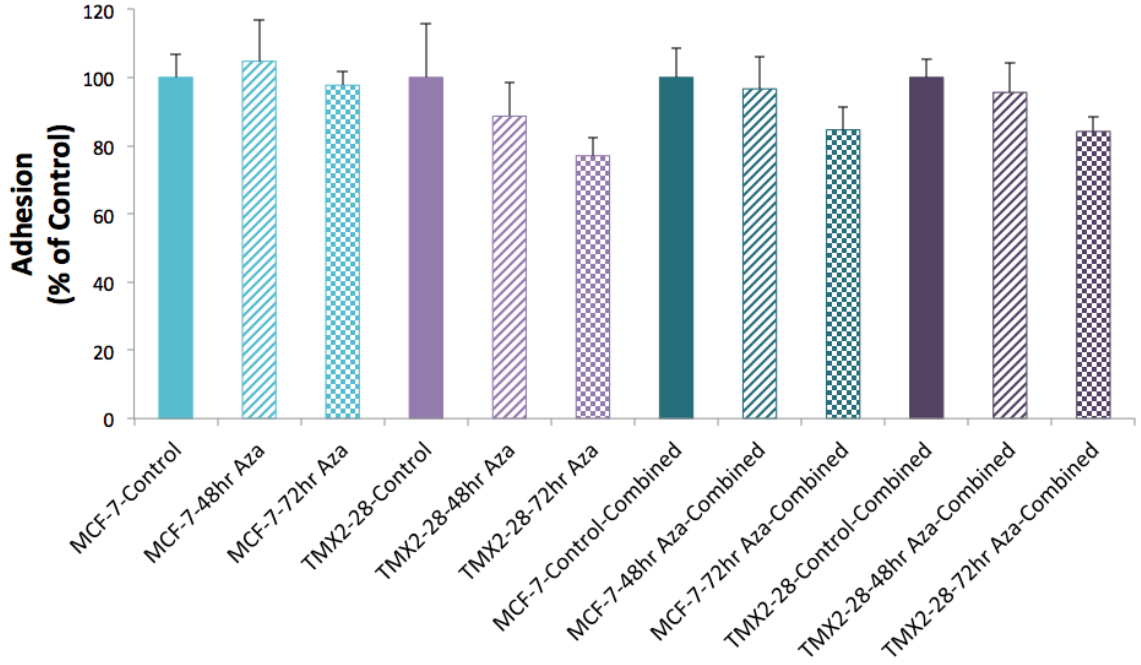
Adhesion (% of Control)
120
100
80
60
40
20
0
MCF-7-Control
MCF-7-48hr Aza
MCF-7-72hr Aza
TMX2-28-Control
TMX2-28-48hr Aza
TMX2-28-72hr Aza
MCF-7-Control-Combined
MCF-7-48hr Aza-Combined
MCF-7-72hr Aza-Combined
TMX2-28-Control-Combined
TMX2-28-48hr Aza-Combined
TMX2-28-72hr Aza-Combined

(B)

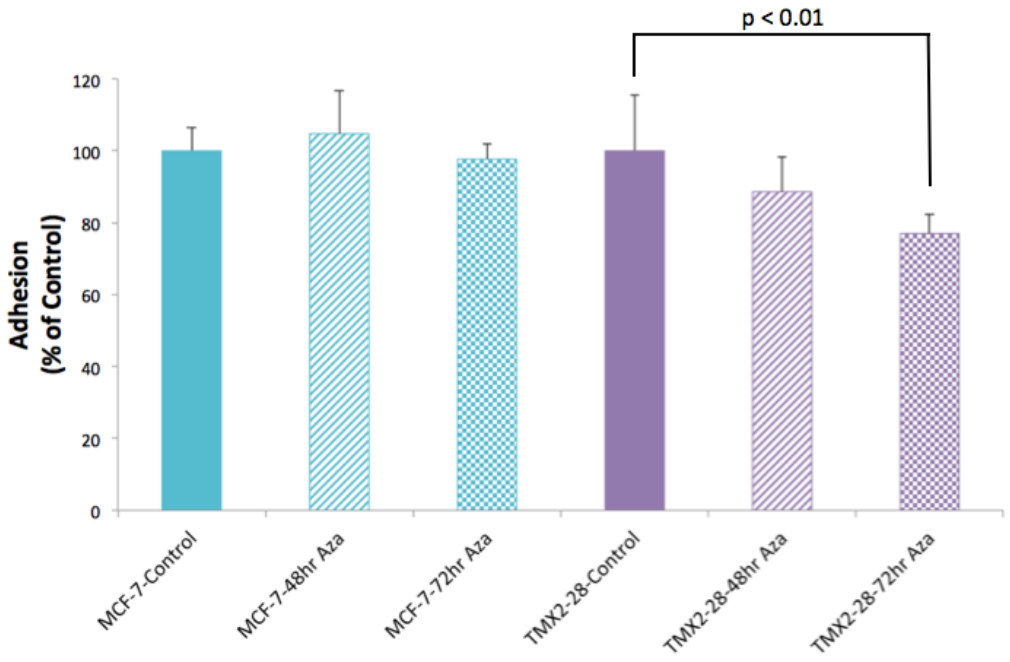
p < 0.01
Adhesion (% of Control)
120
100
80
60
40
20
0
MCF-7-Control
MCF-7-48hr Aza
MCF-7-72hr Aza
TMX2-28-Control
TMX2-28-48hr Aza
TMX2-28-72hr Aza

(Figure D.1)

(C)

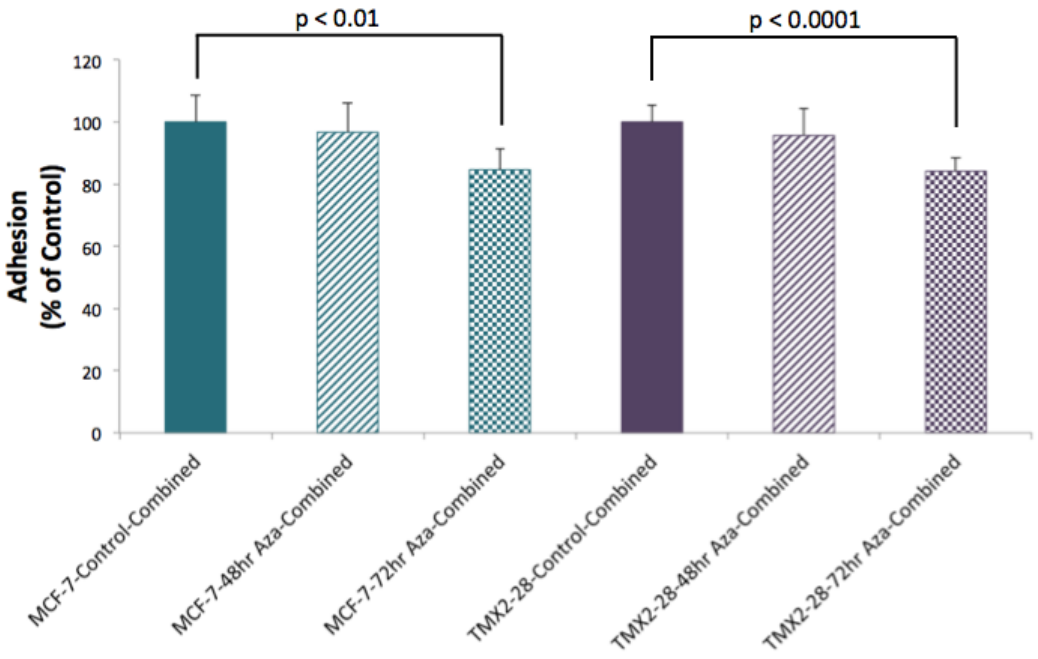

Figure D.1: Adhesion of Adherent Cell Populations and Combined Cell Populations. Cells were seeded in duplicate flasks and treated with DMSO control or 5-Aza-2'-deoxycytidne for 48 or 72 hours prior to seeding on a pre-coated fibronectin plate for adhesion assay. For one set of flasks, the spent media was removed and only the cells adhered to the flask were used in the adhesion assay. For the second set, cells floating in the spent media were combined with cells adhered to the flask (combined) and seeded for the adhesion assay. Adhesion to fibronectin-coated plate represented as percentage of control for MCF-7 and TMX2-28 for adherent cells only and adherent cells combined with cells in suspension (combined) (n = 8). Percent adhesion of all cell populations, normalized to the control for each cell line (A). Percent adhesion of only the adherent populations (B). Percent adhesion of only the combined populations (C).

BIBLIOGRAPHY

1. Anonymousbreastcancer.org. *http://www.breastcancer.org* (accessed 9/10, 2015).

2. AnonymousAmerican Cancer Society. *http://www.cancer.org/cancer/breastcancer/detailedguide/breast-cancer-key-statistics* (accessed 9/10, 2015).

3. Scully, O. J.; Bay, B. H.; Yip, G.; Yu, Y. Breast cancer metastasis. *Cancer. Genomics Proteomics* **2012**, *9*, 311-320.

4. Eroles, P.; Bosch, A.; Perez-Fidalgo, J. A.; Lluch, A. Molecular biology in breast cancer: intrinsic subtypes and signaling pathways. *Cancer Treat. Rev.* **2012**, *38*, 698-707.

5. Anderson, W. F.; Rosenberg, P. S.; Prat, A.; Perou, C. M.; Sherman, M. E. How many etiological subtypes of breast cancer: two, three, four, or more? *J. Natl. Cancer Inst.* **2014**, *106*, 10.1093/jnci/dju165. Print 2014 Aug.

6. Wong, E.; Chaudhry, S.; Rossi, M. McMaster Pathophysiology Review - Breast Cancer. *http://www.pathophys.org/breast-cancer/* (accessed 9/10, 2015).

7. Hanahan, D.; Weinberg, R. A. The hallmarks of cancer. *Cell* **2000**, *100*, 57-70.

8. Hanahan, D.; Weinberg, R. A. Hallmarks of cancer: the next generation. *Cell* **2011**, *144*, 646-674.

9. Bernstein, B. E.; Meissner, A.; Lander, E. S. The mammalian epigenome. *Cell* **2007**, *128*, 669-681.

10. Feinberg, A. P. The epigenetics of cancer etiology. *Semin. Cancer Biol.* **2004**, *14*, 427-432.

11. Sharma, S.; Kelly, T. K.; Jones, P. A. Epigenetics in cancer. *Carcinogenesis* **2010**, *31*, 27-36.

12. Luger, K.; Mader, A. W.; Richmond, R. K.; Sargent, D. F.; Richmond, T. J. Crystal structure of the nucleosome core particle at 2.8 A resolution. *Nature* **1997**, *389*, 251-260.

13. Azad, N.; Zahnow, C. A.; Rudin, C. M.; Baylin, S. B. The future of epigenetic therapy in solid tumours--lessons from the past. *Nat. Rev. Clin. Oncol.* **2013**, *10*, 256-266.

14. Baylin, S. B.; Jones, P. A. A decade of exploring the cancer epigenome - biological and translational implications. *Nat. Rev. Cancer.* **2011**, *11*, 726-734.

15. Razin, A.; Riggs, A. D. DNA methylation and gene function. *Science* **1980**, *210*, 604-610.

16. Widschwendter, M.; Jones, P. DNA methylation and breast carcinogenesis. *Oncogene* **2002**, *21*, 5462-5482.

17. Miranda, T. B.; Jones, P. A. DNA methylation: the nuts and bolts of repression. *J. Cell. Physiol.* **2007**, *213*, 384-390.

18. Gibney, E. R.; Nolan, C. M. Epigenetics and gene expression. *Heredity (Edinb)* **2010**, *105*, 4-13.

19. Jones, P. Functions of DNA methylation: islands, start sites, gene bodies and beyond. *Nature reviews.Genetics* **2012**, *13*, 484-492.

20. Lay, F. D.; Liu, Y.; Kelly, T. K.; Witt, H.; Farnham, P. J.; Jones, P. A.; Berman, B. P. The role of DNA methylation in directing the functional organization of the cancer epigenome. *Genome Res.* **2015**, *25*, 467-477.

21. Yang, X.; Yan, L.; Davidson, N. E. DNA methylation in breast cancer. *Endocr. Relat. Cancer* **2001**, *8*, 115-127.

22. Stefanska, B.; Karlic, H.; Varga, F.; Fabianowska-Majewska, K.; Haslberger, A. Epigenetic mechanisms in anti-cancer actions of bioactive food components--the implications in cancer prevention. *Br. J. Pharmacol.* **2012**, *167*, 279-297.

23. Musgrove, E.; Sutherland, R. Biological determinants of endocrine resistance in breast cancer. *Nature Reviews.Cancer* **2009**, *9*, 631-643.

24. Jeselsohn, R.; Buchwalter, G.; De Angelis, C.; Brown, M.; Schiff, R. ESR1 mutations-a mechanism for acquired endocrine resistance in breast cancer. *Nat. Rev. Clin. Oncol.* **2015**.

25. Fan, M.; Yan, P.; Hartman-Frey, C.; Chen, L.; Paik, H.; Oyer, S.; Salisbury, J.; Cheng, A. S. L.; Li, L.; Abbosh, P.; Huang, T. H.; Nephew, K. Diverse gene expression and DNA methylation profiles correlate with differential adaptation of breast cancer cells to the antiestrogens tamoxifen and fulvestrant. *Cancer Res.* **2006**, *66*, 11954-11966.

26. Early Breast Cancer Trialists' Collaborative Group (EBCTCG) Effects of chemotherapy and hormonal therapy for early breast cancer on recurrence and 15-year survival: an overview of the randomised trials. *Lancet (London, England)* **2005**, *365*, 1687-1717.

27. Lin, X.; Li, J.; Yin, G.; Zhao, Q.; Elias, D.; Lykkesfeldt, A.; Stenvang, J.; Brünner, N.; Wang, J.; Yang, H.; Bolund, L.; Ditzel, H. Integrative analyses of gene expression and DNA methylation profiles in breast cancer cell line models of tamoxifen-resistance indicate a potential role of cells with stem-like properties. *Breast cancer research* **2013**, *15*, R119-R119.

28. Nass, N.; Kalinski, T. Tamoxifen resistance: from cell culture experiments towards novel biomarkers. *Pathol. Res. Pract.* **2015**, *211*, 189-197.

29. Osborne, C. K.; Schiff, R. Mechanisms of endocrine resistance in breast cancer. *Annu. Rev. Med.* **2011**, *62*, 233-247.

30. Connolly, R.; Stearns, V. Epigenetics as a therapeutic target in breast cancer. *J. Mammary Gland Biol. Neoplasia* **2012**, *17*, 191-204.

31. Williams, K. E.; Anderton, D. L.; Lee, M. P.; Pentecost, B. T.; Arcaro, K. F. High-density array analysis of DNA methylation in Tamoxifen-resistant breast cancer cell lines. *Epigenetics* **2014**, *9*, 297-307.

32. Curtit, E.; Nerich, V.; Mansi, L.; Chaigneau, L.; Cals, L.; Villanueva, C.; Bazan, F.; Montcuquet, P.; Meneveau, N.; Perrin, S.; Algros, M. P.; Pivot, X. Discordances in estrogen receptor status, progesterone receptor status, and HER2 status between primary breast cancer and metastasis. *Oncologist* **2013**, *18*, 667-674.

33. Idirisinghe, P. K.; Thike, A. A.; Cheok, P. Y.; Tse, G. M.; Lui, P. C.; Fook-Chong, S.; Wong, N. S.; Tan, P. H. Hormone receptor and c-ERBB2 status in distant metastatic and locally recurrent breast cancer. Pathologic correlations and clinical significance. *Am. J. Clin. Pathol.* **2010**, *133*, 416-429.

34. Zhao, M.; Ramaswamy, B. Mechanisms and therapeutic advances in the management of endocrine-resistant breast cancer. *World J. Clin. Oncol.* **2014**, *5*, 248-262.

35. Ciruelos Gil, E. M. Targeting the PI3K/AKT/mTOR pathway in estrogen receptor-positive breast cancer. *Cancer Treat. Rev.* **2014**, *40*, 862-871.

36. Martin, L. A.; Andre, F.; Campone, M.; Bachelot, T.; Jerusalem, G. mTOR inhibitors in advanced breast cancer: ready for prime time? *Cancer Treat. Rev.* **2013**, *39*, 742-752.

37. Fasco, M.; Amin, A.; Pentecost, B.; Yang, Y.; Gierthy, J. Phenotypic changes in MCF-7 cells during prolonged exposure to tamoxifen. *Mol. Cell. Endocrinol.* **2003**, *206*, 33-47.

38. Fagan-Solis, K. D.; Schneider, S. S.; Pentecost, B. T.; Bentley, B. A.; Otis, C. N.; Gierthy, J. F.; Arcaro, K. F. The RhoA pathway mediates MMP-2 and MMP-9-independent invasive behavior in a triple-negative breast cancer cell line. *J. Cell. Biochem.* **2013**, *114*, 1385-1394.

39. Fagan-Solis, K. D.; Pentecost, B. T.; Gozgit, J. M.; Bentley, B. A.; Marconi, S. M.; Otis, C. N.; Anderton, D. L.; Schneider, S. S.; Arcaro, K. F. SKP2 overexpression is associated with increased serine 10 phosphorylation of p27 (pSer10p27) in triple-negative breast cancer. *J. Cell. Physiol.* **2014**, *229*, 1160-1169.

40. van Agthoven, T.; Godinho, M. F.; Wulfkuhle, J. D.; Petricoin, E. F.,3rd; Dorssers, L. C. Protein pathway activation mapping reveals molecular networks associated with antiestrogen resistance in breast cancer cell lines. *Int. J. Cancer* **2012**, *131*, 1998-2007.

41. Saini, K. S.; Loi, S.; de Azambuja, E.; Metzger-Filho, O.; Saini, M. L.; Ignatiadis, M.; Dancey, J. E.; Piccart-Gebhart, M. J. Targeting the PI3K/AKT/mTOR and Raf/MEK/ERK pathways in the treatment of breast cancer. *Cancer Treat. Rev.* **2013**, *39*, 935-946.

42. Fagan, D. H.; Yee, D. Crosstalk between IGF1R and estrogen receptor signaling in breast cancer. *J. Mammary Gland Biol. Neoplasia* **2008**, *13*, 423-429.

43. Farabaugh, S. M.; Boone, D. N.; Lee, A. V. Role of IGF1R in Breast Cancer Subtypes, Stemness, and Lineage Differentiation. *Front. Endocrinol. (Lausanne)* **2015**, *6*, 59.

44. Reymond, N.; d'Agua, B. B.; Ridley, A. J. Crossing the endothelial barrier during metastasis. *Nat. Rev. Cancer.* **2013**, *13*, 858-870.

45. Eckhardt, B. L.; Francis, P. A.; Parker, B. S.; Anderson, R. L. Strategies for the discovery and development of therapies for metastatic breast cancer. *Nat. Rev. Drug Discov.* **2012**, *11*, 479-497.

46. Fornaro, M.; Dell'Arciprete, R.; Stella, M.; Bucci, C.; Nutini, M.; Capri, M. G.; Alberti, S. Cloning of the gene encoding Trop-2, a cell-surface glycoprotein expressed by human carcinomas. *Int. J. Cancer* **1995**, *62*, 610-618.

47. Shvartsur, A.; Bonavida, B. Trop2 and its overexpression in cancers: regulation and clinical/therapeutic implications. *Genes Cancer.* **2015**, *6*, 84-105.

48. Lipinski, M.; Parks, D. R.; Rouse, R. V.; Herzenberg, L. A. Human trophoblast cell-surface antigens defined by monoclonal antibodies. *Proc. Natl. Acad. Sci. U. S. A.* **1981**, *78*, 5147-5150.

49. Szala, S.; Froehlich, M.; Scollon, M.; Kasai, Y.; Steplewski, Z.; Koprowski, H.; Linnenbach, A. J. Molecular cloning of cDNA for the carcinoma-associated antigen GA733-2. *Proc. Natl. Acad. Sci. U. S. A.* **1990**, *87*, 3542-3546.

50. Basu, A.; Goldenberg, D. M.; Stein, R. The epithelial/carcinoma antigen EGP-1, recognized by monoclonal antibody RS7-3G11, is phosphorylated on serine 303. *Int. J. Cancer* **1995**, *62*, 472-479.

51. El Sewedy, T.; Fornaro, M.; Alberti, S. Cloning of the murine TROP2 gene: conservation of a PIP2-binding sequence in the cytoplasmic domain of TROP-2. *Int. J. Cancer* **1998**, *75*, 324-330.

52. Ciccarelli, F. D.; Acciarito, A.; Alberti, S. Large and diverse numbers of human diseases with HIKE mutations. *Hum. Mol. Genet.* **2000**, *9*, 1001-1007.

53. Alberti, S. HIKE, a candidate protein binding site for PH domains, is a major regulatory region of Gbeta proteins. *Proteins* **1999**, *35*, 360-363.

54. McDougall, A. R.; Tolcos, M.; Hooper, S. B.; Cole, T. J.; Wallace, M. J. Trop2: From development to disease. *Dev. Dyn.* **2014**.

55. Tsujikawa, M.; Kurahashi, H.; Tanaka, T.; Nishida, K.; Shimomura, Y.; Tano, Y.; Nakamura, Y. Identification of the gene responsible for gelatinous drop-like corneal dystrophy. *Nat. Genet.* **1999**, *21*, 420-423.

56. Zhang, K.; Jones, L.; Lim, S.; Maher, C. A.; Adkins, D.; Lewis, J.; Kimple, R. J.; Fertig, E. J.; Chung, C. H.; Van Tine, B. A.; Ellis, M. J.; Herrlich, A.; Michel, L. S. Loss of Trop2 causes ErbB3 activation through a neuregulin-1-dependent mechanism in the mesenchymal subtype of HNSCC. *Oncotarget* **2014**, *5*, 9281-9294.

57. Trerotola, M.; Jernigan, D. L.; Liu, Q.; Siddiqui, J.; Fatatis, A.; Languino, L. R. Trop-2 promotes prostate cancer metastasis by modulating beta(1) integrin functions. *Cancer Res.* **2013**, *73*, 3155-3167.

58. Stoyanova, T.; Goldstein, A. S.; Cai, H.; Drake, J. M.; Huang, J.; Witte, O. N. Regulated proteolysis of Trop2 drives epithelial hyperplasia and stem cell self-renewal via beta-catenin signaling. *Genes Dev.* **2012**, *26*, 2271-2285.

59. Cubas, R.; Zhang, S.; Li, M.; Chen, C.; Yao, Q. Trop2 expression contributes to tumor pathogenesis by activating the ERK MAPK pathway. *Mol. Cancer.* **2010**, *9*, 253-4598-9-253.

60. Guerra, E Trerotola, M Aloisi, A L Tripaldi, R Vacca, G La Sorda, R Lattanzio, R Piantelli,M Alberti, S. The Trop-2 signalling network in cancer growth. *Oncogene* **2013**, *32*, 1594-1600.

61. Lin, J.; Wu, Y.; Wu, J.; Lin, T.; Wu, C.; Chang, Y.; Jou, Y.; Hong, T.; Yang, P. TROP2 is epigenetically inactivated and modulates IGF-1R signalling in lung adenocarcinoma. *EMBO molecular medicine* **2012**, *4*, 472-485.

62. McDougall, A. R.; Hooper, S. B.; Zahra, V. A.; Cole, T. J.; Lo, C. Y.; Doran, T.; Wallace, M. J. Trop2 regulates motility and lamellipodia formation in cultured fetal lung fibroblasts. *Am. J. Physiol. Lung Cell. Mol. Physiol.* **2013**, *305*, L508-21.

63. Ripani, E.; Sacchetti, A.; Corda, D.; Alberti, S. Human Trop-2 is a tumor-associated calcium signal transducer. *Int. J. Cancer* **1998**, *76*, 671-676.

64. Trerotola, M.; Cantanelli, P.; Guerra, E.; Tripaldi, R.; Aloisi, A. L.; Bonasera, V.; Lattanzio, R.; de Lange, R.; Weidle, U. H.; Piantelli, M.; Alberti, S. Upregulation of Trop-2 quantitatively stimulates human cancer growth. *Oncogene* **2013**, *32*, 222-233.

65. Ambrogi, F.; Fornili, M.; Boracchi, P.; Trerotola, M.; Relli, V.; Simeone, P.; La Sorda, R.; Lattanzio, R.; Querzoli, P.; Pedriali, M.; Piantelli, M.; Biganzoli, E.; Alberti, S. Trop-2 is a determinant of breast cancer survival. *PLoS One* **2014**, *9*, e96993.

66. Lindner, D.; Wu, Y.; Haney, R.; Jacobs, B.; Fruehauf, J.; Tuthill, R.; Borden, E. Thrombospondin-1 expression in melanoma is blocked by methylation and targeted reversal by 5-Aza-deoxycytidine suppresses angiogenesis. *Matrix biology* **2013**, *32*, 123-132.

67. Sooman, L.; Ekman, S.; Tsakonas, G.; Jaiswal, A.; Navani, S.; Edqvist, P.; Pontén, F.; Bergström, S.; Johansson, M.; Wu, X.; Blomquist, E.; Bergqvist, M.; Gullbo, J.; Lennartsson, J. PTPN6 expression is epigenetically regulated and influences survival and response to chemotherapy in high-grade gliomas. *Tumor Biol.* **2014**, 4479-4488.

68. Tessema, M.; Yingling, C.; Liu, Y.; Tellez, C.; Van Neste, L.; Baylin, S.; Belinsky, S. Genome-wide unmasking of epigenetically silenced genes in lung adenocarcinoma from smokers and never smokers. *Carcinogenesis* **2014**, 1248-1257.

69. Zhao, R.; Meng, F.; Wang, N.; Ma, W.; Yan, Q. Silencing of CHD5 Gene by Promoter Methylation in Leukemia. *PLoS ONE* **2014**, *9*, e85172-e85172.

70. Ghoshal, K.; Bai, S. DNA methyltransferases as targets for cancer therapy. *Drugs of today* **2007**, *43*, 395-422.

71. Momparler, R. Epigenetic therapy of cancer with 5-aza-2'-deoxycytidine (decitabine). *Semin. Oncol.* **2005**, *32*, 443-451.

72. Karahoca, M.; Momparler, R. Pharmacokinetic and pharmacodynamic analysis of 5-aza-2'-deoxycytidine (decitabine) in the design of its dose-schedule for cancer therapy. *Clinical Epigenetics* **2013**, *5*, 3-3.

73. Stone, A.; Valdés-Mora, F.; Gee, J. M.; Farrow, L.; McClelland, R.; Fiegl, H.; Dutkowski, C.; McCloy, R.; Sutherland, R.; Musgrove, E.; Nicholson, R. Tamoxifen-induced epigenetic silencing of oestrogen-regulated genes in anti-hormone resistant breast cancer. *PLoS ONE* **2012**, *7*, e40466-e40466.

74. Gozgit, J.; Pentecost, B.; Marconi, S.; Otis, C.; Wu, C.; Arcaro, K. Use of an aggressive MCF-7 cell line variant, TMX2-28, to study cell invasion in breast cancer. *Molecular cancer research* **2006**, *4*, 905-913.

75. Gozgit, J. M.; Pentecost, B. T.; Marconi, S. A.; Ricketts-Loriaux, R. S.; Otis, C. N.; Arcaro, K. F. PLD1 is overexpressed in an ER-negative MCF-7 cell line variant and a subset of phospho-Akt-negative breast carcinomas. *Br. J. Cancer* **2007**, *97*, 809-817.

76. Sandoval, J.; Heyn, H.; Moran, S.; Serra-Musach, J.; Pujana, M.; Bibikova, M.; Esteller, M. Validation of a DNA methylation microarray for 450,000 CpG sites in the human genome. *Epigenetics* **2011**, *6*, 692-702.

77. Clark, G. M.; Osborne, C. K.; McGuire, W. L. Correlations between estrogen receptor, progesterone receptor, and patient characteristics in human breast cancer. *J. Clin. Oncol.* **1984**, *2*, 1102-1109.

78. Fenaux, P. Inhibitors of DNA methylation: beyond myelodysplastic syndromes. *Nat. Clin. Pract. Oncol.* **2005**, *2 Suppl 1*, S36-44.

79. Feitelson, M. A.; Arzumanyan, A.; Kulathinal, R. J.; Blain, S. W.; Holcombe, R. F.; Mahajna, J.; Marino, M.; Martinez-Chantar, M. L.; Nawroth, R.; Sanchez-Garcia, I.; Sharma, D.; Saxena, N. K.; Singh, N.; Vlachostergios, P. J.; Guo, S.; Honoki, K.; Fujii, H.; Georgakilas, A. G.; Bilsland, A.; Amedei, A.; Niccolai, E.; Amin, A.; Ashraf, S. S.; Boosani, C. S.; Guha, G.; Ciriolo, M. R.; Aquilano, K.; Chen, S.; Mohammed, S. I.; Azmi, A. S.; Bhakta, D.; Halicka, D.; Keith, W. N.; Nowsheen, S. Sustained proliferation in cancer: Mechanisms and novel therapeutic targets. *Semin. Cancer Biol.* **2015**.

80. Guo, H.; Wu, F.; Wang, Y.; Yan, C.; Su, W. Overexpressed ubiquitin ligase Cullin7 in breast cancer promotes cell proliferation and invasion via down-regulating p53. *Biochem. Biophys. Res. Commun.* **2014**, *450*, 1370-1376.

81. Luo, H.; Tu, G.; Liu, Z.; Liu, M. Cancer-associated fibroblasts: a multifaceted driver of breast cancer progression. *Cancer Lett.* **2015**, *361*, 155-163.

82. Mohamed, A.; Krajewski, K.; Cakar, B.; Ma, C. X. Targeted therapy for breast cancer. *Am. J. Pathol.* **2013**, *183*, 1096-1112.

83. Lu, X.; Kang, Y. Organotropism of breast cancer metastasis. *J. Mammary Gland Biol. Neoplasia* **2007**, *12*, 153-162.

84. Kennecke, H.; Yerushalmi, R.; Woods, R.; Cheang, M. C.; Voduc, D.; Speers, C. H.; Nielsen, T. O.; Gelmon, K. Metastatic behavior of breast cancer subtypes. *J. Clin. Oncol.* **2010**, *28*, 3271-3277.

85. Chikarmane, S. A.; Tirumani, S. H.; Howard, S. A.; Jagannathan, J. P.; DiPiro, P. J. Metastatic patterns of breast cancer subtypes: what radiologists should know in the era of personalized cancer medicine. *Clin. Radiol.* **2015**, *70*, 1-10.

86. Zhang, H.; Qi, F.; Cao, Y.; Zu, X.; Chen, M.; Li, Z.; Qi, L. 5-Aza-2'-deoxycytidine enhances maspin expression and inhibits proliferation, migration, and invasion of the bladder cancer T24 cell line. *Cancer Biother. Radiopharm.* **2013**, *28*, 343-350.

87. Guo, J.; Feng, X. Q.; Nie, S. M.; Su, Z.; Shi, X.; Cui, Z. G.; Zhang, L.; Liu, S. G.; Meng, F. J.; Zhao, C. T. Effect of 5-aza-2'-deoxycytidine combined with trichostatin A on RPMI-8226 cell proliferation, apoptosis and DLC-1 gene expression. *Zhongguo Shi Yan Xue Ye Xue Za Zhi* **2014**, *22*, 357-363.

88. Yao, T. T.; Mo, S. M.; Liu, L. Y.; Lu, H. W.; Huang, M. L.; Lin, Z. Q. 5-Aza-2'-deoxycytidine may influence the proliferation and apoptosis of cervical cancer cells via demethylation in a dose- and time-dependent manner. *Genet. Mol. Res.* **2013**, *12*, 312-318.

89. Yang, Q.; Shan, L.; Yoshimura, G.; Nakamura, M.; Nakamura, Y.; Suzuma, T.; Umemura, T.; Mori, I.; Sakurai, T.; Kakudo, K. 5-Aza-2'-Deoxycytidine Induces Retinoic Acid Receptor Beta 2 Demethylation, Cell Cycle Arrest and Growth Inhibition in Breast Carcinoma Cells. *Anticancer Res.* **2002**, *22*, 2753-2756.

90. Xiong, H.; Qiu, H.; Zhuang, L.; Xiong, H.; Jiang, R.; Chen, Y. Effects of 5-Aza-CdR on the proliferation of human breast cancer cell line MCF-7 and on the expression of Apaf-1 gene. *J. Huazhong Univ. Sci. Technolog Med. Sci.* **2009**, *29*, 498-502.

91. Zeng, L.; Jarrett, C.; Brown, K.; Gillespie, K. M.; Holly, J. M.; Perks, C. M. Insulin-like growth factor binding protein-3 (IGFBP-3) plays a role in the anti-tumorigenic effects of 5-Aza-2'-deoxycytidine (AZA) in breast cancer cells. *Exp. Cell Res.* **2013**, *319*, 2282-2295.

92. Shi, X.; Liu, H.; Cao, J.; Liu, Q.; Tang, G.; Liu, W.; Liu, H.; Deng, D.; Qiao, F.; Wu, Y. Promoter Hypomethylation of Maspin Inhibits Migration and Invasion of Extravillous Trophoblast Cells during Placentation. *PLoS One* **2015**, *10*, e0135359.

93. Li, Z.; Zhang, G.; Li, D.; Jie, Z.; Chen, H.; Xiong, J.; Liu, Y.; Cao, Y.; Jiang, M.; Le, Z.; Tan, S. Methylation-associated silencing of miR-495 inhibit the migration and invasion of human gastric cancer cells by directly targeting PRL-3. *Biochem. Biophys. Res. Commun.* **2015**, *456*, 344-350.

94. Ateeq, B.; Unterberger, A.; Szyf, M.; Rabbani, S. Pharmacological inhibition of DNA methylation induces proinvasive and prometastatic genes in vitro and in vivo. *Neoplasia* **2008**, *10*, 266-278.

95. Sorm, F.; Veselý, J. Effect of 5-aza-2'-deoxycytidine against leukemic and hemopoietic tissues in AKR mice. *Neoplasma* **1968**, *15*, 339-43.

96. Notari, R. E.; DeYoung, J. L. Kinetics and mechanisms of degradation of the antileukemic agent 5-azacytidine in aqueous solutions. *J. Pharm. Sci.* **1975**, *64*, 1148-1157.

97. Jones, P. A.; Taylor, S. M. Cellular differentiation, cytidine analogs and DNA methylation. *Cell* **1980**, *20*, 85-93.

98. Visconte, V.; Tiu, R. V.; Rogers, H. J. Pathogenesis of myelodysplastic syndromes: an overview of molecular and non-molecular aspects of the disease. *Blood Res.* **2014**, *49*, 216-227.

99. Creusot, F.; Acs, G.; Christman, J. K. Inhibition of DNA methyltransferase and induction of Friend erythroleukemia cell differentiation by 5-azacytidine and 5-aza-2'-deoxycytidine. *J. Biol. Chem.* **1982**, *257*, 2041-2048.

100. Gius, D.; Cui, H.; Bradbury, C. M.; Cook, J.; Smart, D. K.; Zhao, S.; Young, L.; Brandenburg, S. A.; Hu, Y.; Bisht, K. S.; Ho, A. S.; Mattson, D.; Sun, L.; Munson, P. J.; Chuang, E. Y.; Mitchell, J. B.; Feinberg, A. P. Distinct effects on gene expression of chemical and genetic manipulation of the cancer epigenome revealed by a multimodality approach. *Cancer. Cell.* **2004**, *6*, 361-371.

101. Ghoshal, K.; Datta, J.; Majumder, S.; Bai, S.; Kutay, H.; Motiwala, T.; Jacob, S. T. 5-Aza-deoxycytidine induces selective degradation of DNA methyltransferase 1 by a proteasomal pathway that requires the KEN box, bromo-adjacent homology domain, and nuclear localization signal. *Mol. Cell. Biol.* **2005**, *25*, 4727-4741.

102. Williams, K. E. DNA-Based Epigenetic Changes in Recurrent and Tamoxifen-Resistant Breast Cancer. **2016**.

103. Ibragimova, I.; Ibanez de Caceres, I.; Hoffman, A. M.; Potapova, A.; Dulaimi, E.; Al-Saleem, T.; Hudes, G. R.; Ochs, M. F.; Cairns, P. Global reactivation of epigenetically silenced genes in prostate cancer. *Cancer. Prev. Res. (Phila)* **2010**, *3*, 1084-1092.

104. Kanai, Y.; Ushijima, S.; Saito, Y.; Nakanishi, Y.; Sakamoto, M.; Hirohashi, S. MRNA expression of genes altered by 5-azacytidine treatment in cancer cell lines is associated with clinicopathological parameters of human cancers. *J. Cancer Res. Clin. Oncol.* **2001**, *127*, 697-706.

105. Tsukahara, Y.; Tanaka, M.; Miyajima, A. TROP2 expressed in the trunk of the ureteric duct regulates branching morphogenesis during kidney development. *PLoS One* **2011**, *6*, e28607.

106. Trerotola, M.; Li, J.; Alberti, S.; Languino, L. R. Trop-2 inhibits prostate cancer cell adhesion to fibronectin through the beta1 integrin-RACK1 axis. *J. Cell. Physiol.* **2012**, *227*, 3670-3677.

107. Gardel, M. L.; Schneider, I. C.; Aratyn-Schaus, Y.; Waterman, C. M. Mechanical integration of actin and adhesion dynamics in cell migration. *Annu. Rev. Cell Dev. Biol.* **2010**, *26*, 315-333.

108. Wang, X. D.; Wang, Q.; Chen, X. L.; Huang, J. F.; Yin, Y.; Da, P.; Wu, H. Trop2 inhibition suppresses the proliferation and invasion of laryngeal carcinoma cells via the extracellular signal-regulated kinase/mitogen-activated protein kinase pathway. *Mol. Med. Rep.* **2015**, *12*, 865-870.

109. Huang, H.; Groth, J.; Sossey-Alaoui, K.; Hawthorn, L.; Beall, S.; Geradts, J. Aberrant expression of novel and previously described cell membrane markers in human breast cancer cell lines and tumors. *Clin. Cancer Res.* **2005**, *11*, 4357-4364.

110. McDougall, A. R.; Hooper, S. B.; Zahra, V. A.; Sozo, F.; Lo, C. Y.; Cole, T. J.; Doran, T.; Wallace, M. J. The oncogene Trop2 regulates fetal lung cell proliferation. *Am. J. Physiol. Lung Cell. Mol. Physiol.* **2011**, *301*, L478-89.

111. Liu, T.; Liu, Y.; Bao, X.; Tian, J.; Liu, Y.; Yang, X. Overexpression of TROP2 predicts poor prognosis of patients with cervical cancer and promotes the proliferation and invasion of cervical cancer cells by regulating ERK signaling pathway. *PLoS One* **2013**, *8*, e75864.

112. Ning, S.; Liang, N.; Liu, B.; Chen, X.; Pang, Q.; Xin, T. TROP2 expression and its correlation with tumor proliferation and angiogenesis in human gliomas. *Neurol. Sci.* **2013**, *34*, 1745-1750.

113. Zhao, P.; Yu, H. Z.; Cai, J. H. Clinical investigation of TROP-2 as an independent biomarker and potential therapeutic target in colon cancer. *Mol. Med. Rep.* **2015**, *12*, 4364-4369.

114. Lin, H.; Huang, J. F.; Qiu, J. R.; Zhang, H. L.; Tang, X. J.; Li, H.; Wang, C. J.; Wang, Z. C.; Feng, Z. Q.; Zhu, J. Significantly upregulated TACSTD2 and Cyclin D1 correlate with poor prognosis of invasive ductal breast cancer. *Exp. Mol. Pathol.* **2013**, *94*, 73-78.

115. Ohmachi, T.; Tanaka, F.; Mimori, K.; Inoue, H.; Yanaga, K.; Mori, M. Clinical significance of TROP2 expression in colorectal cancer. *Clin. Cancer Res.* **2006**, *12*, 3057-3063.

116. Fang, Y. J.; Lu, Z. H.; Wang, G. Q.; Pan, Z. Z.; Zhou, Z. W.; Yun, J. P.; Zhang, M. F.; Wan, D. S. Elevated expressions of MMP7, TROP2, and survivin are associated with survival, disease recurrence, and liver metastasis of colon cancer. *Int. J. Colorectal Dis.* **2009**, *24*, 875-884.

117. Wang, J.; Day, R.; Dong, Y.; Weintraub, S. J.; Michel, L. Identification of Trop-2 as an oncogene and an attractive therapeutic target in colon cancers. *Mol. Cancer. Ther.* **2008**, *7*, 280-285.

118. Trerotola, M.; Ganguly, K. K.; Fazli, L.; Fedele, C.; Lu, H.; Dutta, A.; Liu, Q.; De Angelis, T.; Riddell, L. W.; Riobo, N. A.; Gleave, M. E.; Zoubeidi, A.; Pestell, R. G.; Altieri, D. C.; Languino, L. R. Trop-2 is up-regulated in invasive prostate cancer and displaces FAK from focal contacts. *Oncotarget* **2015**, *6*, 14318-14328.

119. Fackler, Mary Umbricht, Christopher Williams, Danielle Argani, Pedram Cruz, Leigh-Ann Merino, Vanessa Teo, Wei Zhang, Zhe Huang, Peng Visvananthan, Kala Marks, Jeffrey Ethier, Stephen Gray, Joe Wolff, Antonio Cope,Leslie Sukumar, Saraswati Genome-wide methylation analysis identifies genes specific to breast cancer hormone receptor status and risk of recurrence. *Cancer Res.* **2011**, *71*, 6195-6207.

120. Xu, Z.; Bolick, S. C.; DeRoo, L. A.; Weinberg, C. R.; Sandler, D. P.; Taylor, J. A. Epigenome-wide association study of breast cancer using prospectively collected sister study samples. *J. Natl. Cancer Inst.* **2013**, *105*, 694-700.

121. Karantza, V. Keratins in health and cancer: more than mere epithelial cell markers. *Oncogene* **2011**, *30*, 127-138.

122. Joosse, S. A.; Hannemann, J.; Spotter, J.; Bauche, A.; Andreas, A.; Muller, V.; Pantel, K. Changes in keratin expression during metastatic progression of breast cancer: impact on the detection of circulating tumor cells. *Clin. Cancer Res.* **2012**, *18*, 993-1003.

123. Moll, R.; Franke, W. W.; Schiller, D. L.; Geiger, B.; Krepler, R. The catalog of human cytokeratins: patterns of expression in normal epithelia, tumors and cultured cells. *Cell* **1982**, *31*, 11-24.

124. Shao, M. M.; Chan, S. K.; Yu, A. M.; Lam, C. C.; Tsang, J. Y.; Lui, P. C.; Law, B. K.; Tan, P. H.; Tse, G. M. Keratin expression in breast cancers. *Virchows Arch.* **2012**, *461*, 313-322.

125. Gusterson, B. A.; Ross, D. T.; Heath, V. J.; Stein, T. Basal cytokeratins and their relationship to the cellular origin and functional classification of breast cancer. *Breast Cancer Res.* **2005**, *7*, 143-148.

126. Celardo, I.; Antonov, A.; Amelio, I.; Annicchiarico-Petruzzelli, M.; Melino, G. P63 Transcriptionally Regulates the Expression of Matrix Metallopeptidase 13. *Oncotarget* **2014**, *5*, 1279-1289.

127. Yallowitz, A. R.; Alexandrova, E. M.; Talos, F.; Xu, S.; Marchenko, N. D.; Moll, U. M. p63 is a prosurvival factor in the adult mammary gland during post-lactational involution, affecting PI-MECs and ErbB2 tumorigenesis. *Cell Death Differ.* **2014**, *21*, 645-654.

128. Memmi, E. M.; Sanarico, A. G.; Giacobbe, A.; Peschiaroli, A.; Frezza, V.; Cicalese, A.; Pisati, F.; Tosoni, D.; Zhou, H.; Tonon, G.; Antonov, A.; Melino, G.; Pelicci, P. G.; Bernassola, F. p63 Sustains self-renewal of mammary cancer stem cells through regulation of Sonic Hedgehog signaling. *Proc. Natl. Acad. Sci. U. S. A.* **2015**, *112*, 3499-3504.

129. Nakayama, K.; Inokuchi, K.; Dan, K. Hypermethylation of the putative tumor-suppressor genes DCC, p51/63 and O6-methylguanine-DNA methyltransferase (MGMT) and loss of

their expressions in cell lines of hematological malignancies. *J. Nippon Med. Sch.* **2005**, *72*, 270-277.

130. Humphries, L. A.; Godbersen, J. C.; Danilova, O. V.; Kaur, P.; Christensen, B. C.; Danilov, A. V. Pro-apoptotic TP53 homolog TAp63 is repressed via epigenetic silencing and B-cell receptor signalling in chronic lymphocytic leukaemia. *Br. J. Haematol.* **2013**, *163*, 590-602.

131. Park, B. J.; Lee, S. J.; Kim, J. I.; Lee, S. J.; Lee, C. H.; Chang, S. G.; Park, J. H.; Chi, S. G. Frequent alteration of p63 expression in human primary bladder carcinomas. *Cancer Res.* **2000**, *60*, 3370-3374.

132. Sartor, M. A.; Dolinoy, D. C.; Jones, T. R.; Colacino, J. A.; Prince, M. E.; Carey, T. E.; Rozek, L. S. Genome-wide methylation and expression differences in HPV(+) and HPV(-) squamous cell carcinoma cell lines are consistent with divergent mechanisms of carcinogenesis. *Epigenetics* **2011**, *6*, 777-787.

133. Salhia, B.; Kiefer, J.; Ross, J. T.; Metapally, R.; Martinez, R. A.; Johnson, K. N.; DiPerna, D. M.; Paquette, K. M.; Jung, S.; Nasser, S.; Wallstrom, G.; Tembe, W.; Baker, A.; Carpten, J.; Resau, J.; Ryken, T.; Sibenaller, Z.; Petricoin, E. F.; Liotta, L. A.; Ramanathan, R. K.; Berens, M. E.; Tran, N. L. Integrated genomic and epigenomic analysis of breast cancer brain metastasis. *PLoS One* **2014**, *9*, e85448.

134. Zhou, Y.; Hu, Z. Genome-wide demethylation by 5-aza-2'-deoxycytidine alters the cell fate of stem/progenitor cells. *Stem Cell. Rev.* **2015**, *11*, 87-95.

135. Kwan, R.; Looi, K.; Omary, M. B. Absence of keratins 8 and 18 in rodent epithelial cell lines associates with keratin gene mutation and DNA methylation: Cell line selective effects on cell invasion. *Exp. Cell Res.* **2015**, *335*, 12-22.

136. Escobar-Hoyos, L. F.; Shah, R.; Roa-Pena, L.; Vanner, E. A.; Najafian, N.; Banach, A.; Nielsen, E.; Al-Khalil, R.; Akalin, A.; Talmage, D.; Shroyer, K. R. Keratin-17 Promotes p27KIP1 Nuclear Export and Degradation and Offers Potential Prognostic Utility. *Cancer Res.* **2015**, *75*, 3650-3662.

137. Dabbs, D. J.; Chivukula, M.; Carter, G.; Bhargava, R. Basal phenotype of ductal carcinoma in situ: recognition and immunohistologic profile. *Mod. Pathol.* **2006**, *19*, 1506-1511.

138. Perou, C. M.; Sorlie, T.; Eisen, M. B.; van de Rijn, M.; Jeffrey, S. S.; Rees, C. A.; Pollack, J. R.; Ross, D. T.; Johnsen, H.; Akslen, L. A.; Fluge, O.; Pergamenschikov, A.; Williams, C.; Zhu, S. X.; Lonning, P. E.; Borresen-Dale, A. L.; Brown, P. O.; Botstein, D. Molecular portraits of human breast tumours. *Nature* **2000**, *406*, 747-752.

139. Ramos-Vara, J. A. Technical aspects of immunohistochemistry. *Vet. Pathol.* **2005**, *42*, 405-426.

140. AnonymousMedicine Conspectus: Cytoskeleton. Cell Components. Cell Structure and Function. *http://medicineconspectus.blogspot.com/2014/01/cytoskeleton-cell-components-cell.html* (accessed 11/17, 2015).

141. Pu, R. T.; Laitala, L. E.; Alli, P. M.; Fackler, M. J.; Sukumar, S.; Clark, D. P. Methylation profiling of benign and malignant breast lesions and its application to cytopathology. *Mod. Pathol.* **2003**, *16*, 1095-1101.

142. Fackler, M. J.; McVeigh, M.; Evron, E.; Garrett, E.; Mehrotra, J.; Polyak, K.; Sukumar, S.; Argani, P. DNA methylation of RASSF1A, HIN-1, RAR-beta, Cyclin D2 and Twist in in situ and invasive lobular breast carcinoma. *Int. J. Cancer* **2003**, *107*, 970-975.

143. Hill, V. K.; Ricketts, C.; Bieche, I.; Vacher, S.; Gentle, D.; Lewis, C.; Maher, E. R.; Latif, F. Genome-wide DNA methylation profiling of CpG islands in breast cancer identifies novel genes associated with tumorigenicity. *Cancer Res.* **2011**, *71*, 2988-2999.

144. Murphy, J. P.; Pinto, D. M. Temporal proteomic analysis of IGF-1R signalling in MCF-7 breast adenocarcinoma cells. *Proteomics* **2010**, *10*, 1847-1860.

145. Lu, P.; Weaver, V. M.; Werb, Z. The extracellular matrix: a dynamic niche in cancer progression. *J. Cell Biol.* **2012**, *196*, 395-406.

146. Oskarsson, T. Extracellular matrix components in breast cancer progression and metastasis. *Breast* **2013**, *22 Suppl 2*, S66-72.

147. Nakanishi, H.; Taccioli, C.; Palatini, J.; Fernandez-Cymering, C.; Cui, R.; Kim, T.; Volinia, S.; Croce, C. M. Loss of miR-125b-1 contributes to head and neck cancer development by dysregulating TACSTD2 and MAPK pathway. *Oncogene* **2014**, *33*, 702-712.

148. Sharkey, R. M.; van Rij, C. M.; Karacay, H.; Rossi, E. A.; Frielink, C.; Regino, C.; Cardillo, T. M.; McBride, W. J.; Chang, C. H.; Boerman, O. C.; Goldenberg, D. M. A new Tri-Fab bispecific antibody for pretargeting Trop-2-expressing epithelial cancers. *J. Nucl. Med.* **2012**, *53*, 1625-1632.

149. van Rij, C. M.; Lutje, S.; Frielink, C.; Sharkey, R. M.; Goldenberg, D. M.; Franssen, G. M.; McBride, W. J.; Rossi, E. A.; Oyen, W. J.; Boerman, O. C. Pretargeted immuno-PET and radioimmunotherapy of prostate cancer with an anti-TROP-2 x anti-HSG bispecific antibody. *Eur. J. Nucl. Med. Mol. Imaging* **2013**, *40*, 1377-1383.

150. Liu, D.; Cardillo, T. M.; Wang, Y.; Rossi, E. A.; Goldenberg, D. M.; Chang, C. H. Trop-2-targeting tetrakis-ranpirnase has potent antitumor activity against triple-negative breast cancer. *Mol. Cancer.* **2014**, *13*, 53-4598-13-53.

151. Liu, T.; Tian, J.; Chen, Z.; Liang, Y.; Liu, J.; Liu, S.; Li, H.; Zhan, J.; Yang, X. Anti-TROP2 conjugated hollow gold nanospheres as a novel nanostructure for targeted photothermal destruction of cervical cancer cells. *Nanotechnology* **2014**, *25*, 345103-4484/25/34/345103. Epub 2014 Aug 7.

152. Lin, H.; Zhang, H.; Wang, J.; Lu, M.; Zheng, F.; Wang, C.; Tang, X.; Xu, N.; Chen, R.; Zhang, D.; Zhao, P.; Zhu, J.; Mao, Y.; Feng, Z. A novel human Fab antibody for Trop2 inhibits breast cancer growth in vitro and in vivo. *Int. J. Cancer* **2014**, *134*, 1239-1249.

153. Starodub, A. N.; Ocean, A. J.; Shah, M. A.; Guarino, M. J.; Picozzi, V. J.,Jr; Vahdat, L. T.; Thomas, S. S.; Govindan, S. V.; Maliakal, P. P.; Wegener, W. A.; Hamburger, S. A.; Sharkey, R. M.; Goldenberg, D. M. First-in-Human Trial of a Novel Anti-Trop-2 Antibody-SN-38 Conjugate, Sacituzumab Govitecan, for the Treatment of Diverse Metastatic Solid Tumors. *Clin. Cancer Res.* **2015**, *21*, 3870-3878.